

Mars Reconnaissance Orbiter

CRISM DATA PRODUCT SOFTWARE INTERFACE SPECIFICATION

Version 1.3.7.1

Prepared by:

Scott Murchie
JHU/APL

Edward Guinness and Susan Slavney
PDS Geosciences Node
Washington University

Approved by:

Scott Murchie
Principal Investigator, CRISM

Richard Zurek
Project Scientist, MRO

Raymond E. Arvidson
Director, PDS Geosciences Node

Steve Noland
MRO Science Operations System
Engineer, MRO

February 29, 2012

DOCUMENT CHANGE LOG

| Date | Description | Sections affected |
|-----------|--|-------------------|
| 12/15/03 | Initial Draft | All |
| 11/22/04 | Calibration data records redefined based on instrument calibration results; data processing details (App. I) added; descriptions of macros updated; EDR and TRDR labels updated based on needs of data processing; housekeeping file updated for consistency with flight software | All |
| 3/2/2005 | Revisions upon recommendation of reviewers | All |
| 9/14/2005 | <p>Added distinguishing features of wavelength filters, exp, and frame rates for level 4 CDRs</p> <p>Distinguished MRO:WAV file for CDR and RDR</p> <p>Added metakernel list files, wavelength files to MRDRs and MTRDRs in figures and text</p> <p>Updated alarm limits</p> <p>Added 12 to 8 bit inverse table to level 6 CDRs</p> <p>Updated labels for level 4 and level 6 CDRs</p> <p>Updated summary parameters</p> <p>Added wavelength filter as keyword and included in EDRs and CDRs</p> <p>Added functional test to cases where macro \neq EDR</p> <p>Added image source to variable settings</p> <p>Fixed sphere lamp 1 and 2 confusion</p> <p>Changed gain_offset to pixel_proc in CDR filename</p> <p>Added compression_type = none, 8_bit to EDR labels</p> <p>Added MRO:SPHERE_TEMPERATURE to CDR labels</p> <p>Added MRO:FRAME_RATE to LDD list for EDR</p> <p>Added exp time parameter to CDR file name</p> <p>Added MRO:WAVELENGTH_FILTER to LDD for EDRs</p> <p>Made underscores in file names and product IDs consistent</p> <p>Renamed MTRDRs using convention for MRDRs; add required layers (observation ID, counter, column)</p> <p>Added column(s) to MRDR geometry image</p> <p>Made observation ID hexadecimal, and corrected its length in all example labels</p> <p>Reformatted MTRDR sample label to parallel MRDR</p> <p>Added SUBTYPE of product to MRDR and MTRDR name</p> <p>Updated graphics</p> <p>Made 1 label per image file</p> <p>Redefined MTRDRs along line of data archive SIS</p> <p>Added MRO:EXPOSURE_PARAMETER to LDD list, to CDR name, EDR and CDR labels</p> <p>Added correction for shutter position to sphere radiance</p> | All |
| 5/3/2006 | <p>split TP into different test patterns</p> <p>add VNIR and IR FPU electronics temperatures as keywords and included in CDR labels and table of CRISM-specific keywords</p> <p>added prefix bytes to TRDR label</p> <p>copy applicable changes to Data Archive SIS</p> <p>specify which value is used for sphere, spec housing temp, detector temp, FPE temp</p> <p>add VL (valid limit) 14-bit DN level 6 CDR</p> <p>revise MRO:activity CAT file</p> <p>add event log, instrument settings and data compressibility level 6 CDRs</p> <p>revise observation description</p> <p>make heater zone definitions consistent</p> <p>update definition of how bad pixels are filled</p> <p>update macros</p> | All |

| | | |
|-----------|--|-----|
| | <p>add example labels for MRDR, MTRDR wavelength files</p> <p>add section on SPICE files</p> <p>add section on browse files</p> <p>add section on extras; move target list stuff to extras</p> <p>update description of observation ID files</p> <p>removed specific values of alarm limits and referenced appropriate CDR6</p> <p>update calibration appendix</p> <p>add compression_type = none, 8_bit to EDR keyword list</p> <p>made observation_id and observation_number hexadecimal</p> <p>update parameter formulations</p> <p>create LDD keywords INVALID_PIXEL_COORDINATES, REPLACED_PIXEL_COORDINATES and corresponding CAT file</p> <p>modify SC CDR4 for sphere correction; add VNIR image in units of 14-bit DN to use as a reference for the correction</p> <p>add CDR6 BS for bias step</p> <p>modify descriptions of DB, EB, and GH CDR6's</p> <p>fixed CDR4 sample label sphere nomenclature</p> <p>specify DDR geometry to 610, 2300 nm</p> <p>add CDR for daily housekeeping</p> <p>changed format of CDR4 images from IEEE_REAL to PC_REAL</p> <p>defined 000 as inapplicable exposure time parameter</p> <p>rename WV to WA for level-4 CDR</p> <p>rename SR to SS for sphere radiance model</p> <p>updated EDR, TRDR, DDR sample labels</p> <p>deleted appendix a</p> <p>added sample ADR label</p> <p>Redefined definition of nonuniformity files</p> <p>Eliminated CDR6 tables of CDR4s created inflight</p> <p>Added ST CDR6s</p> <p>Added ACT and PRE CDR6s and defined their distinct nomenclature</p> <p>Refined definition of AS CDR6</p> <p>Added BW CDR6</p> <p>Added HV CDR6</p> <p>Added PS CDR4</p> <p>Added RW CDR4</p> <p>Added RF CDR4</p> <p>Renamed WV CDR4 to WA CDR4, to eliminate confusion with the WV CDR6</p> <p>Added SH CDR4</p> <p>Added SL and VL CDR6s</p> <p>Renamed SR CDR4 to SS</p> <p>Added SW CDR6</p> <p>Made the counter in the EDR or TRDR file name hexadecimal</p> <p>Updated nomenclature of CDR4s to include additional identifiers</p> <p>Added resampled TRDR, filetype "RTR"</p> <p>Refined ADR definitions</p> <p>Made the counter in the EDR or TRDR file name hexadecimal</p> <p>Updated nomenclature of CDR4s to include additional identifiers</p> <p>Added resampled TRDR, filetype "RTR"</p> <p>Added ADR directory</p> <p>Made DDRs band sequential</p> | |
| 7/10/2006 | <p>Renamed ACT and PRE CDR6s to BTF and ATF</p> <p>Updated calibration description in Appendix I</p> <p>Redefined last 3 layers of a DDR to exclude CRISM-derived data</p> <p>Added missing commas in sample DDR label</p> <p>Changed units of radiance to W/(m**2 micrometer sr)</p> <p>Replaced local data dictionary keyword</p> | All |

| | | |
|------------|---|-----|
| | MRO:FPE_ELECTRONICS_TEMPERATURE with MRO:FPE_TEMPERATURE | |
| 10/1/2006 | Added INVALID_PIXEL_LOCATION or to TRDR labels Added keywords specific to resampling and atmospheric corrections to TRDR label Added keywords specific to resampling and atmospheric corrections to LDD, and tables of CRISM-specific keywords Updated list of summary products Added keywords specific to resampling and atmospheric corrections to tables of CRISM-specific keywords Added definitions of RTRs Described and differentiated version 0 and 1 DDR Added EDR, TRDR, and MRDR browse product labels to appendix Describe SPICE kernels generated by CRISM Updated definition of DDR browse products Added DDR browse product labels to appendix | All |
| 2/7/2007 | Added AT and RT CDR4s and CT CDR6 describing wavelength-dependent atmospheric transmission, for post-calibration data processing Changed primary source of MRO:DETECTOR_TEMPERATURE from IR temperature sensor 2 to IR temperature sensor 1 Change of definition of wavelength filters on 11 Dec 2006 noted Changed units of elevation layer in DDR to kilometers Changed latitude range separating MRDR map tiles projected equirectangularly and polar stereographically Redefined calibrated data layer of MRDRs and MTRDRs to be I/F instead of radiance Redefined "HYD" IR browse product into three separate products based on first results from Mars | All |
| 5/16/2007 | Changed units of MOLA elevation in DDR description Fixed nomenclature of OTT tables in EXTRAS directory Updated descriptions of SB and NU CDRs | All |
| 8/23/2007 | Corrected character string in file names to designate EPFs Added definition of TOD observing mode Updated descriptions of SPICE kernels Added information on number of wavelengths to descriptions of EDRs generated by each observation type Defined separate backplane files for I/F and Lambert albedo versions of MRDR and MTRDR because they may not be filled identically Updated definitions of summary products, including replace D2400 with SINDEX and add BD920 Updated nomenclature of MRDRs to include tile number Deleted UR CDR6 and RA CDR4 which aren't being generated | All |
| 11/29/2010 | Added description of LDR data set Added descriptions of limb scans and hyperspectral survey Updated definition of MTRDRs and associated browse products Updated archive data volume estimates Updated descriptions of procedures to represent actual flight processes Updated calibration summary in Appendix Replaced sample labels with current formats Updated description of summary products to include OLINDEX2 | All |
| 2/29/2012 | Added description of TRR3 data filtering | All |

TBD ITEMS

| Section | Description |
|---------|---|
| All | Add appendix explaining usage of ADRs Update calibration description to TRRs Add description of filtering of TRR3 I/F files |

CONTENTS

| | |
|--|-----------|
| 1. INTRODUCTION | 12 |
| 1.1 Purpose and Scope | 12 |
| 1.2 Contents | 13 |
| 1.3 Applicable Documents and Constraints | 13 |
| 1.4 Relationships with Other Interfaces | 14 |
| 2. DATA PRODUCT CHARACTERISTICS AND ENVIRONMENT | 14 |
| 2.1 Instrument Overview | 14 |
| 2.1.1 Hardware overview. | 15 |
| 2.1.2 Key variables in observing modes | 17 |
| 2.1.3 Summary of orbital observing modes..... | 19 |
| 2.1.4 Details of observing modes..... | 22 |
| 2.2 Data Product Overview | 28 |
| 2.2.1 EDRs..... | 29 |
| 2.2.2 CDRs..... | 30 |
| 2.2.3 ADRs..... | 30 |
| 2.2.4 TRDRs | 30 |
| 2.2.5 DDRs..... | 30 |
| 2.2.6 LDRs | 31 |
| 2.2.7 MRDRs..... | 31 |
| 2.2.8 MTRDRs..... | 31 |
| 2.2.9 SPICE Files..... | 31 |
| 2.2.10 Browse Products..... | 31 |
| 2.2.11 Extra Products..... | 32 |
| 2.3 Data Processing | 34 |
| 2.3.1 Data Processing Level | 34 |
| 2.3.2 Data Product Generation | 34 |
| 2.3.3 Data Flow and Delivery | 37 |
| 2.3.4 Labeling and Identification | 38 |
| 2.4 Standards Used in Generating Data Products..... | 53 |
| 2.4.1 PDS Standards | 53 |
| 2.4.2 Time Standards..... | 53 |
| 2.4.3 Coordinate Systems..... | 54 |
| 2.5 Data Validation..... | 54 |
| 2.5.1 EDR level | 54 |
| 2.5.2 EDR to RDR level | 54 |
| 2.5.3 RDR level | 55 |
| 3. DETAILED DATA PRODUCT SPECIFICATIONS..... | 57 |
| 3.1 EDR..... | 57 |
| 3.1.1 Data Product Structure and Organization | 57 |
| 3.1.2 Label Description | 74 |
| 3.2 DDR..... | 76 |
| 3.2.1 Data Product Structure and Organization | 76 |
| 3.2.2 Label Description | 78 |
| 3.3 LDR | 79 |
| 3.3.1 Data Product Structure and Organization | 79 |
| 3.3.2 Label Description | 80 |
| 3.4 Targeted RDR..... | 81 |
| 3.4.1 Data Product Structure and Organization | 81 |
| 3.4.2 Label Description | 85 |

| | |
|--|------------|
| 3.5 Map-Projected Multispectral RDR | 90 |
| 3.5.1 Data Product Structure and Organization | 90 |
| 3.5.2 Map projection standards | 91 |
| 3.5.3 Label Description | 93 |
| 3.6 Map-Projected Targeted RDR | 94 |
| 3.6.1 Data Product Structure and Organization | 94 |
| 3.6.2 Label Description | 95 |
| 3.7 Level-6 CDR | 99 |
| 3.7.1 Data Product Structure and Organization | 99 |
| 3.7.2 Label Description | 99 |
| 3.8 Level-4 CDR | 102 |
| 3.8.1 Data Product Structure and Organization | 102 |
| 3.8.2 Label Description | 102 |
| 3.9 ADR | 106 |
| 3.10 CRISM-Generated SPICE Files | 108 |
| 3.11 Browse Products | 109 |
| 3.11.1 EDR Browse Products | 109 |
| 3.11.2 MTRDR Browse Products | 110 |
| 3.11.3 MRDR Browse Products | 113 |
| 3.12 Extra Products | 113 |
| 4. APPLICABLE SOFTWARE | 116 |
| 4.1 Utility Programs | 116 |
| 4.2 Applicable PDS Software Tools | 117 |
| APPENDIX A. EDR LABEL | 118 |
| APPENDIX B. DDR LABEL | 121 |
| APPENDIX C1. TRDR LABEL (RADIANCE IMAGE + LISTFILE) | 123 |
| APPENDIX C2. TRDR LABEL (I/F IMAGE) | 127 |
| APPENDIX D1. MRDR LABEL (I/F IMAGE) | 131 |
| APPENDIX D2. MRDR LABEL (DERIVED DATA IMAGE) | 133 |
| APPENDIX D3. MRDR LABEL (SUMMARY PRODUCT IMAGE) | 135 |
| APPENDIX D4. MRDR LABEL (WAVELENGTH FILE) | 138 |
| APPENDIX E. MTRDR LABEL (CORRECTED I/F FILE) | 140 |
| APPENDIX F. LEVEL 6 CDR LABEL | 142 |
| APPENDIX G. LEVEL 4 CDR LABEL | 144 |
| APPENDIX H. LDR LABEL | 147 |
| APPENDIX I1. EDR BROWSE PRODUCT HTML FILE LABEL | 149 |
| APPENDIX I2. EDR BROWSE PRODUCT PNG FILE LABEL | 150 |
| APPENDIX J. MTRDR BROWSE PRODUCT 'TRU' PNG FILE LABEL | 152 |
| APPENDIX K. MRDR BROWSE PRODUCT 'TRU' PNG FILE LABEL | 155 |
| APPENDIX L. DATA PROCESSING DETAILS | 157 |
| 1. CALIBRATION OVERVIEW | 157 |
| 1.1 Collection of calibration data in flight | 157 |
| 1.2 Reduction of flight target image data using calibration data | 157 |
| 2. CALIBRATION DESCRIPTION | 159 |
| 2.1 Overview of calibration equation | 159 |
| 2.2 Uncompression and conversion to 14-bit DN | 162 |

| | |
|--|-----|
| 2.3 Remove bias | 163 |
| 2.4 Remove detector quadrant electronics ghost | 166 |
| 2.5 Flag saturated pixels | 167 |
| 2.6 Apply a priori bad pixel mask to all images | 168 |
| 2.7 Detector average nonlinearity correction | 171 |
| 2.8 Divide by integration time to get counts/second | 172 |
| 2.9 Background subtraction | 173 |
| 2.10 Scattered light correction | 174 |
| 2.11 Subtraction of second-order stray light | 179 |
| 2.12 Correction of instrument responsivity for detector temperature | 180 |
| 2.13 Apply binning and detector masks to responsivity | 182 |
| 2.14 Calculate scene radiance at instrument aperture and divide by flat field | 183 |
| 2.15 Ex post facto bad pixel removal and apply detector masks | 183 |
| 2.16 Measurement uncertainties due to nonrepeatability | 185 |
| 2.17 Processing from radiance to I/F | 186 |
| 3. ADDITIONAL MINI-PIPELINES FOR GENERATING CALIBRATION TABLES FROM FLIGHT CALIBRATION DATA | 187 |
| 3.1 Calculation of IR bias images | 187 |
| 3.2 Mini-pipeline for IR background and VNIR bias images (darks) | 189 |
| 3.3 Generation of the flat fields | 190 |
| 3.4 Calculating sphere radiance including sphere temperature and shutter mirror position | 191 |
| 3.5 Calculation of instrument responsivity from sphere radiance | 194 |
| 4. IMPLEMENTATION IN PIPE | 197 |
| 4.1 Data flow of flight calibration and scene EDRs to flight CDR4s and TRDRs | 197 |
| 4.2 Logic for choosing specific flight calibration EDRs to use with a given scene EDR | 199 |
| APPENDIX M. TEMPERATURE SENSOR AND HEATER LOCATIONS | 204 |
| APPENDIX N. DESCRIPTION OF TRR3 FILTERING | 210 |
| APPENDIX O. DESCRIPTION AND USAGE OF ADRS | 221 |

FIGURES AND TABLES

| | |
|--|-----|
| DOCUMENT CHANGE LOG | 2 |
| CONTENTS | 6 |
| FIGURES AND TABLES | 9 |
| ACRONYMS | 10 |
| Table 2-1 CRISM Investigation Objectives and Implementation | 14 |
| Figure 2-2a. Photographs of CRISM OSU, DPU, GME | 16 |
| Figure 2-2b. CRISM block diagram. | 16 |
| Figure 2-2c. CRISM Optical Sensor Unit (OSU) configuration. | 16 |
| Figure 2-2d. CRISM optical diagram. | 17 |
| Figure 2-3. Sample VNIR and IR image frames (viewing internal integrating sphere). | 17 |
| Table 2-4. CRISM Observing Modes | 21 |
| Figure 2-5. Elements to a CRISM targeted observation. | 22 |
| Table 2-6. Translation of different observation classes into EDRs. | 26 |
| Figure 2-7. Translation of 12-bit DN's into 8-bit DN's using LUTs. | 28 |
| Table 2-8. Definitions of CRISM data products. | 32 |
| Figure 2-9. Sequential processing of EDRs to yield RDRs of Mars data. | 33 |
| Figure 2-10. Tiling scheme for the map-projected multispectral survey. | 33 |
| Table 2-11. Processing Levels for Science Data Sets | 34 |
| Table 2-12. Contents of each type of CRISM observation | 36 |
| Table 2-13. Representative CRISM data acquisition during 1 Mars year. | 37 |
| Table 2-14. Nomenclature of Observation Tracking Tables | 53 |
| Figure 3-1. Contents of a CRISM Experiment Data Record (EDR). | 58 |
| Table 3-2. Items in housekeeping list file | 59 |
| Table 3-3. Bit mapping of scan motor status word | 71 |
| Table 3-4. Bit mapping of scan motor control word | 71 |
| Table 3-5. Alarms coded in housekeeping | 72 |
| Table 3-6. Alarms for monitored housekeeping and responses | 73 |
| Table 3-7. CRISM-specific values for EDR label keywords | 74 |
| Figure 3-8. Contents of a CRISM Derived Data Record (DDR). | 78 |
| Table 3-9. CRISM-specific values for DDR label keywords | 79 |
| Table 3-10. CRISM-specific values for LDR label keywords | 81 |
| Figure 3-11. Contents of a CRISM Reduced Data Record for a single observation (TRDR). | 83 |
| Table 3-12. Formulation of parameters for summary products | 83 |
| Table 3-13. CRISM-specific values for TRDR label keywords | 86 |
| Figure 3-14. Contents of a CRISM Reduced Data Record for a multispectral map tile (MRDR). | 93 |
| Table 3-15. CRISM-specific values for MRDR label keywords | 94 |
| Figure 3-16. Contents of a CRISM Reduced Data Record for a MTRDR | 95 |
| Table 3-17. CRISM-specific values for MTRDR label keywords | 95 |
| Figure 3-18. Contents of a CRISM Calibration Data Record (CDR). | 99 |
| Table 3-19. Descriptions of calibration-related level-6 CDRs | 100 |
| Table 3-20. Descriptions of operational level-6 CDRs | 101 |
| Table 3-21. Descriptions of level-4 CDRs | 102 |
| Table 3-22. CRISM-specific values for CDR label keywords | 104 |
| Table 3-23. LUT for atmospheric opacity (ADR type = CL) | 107 |
| Table 3-24. LUT for predicted atmospheric / photometric / thermal correction (ADR type = AC) | 107 |
| Table 3-25. LUT for local surface temperature (ADR type = TE) | 107 |
| Figure 3-26. Example EDR browse product | 109 |
| Table 3-27. Contents of OBS_ID Table. | 113 |

ACRONYMS

| | |
|---------|---|
| A/D | Analog to Digital Converter |
| ADC | Analog to Digital Converter |
| ADR | Ancillary Data Record |
| APL | The Johns Hopkins University Applied Physics Laboratory |
| CAT | CRISM Analysis Tool |
| CRISM | Compact Reconnaissance Imaging Spectrometer for Mars |
| CDR | Calibration Data Record |
| CSV | Comma-Separated Value (a format for organizing tabular data in ASCII format) |
| CTX | Context Imager (on Mars Reconnaissance Orbiter) |
| DAC | Digital to Analog Converter |
| DDR | Derived Data Record |
| DPCM | Differential Pulse-Code Modulation (compression) |
| DPU | CRISM Data Processing Unit |
| EDR | Experiment Data Record |
| EPF | Emission Phase Function |
| FOV | Field-of-View |
| FPU | Focal Plane Unit |
| Gb | Gigabit (10^9 bits) |
| GME | CRISM Gimbal Motor Electronics |
| HIRISE | High-Resolution Imaging Science Experiment (on Mars Reconnaissance Orbiter) |
| HOP | High-output Paraffin actuator; on CRISM a HOP deploys the cover |
| I/F | Intensity divided by flux, or the ratio of radiance to incident solar radiation |
| IR | Infrared |
| JHU/APL | The Johns Hopkins University Applied Physics Laboratory |
| JPL | Jet Propulsion Laboratory |
| LDR | Limb Data Record |
| LED | Light-emitting diode |
| LOS | Line-of Sight |
| LS | Solar longitude; a measure of Mars' motion in its orbit, in degrees, since northern hemisphere vernal equinox |
| LUT | Look-up Table |
| LVDS | Low-Voltage Differential Signal |
| MOC | Mars Orbiter Camera (on Mars Global Surveyor) |
| MOLA | Mars Orbiter Laser Altimeter (on Mars Global Surveyor) |
| MRDR | Map-projected Reduced Data Record |
| MRO | Mars Reconnaissance Orbiter |
| MTRDR | Map-projected Targeted Reduced Data Record |
| MUX | Multiplexed or multiplexer |
| OMEGA | Observatoire pour la Minéralogie, l'Eau, les Glaces et l'Activité (on Mars Express) |
| OSU | CRISM Optical Sensor Unit |
| PDS | Planetary Data System |
| RDR | Reduced Data Record |
| SIS | Software Interface Specification |

| | |
|--------|---|
| SOC | Science Operations Center |
| SNR | Signal-to-noise ratio |
| SPICE | SPacecraft, Instrument, Camera, and Events; a set of data formats for spacecraft ephemeris, attitude, and instrument pointing |
| Tb | Terabit (10^{12} bits) |
| TBD | To Be Determined |
| TES | Thermal Emission Spectrometer (on Mars Global Surveyor) |
| THEMIS | Thermal Emission Imaging System (on Mars Odyssey) |
| TRDR | Targeted Reduced Data Record |
| VNIR | Visible / near-infrared |

1. INTRODUCTION

1.1 Purpose and Scope

The purpose of this Data Product Software Interface Specification (SIS) is to provide users of the data products from the Compact Reconnaissance Imaging Spectrometer for Mars (CRISM) with:

- a detailed description of the products
- a guide to interpreting and using their contents
- a description of how they were generated, including data sources and destinations
- a description of how raw data can be calibrated, including what archived data products are necessary and the procedures to use

Although this is beyond the scope of the strictest definition of the contents of a Planetary Data System (PDS) SIS, this approach is adopted because CRISM is a sophisticated instrument which will generate an extremely large data set that include multiple observing modes. The authors believe that detailed information is required for users to correctly utilize the data products described herein.

There are ten CRISM data products defined in this SIS document. These include:

- 1) Experiment Data Record (EDR) consisting of raw, uncalibrated CRISM spectra;
- 2) Derived Data Record (DDR) containing pointing and other ancillary information for observations pointed at Mars' surface;
- 3) Limb Data Record (LDR) containing pointing and other ancillary information for observations pointed at Mars' limb;
- 4) Targeted Reduced Data Record (TRDR), which is a radiometrically calibrated EDR;
- 5 and 6) two types of Calibration Data Records (CDRs), which are files used to generate radiance or radiance/solar irradiance (I/F) values in a TRDR from an EDR;
- 7) Ancillary Data Records (ADRs), which are files used to correct I/F values for atmospheric, photometric, or thermal effects, and which document the data set
- 8) Map-Projected Multispectral Reduced Data Record (MRDR);
- 9) Map-Projected Targeted Reduced Data Record (MTRDR); and
- 10) browse products for EDRs, MTRDRs, and MRDRs.

This SIS is intended to provide enough information to enable users to read and understand the data products. The users for whom this SIS is intended are the scientists who will analyze the data, including those associated with the Mars Reconnaissance Orbiter Project and those in the general planetary science community.

1.2 Contents

This Data Product SIS describes how data products generated by the CRISM are processed, formatted, labeled, and uniquely identified. The document details standards used in generating the products and software that may be used to access the product. Data product structure and organization is described in sufficient detail to enable a user to read the product. Finally, an example of each product label is provided.

The CRISM investigation team has also delivered, in parallel with flight data, a spectral library of analog materials that is useful to interpreting flight data. That is described in:

1. CRISM Spectral Library Software Interface Specification, S. Slavney, rev. 0, Nov. 24, 2003.

1.3 Applicable Documents and Constraints

This Data Product SIS is responsive to the following Mars Reconnaissance Orbiter documents:

2. Mars Exploration Program Data Management Plan, R. E. Arvidson and S. Slavney, Rev. 2, Nov. 2, 2000.
3. Mars Reconnaissance Orbiter Project Data Archive Generation, Validation and Transfer Plan, R. E. Arvidson, S. Noland and S. Slavney, Jan. 26, 2006.
4. Mars Reconnaissance Orbiter (MRO) Compact Reconnaissance Imager and Spectrometer for Mars (CRISM) Experiment Operations Plan, S. L Murchie, version 1.7, June 2005.
5. CRISM Archive Volume Software Interface Specification, S. L Murchie, E. Guinness, and S. Slavney, version 1.2.7, May 6, 2011.

This SIS is also consistent with the following Planetary Data System documents:

6. Planetary Data System Data Preparation Workbook, Version 3.1, Jet Propulsion Laboratory (JPL) D-7669, Part 1, February 1, 1995.
7. Planetary Data System Data Standards Reference, Version 3.6, JPL D-7669, Part 2, August 1, 2003.
8. Planetary Science Data Dictionary Document, JPL D-7116, Rev. E, August 28, 2002.

The reader is referred to the following documents for additional information:

9. Seidelmann, P. K., V. K. Abalakin, M. Bursa, M. E. Davies, C. de Bergh, J. H. Lieske, J. Oberst, J. L. Simon, E. M. Standish, P. Stooke, and P. C. Thomas, Report of the IAU/IAG working group on cartographic coordinates and rotational elements of the planets and satellites: 2000, *Celestial Mechanics and Dynamical Astronomy*, 82, 83-111, 2002.

Finally, this SIS is meant to be consistent with the contract negotiated between the Mars Reconnaissance Orbiter Project and the CRISM Principal Investigator (PI) in which reduced data records and documentation are explicitly defined as deliverable products.

1.4 Relationships with Other Interfaces

Data products described in this SIS are produced by the CRISM Science Operations Center (SOC). Changes to the SOC processing algorithms may cause changes to the data products and, thus, this SIS. The RDR products are dependent on the CRISM EDR products. As such, changes to the EDR product may affect the RDR products.

Changes in CRISM data products or this SIS may affect the design of the CRISM archive volumes.

2. DATA PRODUCT CHARACTERISTICS AND ENVIRONMENT

2.1 Instrument Overview

CRISM addresses the objectives of characterizing Martian aqueous mineralogy and crustal composition, seasonal variation in the surface and atmosphere, and identifying new targets of scientific interest using the three-pronged strategy described in Table 2-1.

Table 2-1 CRISM Investigation Objectives and Implementation

| Objective | Implementation / Measurement Strategy | Observation / Planning Design |
|---|---|--|
| Find new targets of interest: aqueous deposits, crustal composition | Target observations using previous geologic studies and results from the Thermal Emission Spectrometer (TES), Thermal Emission Imaging System (THEMIS), Mars Orbiter Camera (MOC), etc. | Target list assembled from previous studies Screened / added to using targeting basemap |
| | Use Mars Express OMEGA data to find new targets lacking morphologic or thermal IR signatures | Derived products from OMEGA included in targeting basemap |
| | Find targets below OMEGA's resolution using near-global multispectral survey at key wavelengths | 72-channel, ~200-m/pixel multispectral survey |
| Separate the surface and atmosphere Provide information on spatial/seasonal variations in aerosols, H ₂ O, CO ₂ , and ices | Observe emission phase function (EPF) at each targeted observation to quantify atmospheric effects | ±60° EPF inherent to full and half resolution targeted observations |
| | Regularly acquire global grids of EPFs to monitor seasonal variations in surface and atmospheric properties | High time-resolution (atmospheric monitoring campaign) High spatial-resolution (seasonal change campaign) |
| | Sample compositional layering and seasonal change of polar ices | Key areas targeted with full and half resolution Monitor seasonal cap with multispectral windows |
| Measure surface targets with high spatial and spectral resolutions and high signal-to-noise ratio (SNR) | Measure thousands of targets at full spectral resolution and high spatial resolution | Full and half resolution targeted observations provide coverage at 6.55 nm/channel, 15-40 m/pixel (at nadir) |
| | Measure key regions of the surface at key wavelengths at higher resolutions than multispectral survey | Multispectral windows or trips of multispectral survey provide coverage of key regions of the planet at ~100 m/pixel, including seasonal polar caps to track |

| | |
|---|--|
| | seasonal changes |
| Conduct inflight calibration of background and responsivity to provide radiometric accuracy | Radiometric calibration using integrating sphere Background calibrations using shutter are integrated with each observation |

2.1.1 Hardware overview.

The CRISM system, design, and function are illustrated in Figure 2-2. CRISM consists of three boxes: the Optical Sensor Unit (OSU) which includes the optics, gimbal, focal planes, cryocoolers and radiators, and focal plane electronics; the Gimbal Motor Electronics (GME), which commands and powers the gimbal motor and encoder and analyzes data from the encoder in a feedback loop; and the Data Processing Unit (DPU), which accepts and processes commands from the spacecraft and accepts and processes data from the OSU and communicates it to the spacecraft. The CRISM OSU has a one-time deployable cover that protects the instrument optics from contamination. The cover will be opened following MRO's aerobraking into its science orbit.

The optical and sensor assembly in the OSU consists of a visible/near-infrared (VNIR) focal plane covering 362-1053 nm at 6.55 nm/channel and a cryogenically cooled infrared (IR) focal plane covering 1002-3920 nm at 6.55 nm/channel. Each field-of-view (FOV) is approximately 605 61.5- μ rad pixels wide. On each side of the VNIR FOV and one side of the IR FOV there are detector elements not illuminated through the spectrometer slit, that measure instrument and scattered light in the spectrometer cavity simultaneously with each scene measurement (Figure 2-3). A shutter can block the FOV to interleave full-field background measurements. The shutter can also be positioned to view a closed-loop controlled integrating sphere simultaneously by each focal plane, providing radiometric response and flat-field calibration. In addition, either of two redundant lamps can illuminate each focal plane directly to measure detector non-uniformity. Each focal plane has a dedicated electronics board that provides the required clock signals and bias voltages, and digitizes the video data from the focal plane. The digitized data is transmitted through the twist capsule to the DPU. The infrared focal plane is cooled to ~110K by one of three cryocoolers (selectable by the DPU).

The scanning subsystem consists of the Gimbal Motor Electronics (GME), a high-resolution angular encoder, and the gimbal drive motor. The GME contains the motor driver circuitry, and responds to a commanded profile from the DPU. Software in the DPU implements a control algorithm, utilizing feedback information from the 20-bit encoder to maintain closed-looped control. The system accurately follows a programmed scan pattern that is carefully designed to compensate for orbital motion and to accomplish the desired scan pattern across the Martian surface.

The DPU receives unregulated 28-32 volt power from MRO and provides regulated secondary power to CRISM, receives and processes commands from the MRO, controls the CRISM subsystems, and acquires and formats CRISM science and housekeeping data that is then sent to the spacecraft solid state recorder for downlink to earth.

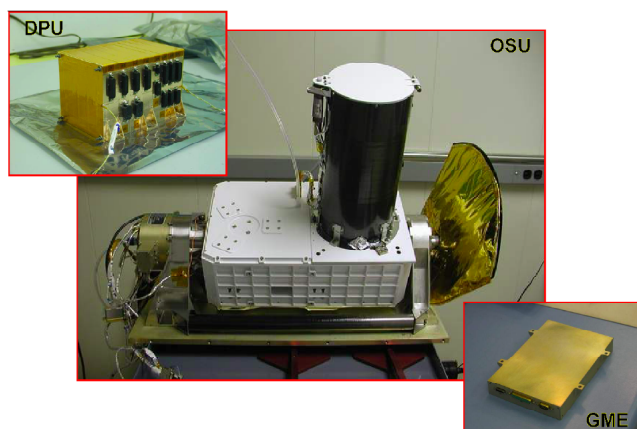


Figure 2-2a.
Photographs
of CRISM OSU,
DPU, GME.

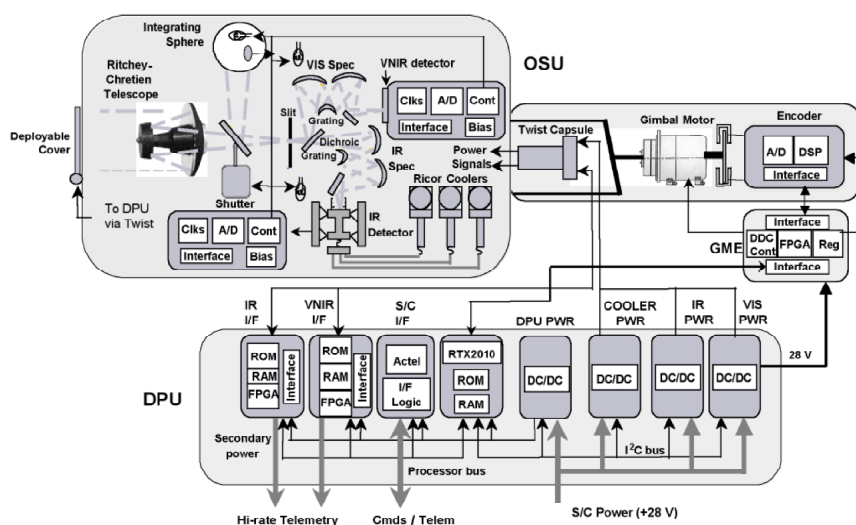


Figure 2-2b.
CRISM block
diagram.

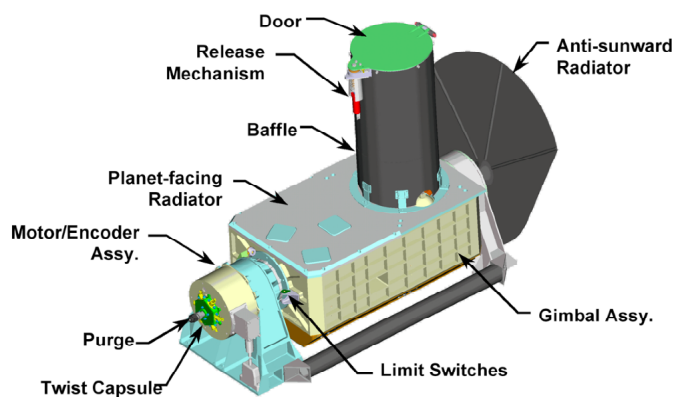


Figure 2-2c.
CRISM Optical
Sensor Unit
(OSU)
configuration.

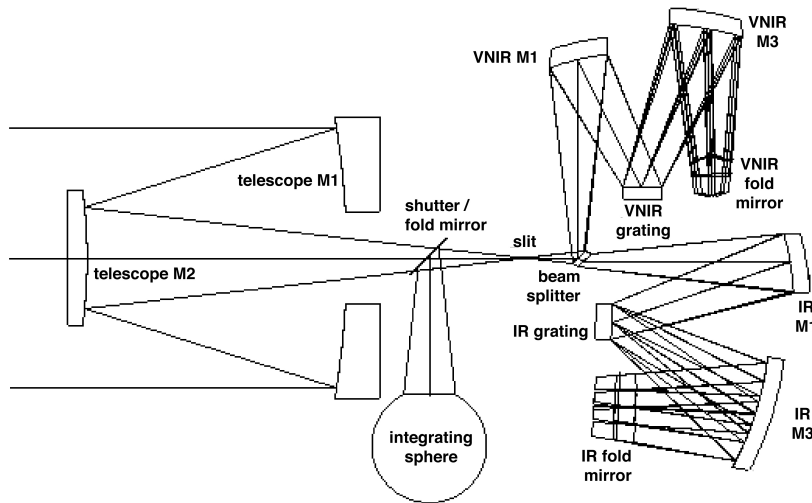
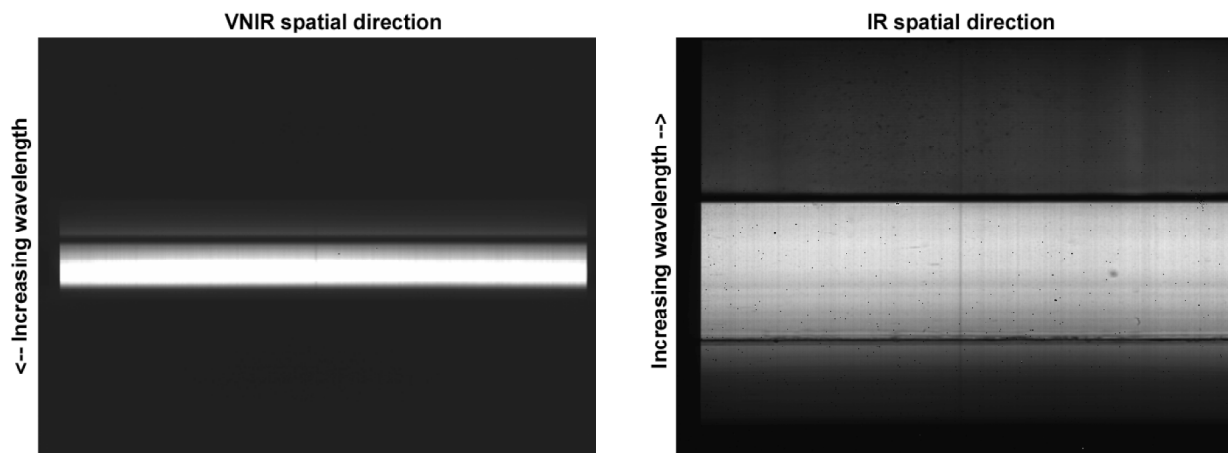


Figure 2-2d.
**CRISM optical
diagram.**



**Figure 2-3. Sample VNIR and IR image frames (viewing internal
integrating sphere).**

2.1.2 Key variables in observing modes

Key variables ("configurations") in constructing observing scenarios include the following. All are selectable separately for the VNIR and IR detectors.

- Image source. Image data may be generated using digitized output from the detector, or using one of up to seven test patterns.
- Detector row selection. All detector rows, sampling different wavelengths, having useful signal can be saved. Alternatively an arbitrary, commandable subset of rows can be saved. The number of rows with useful signal is 545, 107 in the VNIR and 438 in the IR, and these subsets of VNIR and IR detector rows are used for hyperspectral observing. Prior to 10 Dec 2006 the nominal number of rows for multispectral mode was 73, 18 in the VNIR and 55 in the IR. On 10 Dec 2006 an extra channel was added to the VNIR for calibration purposes, for a total of 19. For each detector, there are four options of channel selection to choose from rapidly by command:

hyperspectral (545 total channels), multispectral (73 total channels prior to 10 Dec 2006, 74 total channels on and after 10 Dec 2006), and two sets of expanded multispectral (84 and 92 channels prior to 10 Dec 2006, 85 and 93 channels on and after 10 Dec 2006). New options are set by uploading a data structure to the DPU. On 12 Jan 2010, the smaller of the two expanded multispectral channel selections was replaced with the largest value supportable at a 15 Hz frame rate, all 107 VNIR channels and 155 IR channels; most of the IR channels are contiguous from 1.8-2.55 μm to cover key mineral absorptions.

- Pixel binning . Pixels can be saved unbinned or binned 2x, 5x, or 10x in the spatial direction. No pixel binning in the spectral direction is supported.

- Compression. All CRISM data are read off the detector in 14-bit format and are compressed real-time in hardware. Compression options, in succession, are:

- Subtraction of an offset, on a line by line basis. Offsets are set by uploading a data structure to the DPU.

- Multiplication by a gain, on a line by line basis, with the output in 12-bit format. Gains are set by uploading a data structure to the DPU. (Raw 12-bit data are stored onground in data products as 16-bit numbers.)

- Optionally, conversion from 12 to 8 bits using one of eight look-up tables (LUTs) specified on a line by line basis. These choices are set by uploading a data structure to the DPU.

- Optionally, lossless Fast + differential pulse-code modulation (DPCM) compression

- Pointing. CRISM has two basic gimbal pointing configurations and two basic superimposed scan patterns. Pointing can be (1) fixed (nadir-pointed in the primary science orbit) or (2) dynamic, tracking a target point on the surface of Mars and taking out ground track motion. Two types of superimposed scans are supported: (1) a short, 4-second duration fixed-rate ("EPF-type") scan which superimposes a constant angular velocity scan on either of the basic pointing profiles, or (2) a long, minutes-duration fixed-rate ("target swath-type") scan.

- Frame rate . Frame rates of 1, 3.75, 5, 15, and 30 Hz are supported. The 1 Hz frame rate is used for hyperspectral measurements of the onboard integrating sphere, because the long exposures possible at 1 Hz are needed for appreciable SNR at the shortest wavelengths. 3.75 Hz is used for hyperspectral measurements of Mars; this is the highest frame rate at which the DPU electronics support onboard compression options over the range of wavelengths imaged onto the detectors with useful SNR. 15 and 30 Hz frame rates are used for nadir-pointed multispectral measurements that return only selected wavelengths. The 5 Hz frame rate is not planned for use in flight, because at that rate the electronics do not support compression of a hyperspectral wavelength selection, and it would produce excessive along-track smear in a nadir-pointed observation.

- Integration time. Integration times are in increments of 1/480th of the inverse of the frame rate. At 1 Hz, for example, available integration times are 1/480th sec, 2/480th sec...480/480th , and at 15 Hz, 1/7200th sec, 2/7200th sec...480/7200th sec.

- Calibration lamps. Radiometric calibration is provided inflight by either of a pair of lamps that directly illuminates each focal plane with "white" light, and in two lamps in the integrating sphere. All focal plane lamp settings are open-loop with 4095 possible levels, meaning that current is commanded directly. For the integrating sphere, closed loop control is available at

4095 levels. For closed loop control, the setting refers to output from a photodiode viewing the interior of the integrating sphere; current is adjusted dynamically to attain the commanded photodiode output. In flight, all regular radiometric calibrations have used the integrating sphere running under closed-loop control, and specifically the IR-controlled lamp which provides more uniform illumination. The focal plane lamps were used for restricted cruise tests of linearity of the detectors' response.

- Shutter position. Open, closed, or viewing the integrating sphere. The shutter is actually commandable directly to position 0 through 32. In software, open=3, sphere=17, closed=32. NOTE: during integration and testing, it was discovered that at positions ≤ 2 the hinge end of the shutter is directly illuminated and creates scattered light. Position 3 does not cause this effect, but the other end of the shutter slightly vignettes incoming light.

2.1.3 Summary of orbital observing modes

During the primary science orbit, CRISM uses combinations of instrument settings to acquire several basic types of observations as described in Table 2-4. Targeted mode (Figure 2-5) is intended to provide high-resolution hyperspectral measurements of the surface, with accompanying measurements of atmospheric opacity and trace gases. As a target is over flown it is covered by a slow, continuous scan of the field-of-view, taking out most ground track motion. During this operation, the instrument gimbal covers angles $\pm 35^\circ$. This central scan is bracketed by five incoming and five outgoing $\pm 0.3^\circ$ scans centered on the center point of the target, at 5° increments in gimbal position over the range of 40° - 60° in gimbal angle. The total of eleven scans provides an 11-angle emission phase function¹ (EPF) that contains information needed for photometric and atmospheric correction of the central targeted scan. Beginning in August 2010, aging of the gimbal led to restriction of the range of gimbal motion, eliminating the 5 incoming $\pm 0.3^\circ$ scans.

In atmospheric EPF mode, the central scan is replaced by 1 or 3 $\pm 0.3^\circ$ scans covering a geographically restricted region. The main purpose is recovery of an 11- or 13-position EPF to estimate atmospheric opacity and collect additional hyperspectral measurements of trace gases. Atmospheric EPF mode is used every $\sim 9^\circ$ of solar longitude (Ls; a measure of Martian season, where 0° is northern hemisphere vernal equinox) to acquire a low spatial density global grid of EPFs to track seasonal variations in surface and atmospheric properties. The grid is covered in 1 solar day. Every $\sim 36^\circ$ of Ls, a cluster of grids is taken on non-contiguous days to provide a higher spatial density grid to monitor seasonal change in surface material spectral properties. The grids are overlain on a best-effort basis; repeat coverage to ± 25 km can be accomplished from careful selection of the orbits along which the EPFs are taken. Restrictions on gimbal motion beginning in August 2010 leave an 8-position EPF measurement in this type of observation.

¹ An emission phase function is a set of observations of a location on the Martian surface at near-constant solar incidence angle but variable emission angle (and thus phase angle). Because the atmospheric path length varies while illumination is held constant, an EPF enables simultaneous solution for atmospheric and surface components to radiance using estimated surface and atmospheric wavelength-dependent scattering functions. The EPF geometries envelope that of the central scan, so the estimated atmospheric and surface components of its measured radiance can be separated.

Beginning in late 2008, approximately every 2 months the grids of EPFs have been supplemented with a cluster of two or more orbits of limb-scan measurements, located at longitudes nearest to Nili Fossae and Ascraeus Mons. In this type of observation the spacecraft is pitched to allow the gimbal access to the limb, and gimbal motion is used to scan the field-of-view (FOV) from below the horizon to at least 120 km above it. Over each orbit ~15 scans are collected over the day side of Mars, and several additional scans past the ascending and descending terminators look for airglow over the polar regions.

In multispectral mode, the instrument is fixed pointing at nadir, and selected wavelengths are measured at spatial resolution that is reduced by binning pixels in the spatial direction, to manage data volume. This mode of operation is intended to search for new targets of interest and to provide moderate spatial and spectral resolution contextual mapping of surface composition. Two modes of multispectral operation were used initially: ~200 m/pixel "multispectral survey" mode which is designed to accomplish coverage rapidly, and ~100 m/pixel "multispectral window" mode which is intended for higher spatial resolution in key areas.

Beginning 12 January 2010, ~200 m/pixel "hyperspectral survey" mode using an expanded set of detector rows was initiated, to provide a contextual hyperspectral mapping mode for target-rich regions of the planet.

In optical depth tracking mode, the instrument is fixed pointing at nadir, and a short burst of data is taken periodically with CRISM's full wavelength selection, but at spatial resolution that is reduced by binning pixels in the spatial direction to manage data volume. This mode of operation is intended to supplement EPFs with high spatial density measurements with full hyperspectral capability, to provide additional monitoring of trace gases.

In addition, radiometric calibrations using the onboard integrated sphere and measurements of detector bias are taken at least daily. Background measurements are integrated with each type of observation.

On a monthly basis, the flat-field response is assessed by imaging bland regions of Mars.

Table 2-4. **CRISM Observing Modes**

| Mode | Pointing | Description | Coverage |
|-----------------------------------|--|--|---|
| Targeted (hyperspectral) | Tracking as shown, once per target | Full resolution (FRT) Spatial pixels unbinned for target - 18 m/pixel @300 km, 10x binned for EPF | ~6500 per Mars year |
| | | Half resolution short (HRS) Spatial pixels 2x binned for target - 36 m/pixel @300 km, 10x binned for EPF; same swath length as above | |
| | | Half resolution long (HRL) Spatial pixels 2x binned for target - 36 m/pixel @300 km, 10x binned for EPF; twice swath length as above | |
| | | EPFs Spatial pixels 10x binned (~200 m/pixel @300 km) | |
| Atmospheric (hyperspectral) | Tracking as shown but only center of target measured | | Lat./lon. grids every ~9° of Ls |
| | Nadir-pointed | Tracking Optical Depth (TODs) Spatial pixels 10x binned (~200 m/pixel @300 km) | Between other scheduled observations |
| | Limb scans | Limb scan measurements (LMBs) Spatial pixels 10x binned; ~200 m vertical sampling) | 2 orbits every 2 months |
| Mapping (selected wavelengths) | Nadir-pointed | Multispectral survey 73/74 or 94/95 selected channels, spatial pixels 10x binned (~200 m/pixel @300 km) | ~80% of Mars |
| | | Multispectral windows 73/74 or 94/95 selected channels, spatial pixels 5x binned (~100 m/pixel @300 km) | Select areas plus sampling of seasonal variation at polar cap |
| | | Hyperspectral survey 262 channels, spatial pixels 10x binned (~200 m/pixel @300 km) | Select areas plus sampling of seasonal variation at polar cap |
| | | | |
| Radiometric Calibration | - | Observations of onboard integrating sphere | Daily |
| Bias Calibration | - | Dark observations at multiple exposure times | Daily |
| Flat-Field Calibration | Nadir-pointed | Observations of bland regions of Mars | Every month |

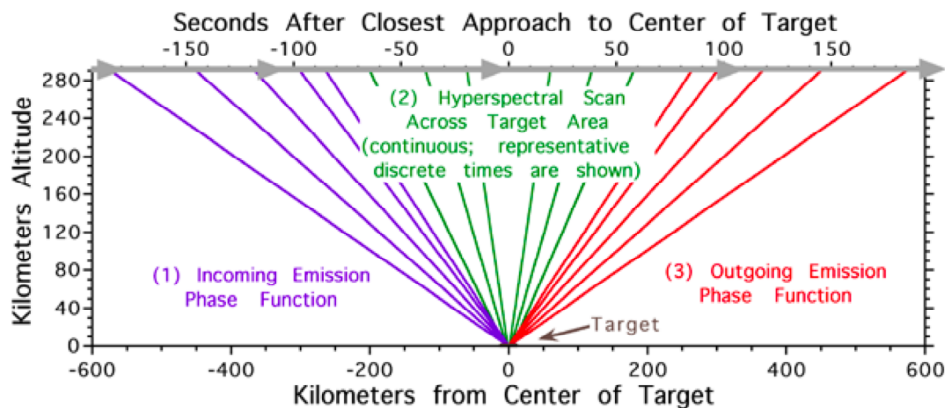


Figure 2-5. Elements to a CRISM targeted observation.

2.1.4 Details of observing modes

Commanding of CRISM uses onboard macros, sequences of commands that configure the instrument for a particular operation, acquire data, and then return the instrument to a reference configuration. Up to 255 macros are stored onboard, and the data acquired by part or all of one macro is the fundamental data unit that populates a single EDR.

CRISM science observations use nine basic sequences of macros that translate into different sequences of EDRs (Table 2-6). All of the sequences use an onboard target list for autonomous pointing and time of observations by the spacecraft guidance and controls system. A target ID² is used to uniquely identify a target on this list.

2.1.4.1 Gimbaled Observations: Targeted, EPF, and limb scan measurements

Four of the macro sequences are intended for execution while the gimbal is tracking a target, and superimposing 11 slow scans: Full resolution targeted observation, half resolution (long or short) targeted observation, and atmospheric survey EPF. All follow the same basic outline. The gimbal is first set to +60° to begin the scan (+30° beginning in August 2010), which then starts at the commanded time. During approach to the target, the scan profile is designed to slowly sweep the optical line-of-sight (LOS) back and forth across the target. Thus, instead of holding the target still within the FOV, short $\pm 0.3^\circ$ scans are superimposed (part 1 in Figure 2-5, only prior to August 2010). These short scans are called EPF scans. During target over-flight (+35° to -35° gimbal angle; part 2 in Figure 2-5), the gimbal takes a much longer sweep across the target. It is this long central scan that differentiates the classes of observations. The incoming EPF sequence is repeated outgoing, except in reverse order (part 3 in Figure 2-5). Four "dark" measurements of instrument background are taken, marking the start and end of each group of EPF scans, effectively bracketing the incoming and outgoing EPF scans and the central scan.

² MRO autonomously determines spacecraft attitude and time to execute a CRISM observation. The inputs include latitude, longitude, and elevation of the target and the command macro sequence and gimbal profile to signal to CRISM to execute. Each observation is given a unique tag or "target ID" to identify it. On MRO this nomenclature is diagnostic of a particular mode of targeting so it is preserved in this SIS. However in PDS data product labels it is replaced by the term "observation ID" and is equivalent to it.

The character of the central scan is what differentiates the four types of gimbaled science observations:

A full resolution targeted measurement utilizes CRISM's full resolution capabilities, at the expense of a relatively large data volume. The gimbal is first moved to the starting position of the central scan, which depends on the scan's length, scans at a rate of 1 pixel (approximated as 60 μ rad) per integration time, and crosses the target at mid-scan. The number of integrations is selected to mostly occupy the range of gimbal angles between $\pm 35^\circ$. Depending on the altitude above a particular target, one of several choices of macros is used to mostly occupy but not overfill this gimbal range, and a corresponding gimbal setup macro is used. The data are taken without spatial pixel binning, and accompanying dark data are correspondingly taken without pixel binning. However to conserve data volume, the EPF scans are taken with 10x pixel binning; the gimbal scan rate for the EPFs yields approximately square pixels projected onto the surface.

A half resolution long targeted measurement covers a larger area, but at half the spatial resolution. It is intended for targets for which areal coverage is more important than the highest possible resolution. The LOS is scanned at a rate of 2 pixels (120 μ rad) per integration time, and sufficient integrations are executed to mostly occupy the range of gimbal angles between $\pm 35^\circ$. Depending on the altitude above a particular target, one of several choices of macros is used to mostly occupy but not overfill this gimbal range, and the corresponding gimbal setup macro is used. The duration of the scan is the same as for a full resolution targeted measurement taken from the same altitude. The data are taken with 2x spatial pixel binning; the higher scan rate yields approximately square pixel footprints projected onto the planet surface. The area covered by the central scan is approximately twice that as for a full resolution targeted measurement. The dark data are correspondingly taken with 2x pixel binning. However to conserve data volume, the EPF scans are taken with 10x pixel binning; the gimbal scan rate yields approximately square pixels projected onto the surface.

A half resolution short targeted measurement is a lower data volume alternative to the two types of targeted observations just described, intended to provide flexibility in covering more targets. The LOS is scanned at a rate of 2 pixels (120 μ rad) per integration time, and sufficient integrations are executed to occupy approximately half the range of gimbal angles between $\pm 35^\circ$. Depending on the altitude above a particular target, one of several choices of macros is used, and the corresponding gimbal setup macro is used. The duration of data collection over the central scan is half that of a full resolution targeted measurement taken from the same altitude. The data are taken with 2x spatial pixel binning; the higher scan rate yields approximately square pixel footprints projected onto the planet surface. The area covered by the central scan is approximately the same as that as for a full resolution targeted measurement. The dark data are correspondingly taken with 2x pixel binning. However to conserve data volume, the EPF scans are taken with 10x pixel binning; the gimbal scan rate yield approximately square pixels projected onto the surface.

In an EPF measurement, the central scan is replaced with 1 or 3 EPF scans. The EPFs and dark data are all taken with 10x pixel binning. An EPF measurement is intended to characterize the atmosphere or the average surface properties of a kilometers-sized area, as a part of tracking seasonal changes.

In a limb scan measurement, a 16° spacecraft pitch puts the limb just inside the gimbal range. Images are binned spatially as with EPF measurements, but the FOV is scanned across the limb at a rate of 1 pixel per integration time to maximize vertical sampling. Dark measurements are located between each measurement of the limb.

2.1.4.2 *Nadir observations: Multispectral and hyperspectral survey, multispectral windows, and TODs*

The multispectral survey is intended to map large areas Mars Odyssey/THEMIS-IR scale of resolution, for two purposes: (a) to find sites for targeted measurements, or (b) to characterize composition over large, contiguous areas. This type of observation does not use a scan profile, but is nadir-pointed and measures selected wavelengths at elevated frame rates. The basic configuration is a repeating sequence of alternating Mars-viewing and background measurement macros. The Mars-viewing periods are constrained to be in blocks of 3 minutes so that adequate interpolation of background is possible. CRISM spends most of its observing time in this mode.

There are two versions of multispectral survey, one in which data are retained in 12-bit form (MSP), and one in which the data are converted from 12 to 8 bits using a variety of LUTs that can be specified by detector row to provide a least-information-loss choice for any given wavelength (MSS). In Mars orbit only the 12-bit version has been used.

Multispectral survey data and accompanying background calibrations are taken in 10x pixel binning mode, with 73/74 or 94/95 channels selected (before or after 6 Dec 2006). Dark and Mars data are all taken at 15 Hz, yielding 200-m effective pixels.

The hyperspectral survey is an augmentation of the multispectral survey, with the increased density of wavelength sampling providing capability to separate subtly different spectral signatures and to provide improved capability to detect and map carbonate absorptions. It is intended to map regions rich in mineral diversity where contiguous coverage by targeted observations is impractical over the lifetime of MRO. As with multispectral survey, the basic configuration is a repeating sequence of alternating Mars-viewing and background measurement macros. The data are always taken in 12-bit format. Scene data and accompanying background calibrations are taken in 10x pixel binning mode at 15 Hz frame rate, yielding 200-m effective pixels.

Multispectral windows resemble the above multispectral survey, except that they are taken at 30 Hz with 5x pixel binning, yielding 100-m effective pixels projected on Mars. In practice they were used mainly as "ride-along" observations: if a High-Resolution Imaging Science Experiment (HiRISE) or Context Imager (CTX) measurement was not coordinated with a CRISM targeted measurement, then a 15-second duration multispectral window measurement was commonly executed, with the window centered on the center of the HiRISE or CTX target. This assured that observations by either of those instruments are accompanied by at least a minimal CRISM observation. The data were always taken in 12-bit format. Multispectral windows were discontinued in 2007; subsequently strips of multispectral or hyperspectral survey data have been used for the same purpose.

Tracking optical depth measurements (TODs) resemble the multispectral survey, except that they are taken with all wavelengths in brief bursts every approximately 48 seconds, yielding 10 x 10 km footprints every 2° of latitude. These data are always taken in 12-bit format. TODs are

designed to fill time between other observations to maintain a high spatial density of sampling of atmospheric properties.

2.1.4.3 *Other calibrations*

Radiometric calibration is performed at least daily. A radiometric calibration consists of a set of sphere measurements (with the sphere operated closed-loop) with bracketing measurements of the ambient background with the shutter viewing the darkened sphere. These data are used to recover radiometric responsivity.

Bias calibration is performed at least daily. A bias calibration consists of a set of shutter-closed measurements at each frame rate, at 4-5 integration times per frame rate. These data are used to recover detector bias, i.e., the offset image with zero scene radiance or thermal background.

Flat-field calibration is performed at months. A flat-field calibration consists of a set of of a bland region of Mars with bracketing background measurements. These data are used to recover non-uniformity of the VNIR detector. (The integrating sphere provides sufficient signal for this to be measured in the IR, but in the VNIR, at wavelengths <600 nm there is insufficient signal at a single detector element to determine non-uniformity at the desired accuracy of 0.001.)

Table 2-6. Translation of different observation classes into EDRs.

| Full resolution targeted observation (3.75 Hz) | Half resolution (long or short) targeted observation (3.75 Hz) | Atmospheric survey EPF (3.75 Hz) |
|---|---|--|
| full spatial resolution background measurement with shutter closed | half spatial resolution background measurement with shutter closed | reduced spatial resolution (10x-pixel-binned) background measurement with shutter closed |
| reduced spatial resolution (10x-pixel-binned) measurement of Mars for EPF (5 times) | reduced spatial resolution (10x-pixel-binned) measurement of Mars for EPF (5 times) | reduced spatial resolution (10x-pixel-binned) measurement of Mars for EPF (5 times) |
| full spatial resolution background measurement with shutter closed | half spatial resolution background measurement with shutter closed | reduced spatial resolution (10x-pixel-binned) background measurement with shutter closed |
| full spatial resolution measurement of Mars | half spatial resolution measurement of Mars | reduced spatial resolution (10x-pixel-binned) measurement of Mars for EPF |
| full spatial resolution background measurement with shutter closed | half spatial resolution background measurement with shutter closed | reduced spatial resolution (10x-pixel-binned) background measurement with shutter closed |
| reduced spatial resolution (10x-pixel-binned) measurement of Mars for EPF (5 times) | reduced spatial resolution (10x-pixel-binned) measurement of Mars for EPF (5 times) | reduced spatial resolution (10x-pixel-binned) measurement of Mars for EPF (5 times) |
| full spatial resolution background measurement with shutter closed | half spatial resolution background measurement with shutter closed | reduced spatial resolution (10x-pixel-binned) background measurement with shutter closed |

| Tracking optical depth observation (3.75 Hz) | Limb scan observation (3.75) |
|--|--|
| reduced spatial resolution (10x-pixel-binned) background measurement with shutter closed | reduced spatial resolution (10x-pixel-binned) background measurement with shutter closed |
| reduced spatial resolution (10x-pixel-binned) measurement of Mars (4 times) | reduced spatial resolution (10x-pixel-binned) measurement of Mars |
| <i>(repeat last 2 sequences n times)</i> | <i>(repeat last 2 sequences n times)</i> |
| reduced spatial resolution (10x-pixel-binned) background measurement with shutter closed | reduced spatial resolution (10x-pixel-binned) background measurement with shutter closed |

| Multispectral or hyperspectral survey (15 Hz) | Multispectral window (30 Hz) |
|--|---|
| reduced spatial resolution (10x-pixel-binned) background measurement with shutter closed | reduced spatial resolution (5x-pixel-binned) background measurement, shutter closed |
| reduced spatial resolution (10x-pixel-binned) measurement of Mars | reduced spatial resolution (5x-pixel-binned) measurement of Mars |
| <i>(repeat last 2 sequences n times)</i> | <i>(repeat last 2 sequences n times)</i> |
| reduced spatial resolution (10x-pixel-binned) background measurement with shutter closed | reduced spatial resolution (5x-pixel-binned) background measurement, shutter closed |

| Radiometric Calibration | |
|---|---|
| full spatial resolution background measurement of the internal integrating sphere before it is powered on (VNIR 1 Hz, IR 1 Hz) | reduced spatial resolution (10x-binned) background measurement of the internal integrating sphere before it is powered on (VNIR 1 Hz, IR 15 Hz) |
| full spatial resolution measurement of the internal integrating sphere illuminated under closed-loop control using primary lamp (VNIR 1 Hz, IR 1 Hz) | reduced spatial resolution (10x-binned) measurement of the internal integrating sphere illuminated under closed-loop control using primary lamp (VNIR 1 Hz, IR 15 Hz) |
| full spatial resolution background measurement of the internal integrating sphere after it is powered on (VNIR 1 Hz, IR 1 Hz) | reduced spatial resolution (10x-binned) background measurement of the internal integrating sphere after it is powered on (VNIR 1 Hz, IR 15 Hz) |
| full spatial resolution background measurement of the internal integrating sphere before it is powered on (VNIR 1 Hz, IR 3.75 Hz) | reduced spatial resolution (5x-binned) background measurement of the internal integrating sphere before it is powered on (VNIR 1 Hz, IR 30 Hz) |
| full spatial resolution measurement of the internal integrating sphere illuminated under closed-loop control using primary lamp (VNIR 1 Hz, IR 3.75 Hz) | reduced spatial resolution (5x-binned) measurement of the internal integrating sphere illuminated under closed-loop control using primary lamp (VNIR 1 Hz, IR 30 Hz) |
| full spatial resolution background measurement of the internal integrating sphere after it is powered on (VNIR 1 Hz, IR 3.75 Hz) | reduced spatial resolution (5x-binned) background measurement of the internal integrating sphere after it is powered on (VNIR 1 Hz, IR 30 Hz) |

| Flat-field Calibration | |
|---|---|
| full spatial resolution background measurement with shutter closed, 1 Hz | reduced spatial resolution (10x-binned) background measurement with shutter closed, 15 Hz |
| full spatial resolution measurement of bland scene on Mars, 1 Hz | reduced spatial resolution (10x-binned) measurement of bland scene on Mars, 15 Hz |
| full spatial resolution background measurement with shutter closed, 1 Hz | reduced spatial resolution (10x-binned) background measurement with shutter closed, 15 Hz |
| full spatial resolution background measurement with shutter closed, 3.75 Hz | reduced spatial resolution (5x-binned) background measurement with shutter closed, 30 Hz |
| full spatial resolution measurement of bland scene on Mars, 3.75 Hz | reduced spatial resolution (5x-binned) measurement of bland scene on Mars, 30 Hz |
| full spatial resolution background measurement with shutter closed, 3.75 Hz | reduced spatial resolution (5x-binned) background measurement with shutter closed, 30 Hz |

| Bias Calibration (IR only) |
|--|
| full spatial resolution background measurement with shutter closed, series of integration times, 1 Hz |
| full spatial resolution background measurement with shutter closed, series of integration times, 3.75 Hz |
| reduced spatial resolution (10x-binned) background measurement with shutter closed, series of integration times, 15 Hz |
| reduced spatial resolution (5x-binned) background measurement with shutter closed, series of integration times, 30 Hz |

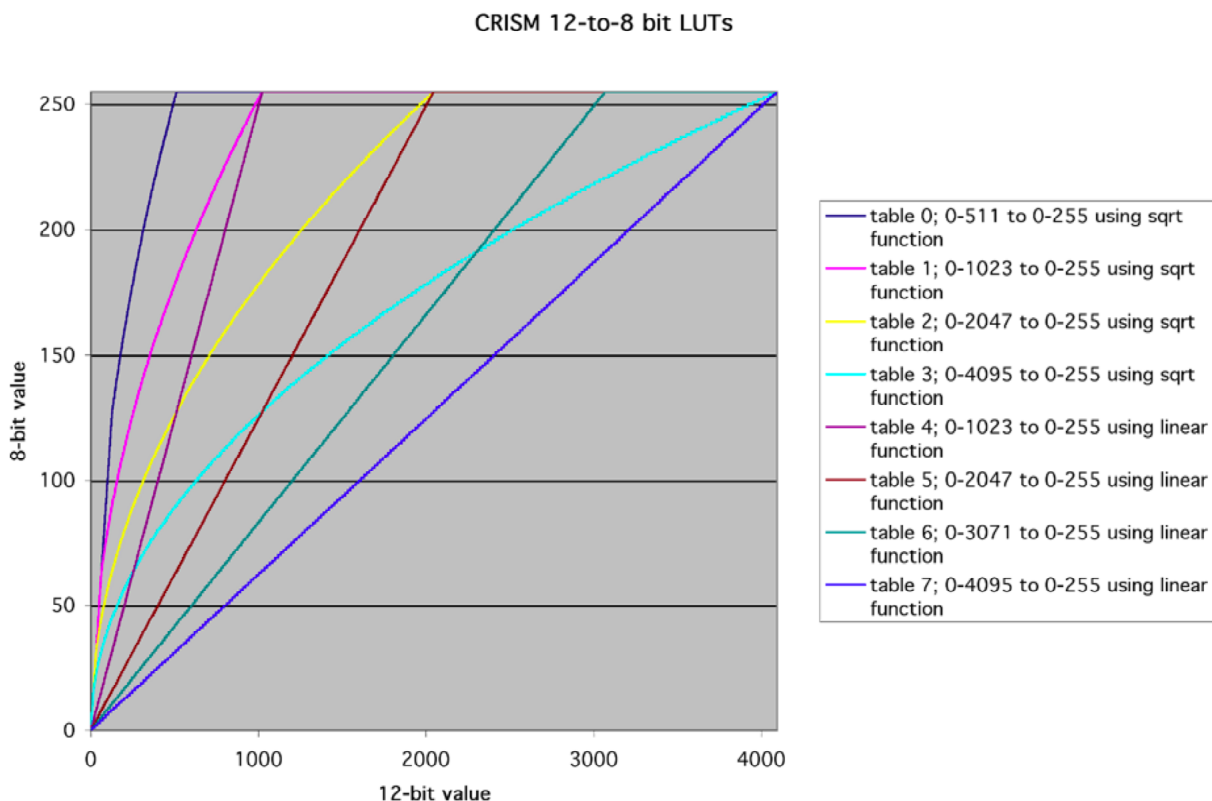


Figure 2-7. Translation of 12-bit DNs into 8-bit DNs using LUTs.

2.2 Data Product Overview

The CRISM data stream downlinked by the spacecraft unpacks into a succession of compressed image frames with binary headers containing housekeeping. In each image, one direction is spatial and one is spectral. There is one image for the VNIR focal plane and one image for the IR focal plane. The image from each focal plane has a header with 220 housekeeping items that contain full status of the instrument hardware, including data configuration, lamp and shutter status, gimbal position, a time stamp, and the target ID and macro within which the frame of data was taken. A number of the housekeeping items are particular to the image frame to which they are attached; others represent instrument hardware or software status and are identically represented in the header from each focal plane.

CRISM standard data products (Table 2-8) and the supplementary browse products represent rearranged values from the data stream, or corresponding derived products, with the basic unit of organization being that portion of the output from one macro which has a consistent instrument configuration (shutter position, frame rate, pixel binning, compression, exposure time, on/off status and setting of different lamps). The flow of data processing and the relationship of data products is shown in Figure 2-9.

2.2.1 EDRs

In an EDR (Figure 3-1) the values are unmodified but are rearranged: the headers are stripped off and placed into a text list file, and the frames are merged into a multiple-band image. The multiple-band image may consist of 8- or 12-bit data, stored as 16-bit values. There is one EDR per focal plane.

The list file is based on the 220 housekeeping items. 5 of the items are composite in that each bit of a 32-bit word encodes particular information on gimbal status or control. These separate items are not broken out, except for the gimbal status at the beginning, middle, and end of each exposure, from which gimbal position is broken out (3 additional items). The housekeeping is pre-pended with spaces for 10 additional frame-specific items useful in data validation, processing, and sorting, for a total of 233 items per frame:

- A data quality parameter produced during data validation, as discussed in section 2.5
- L_s , degrees
- Solar distance, km
- Time of day at center of FOV, hhmm.ss with 1 Mars solar day = 2400.00
- Preliminary latitude, longitude at center and edges of FOV, degrees
- Preliminary i (incidence angle) at center of FOV, degrees
- Preliminary e (emission angle) at center of FOV, degrees
- Preliminary g (phase angle) at center of FOV, degrees
- Predicted dust opacity, unitless

For the most part, the output from one macro from one focal plane equals an EDR. However there are only 255 available macro slots, so to best utilize available macro space, three types of complex inflight calibrations are lumped into one macro from which several EDRs are generated:

- At times when the focal plane lamps were used, output from a focal plane lamp macro consists of sequential frames taken at different focal plane lamp settings. These different settings are NOT distinguished by a separate macro ID, but they are stored in separate EDRs.
- The output from a bias calibration macro consists of sequential frames taken at different exposure times with the shutter closed. These different exposures are NOT distinguished by a separate macro ID, but they are stored in separate EDRs.
- Onboard functional test macros cycle the instrument through different frame rate, binning, and compression configurations. These different configurations are NOT distinguished by a separate macro ID, but they are stored in separate EDRs.

In the data archive, EDRs are grouped into the outputs from one observation. For each observation, there is also a text report on data validation for the EDRs generated by each detector.

2.2.2 CDRs

EDRs containing bias measurements or measurements of background, bias, or the internal integrating sphere are processed into level-4 CDRs. A level-4 CDR contains derived values needed to convert a scene-viewing EDR into units of radiance. These are in image format, with multiple versions corresponding to different pixel binning states. Other level 4 CDRs are derived from ground measurements. A level-6 CDR contains tabulated information, for example for correcting for detector non-linearity, converting housekeeping to physical units, or converting EDRs from 12 to the original at-sensor 14 bits prior to calibration.

2.2.3 ADRs

An Ancillary Data Record (ADR) is used to correct scene measurements calibrated to units of radiance for photometric, thermal emission, or atmospheric effects. An ADR is a hyperdimensional binary table or cube containing reference information used by algorithms that correct at-sensor radiance to the reflected solar component of I/F with thermal and atmospheric effects removed.

2.2.4 TRDRs

A Targeted Reduced Data Record or TRDR (Figure 3-4) is comparable to a scene-viewing EDR except that image data has been converted to units of radiance using level-4 and level-6 CDRs, and the list file is converted into physical units using a level-6 CDR. A TRDR may also contain I/F, in a separate file. Lambert albedo, or a set of derived spectral parameters (summary products) that provide an overview of the data set. Summary products include Lambert albedo at key wavelengths, or key band depths or spectral reflectance ratios. To create these products, estimated corrections for atmospheric, photometric, and thermal effects are applied to the radiance data using corrections given in ADRs. The formulations for all of the summary products have been validated using data from Mars Express/OMEGA.

TRDRs may be resampled in the spectral or spatial direction, to remove optical distortions in the data. If resampling has been performed, that is indicated in the label and file name.

2.2.5 DDRs

A Derived Data Records (DDR, Figure 3-3) accompanies each observation pointed at Mars' surface, and includes information needed to map project data calibrated to units of radiance or I/F, or to process them further to Lambert albedo corrected for photometric, atmospheric, and thermal effects.

There are two types of information in DDRs: geometric information (latitude, longitude, incidence, emission and phase angles) and information on surface physical properties (slope magnitude and azimuth, thermal inertia). The physical information is derived by retrieving information from other data sets for the latitudes and longitudes corresponding to each detector element, and thus is in non-resampled sensor space.

2.2.6 LDRs

A Limb Data Record (LDR) accompanies each observation scanned across Mars' limb, and includes information on the tangent height of each pixel above Mars' surface and photometric angles to analyze the measured radiances..

2.2.7 MRDRs

A map-projected multispectral RDR (MRDR, Figure 3-6) consists of several or more strips of multispectral survey data mosaicked into a map tile. Thus a map tile is constructed from a large number of TRDRs. The mosaic is uncontrolled (accepting existing pointing data with image mismatch at seams generally <1 200-m pixel). A global pattern of 1964 such tiles (Figure 2-9) has been developed, forming a major data product for multispectral survey observations. Each tile contains data in units of I/F extracted from a TRDR, plus Lambert albedo, summary products, and the DDR data used to generate them. So, for every latitude or longitude in an MRDR, there is both an I/F and all the information providing traceability to a companion I/F corrected for atmospheric, photometric, and thermal emission effects (Lambert albedo). The MRDRs also include text files having information on the wavelength of the layers of the Lambert albedo and I/F multiband images.

2.2.8 MTRDRs

A map-projected TRDR (MTRDR, Figure 3-8) is analogous to an MRDR, except that it contains hyperspectral data from a targeted, hyperspectral observation, map-projected and converted to I/F, with additional corrections applied to normalize photometric and atmospheric effects, and with channels having questionable calibration ("bad channels") removed. There may be an additional file with summary products, and a list file with wavelengths of the channels present.

2.2.9 SPICE Files

Four types of SPICE kernels are needed to calculate CRISM's pointing:

- Frames kernel (FK). This file defines the relationships of the of CRISM's field of view to the spacecraft, with the gimbal at "nadir".
- Instrument kernel (IK). This file describes the relationship of position of each detector element (at a row or wavelength and spatial or column position) to a zero position within the field of view.
- Gimbal C kernel. This file gives a time history of the angle of the gimbal within the gimbal plane, relative to its commanded nadir.
- Metakernel. This file gives, for any time span covered by a gimbal C kernel, the MRO and CRISM SPICE kernels used to create DDRs for observations occurring during that time period.

2.2.10 Browse Products

Browse products are PNG files that show a summary of EDR, MTRDR, or MRDR data characteristics in the spatial plane of the data. For the EDRs, the PNG files show median values

from a selected wavelength range. For MTRDRs or MRDRs, the PNG files show scaled values of key layers of the data. Accompanying labels describe scaling to the 8-bit PNG files. The PNG files may be accompanied by an HTML file that describes the EDR or MTRDR browse products for one observation, or the MRDR browse products for one map tile.

2.2.11 Extra Products

Extra products in the CRISM archive are all ASCII text files and include a time ordered history of observations and the characteristics of the sites observed, as well as the configuration-managed history of the hardware and software state of the CRISM instrument.

Several engineering-related files, which have a format and nomenclature like that of level 6 CDRs, include a history of alarms settings and software control parameters that are uploaded as binary tables ("data structures"), and events log, heater settings, and the model of data compressibility that is used in observation sequence planning.

Other files document the characteristics of flight macros that were active during different periods of the MRO mission. There are three files for each macro load: the macro dictionary itself, a summary of each macro's function, and a description of the image data generated by each macro.

Finally, a table connects specific observations with regions of interest on Mars, science objectives, and specific observation conditions.

Table 2-8. Definitions of CRISM data products.

| Data Product | PDS Data Set ID | Data Processing Level | Example PDS Labels |
|-------------------------------|--------------------------------------|------------------------------|---------------------------|
| Experiment Data Record (EDR) | MRO-M-CRISM-2-EDR-V1.0 | 2 | Figure 3-1; Appendix A |
| Calibration Data Record (CDR) | MRO-M-CRISM-4/6-CDR-V1.0 | 4, 6 | Appendices F,G |
| Derived Data Record (DDR) | MRO-M-CRISM-6-DDR-V1.0 | 6 | Figure 3-3; Appendix B |
| Limb Data Record (LDR) | MRO-M-CRISM-6-LDR-V1.0 | 6 | Appendix H |
| Targeted RDR (TRDR) | MRO-M-CRISM-3-RDR-TARGETED-V1.0 | 3 | Figure 3-4; Appendix C |
| Multispectral RDR (MRDR) | MRO-M-CRISM-5-RDR-MULTISPECTRAL-V1.0 | 5 | Figure 3-6; Appendix D |
| Map-Projected TRDR (MTRDR) | MRO-M-CRISM-5-RDR-MPTARGETED-V1.0 | 5 | Figure 3-8; Appendix E |

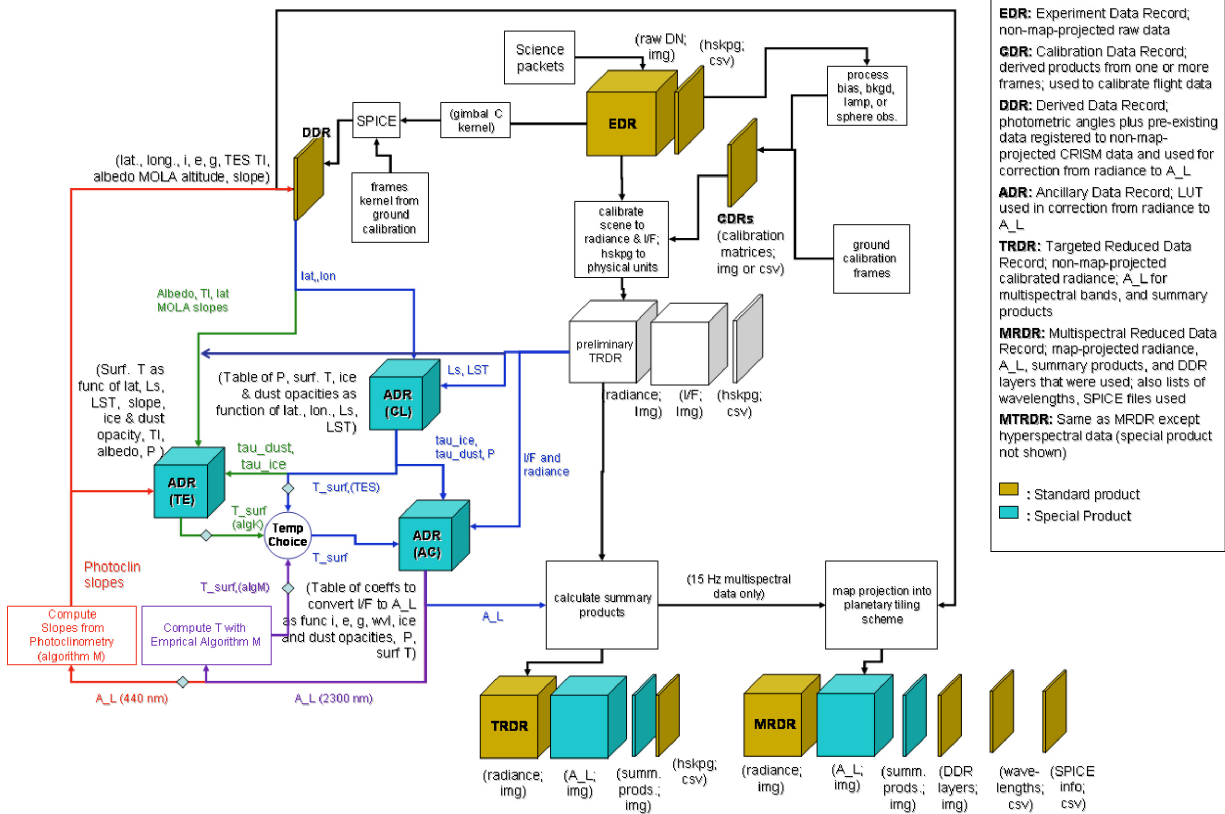


Figure 2-9. Sequential processing of EDRs to yield RDRs of Mars data, showing the roles of CDRs and ADRs.

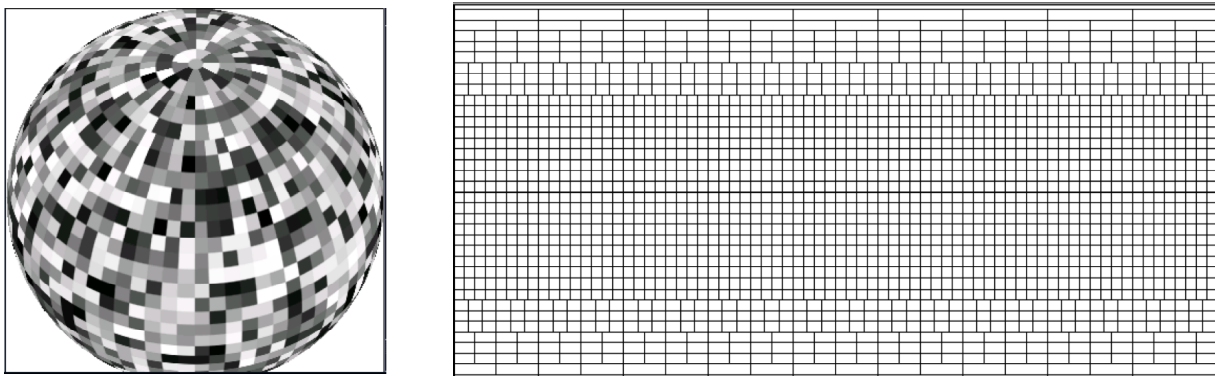


Figure 2-10. Tiling scheme for the map-projected multispectral survey, shown in orthographic view and as a global, EQUIRECTANGULAR map form.

2.3 Data Processing

2.3.1 Data Processing Level

This SIS uses the Committee On Data Management And Computation (CODMAC) data level numbering system to describe the processing level of the CRISM data products. Table 2-11 shows the description of the CODMAC data processing levels and the correlation with the NASA processing levels. The CODMAC system is used here because it is the standard used by the PDS. CODMAC data processing levels for CRISM data products are listed in Table 2-8.

Table 2-11. Processing Levels for Science Data Sets

| NASA | CODMAC | Description |
|-------------|----------------------|--|
| Packet data | Raw - Level 1 | Telemetry data stream as received at the ground station, with science and engineering data embedded. |
| Level-0 | Edited - Level 2 | Instrument science data (e.g., raw voltages, counts) at full resolution, time ordered, with duplicates and transmission errors removed. |
| Level 1-A | Calibrated - Level 3 | Level 0 data that have been located in space and may have been transformed (e.g., calibrated, rearranged) in a reversible manner and packaged with needed ancillary and auxiliary data (e.g., radiances with the calibration equations applied). |
| Level 1-B | Resampled - Level 4 | Irreversibly transformed (e.g., resampled, remapped, calibrated) values of the instrument measurements (e.g., radiances, magnetic field strength). |
| Level 1-C | Derived - Level 5 | Level 1A or 1B data that have been resampled and mapped onto uniform space-time grids. The data are calibrated (i.e., radiometrically corrected) and may have additional corrections applied (e.g., terrain correction). |
| Level 2 | Derived - Level 5 | Geophysical parameters, generally derived from Level 1 data, and located in space and time commensurate with instrument location, pointing, and sampling. |
| Level 3 | Derived - Level 5 | Geophysical parameters mapped onto uniform space-time grids. |
| | Ancillary – Level 6 | Data needed to generate calibrated or resampled data sets. |

2.3.2 Data Product Generation

2.3.2.1 Data acquisition

The high-level observation plan in Table 2-4 has been translated into a preliminary timeline for a number of types of targets. This has involved internal planning of CRISM observations as described above, as well as coordination with MRO Project objectives and spacecraft resource constraints.

- First, based on the data expected from the sequence of macros executed for each type of observations, a predicted data volume for each type of observation is calculated. This is summarized in Table 2-12.
- Second, the MRO project has allocated CRISM and other instruments a fraction of spacecraft resources, downlink and spacecraft pointing.
- Third, based on coverage goals summarized in Table 2-4, observing opportunities are identified that both address the science objectives and fit within allocated downlink. The numbers of opportunities and the subsequent ground processing result in numbers and volumes of EDRs and higher-order products (Table 2-13).

During the first 6 months of the mission, approximately half of the orbits were devoted to nadir pointing for multispectral survey observations, with off-nadir observations requiring spacecraft pointing mostly on remaining orbits. After that 6-month period, multispectral survey was collected between off-nadir observations requiring spacecraft pointing. The off-nadir opportunities are of 3 types: (a) Mars Exploration Program (MEP)-selected targets, the highest priority, for which all instruments observe the same target at high spatial resolution; (b) coordinated targets, observed in the same way, of which each instrument chooses a fraction; and (c) single-instrument targets for which other instruments may or may not operate at high spatial resolution. Remaining downlink allocation is filled with targets that are observed at high spatial resolution but without off-nadir pointing. In addition, some non-coordinated HiRISE or CTX observations are accompanied by a short, reduced-resolution CRISM observation (a ridealong).

Table 2-12. Contents of each type of CRISM observation

| Class of observation | Frame rate, Hz | Activity | Pixel binning | # | Wave-lengths | Frames (typical) |
|--|---------------------|--|---------------|----------|----------------|------------------|
| Full resolution targeted | 3.75 | central scan | 1 | 1 | 545 | 390 |
| | 3.75 | EPF scans | 10 | 10 | 545 | 15 |
| | 3.75 | dark sets | 1 | 4 | 545 | 12 |
| Half resolution short targeted | 3.75 | central scan | 2 | 1 | 545 | 243 |
| | 3.75 | EPF scans | 10 | 10 | 545 | 15 |
| | 3.75 | dark sets | 2 | 4 | 545 | 12 |
| Half resolution long targeted | 3.75 | central scan | 2 | 1 | 545 | 487 |
| | 3.75 | EPF scans | 10 | 10 | 545 | 15 |
| | 3.75 | dark sets | 2 | 4 | 545 | 12 |
| EPF | 3.75 | EPF scans | 10 | 11 or 13 | 545 | 15 |
| | 3.75 | dark sets | 10 | 4 | 545 | 12 |
| Limb scan | 3.75 | Individual scans | 10 | variable | 545 | 540 |
| | 3.75 | dark sets | 10 | same | 545 | 12 |
| TOD | 3.75 | 3-second segments | 10 | 12 | 545 | 12 |
| | 3.75 | dark sets | 10 | 4 | 545 | 12 |
| Multispectral survey | 15 | 3-minute segments | 10 | 8 | 73/74 or 94/95 | 2700 |
| | 15 | dark sets | 10 | 9 | 73/74 or 94/95 | 12 |
| Hyperspectral survey | 15 | 3-minute segments | 10 | 8 | 262 | 2700 |
| | 15 | dark sets | 10 | 9 | 262 | 12 |
| Multispectral window | 30 | 1 3-minute segment | 5 | 1 | 73/74 or 94/95 | 5400 |
| | 30 | dark sets | 5 | 2 | 73/74 or 94/95 | 12 |
| Radiometric calibration | 1 (VNIR), 1 (IR) | sphere background | 1 | 2 | 545 | 12 |
| | 1 (VNIR), 1 (IR) | sphere frames | 1 | 1 | 545 | 32 |
| | 1 (VNIR), 3.75 (IR) | sphere background | 1 | 2 | 545 | 12 |
| | 1 (VNIR), 3.75 (IR) | sphere frames | 1 | 1 | 545 | 32 |
| | 1 (VNIR), 15 (IR) | sphere background | 10 | 2 | 73 | 12 |
| | 1 (VNIR), 15 (IR) | sphere frames | 10 | 1 | 73 | 32 |
| | 1 (VNIR), 30 (IR) | sphere background | 5 | 2 | 73 | 12 |
| | 1 (VNIR), 30 (IR) | sphere frames | 5 | 1 | 73 | 32 |
| Bias calibration | 1 | dark frames, several integration times | 1 | 4 | 438 (IR only) | 10 |
| | 3.75 | dark frames, several integration times | 1 | 5 | 438 (IR only) | 10 |
| | 15 | dark frames, several integration times | 10 | 4 | 55 (IR only) | 10 |
| | 30 | dark frames, several integration times | 5 | 4 | 55 (IR only) | 10 |
| Flat-field calibration (only 1 frame rate at a time) | 1 | dark sets | 1 | 2 | 545 | 12 |
| | 1 | 3-minute segments | 1 | 1 | 545 | 180 |
| | 3.75 | dark sets | 1 | 2 | 545 | 12 |
| | 3.75 | 3-minute segments | 1 | 1 | 545 | 675 |
| | 15 | dark sets | 10 | 2 | 73 | 12 |
| | 15 | 3-minute segments | 10 | 1 | 73 | 2700 |
| | 30 | dark sets | 5 | 2 | 73 | 12 |
| | 30 | 3-minute segments | 5 | 1 | 73 | 5400 |

Table 2-13. Representative CRISM data acquisition during 1 Mars year.

| Class of observation | # | Approx. EDR vol per observation, Gb | Approx. data vol., associated cal. files, Gb | PDS deliveries | Data vol per TRDR+DDR or per MRDR, Gb | PDS deliveries (initial, redelivery) | Delivered volume, Tb |
|--------------------------------|-------|-------------------------------------|--|----------------|---------------------------------------|--------------------------------------|----------------------|
| Full-res targets | 5000 | 2.10 | 0.23 | 1 | 4.33 | 2 | 53.72 |
| Half-res long targets | 1500 | 1.09 | 0.05 | 1 | 2.25 | 2 | 8.26 |
| Half-res short targets | 1000 | 0.62 | 0.05 | 1 | 1.28 | 2 | 3.17 |
| EPFs | 3000 | 0.10 | 0.03 | 1 | 0.21 | 2 | 1.61 |
| TODs | 6000 | 0.03 | 0.05 | 1 | 0.06 | 2 | 1.23 |
| Strips of multispectral survey | 12000 | 0.75 | 0.002 | 1 | 1.83 | 2 | 51.80 |
| Strips of hyperspectral survey | 6000 | 2.70 | 0.002 | 1 | 5.73 | 2 | 82.93 |
| Multispectral survey tiles | 1764 | | | | 9.47 | 1 | 16.32 |
| Multispectral windows | 2000 | 0.75 | 0.0014 | 1 | 1.83 | 2 | 8.63 |
| Total | | | | | | | 227.66 |

2.3.2.2 Data processing overview

Data processing to standard products for delivery to the PDS (EDRs, CDRs, TRDRs, DDRs, LDRs, and MRDRs) occurs in the CRISM Science Operations Center (SOC). ADRs are created by the science team and delivered to the SOC for application to the data. Additional processing to special products (MTRDRs) is the responsibility of individual CRISM science team members.

The sequence of processing used to create deliverable data products is discussed in section 2.2 and shown graphically in Figure 2-9. Appendix L provides detailed mathematical formations of CDRs, and of the derivation of radiance in TRDRs using the CDRs.

2.3.3 Data Flow and Delivery

Downlinked CRISM data are forwarded with spacecraft housekeeping and pointing information from JPL to the CRISM Science Operations Center (SOC) at The Johns Hopkins University Applied Physics Laboratory (APL), where they are processed to EDRs in near-real time. DDRs and LDRs are generated at the SOC using SPacecraft, Instrument, Camera, and Events (SPICE) and other data sources. TRDRs are also generated at the SOC from EDR products, and for multispectral survey, MRDRs are generated from TRDR strips. After validation CRISM data products are transferred to the PDS Geosciences Node for archiving and distribution.

CRISM data archival is overseen by Co-I Arvidson, manager of the PDS Geosciences Node. The approach outlined above is consistent with the MRO Data Archive Plan (R. Arvidson, author). Ground data including calibration files and the spectral library were delivered at various times through Mars orbit insertion. For flight data, delivery of EDRs, DDRs, LDRs, TRDRs, and CDRs occurs at 3-month intervals following 6 months of validation, on hard drives and deep-archive media to be determined by the PDS. Additionally, at selected delivery times, MRDRs covering selected tiles of the global maps are delivered, part of the planet at each delivery.

When upgrades occur to data calibration, TRDRs and/or MRDRs are redelivered with an increment to version numbers. Through 2 Mars years, there we 2 TRDR upgrades early in the mission, and a pending upgrade of both TRDRs and MRDRs necessitating a redelivery of both data sets.

Tables 2-13 shows how the numbers of acquired observations translates to EDRs, DDRs, TRDRs, CDRs, and MRDRs.

2.3.4 Labeling and Identification

2.3.4.1 EDR, DDR, LDR, and TRDR

EDRs, DDRs, LDRs, and TRDRs are CRISM standard products representing raw and calibrated data with geometric and timing information necessary for map projection and various post-processing correction. In summary:

- a) EDRs represent raw data and TRDRs represent calibrated data. Both are in units of sensor space. They contain the optical and spatial distortions present at the sensor.
- b) DDRs represent geometric information for observations pointed at Mars' surface, indexed to the wavelength bands of EDRs and TRDRs that are closest to 610 nm (VNIR) and 2300 nm (IR).
- c) LDRs represent geometric information for observations pointed at Mars' limb, indexed to the wavelength bands of EDRs and TRDRs that are closest to 610 nm (VNIR) and 2300 nm (IR).

Optical distortions may be removed from TRDRs by resampling in the spectral or spatial direction. Three types of resampling can occur: (a) resampling in the wavelength direction occurs using nearest-neighbor resampling, as coded in the PS CDR4; (b) resampling in the spatial direction, to remove differences in spatial scale with wavelength or band, using the CM CDR4; and (c) VNIR data may be rescaled to match the slightly different magnification of the IR spectrometer, also using the CM CDR4. A resampled TRDR is distinguished by its label and file name. The label uses local data dictionary keywords to document the type of resampling that has occurred. The file name parallels that of the source TRDR except for file type.

The file naming convention for EDR, DDR, LDR, and TRDR products is as follows.

(ClassType)(ObsID)_(Counter)_(Activity)(SensorID)_(Filetype)(version).(Ext)

where:

Class Type =

FRT (Full Resolution Targeted Observation)
HRL (Half Resolution Long Targeted Observation)
HRS (Half Resolution Short Targeted Observation)
EPF (Atmospheric Survey EPF)
TOD (Tracking Optical Depth Observation)
LMB (Limb Scan Observation)
MSS (Multispectral Survey, lossy compressed)
MSP (Multispectral Survey, losslessly compressed)
HSP (Hyperspectral Survey, losslessly compressed)
HSV (Hyperspectral Survey - VNIR only, losslessly compressed)
MSW (Multispectral Window)
CAL (Radiometric Calibration)
FFC (Flat Field Calibration)
ICL (Calibration source intercalibration)
STO (Star Observation)
FUN (Functional test)
UNK (no valid EDRs within observation that indicate class type)

ObsID = nnnnnnnn, Observation ID, unique for the whole CRISM mission, expressed as a hexadecimal number

Counter= nn, a monotonically increasing ordinal counter of EDRs from one Observation ID, expressed as a hexadecimal number

Activity = for an EDR, type of observation, e.g.

BI#### – Bias measurements / Macro#
DF#### – Dark field measurements / Macro#
LP#### – Lamp measurements / Macro #
SP#### – Sphere measurements / Macro #
SC#### – Scene measurements / Macro #
T1#### – Focal plane electronics test pattern 1 / Macro #
T2#### – Focal plane electronics test pattern 2 / Macro #
T3#### – Focal plane electronics test pattern 3 / Macro #
T4#### – Focal plane electronics test pattern 4 / Macro #
T5#### – Focal plane electronics test pattern 5 / Macro #

T6### – Focal plane electronics test pattern 6 / Macro #

T7### – Focal plane electronics test pattern 7 / Macro #

UN### – Instrument configuration does not match macro library / Macro #

for a TRDR, type of product, e.g.

RA### – Radiance / Macro#

SU### – Summary Products / Macro #

IF### – I/F / Macro #

AL### – Lambert albedo / Macro #

for a DDR or LDR, type of product, e.g.

DE### – Derived product / Macro#

Sensor ID = S or L for VNIR or IR

filetype = EDR, DDR, LDR, or "TRR" for TRDR, "RTR" for resampled TRDR

version = 0, 1,...,9, a, ..., z

Ext = IMG or TAB

Each CRISM data product of these types will also have a product ID that is unique within its data set. The product ID scheme for CRISM EDR, DDR, and TRDR products is as follows (see file naming convention for allowable values for each field):

CCCNNNNNNNN_XX_AAAAAS_TTTV

Where:

| | | |
|----------|---|--|
| CCC | = | Class Type |
| NNNNNNNN | = | Observation ID as a hexadecimal number |
| XX | = | Counter within this observation |
| AAAAA | = | Activity Type |
| S | = | Sensor ID |
| TTT | = | Product Type (EDR, DDR, LDR, "TRR" for TRDR, "RTR" for resampled TRDR) |
| V | = | Product version number |

2.3.4.2 EDR Validation Reports

The file naming convention for EDR validation report is as follows.

(ClassType)(ObsID)_(SensorID)_VALIDATION.TXT

where:

Class Type =

FRT (Full Resolution Targeted Observation)
HRL (Half Resolution Long Targeted Observation)
HRS (Half Resolution Short Targeted Observation)
EPF (Atmospheric Survey EPF)
TOD (Tracking Optical Depth Observation)
LMB (Limb Scan Observation)
MSS (Multispectral Survey, lossy compressed)
MSP (Multispectral Survey, losslessly compressed)
HSP (Hyperspectral Survey, losslessly compressed)
HSV (Hyperspectral Survey - VNIR only, losslessly compressed)
MSW (Multispectral Window)
CAL (Radiometric Calibration)
FFC (Flat Field Calibration)
ICL (Calibration source intercalibration)
STO (Star Observation)
FUN (Functional test)
UNK (no valid EDRs within observation that indicate class type)

ObsID = nnnnnnnn, Observation ID, unique for the whole CRISM mission, expressed as a hexadecimal number

Sensor ID = S or L (or J=joint for an MTRDR)

Each validation report will also have a product ID that is unique within its data set. The product ID scheme for CRISM EDR validation reports is as follows (see file naming convention for allowable values for each field):

CCCNNNNNNNN_S_VALIDATION

Where:

| | | |
|----------|---|--|
| CCC | = | Class Type |
| NNNNNNNN | = | Observation ID as a hexadecimal number |
| S | = | Sensor ID |

2.3.4.3 *EDR Browse Products*

The file naming convention for the HTML browse products for EDRs is as follows.

(ClassType)(ObsID)_BROWSE_EDR(version).(Ext)

where:

Class Type =

FRT (Full Resolution Targeted Observation)

HRL (Half Resolution Long Targeted Observation)

HRS (Half Resolution Short Targeted Observation)

EPF (Atmospheric Survey EPF)

TOD (Tracking Optical Depth Observation)

LMB (Limb Scan Observation)

MSS (Multispectral Survey, lossy compressed)

MSP (Multispectral Survey, losslessly compressed)

HSP (Hyperspectral Survey, losslessly compressed)

HSV (Hyperspectral Survey - VNIR only, losslessly compressed)

MSW (Multispectral Window)

CAL (Radiometric Calibration)

FFC (Flat Field Calibration)

ICL (Calibration source intercalibration)

STO (Star Observation)

FUN (Functional test)

UNK (no valid EDRs within observation that indicate class type)

ObsID= nnnnnnnn, Observation ID, unique for the whole CRISM mission, expressed as a hexadecimal number

version= 0, 1,...,9, a, ..., z

Ext= HTML

Each EDR HTML browse product will have a product ID that is unique within its data set. The product ID scheme for CRISM EDR HTML browse products is as follows:

CCCNNNNNNNN_BROWSE_EDRV

Where:

CCC = Class Type

NNNNNNNN = Observation ID as a hexadecimal number

TTT = Product Type (EDR)

V = Product version number

The file naming convention for the PNG browse products for EDRs is as follows.

(ClassType)(ObsID)_(Counter)_(Activity)(SensorID)_RAW(version).(Ext)

where:

Counter= nn, a monotonically increasing ordinal counter of EDRs from one Observation ID

Activity= for an EDR, type of observation, e.g.

BI_{nnn} – Bias measurements / Macro#

DF_{nnn} – Dark field measurements / Macro#

LP_{nnn} – Lamp measurements / Macro #

SP_{nnn} – Sphere measurements / Macro #

SC_{nnn} – Scene measurements / Macro #

T1_{nnn} – Focal plane electronics test pattern 1 / Macro #

T2_{nnn} – Focal plane electronics test pattern 2 / Macro #

T3_{nnn} – Focal plane electronics test pattern 3 / Macro #

T4_{nnn} – Focal plane electronics test pattern 4 / Macro #

T5_{nnn} – Focal plane electronics test pattern 5 / Macro #

T6_{nnn} – Focal plane electronics test pattern 6 / Macro #

T7_{nnn} – Focal plane electronics test pattern 7 / Macro #

UN_{nnn} – Instrument configuration does not match macro library / Macro #

Sensor ID= S for VNIR, or L for IR

version= 0, 1,...,9, a, ..., z

Ext= PNG

Each EDR PNG browse product will have a product ID that is unique within its data set. The product ID scheme for CRISM EDR PNG browse products is as follows:

CCCN_{NNNNNNNN}_XX_AAAAAS_RAWV

Where:

CCC = Class Type

NNNNNNNN = Observation ID as a hexadecimal number

XX = Counter within this observation

AAAAA = Activity Type

S = Sensor ID

V = Product version number

2.3.4.4 *MRDRs*

The file naming convention for MRDR products is as follows.

(Tile)_(ProductType)(Subtype)_(CLat)(Hemisphere) (CLon)_(Resolution)_version.(Ext)

where:

Tile = Tnnnn, tile number with tile 0000 at the south pole, increasing spiraling northward

Product Type = "MRR" for MRDR

Subtype of product, e.g.

IF – I/F

AL – Lambert albedo

SU – Summary Products

DE – Derived Products for I/F

DL – Derived Products for Lambert albedo

WV – List of wavelengths and wavelength ranges of radiance and I/F images

CLat = nn, Planetocentric latitude of tile center

Hemisphere = #, N or S for north or south latitude

CLon = nnn, East longitude of tile center

Resolution = nnnn, in map-projected pixels per degree, e.g. 256 pixels per degree

version = 0, 1,..., 9, a,..., z

Ext = IMG or TAB

The product ID scheme for the CRISM MRDRs is as follows:

TNNNN_TTTSS_XXDYYY_RRRR_V

Where:

| | | |
|-------|---|--|
| TNNNN | = | Tile number |
| TTT | = | Product Type ("MRR" for MRDR) |
| SS | = | Product subtype, i.e., IF, AL, SU, DE, DL, or WV |
| XX | = | Planetocentric latitude of tile center |
| D | = | N or S for north or south latitude |
| YYY | = | East longitude of tile center |
| RRRR | = | Map resolution in pixels per degree, e.g. 0256 or 2048 |
| V | = | Product version number |

2.3.4.5 *MRDR Browse Products*

Browse products for MRDRs are only PNG files. Their nomenclature follows that of MRDRs except that browse products type (following the browse product types for TRDRs) is substituted for the type of image product:

(Tile)_(ProductType)(BrowseProductType)_ (CLat)(Hemisphere) (CLon)_(Resolution)_
version.(Ext)

where:

Tile = Tnnnn, tile number with tile 0000 at the south pole, increasing spiraling northward

Product Type = MRR

BrowseProductType = TRU, VNA, FEM, FM2, FAL, IRA, MAF, PHY, PH2, HYD, or ICE

CLat = nn, Planetocentric latitude of tile center

Hemisphere = #, N or S for north or south latitude

CLon = nnn, East longitude of tile center

Resolution= nnnn, in map-projected pixels per degree, e.g. 256 pixels per degree

version= 0, 1,..., 9, a,..., z

Ext= PNG

The product ID scheme for the CRISM MRDRs is as follows:

TNNNN_TTTBBB_XXDYYY_RRRR_V

Where:

| | | |
|-------|---|---|
| TNNNN | = | Tile number |
| TTT | = | Product Type ("MRR" for MRDR) |
| BBB | = | Browse Product Type, TRU, VNA, FEM, FM2, FAL, IRA, MAF, PHY, PH2, HYD, or ICE |
| XX | = | Planetocentric latitude of tile center |
| D | = | N or S for north or south latitude |
| YYY | = | East longitude of tile center |
| RRRR | = | Map resolution in pixels per degree, e.g. 0256 or 2048 |
| V | = | Product version number |

2.3.4.6 *MTRDRs*

The file naming convention for MTRDRs closely parallels that for TRDRs:

(ClassType)(ObsID)_(Counter)_ (Activity)(SensorID)_(Filetype)(version).(Ext)

where:

Class Type =

FRT (Full Resolution Targeted Observation)

HRL (Half Resolution Long Targeted Observation)

HRS (Half Resolution Short Targeted Observation)

ObsID= nnnnnnnn, Observation ID, unique for the whole CRISM mission, expressed as a hexadecimal number

Counter= nn, the ordinal counter carried through from the source EDR, expressed as a hexadecimal number

Activity= for a TRDR, type of product, e.g.

IFnnn – corrected I/F / Macro #

SUnnn – Summary Products / Macro #

WV – List of wavelengths of I/F images

Sensor ID= J (for joined S and L)

filetype = "MTR" for MTRDR

version= 0, 1,...,9, a, ..., z

Ext= IMG

The product ID scheme for the CRISM MTRDRs is as follows:

CCCNNNNNNNN_XX_AAAAAJ_TTTV

Where:

| | | |
|----------|---|--|
| CCC | = | Class Type |
| NNNNNNNN | = | Observation ID as a hexadecimal number |
| XX | = | Counter within this observation |
| AAAAA | = | Activity Type |
| J | = | Sensor ID |
| TTT | = | Product Type (MTR) |
| V | = | Product version number |

2.3.4.7 MTRDR Browse Products

The file naming convention for the HTML browse products for MTRDRs is as follows.

(ClassType)(ObsID)_BROWSE_MTR(version).(Ext)

where:

Class Type =

FRT (Full Resolution Targeted Observation)

HRL (Half Resolution Long Targeted Observation)

HRS (Half Resolution Short Targeted Observation)

ObsID = nnnnnnnn, Observation ID, unique for the whole CRISM mission, expressed as a hexadecimal number

version=0, 1,...,9, a, ..., z

Ext= HTML

Each EDR HTML browse product will have a product ID that is unique within its data set. The product ID scheme for CRISM EDR HTML browse products is as follows:

CCCNNNNNNNN_BROWSE_MTRV

Where:

CCC = Class Type

NNNNNNNN = Observation ID as a hexadecimal number

TTT = Product Type (EDR)

V = Product version number

The file naming convention for the PNG browse products for MTRDRs is as follows.

(ClassType)(ObsID)_(Counter)_(Activity)(SensorID)_(BrowseProductType)(version).(Ext)

where:

Counter= nn, the ordinal counter carried through from the source EDR

Activity = type of product, e.g.

IF### – I/F / Macro#

SU### – Summary Products / Macro #

BrowseProductType = TRU, VNA, FEM, FM2, FAL, IRA, MAF, PHY, PH2, HYD, ICE, IC2, CAR, CR2, or GLO

version= 0, 1,...,9, a, ..., z

Ext= PNG

Each MTRDR PNG browse product will have a product ID that is unique within its data set. The product ID scheme for CRISM EDR PNG browse products is as follows:

CCCNNNNNNNN_XX_AAAAJ_RAWV

Where:

CCC = Class Type

NNNNNNNN = Observation ID as a hexadecimal number

XX = Counter within this observation

AAAAA = Activity Type

J = Sensor ID

V = Product version number

2.3.4.8 CDRs

There are three formats for CDRs:

- tabulated ground or flight ancillary data used during processing from an EDR to radiance (level-6 CDRs)
- tables of scene and accompanying calibration EDRs, to process to CDR4s or TRDRs (level-6 CDRs, with distinct nomenclature to distinguish them from data-containing files.)
- derived, image-format ground or flight data used during processing from an EDR to radiance or I/F (level-4 CDRs)

The file naming convention for data-containing level-6 CDRs is as follows.

(ProductType)(Level)_(Partition)_(Time)_(Product)_(SensorID)_version.(Ext)

where:

Product Type = CDR

Level = 6

Partition = n, partition of the spacecraft clock.

Time = nnnnnnnnnn, spacecraft start time of applicability of data product; units are spacecraft clock counts, in units of whole seconds.

Product = nn, acronym describing data product from Table 3-5

Sensor ID = S or L (or J=joint)

Version = 0, 1,..., 9, a,..., z

Ext = TAB

The product ID scheme for data-containing CRISM level 6 CDRs is as follows:

CCCC_P_TTTTTTTTTT_AA_S_V

| | | |
|------------|---|--|
| Where: | | |
| CCCC | = | Product Type (CDR6) |
| P | = | Partition number of sclk counts |
| TTTTTTTTTT | = | Start time of applicability, in units of sclk counts |
| AA | = | Acronym for contents of product |
| S | = | Sensor ID |
| V | = | Version |

The file naming convention for EDR processing tables is as follows.

(Product)_(Sensor)_(YYYY)_(DOY)_version

where:

Product Type = BTF for before-the-fact predicted, or ATF for after-the-fact actual

Sensor = VN or IR

YYYY = year

DOY = day of year

Version = nn

The product ID scheme for the EDR processing tables is as follows:

CCCC_P_TTTTTTTTTT_AA_S_V

| | | |
|--------|---|---------------------------------|
| Where: | | |
| CCC | = | Product (BTF or ATF) |
| S | = | Sensor ID |
| P | = | Partition number of slck counts |
| YYYY | = | Year covered by table |
| DOY | = | Day of year covered by table |
| V | = | Version |

The file naming convention for level-4 CDRs is as follows.

(ProductType)(Level)(Partition)(Time)_

(Product)(FrameRate)(Binning)(ExposureParameter)(WavelengthFilter)(Side)(SensorID)_
version.(Ext)

Product Type = CDR

Level = 4

Partition = n, partition of slck counts

Time = nnnnnnnnnn, spacecraft start time of applicability of ground data product, or spacecraft mean time of acquisition of source EDR of flight data product; units are spacecraft clock counts, in units of whole seconds.

Product = nn, acronym describing data product from Table 3-19

FrameRate = n, rate in Hz at which data are taken (0=1 Hz, 1=3.75 Hz, 3=156 Hz, 4=30 Hz, 5 = N/A)

Binning = n, number of spatial pixels binned (0=unbinned, 1= 2x binned, 2= 5x binned, 3= 10x binned, 4=N/A)

Exposure parameter = nnn, an integer 1-480 indicating commanded exposure time in units of (inverse frame rate)/480; 000 if inapplicable

Wavelength filter = n, and integer 0-3 indicating which onboard menu of rows of the detector are represented

Side = #, 1 or 2 for focal plane or sphere bulbs; or 0 if N/A

Sensor ID = S or L (or J=joint)

version = 0, 1,..., 9, a,..., z

Ext = IMG

The product ID scheme for CRISM level 4 CDRs is as follows:

CCCCPTTTTTTTTTT_AARBEEEWCS_V

| | | |
|-------------|---|--|
| Where: | | |
| CCCC | = | Product Type (CDR4) |
| P | = | Partition number of scik counts |
| TTTTTTTTTTT | = | Start time of applicability, in units of scik counts |
| AA | = | Acronym for contents of product |
| R | = | Frame rate |
| B | = | Binning |
| EEE | = | Exposure parameter |
| W | = | Wavelength filter |
| C | = | Side |
| S | = | Sensor ID |
| V | = | Version |

2.3.4.9 ADRs

ADR's are hyperdimensional binary tables of derived values, where the axes of the matrix represent values of a layer of a DDR (e.g., incidence angle, thermal inertia, etc.), and the element in the matrix is a coefficient used either directly or as an input to correct I/F for predicted atmospheric, photometric, or thermal effects.

The file naming convention for ADR's is as follows.

(ProductType)_(ADR_Type)_(Wavelength)_(Partition)_(Time)_version.(Ext)

where:

Product Type = ADR

ADR_Type = CL, AC, or TE as described in section 3.8

Wavelength = nnnn, in nanometers; 0000 if not applicable

Partition = n, spacecraft clock partition.

Time = nnnnnnnnnn, spacecraft start time of applicability of data product; units are spacecraft clock counts, in units of whole seconds.

version = 0, 1,..., 9, a,..., z

Ext = DAT

The product ID scheme for CRISM ADRs is as follows:

CCC_AA_NNNN_P_TTTTTTTTTT_V

| | | |
|------------|---|--|
| Where: | | |
| CCC | = | Product Type (ADR) |
| AA | = | Acronym for contents of product |
| NNNN | = | Wavelength in nearest whole nanometers |
| P | = | Partition number of sclk counts |
| TTTTTTTTTT | = | Start time of applicability, in units of sclk counts |
| V | = | Version |

2.3.4.10 SPICE Files

The file naming convention CRISM-generated SPICE kernels is as follows.

MRO_CRISM_(KernelType)_(YYYY_DOY)_(Filetype)_(version).(Ext)

where:

Kernel Type =

FK (frames kernel)

IK (instrument kernel)

CK (gimbal C-kernel)

MK (metakernel)

YYYY_DOY is the year and day of year of the start of a 2-week period covered in a single gimbal C kernel or metakernel; or else these fields are filled with zeroes

filetype =

P for predicted

R for reconstructed

N for not applicable

version = 0, 1,...,9, a, ..., z

Ext =

TI (text-format, instrument kernel)

TF (text-format, frames kernel)
BC (binary-format, gimbal C kernel)
BO (binary-format, gimbal offset C kernel)
TM (text-format, metakernel)

2.3.4.11 *Extra Products*

Files that document the history of instrument software settings have a format and nomenclature like that of level 6 CDRs, as described in section 2.3.4.8.

The file naming convention for the macro dictionary is as follows.

MacroDict(YYYYMMDD).PY

where:

YYYYMMDD = year, month, and day of the last onground revision of the macro dictionary

The file naming convention for the description of the image data generated by each macro is as follows.

MacroDict(YYYYMMDD)_BURSTS.CSV

The file naming convention for the summary of each macro's function is as follows.

MacroDict(YYYYMMDD)_SUM.CSV

The nomenclature of tables that connect specific observations with regions of interest on Mars, science objectives, and specific observation conditions is described in Table 2-14. For the SITE_ID, ANCILLARY, REQ_ID, and CORRESP tables may be one table for the mission, and the string YYYY_MM_DD is the date of the last update. For the OBS_ID table, there are multiple tables, as indicated by YYYY_MM_00 for the year and month included in the table.

Table 2-14. Nomenclature of Observation Tracking Tables

| File Name | File Contents |
|-------------------------------------|--|
| SITE_ID_YYYY_MM_DD.TAB | OPTIONAL: Description of the locations and physical features of sites of interest on Mars, compiled by the CRISM science team. Date is last update. |
| SITE_ID_YYYY_MM_DD.HDR | OPTIONAL: Header record to site ID table. |
| SITE_ID_YYYY_MM_DD.LBL | OPTIONAL: Label to site ID table. |
| ANCILLARY_YYYY_MM_DD.TAB | OPTIONAL: Tabulated statistics on physical properties of sites of interest on Mars, compiled by the CRISM science team . Date is last update. |
| ANCILLARY_YYYYMMDD.HDR | OPTIONAL: Header record to ancillary information table. |
| ANCILLARY_YYYYMMDD.LBL | OPTIONAL: Label to ancillary information table. |
| REQ_ID_MC##- ####_YYYY_MM_DD.TAB | OPTIONAL: A table of request IDs, with one or more entries, specifying the desired observing conditions such as Ls. One table per site ID (MC## ####). |
| REQ_ID_MC##- ####_YYYY_MM_DD.HDR | OPTIONAL: Generic header record to request ID tables. |
| REQ_ID_MC##- ####_YYYY_MM_DD.LBL | OPTIONAL: Label to request ID tables. |
| OBS_ID_YYYY_MM_DD.TAB | Table summarizing the date and characteristics of each observation actually taken. |
| OBS_ID_YYYY_MM_DD.HDR | Header record to observation ID table. |
| OBS_ID_YYYY_MM_DD.LBL | Label to observation ID table. |
| CORRESP_YYYY_MM_DD.TAB | OPTIONAL: Correspondence table in which one line gives a site ID, request ID, and target ID where there is geographic overlap. |
| CORRESP_YYYY_MM_DD.HDR | OPTIONAL: Header record to correspondence table. |
| CORRESP_YYYY_MM_DD.LBL | OPTIONAL: Label to correspondence table. |

2.4 Standards Used in Generating Data Products

2.4.1 PDS Standards

The CRISM data product complies with the PDS standards for file formats and labels, specifically the PDS image and table data objects [Applicable Documents 6 and 7].

2.4.2 Time Standards

Two time standards are used in CRISM data products:

- spacecraft time in seconds (PDS label keywords SPACECRAFT_CLOCK_START_COUNT and SPACECRAFT_CLOCK_STOP_COUNT)
- UTC (PDS label keywords START_TIME, STOP_TIME, and PRODUCT_CREATION_TIME)

One additional time-related field is used in CRISM data products:

- target ID, which is a unique identifier associated with each MRO observation (PDS label keyword OBSERVATION_ID)

2.4.3 Coordinate Systems

The cartographic coordinate system used for the CRISM data products conforms to the IAU planetocentric system with East longitudes being positive. The IAU2000 reference system [7] for Mars cartographic coordinates and rotational elements was used for computing latitude and longitude coordinates.

2.5 Data Validation

Data validation is an iterative process throughout the history of processing the data set. Key steps in the process are given below.

2.5.1 EDR level

For each observation, every EDR is compared against frame-by-frame predictions of commanded instrument state. The results of the comparison are written as a data validation report that accompanies the EDRs for that observation.

In the case of a hardware or configuration discrepancy (shutter position, lamp status or level, pixel binning, frame rate, channel selection, power status of detectors), processing of the image data to RDR level does not occur in order to avoid introducing invalid results. Missing frames or portions of frames are replaced with a value of 65535 (this cannot be a valid data value) and only that portion of the EDR is not further processed.

If an expected calibration data set (background, focal plane lamp, or sphere) is not successfully acquired and downloaded, the next closest in time calibration can be used. In this case there is a discrepancy between the predicted EDR processing table and the actual one, and this is recorded in the data quality index upon processing of the scene EDR to the TRDR level.

2.5.2 EDR to RDR level

A data quality keyword is used to encode Figures-of-Merit into one parameter that is included in each line of the list file with the EDR and TRDR. This begins with the EDR and is modified in the TRDR. At the EDR level, missing data, saturation, and basic hardware status are assessed.

At the TRDR level there is the additional option (not currently implemented) to add further information: whether a target's latitude and longitude are within the boundaries of an observation, for the central swath of a targeted observation; whether underexposure occurred; usage of temporally non-adjacent calibration files (due to loss of data from a background, bias, or sphere macro); or high spectrometer housing or detector temperature is flagged. Once the

summary product backplanes are derived, an excessive violet I/F can be flagged as a possible indication of water ice clouds.

The 16-byte data quality field is interpreted as follows:

Byte 0: populated in EDR; 1 = focal planes not properly powered; 0 = focal planes properly powered;

Byte 1: populated in EDR; updated in RDR; 1 = saturated data (8-bit 255; 12-bit 4095; or within 10% of 14-bit saturation) present outside of bad pixel mask; 0 = saturated data not present;

Byte 2: populated in EDR; 1 = missing data (some pixels populated with 65535); 0 = no missing data;

Byte 3: populated in EDR; 1 = shutter out of commanded position; 0 = shutter in position;

Byte 4: populated in EDR; 1 = focal plane lamp setting out of commanded range; 0 = focal plane lamp setting in commanded range;

Byte 5: populated in EDR; 1 = sphere goal out of commanded range; 0 = sphere goal in commanded range;

Byte 6: populated in EDR; 1 = more lines or bands than expected; 0 = not more than expected;

Byte 7: populated in RDR; 1 = VNIR detector out of calibrated temperature range; 0 = VNIR detector within calibrated temperature range

(Byte 8: populated in RDR; 1 = IR detector out of calibrated temperature range; 0 = IR detector within calibrated temperature range)

(Byte 9: populated in RDR; 1 = sphere temperature out of calibrated range; 0 = temperature sphere within calibrated range)

(Byte 10: populated in RDR; 1 = spectrometer housing temperature $>-75^{\circ}\text{C}$; 0 = spectrometer housing temperature $\leq -75^{\circ}\text{C}$)

(Byte 11: populated in RDR; 1 = target not covered; 0 = target covered)

(Byte 12: populated in RDR; 1 = non-adjacent calibration files used; 0 = temporally adjacent calibration files used;)

(Byte 13: populated in RDR; 1 = violet I/F from summary product backplane suggests clouds or ice, value >0.1 ; 0 = low violet I/F)

Byte 14 through Byte 15 spare

Missing frames or portions of frames or saturated data are indicated in an RDR with a value of 65535 (this cannot be a valid data value).

2.5.3 RDR level

Once data are calibrated to units of radiance, some of the pixels that are present in an EDR cannot have meaningful values. These include the regions at the edge of each detector which contain background measurements that are used during application of the calibration algorithm

(see Appendix L). Those pixels are set to a value of exactly 65535, which cannot have a meaningful significant in the units used for radiance or I/F.

3. DETAILED DATA PRODUCT SPECIFICATIONS

3.1 EDR

3.1.1 Data Product Structure and Organization

At the SOC, EDRs are constructed from each observation with a distinct observation ID. An EDR consists of a part or all of the output from one of the constituent command macros that make up one observation tagged by a unique observation ID. The data in one EDR represent a consistent instrument configuration (shutter position, frame rate, pixel binning, compression, exposure time, on/off status and setting of different lamps). This is shown schematically in Figure 3-1. There is a single multiple-band image (suffix *.IMG) stored in one file, plus a detached list file in which each record has information specific to one frame of the multiple-band image (suffix *.TAB). One label points to both files.

The multiple-band image has dimensions of sample, line, and wavelength. The size of the multiple-band image varies according to the observation mode but is deterministic given the macro ID. A typical multiple-band image might have XX pixels in the sample (cross-track) dimension, YY pixels in the line (along-track) dimension, and ZZ pixels in the wavelength dimension, where

- XX=640/binning, where 640 is the number of columns read off the detector, and binning is 1, 2, 5, or 10,
- YY=the number of frames of data with a consistent instrument configuration , and
- ZZ=the number of detector rows (wavelengths) that are retained by the instrument.

Pixels are 16-bit unsigned integer values, most significant bit first.

Appended to the multiple-band image is a binary table of the detector rows that were used, as selected by the wavelength filter. This is a one-column table, with each row containing one detector row number expressed as a 16-bit unsigned integer values, most significant bit first.

Data are not precisely registered in the spectral direction. For one column, the projection onto Mars' surface may vary by as much as ± 0.4 detector elements in the XX dimension depending on position in the FOV (distortions are worst at the edges of the VNIR and IR FOVs). For a single wavelength, its location in the ZZ direction may vary by as much as ± 1 detector element depending on wavelength (distortions are worst at the short- and long-wavelength ends of the IR detector).

The detached comma-separated ASCII file is YY lines in length, containing raw instrument housekeeping plus other frame dependent information. Locations of the temperature sensors and heaters whose states are reported in the housekeeping are shown in Appendix M.

Most of the contents of an EDR represent unmodified but rearranged values from the data stream. The data stream downlinked by the spacecraft unpacks into a succession of image-like frames with binary headers containing housekeeping (Table 3-2). For each focal plane, there are 220 housekeeping items that contain full status of the instrument hardware, including data

configuration, lamp and shutter status, gimbal position, a time stamp, and the target ID and macro within which the frame of data was taken.

To convert to an EDR format, the headers are stripped off and placed into the list file in text form, and the frames are merged into a multiple-band image. The list file is based on the 220 housekeeping items. 5 of the items are composite in that each bit of a 32-bit word encodes particular information on gimbal status or control. These separate items are not broken out, except for the gimbal status at the beginning, middle, and end of each exposure, from which gimbal position is broken out (3 additional items). The housekeeping is pre-pended with spaces for 10 additional frame-specific items useful in data validation, processing, and sorting, for a total of 233 items per frame. Not all of the 10 additional items may be populated:

- A data quality parameter produced during data validation, as discussed in section 2.5
- L_s , degrees
- Solar distance, km
- Time of day at center of FOV, hhmm.ss with 1 Mars solar day = 2400.00
- Preliminary latitude at center of FOV, degrees
- Preliminary longitude at center of FOV, degrees
- Preliminary i (incidence angle) at center of FOV, degrees
- Preliminary e (emission angle) at center of FOV, degrees
- Preliminary g (phase angle) at center of FOV, degrees
- Predicted dust opacity, unitless

The pointing and geometric information is derived from spacecraft positions and quaternions plus the gimbal position. Predicted dust opacity is interpolated from an ADR .

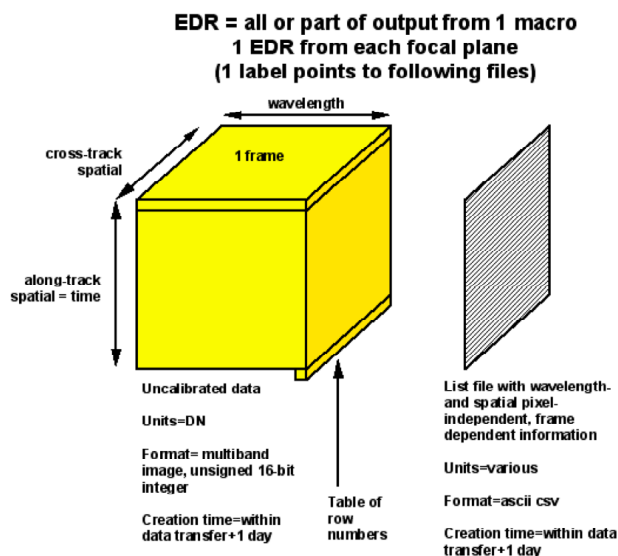


Figure 3-1. Contents of a CRISM Experiment Data Record (EDR).

Table 3-2. Items in housekeeping list file

| Column | Mnemonic | Description | Source of information | Length (bytes) | Format (and range if applicable) | Notes |
|--------|-------------------------|--|---------------------------------------|----------------|---|-------|
| 1 | DATA_QUALITY_CODE | Data quality | Added parameter | 16 | Integer | 1,2 |
| 2 | SOLAR_LONGITUDE | LS | Added parameter | 7 | Float | 1,2 |
| 3 | SOLAR_DISTANCE | Solar distance | Added parameter | 12 | Float | 1,2 |
| 4 | LOCAL_TIME | Local time (hh:mm:ss) | Added parameter | 7 | Character | 1,2 |
| 5 | CENTER_LATITUDE | Estimated latitude | Added parameter | 7 | Float | 1,2 |
| 6 | CENTER_LONGITUDE | Estimated longitude | Added parameter | 7 | Float | 1,2 |
| 7 | CENTER_INCIDENCE_ANGLE | Estimated incidence angle | Added parameter | 7 | Float | 1,2 |
| 8 | CENTER_EMISSION_ANGLE | Estimated emission angle | Added parameter | 7 | Float | 1,2 |
| 9 | CENTER_PHASE_ANGLE | Estimated phase angle | Added parameter | 7 | Float | 1,2 |
| 10 | PREDICTED_DUST_OPACITY | Predicted dust opacity | Added parameter | 5 | Float | 1,2 |
| 11 | SYNCHRONIZATION_PATTERN | Synchronization pattern | Spectrometer Image Header | 10 | Integer; valid value 4277809352 | 1,3 |
| 12 | DATATYPE | Type of data (0 for image data; 1 for encoder diagnostics) | Spectrometer Image Header | 5 | Integer | 1,3 |
| 13 | NUMLINES | Amount of image data sent (lines, 0 - 480) | Spectrometer Image Header | 3 | Integer | 1,3 |
| 14 | EXPOSURE_MET | Spacecraft time of exposure, in spacecraft clock units | Spectrometer Image Header | 10 | Integer | 1,3 |
| 15 | EXPOSURE_SS | Time of exposure fractional second ($1/2^{16}$ seconds) | Spectrometer Image Header | 5 | Integer | 1,3 |
| 16 | SCAN_MOTOR_STATUS1 | Scan motor status word 1 | Spectrometer Image Header | 16 | Character; see Table 3-3 for significance of each character | 1,3 |
| 17 | SCAN_MOTOR_STATUS2 | Scan motor status word 2 | Spectrometer Image Header | 16 | Character; see Table 3-3 for significance of each character | 1,3 |
| 18 | SCAN_MOTOR_STATUS3 | Scan motor status word 3 | Spectrometer Image Header | 16 | Character; see Table 3-3 for significance of each character | 1,3 |
| 19 | SCAN_MOTOR_ENCPOS1 | Angular position of gimbal, beginning of frame | Derived from scan motor status word 1 | 8 | Integer | 1,3 |
| 20 | SCAN_MOTOR_ENCPOS2 | Angular position of gimbal, middle of frame | Derived from scan motor status word 2 | 8 | Integer | 1,3 |
| 21 | SCAN_MOTOR_ENCPOS3 | Angular position of gimbal, end of frame | Derived from scan motor status word 3 | 8 | Integer | 1,3 |
| 22 | SPECT_ID | Spectrometer identifier | Spectrometer Image Header | 1 | Integer; 0 = IR, 1 = VNIR | 1,3 |
| 23 | TEMP_MON | Temperature monitoring enabled or disabled | Spectrometer Image Header | 1 | Integer; 0 = Off, 1 = On | 1,3 |
| 24 | EXPOSURE | Exposure time parameter; number of $1/480$ ths of inverse frame rate; specified separately for each detector | Spectrometer Image Header | 3 | 0 - 480 | 1,3 |

| Column | Mnemonic | Description | Source of information | Length (bytes) | Format (and range if applicable) | Notes |
|--------|----------------------|---|---------------------------|----------------|---|-------|
| 25 | RATE | Rate of frame acquisition; 0 = 1 Hz; 1 = 3.75 Hz; 2 = 5 Hz; 3 = 15 Hz; 4 = 30 Hz | Spectrometer Image Header | 1 | Integer; 0-4 | 1,3 |
| 26 | SOURCE | Data source, either actual detector or a test pattern | Spectrometer Image Header | 1 | Integer; 0 = Detector, 1 - 7 = Test pattern | 1,3 |
| 27 | FILTER | Wavelength filter; which onboard table is used to define which detector rows are recorded | Spectrometer Image Header | 1 | Integer; 0 – 3 | 1,3 |
| 28 | BINNING | Pixel binning mode; 0 = 1:1, 1 = 2:1, 2 = 5:1, 3 = 10:1 | Spectrometer Image Header | 1 | Integer; 0 – 3 | 1,3 |
| 29 | LOSSY | Enable/disable lossy compression | Spectrometer Image Header | 1 | Integer; 0 = Disable, 1 = Enable | 1,3 |
| 30 | FAST | Enable/disable Fast compression | Spectrometer Image Header | 1 | Integer; 0 = Disable, 1 = Enable | 1,3 |
| 31 | DPU_BOARD_TEMP | DPU_PWR_0 (DPU power board temperature) | Analog Status | 5 | Integer | 1,4 |
| 32 | DPU_P5_VOLTAGE | DPU_PWR_1 (DPU +5 voltage) | Analog Status | 5 | Integer | 1,4 |
| 33 | DPU_P5_CURRENT | DPU_PWR_3 (DPU +5 current) | Analog Status | 5 | Integer | 1,4 |
| 34 | SCAN_MOT_CURR | DPU_PWR_4 (Scan motor current) | Analog Status | 5 | Integer | 1,4 |
| 35 | IR_BOARD_TEMP | IR_PWR_0 (IR power board temperature) | Analog Status | 5 | Integer | 1,4 |
| 36 | IR_FPU_P12_VOLTAGE | IR_PWR_1 (IR focal plane unit [FPU] +12 voltage) | Analog Status | 5 | Integer | 1,4 |
| 37 | IR_FPU_P7_VOLTAGE | IR_PWR_2 (IR FPU +7 voltage) | Analog Status | 5 | Integer | 1,4 |
| 38 | IR_FPU_CURRENT | IR_PWR_3 (IR FPU current) | Analog Status | 5 | Integer | 1,4 |
| 39 | HEATER_34_CURRENT | IR_PWR_4 (Heater 3 & 4 current) | Analog Status | 5 | Integer | 1,4 |
| 40 | VNIR_BOARD_TEMP | VNIR_PWR_0 (VNIR power board temperature) | Analog Status | 5 | Integer | 1,4 |
| 41 | VNIR_FPU_P12_VOLTAGE | VNIR_PWR_1 (VNIR FPU +12 voltage) | Analog Status | 5 | Integer | 1,4 |
| 42 | VNIR_FPU_P7_VOLTAGE | VNIR_PWR_2 (VNIR FPU +7 voltage) | Analog Status | 5 | Integer | 1,4 |
| 43 | VNIR_FPU_CURRENT | VNIR_PWR_3 (VNIR FPU current) | Analog Status | 5 | Integer | 1,4 |
| 44 | HEATER_12_CURRENT | VNIR_PWR_4 (Header 1 & 2 current) | Analog Status | 5 | Integer | 1,4 |
| 45 | COOL_BOARD_TEMP | COOL_PWR_0 (Cooler power board temperature) | Analog Status | 5 | Integer | 1,4 |
| 46 | COOL_P15_VOLTAGE | COOL_PWR_1 (Cooler +15 voltage) | Analog Status | 5 | Integer | 1,4 |
| 47 | COOL_CURRENT | COOL_PWR_3 (Cooler current) | Analog Status | 5 | Integer | 1,4 |
| 48 | HOP_HEATER_12_CURR | COOL_PWR_4 (High-output paraffin actuator [HOP] heater 1 & 2 current) | Analog Status | 5 | Integer | 1,4 |

| Column | Mnemonic | Description | Source of information | Length (bytes) | Format (and range if applicable) | Notes |
|--------|------------------------|--|-----------------------|----------------|----------------------------------|-------|
| 49 | SHUT_MOTOR_CURR_IR | IR_FP_0 (Shutter motor current (IR)) | Analog Status | 5 | Integer | 1,4 |
| 50 | IR_DETECTOR_TEMP1 | IR_FP_1 (IR detector temperature 1) | Analog Status | 5 | Integer | 1,4 |
| 51 | IR_DETECTOR_TEMP2 | IR_FP_2 (IR detector temperature 2) | Analog Status | 5 | Integer | 1,4 |
| 52 | COOLER_TEMP1 | IR_FP_3 (Cooler temperature 1) | Analog Status | 5 | Integer | 1,4 |
| 53 | COOLER_TEMP2 | IR_FP_4 (Cooler temperature 2) | Analog Status | 5 | Integer | 1,4 |
| 54 | COOLER_TEMP3 | IR_FP_5 (Cooler temperature 3) | Analog Status | 5 | Integer | 1,4 |
| 55 | SHUT_MOTOR_TEMP_IR | IR_FP_6 (Shutter motor temperature (IR)) | Analog Status | 5 | Integer | 1,4 |
| 56 | SPHERE_TEMP_IR | IR_FP_7 (Integrating sphere temperature (IR)) | Analog Status | 5 | Integer | 1,4 |
| 57 | SPIDER_TEMP_IR | IR_FP_8 (Telescope spider temperature (IR)) | Analog Status | 5 | Integer | 1,4 |
| 58 | SPECT_CAVITY_TEMP_IR | IR_FP_9 (Spectral cavity temperature (IR)) | Analog Status | 5 | Integer | 1,4 |
| 59 | OSU_CAVITY_TEMP_IR | IR_FP_10 (OSU cavity temperature (IR)) | Analog Status | 5 | Integer | 1,4 |
| 60 | IR_FPU_BOARD_TEMP | IR_FP_11 (IR FPU board temperature) | Analog Status | 5 | Integer | 1,4 |
| 61 | IR_SPHERE_CURR | IR_FP_12 (IR sphere lamp current) | Analog Status | 5 | Integer | 1,4 |
| 62 | HOP_TEMP_IR | IR_FP_13 (HOP temperature (IR)) | Analog Status | 5 | Integer | 1,4 |
| 63 | SHUT_MOTOR_CURR_VNIR | VNIR_FP_0 (Shutter motor current (VNIR)) | Analog Status | 5 | Integer | 1,4 |
| 64 | VNIR_DETECTOR_TEMP1 | VNIR_FP_1 (VNIR detector temperature 1) | Analog Status | 5 | Integer | 1,4 |
| 65 | VNIR_DETECTOR_TEMP2 | VNIR_FP_2 (VNIR detector temperature 2) | Analog Status | 5 | Integer | 1,4 |
| 66 | TELESCOPE_TEMP | VNIR_FP_3 (Telescope temperature (VNIR)) | Analog Status | 5 | Integer | 1,4 |
| 67 | OPTICAL_BENCH_TEMP | VNIR_FP_4 (Optical bench temperature (VNIR)) | Analog Status | 5 | Integer | 1,4 |
| 68 | SPIDER_TEMP_VNIR | VNIR_FP_5 (Telescope spider temp. (VNIR)) | Analog Status | 5 | Integer | 1,4 |
| 69 | SPECT_CAVITY_TEMP_VNIR | VNIR_FP_6 (Spectral cavity temperature (VNIR)) | Analog Status | 5 | Integer | 1,4 |
| 70 | OSU_CAVITY_TEMP_VNIR | VNIR_FP_7 (OSU cavity temperature (VNIR)) | Analog Status | 5 | Integer | 1,4 |
| 71 | VNIR_FPU_BOARD_TEMP | VNIR_FP_8 (VNIR FPU board temperature) | Analog Status | 5 | Integer | 1,4 |
| 72 | BAFFLETEMP | VNIR_FP_9 (Baffle temperature (VNIR)) | Analog Status | 5 | Integer | 1,4 |
| 73 | SCAN_PWR | Scan motor power | Digital Status | 1 | Integer; 0 = Off, 3 = On | 1,5 |
| 74 | IR_PRI_PWR | IR FPU primary power | Digital Status | 1 | Integer; 0 = Off, 1 = On | 1,5 |
| 75 | HTR3_PWR | Heater 3 (on cooler radiator) power | Digital Status | 1 | Integer; 0 = Off, 1 = On | 1,5 |

| Column | Mnemonic | Description | Source of information | Length (bytes) | Format (and range if applicable) | Notes |
|--------|--------------------|--|-----------------------|----------------|---|-------|
| 76 | HTR4_PWR | Heater 4 (on spectrometer housing) power | Digital Status | 1 | Integer; 0 = Off, 1 = On | 1,5 |
| 77 | VNIR_PRI_PWR | VNIR FPU primary power | Digital Status | 1 | Integer; 0 = Off, 1 = On | 1,5 |
| 78 | HTR1_PWR | Heater 1 (on gimbal electronics housing) power | Digital Status | 1 | Integer; 0 = Off, 1 = On | 1,5 |
| 79 | HTR2_PWR | Heater 2 (on gimbal electronics housing) power | Digital Status | 1 | Integer; 0 = Off, 1 = On | 1,5 |
| 80 | COOL_PRI_PWR | Cooler primary power | Digital Status | 1 | Integer; 0 = Off, 1 = On | 1,5 |
| 81 | HOP_HTR1_PWR | HOP heater 1 power | Digital Status | 1 | Integer; 0 = Off, 1 = On | 1,5 |
| 82 | HOP_HTR2_PWR | HOP heater 2 power | Digital Status | 1 | Integer; 0 = Off, 1 = On | 1,5 |
| 83 | COVER_TELLTALE_PWR | Imager cover telltale power | Digital Status | 1 | Integer; 0 = Off, 1 = On | 1,5 |
| 84 | COVER_TELLTALE | Cover Telltale | Digital Status | 1 | Integer; 0 = Not closed, 1 = Closed | 1,5 |
| 85 | IR_COOL1_LEVEL | IR Cooler 1 level | Digital Status | 4 | Integer; 0 - 4095 | 1,5 |
| 86 | IR_COOL2_LEVEL | IR Cooler 2 level | Digital Status | 4 | Integer; 0 - 4095 | 1,5 |
| 87 | IR_COOL3_LEVEL | IR Cooler 3 level | Digital Status | 4 | Integer; 0 - 4095 | 1,5 |
| 88 | IR_FLOOD1_LEVEL | IR flood lamp 1 level | Digital Status | 4 | Integer; 0 - 4095 | 1,5 |
| 89 | IR_FLOOD2_LEVEL | IR flood lamp 2 level | Digital Status | 4 | Integer; 0 - 4095 | 1,5 |
| 90 | IR_SPHERE_GOAL | Sphere lamp 1 closed-loop goal (IR) | Digital Status | 4 | Integer; 0 - 4095 | 1,5 |
| 91 | IR_SPHERE_LEVEL | Sphere lamp 1 level (IR); relevant to open-loop operation only | Digital Status | 4 | Integer; 0 - 4095 | 1,5 |
| 92 | IR_SOURCE | IR data source, either actual detector or a test pattern | Digital Status | 1 | Integer; 0 = Detector, 1 - 7 = Test pattern | 1,5 |
| 93 | IR_SHUT_LED | Shutter fiducial light-emitting diode (LED) power (IR) | Digital Status | 1 | Integer; 0 = Off, 1 = On | 1,5 |
| 94 | IR_SPHERE_PWR | Sphere lamp 1 power (IR) | Digital Status | 1 | Integer; 0 = Off, 1 = On | 1,5 |
| 95 | IR_FLOOD1_PWR | IR flood lamp 1 power | Digital Status | 1 | Integer; 0 = Off, 1 = On | 1,5 |
| 96 | IR_FLOOD2_PWR | IR flood lamp 2 power | Digital Status | 1 | Integer; 0 = Off, 1 = On | 1,5 |
| 97 | IR_COOL1_PWR | IR cooler 1 power | Digital Status | 1 | Integer; 0 = Off, 1 = On | 1,5 |
| 98 | IR_COOL2_PWR | IR cooler 2 power | Digital Status | 1 | Integer; 0 = Off, 1 = On | 1,5 |
| 99 | IR_COOL3_PWR | IR cooler 3 power | Digital Status | 1 | Integer; 0 = Off, 1 = On | 1,5 |
| 100 | IR_LVDS_1 | IR low-voltage differential signal (LVDS) driver #1 enable | Digital Status | 1 | Integer; 0 = Disable, 1 = Enable | 1,5 |
| 101 | IR_LVDS_2 | IR LVDS driver #2 enable | Digital Status | 1 | Integer; 0 = Disable, 1 = Enable | 1,5 |
| 102 | IR_DAC_POWER | IR digital-to-analog converter (DAC) power (for coolers and lamps) | Digital Status | 1 | Integer; 0 = Off, 1 = On | 1,5 |
| 103 | IR_DAC_PD | IR DAC power down | Digital Status | 1 | Integer; 0 = Run, 1 = Power down | 1,5 |

| Column | Mnemonic | Description | Source of information | Length (bytes) | Format (and range if applicable) | Notes |
|--------|-------------------------------|---|-----------------------|----------------|----------------------------------|-------|
| 104 | IR_ANA_5V_PWR | IR analog 5V power | Digital Status | 1 | Integer; 0 = Off, 1 = On | 1,5 |
| 105 | IR_ADC_Q1_PWR | IR detector quadrant #1 analog-to-digital converter (ADC, or A/D) power | Digital Status | 1 | Integer; 0 = Off, 1 = On | 1,5 |
| 106 | IR_ADC_Q2_PWR | IR detector quadrant #2 A/D power | Digital Status | 1 | Integer; 0 = Off, 1 = On | 1,5 |
| 107 | IR_ADC_Q3_PWR | IR detector quadrant #3 A/D power | Digital Status | 1 | Integer; 0 = Off, 1 = On | 1,5 |
| 108 | IR_ADC_Q4_PWR | IR detector quadrant #4 A/D power | Digital Status | 1 | Integer; 0 = Off, 1 = On | 1,5 |
| 109 | IR_BIAS_PWR | IR detector bias power | Digital Status | 1 | Integer; 0 = Off, 1 = On | 1,5 |
| 110 | IR_AMP_HI_PWR | IR detector amp high power | Digital Status | 1 | Integer; 0 = Off, 1 = On | 1,5 |
| 111 | IR_CLOCK_DRIVE | IR detector clock driver | Digital Status | 1 | Integer; 0 = Off, 1 = On | 1,5 |
| 112 | IR_COOLER_TEMP3_CONV | IR cooler temperature 3 conversion enable; disabling turns off power to temperature sensor in case of introduced noise in detector | Digital Status | 1 | Integer; 0 = Disable, 1 = Enable | 1,5 |
| 113 | IR_COOLER_TEMP2_CONV | IR cooler temperature 2 conversion enable; disabling turns off power to temperature sensor in case of introduced noise in detector | Digital Status | 1 | Integer; 0 = Disable, 1 = Enable | 1,5 |
| 114 | IR_COOLER_TEMP1_CONV | IR cooler temperature 1 conversion enable; disabling turns off power to temperature sensor in case of introduced noise in detector | Digital Status | 1 | Integer; 0 = Disable, 1 = Enable | 1,5 |
| 115 | IR_TEMP2_CONV | IR detector temperature 2 conversion enable; disabling turns off power to temperature sensor in case of introduced noise in detector | Digital Status | 1 | Integer; 0 = Disable, 1 = Enable | 1,5 |
| 116 | IR_TEMP1_CONV | IR detector temperature 1 conversion enable; disabling turns off power to temperature sensor in case of introduced noise in detector | Digital Status | 1 | Integer; 0 = Disable, 1 = Enable | 1,5 |
| 117 | IR_SHUTTER_MOTOR_CURRENT_CONV | Shutter motor current conversion enable (IR); disabling turns off power to current sensor in case of introduced noise in detector | Digital Status | 1 | Integer; 0 = Disable, 1 = Enable | 1,5 |
| 118 | IR_MUX_TEMP_CONV | IR multiplexed (MUX) temperature conversion enable; disabling turns off power to temperature sensor in case of introduced noise in detector | Digital Status | 1 | Integer; 0 = Disable, 1 = Enable | 1,5 |
| 119 | IR_SHUT_ENB | Shutter motor phase enabled (IR) | Digital Status | 1 | Integer; 0 - 3 | 1,5 |

| Column | Mnemonic | Description | Source of information | Length (bytes) | Format (and range if applicable) | Notes |
|--------|-------------------|--|-----------------------|----------------|---|-------|
| 120 | IR_SHUT_PHASE | Shutter motor phase (IR) | Digital Status | 1 | Integer; 0 - 3 | 1,5 |
| 121 | IR_DAC_STATE | IR DAC power state | Digital Status | 1 | Integer; 0 = Off, 1 = On | 1,5 |
| 122 | IR_SHUT_FID | Shutter fiducial LED (IR) | Digital Status | 1 | Integer; 0 = Off, 1 = On (fiduciated) | 1,5 |
| 123 | IR_ADC_Q1_STATE | IR detector quadrant #1 A/D latch-up | Digital Status | 1 | Integer; 0 = Ok, 1 = Latched | 1,5 |
| 124 | IR_ADC_Q2_STATE | IR detector quadrant #2 A/D latch-up | Digital Status | 1 | Integer; 0 = Ok, 1 = Latched | 1,5 |
| 125 | IR_ADC_Q3_STATE | IR detector quadrant #3 A/D latch-up | Digital Status | 1 | Integer; 0 = Ok, 1 = Latched | 1,5 |
| 126 | IR_ADC_Q4_STATE | IR detector quadrant #4 A/D latch-up | Digital Status | 1 | Integer; 0 = Ok, 1 = Latched | 1,5 |
| 127 | VNIR_FLOOD1_LEVEL | VNIR flood lamp 1 level | Digital Status | 4 | Integer; 0 - 4095 | 1,5 |
| 128 | VNIR_FLOOD2_LEVEL | VNIR flood lamp 2 level | Digital Status | 4 | Integer; 0 - 4095 | 1,5 |
| 129 | VNIR_SPHERE_GOAL | Sphere lamp 1 closed-loop goal (VNIR) | Digital Status | 4 | Integer; 0 - 4095 | 1,5 |
| 130 | VNIR_SPHERE_LEVEL | Sphere lamp 1 level (VNIR); relevant to open-loop operation only | Digital Status | 4 | Integer; 0 - 4095 | 1,5 |
| 131 | VNIR_HEATER | VNIR heater | Digital Status | 1 | 0 = Off 1 = On | 1,5 |
| 132 | VNIR_SOURCE | VNIR data source, either actual detector or a test pattern | Digital Status | 1 | 0 = Detector 1 - 7 = Test pattern | 1,5 |
| 133 | VNIR_SHUT_LED | Shutter fiducial LED power (VNIR) | Digital Status | 1 | Integer; 0 = Off, 1 = On | 1,5 |
| 134 | VNIR_SPHERE_PWR | Sphere lamp 2 power (VNIR) | Digital Status | 1 | Integer; 0 = Off, 1 = On | 1,5 |
| 135 | VNIR_FLOOD1_PWR | VNIR flood lamp 1 power | Digital Status | 1 | Integer; 0 = Off, 1 = On | 1,5 |
| 136 | VNIR_FLOOD2_PWR | VNIR flood lamp 2 power | Digital Status | 1 | Integer; 0 = Off, 1 = On | 1,5 |
| 137 | VNIR_LVDS_1 | VNIR LVDS driver #1 enable | Digital Status | 1 | Integer; 0 = Disable, 1 = Enable | 1,5 |
| 138 | VNIR_LVDS_2 | VNIR LVDS driver #2 enable | Digital Status | 1 | Integer; 0 = Disable, 1 = Enable | 1,5 |
| 139 | VNIR_DAC_POWER | VNIR DAC power (for lamps) | Digital Status | 1 | Integer; 0 = Off, 1 = On | 1,5 |
| 140 | VNIR_DAC_PD | VNIR DAC power down | Digital Status | 1 | 0 = Run 1 = Power down | 1,5 |
| 141 | VNIR_ANA_5V_PWR | VNIR analog 5V power | Digital Status | 1 | Integer; 0 = Off, 1 = On | 1,5 |
| 142 | VNIR_ADC_Q1_PWR | VNIR detector quadrant #1 A/D power | Digital Status | 1 | Integer; 0 = Off, 1 = On | 1,5 |
| 143 | VNIR_ADC_Q2_PWR | VNIR detector quadrant #2 A/D power | Digital Status | 1 | Integer; 0 = Off, 1 = On | 1,5 |
| 144 | VNIR_ADC_Q3_PWR | VNIR detector quadrant #3 A/D power | Digital Status | 1 | Integer; 0 = Off, 1 = On | 1,5 |
| 145 | VNIR_ADC_Q4_PWR | VNIR detector quadrant #4 A/D power | Digital Status | 1 | Integer; 0 = Off, 1 = On | 1,5 |
| 146 | VNIR_CHARGE_PUMP | VNIR detector charge pump power | Digital Status | 1 | Integer; 0 = off; 1 = 500 kHz; 2 = 250 kHz; 3 = 125 kHz (default) | 1,5 |
| 147 | VNIR_BIAS_PWR | VNIR detector bias power | Digital Status | 1 | Integer; 0 = Off, 1 = On | 1,5 |

| Column | Mnemonic | Description | Source of information | Length (bytes) | Format (and range if applicable) | Notes |
|--------|---------------------------------|---|-----------------------|----------------|---------------------------------------|-------|
| 148 | VNIR_AMP_HI_PWR | VNIR detector amp high power | Digital Status | 1 | Integer; 0 = Off, 1 = On | 1,5 |
| 149 | VNIR_CLOCK_DRIVE | VNIR detector clock driver | Digital Status | 1 | Integer; 0 = Off, 1 = On | 1,5 |
| 150 | VNIR_TEMP2_CONV | VNIR detector temperature 2 conversion enable; disabling turns off power to temperature sensor in case of introduced noise in detector | Digital Status | 1 | Integer; 0 = Disable, 1 = Enable | 1,5 |
| 151 | VNIR_TEMP1_CONV | VNIR detector temperature 1 conversion enable; disabling turns off power to temperature sensor in case of introduced noise in detector | Digital Status | 1 | Integer; 0 = Disable, 1 = Enable | 1,5 |
| 152 | VNIR_SHUTTER_MOTOR_CURRENT_CONV | Shutter motor current conversion enable (VNIR); disabling turns off power to current sensor in case of introduced noise in detector | Digital Status | 1 | Integer; 0 = Disable, 1 = Enable | 1,5 |
| 153 | VNIR_MUX_TEMP_CONV | VNIR multiplexed temperature conversion enable; disabling turns off power to temperature sensor in case of introduced noise in detector | Digital Status | 1 | Integer; 0 = Disable, 1 = Enable | 1,5 |
| 154 | VNIR_SHUT_ENB | Shutter motor phase enabled (VNIR) | Digital Status | 1 | Integer; 0 - 3 | 1,5 |
| 155 | VNIR_SHUT_PHASE | Shutter motor phase (VNIR) | Digital Status | 1 | Integer; 0 - 3 | 1,5 |
| 156 | VNIR_DAC_STATE | VNIR DAC power state | Digital Status | 1 | Integer; 0 = Off, 1 = On | 1,5 |
| 157 | VNIR_SHUTTER_FID | Shutter fiducial LED (VNIR) | Digital Status | 1 | Integer; 0 = Off, 1 = On (fiduciated) | 1,5 |
| 158 | VNIR_ADC_Q1_STATE | VNIR detector quadrant #1 A/D latch-up | Digital Status | 1 | Integer; 0 = Ok, 1 = Latched | 1,5 |
| 159 | VNIR_ADC_Q2_STATE | VNIR detector quadrant #2 A/D latch-up | Digital Status | 1 | Integer; 0 = Ok, 1 = Latched | 1,5 |
| 160 | VNIR_ADC_Q3_STATE | VNIR detector quadrant #3 A/D latch-up | Digital Status | 1 | Integer; 0 = Ok, 1 = Latched | 1,5 |
| 161 | VNIR_ADC_Q4_STATE | VNIR detector quadrant #4 A/D latch-up | Digital Status | 1 | Integer; 0 = Ok, 1 = Latched | 1,5 |
| 162 | STATUS_INT | Status interval (seconds); interval at which analog digital and software status are reported in status packets to low-speed telemetry | Software Status | 5 | Integer; 1 – 65535 (0 = Off) | 1,6 |
| 163 | MACRO_BLOCKS | Number of macro blocks free | Software Status | 5 | Integer | 1,6 |
| 164 | TLM_VOLUME | Telemetry volume produced (KB) on the low speed engineering channel since the last CRM_STAT_CLR command | Software Status | 5 | Integer | 1,6 |

| Column | Mnemonic | Description | Source of information | Length (bytes) | Format (and range if applicable) | Notes |
|--------|------------------|---|-----------------------|----------------|--|-------|
| 165 | WATCH_ADDR | Memory watch address | Software Status | 5 | Integer | 1,6 |
| 166 | WATCH_MEM_ID | Memory watch id (page no.) | Software Status | 3 | Integer | 1,6 |
| 167 | WATCH_DATA | Watched memory | Software Status | 5 | Integer | 1,6 |
| 168 | SW_VERSION | Software version number | Software Status | 3 | Integer | 1,6 |
| 169 | ALARM_ID | Latest alarm Id | Software Status | 3 | Integer; see Table 3-5 | 1,6 |
| 170 | ALARM_TYPE | Latest alarm type | Software Status | 1 | Integer; 0 = Persistent, 1 = Transient | 1,6 |
| 171 | ALARM_COUNT | Count of alarms since the last CRM_STAT_CLR command | Software Status | 3 | Integer | 1,6 |
| 172 | CMD_EXEC | Commands executed since the last CRM_STAT_CLR command | Software Status | 3 | Integer | 1,6 |
| 173 | CMD_REJECT | Commands rejected since the last CRM_STAT_CLR command | Software Status | 3 | Integer | 1,6 |
| 174 | MAC_CMD_EXEC | Macro commands executed since the last CRM_STAT_CLR command | Software Status | 3 | Integer | 1,6 |
| 175 | MAC_CMD_REJECT | Macro commands rejected since the last CRM_STAT_CLR command | Software Status | 3 | Integer | 1,6 |
| 176 | MAC_ID | ID of most recent macro executed | Software Status | 3 | Integer | 1,6 |
| 177 | MACRO_LEARN | Macro learn mode; in learn mode commands are appended to a macro being loaded to memory; when not in learn mode commands are executed | Software Status | 1 | Integer; 0 = Not learning, 1 = Learning | 1,6 |
| 178 | MONITOR_RESPONSE | Monitor response enabling; if enabled a persistent out-of-limits condition will cause an onboard safing macro to be executed; 0 = disabled; 1 = enabled | Software Status | 1 | Integer; 0 = Disable, 1 = Enable | 1,6 |
| 179 | MEM_WRITE | Memory write enable; required to upload data structures with commandable monitor limits or pixel procesing value | Software Status | 1 | Integer; 0 = Disable, 1 = Enable | 1,6 |
| 180 | IR_SPECTRA | Last value for number of IR spectra to collect | Software Status | 5 | Integer; 0 – 65534 Remaining; 65535: Forever | 1,6 |
| 181 | VNIR_SPECTRA | Last value for number of VNIR spectra to collect | Software Status | 5 | Integer; 0 – 65534 Remaining; 65535: Forever | 1,6 |
| 182 | COOL_1_SETPOINT | Cooler 1 temperature goal; value corresponds to temperature goal for COOLER_TEMP1 | Software Status | 5 | Integer | 1,6 |

| Column | Mnemonic | Description | Source of information | Length (bytes) | Format (and range if applicable) | Notes |
|--------|------------------------|---|-----------------------|----------------|----------------------------------|-------|
| 183 | COOL_2_SETPOINT | Cooler 2 temperature goal; value corresponds to temperature goal for COOLER_TEMP2 | Software Status | 5 | Integer | 1,6 |
| 184 | COOL_3_SETPOINT | Cooler 3 temperature goal; value corresponds to temperature goal for COOLER_TEMP3 | Software Status | 5 | Integer | 1,6 |
| 185 | VNIR_HEATER_GOAL | VNIR heater temperature goal; value corresponds to temperature goal for VNIR_DETECTOR_TEMP1 | Software Status | 5 | Integer | 1,6 |
| 186 | HEATER_1_GOAL | Heater 1 (on gimbal electronics housing) goal; value corresponds to temperature goal for OSU_CAVITY_TEMP_VNIR | Software Status | 5 | Integer | 1,6 |
| 187 | HEATER_2_GOAL | Heater 2 (on gimbal electronics housing) goal; value corresponds to temperature goal for OSU_CAVITY_TEMP_VNIR | Software Status | 5 | Integer | 1,6 |
| 188 | HEATER_3_GOAL | Heater 3 (on cooler radiator) goal; value corresponds to temperature goal for OSU_CAVITY_TEMP_IR | Software Status | 5 | Integer | 1,6 |
| 189 | HEATER_4_GOAL | Heater 4 (on spectrometer housing) goal; value corresponds to temperature goal for SPECT_CAVITY_TEMP_IR | Software Status | 5 | Integer | 1,6 |
| 190 | HEATER_1_HYSTERESIS | Heater 1 (on gimbal electronics housing) hysteresis | Software Status | 3 | Integer | 1,6 |
| 191 | HEATER_2_HYSTERESIS | Heater 2 (on gimbal electronics housing) hysteresis | Software Status | 3 | Integer | 1,6 |
| 192 | HEATER_3_HYSTERESIS | Heater 3 (on cooler radiator) hysteresis | Software Status | 3 | Integer | 1,6 |
| 193 | HEATER_4_HYSTERESIS | Heater 4 (on spectrometer housing) hysteresis | Software Status | 3 | Integer | 1,6 |
| 194 | VNIR_HEATER_HYSTERESIS | VNIR heater hysteresis | Software Status | 3 | Integer | 1,6 |
| 195 | TARGET_ID | Target Id | Software Status | 10 | Integer | 1,6 |
| 196 | TARGET_TIME | Time of target closest approach (whole second component); same scale as EXPOSURE_MET | Software Status | 10 | Integer | 1,6 |
| 197 | TARGET_SUBSECONDS | Time of target fractional second ($1/2^{16}$ seconds) | Software Status | 5 | Integer | 1,6 |
| 198 | PROFILE_ID | Profile Id | Software Status | 5 | Integer; 0 - 1819 | 1,6 |
| 199 | SCAN_STATUS_WORD | Scan motor status word | Software Status | 16 | Character; see Table 3-3 | 1,6 |

| Column | Mnemonic | Description | Source of information | Length (bytes) | Format (and range if applicable) | Notes |
|--------|-------------------|---|-----------------------|----------------|---|-------|
| 200 | SCAN_CONTROL_WORD | Scan motor control word | Software Status | 16 | Character; see Table 3-4 | 1,6 |
| 201 | SLEW_ANGLE | Gimbal angle (μradians) | Software Status | 11 | Integer | 1,6 |
| 202 | OFFSET_ANGLE | Target for offset angle from gimbal profile defined in PROFILE_ID (μradians) | Software Status | 11 | Integer | 1,6 |
| 203 | OFFSET_RATE | Target for offset rate from gimbal profile defined in PROFILE_ID (μradians/s) | Software Status | 11 | Integer | 1,6 |
| 204 | GOAL_ANGLE | Gimbal goal angle from gimbal profile defined in PROFILE_ID (μradians) | Software Status | 11 | Integer | 1,6 |
| 205 | VNIR_HTR_MODE | VNIR heater control mode | Software Status | 1 | Integer; 0 = Off, 1 = On, 2 = Software control | 1,6 |
| 206 | OBSERVE | Observation state | Software Status | 1 | Integer; 0 = Idle, 1 = Observing | 1,6 |
| 207 | OFFSET_ADJUST | Scan offset adjustment | Software Status | 1 | Integer; 0 = Disable, 1 = Enable | 1,6 |
| 208 | HTR_1_MODE | Heater 1 (on gimbal electronics housing) control mode | Software Status | 1 | Integer; 0 = Off; 1 = On; 2 = Software control | 1,6 |
| 209 | HTR_2_MODE | Heater 2 (on gimbal electronics housing) control mode | Software Status | 1 | Integer; 0 = Off; 1 = On; 2 = Software control | 1,6 |
| 210 | HTR_3_MODE | Heater 3 (on cooler radiator) control mode | Software Status | 1 | Integer; 0 = Off; 1 = On; 2 = Software control | 1,6 |
| 211 | HTR_4_MODE | Heater 4 (on spectrometer housing) control mode | Software Status | 1 | Integer; 0 = Off; 1 = On; 2 = Software control | 1,6 |
| 212 | COVER_MODE | Cover deployment mode | Software Status | 1 | Integer; 0 = Disable deployment; 1 = Enable deployment | 1,6 |
| 213 | SCAN_MODE | Scan platform control mode | Software Status | 1 | Integer; 0 = off; 1 = holding; the gimbal is held at the current position; 2 = slewing; the gimbal is moved to a commanded angle; 3 = following a profile; the gimbal follows a computed and uploaded profile; 4 = home; the gimbal searches for its index fiducial | 1,6 |
| 214 | OBS_MAC_ID | Id of most recent observation macro executed | Software Status | 3 | Integer | 1,6 |
| 215 | SHUTTER_POS | Shutter position from 0 to 32 | Software Status | 2 | Integer; 0 - 32; nominal open is 3; viewing sphere is 17; closed is 32 | 1,6 |

| Column | Mnemonic | Description | Source of information | Length (bytes) | Format (and range if applicable) | Notes |
|--------|-------------------|---|-----------------------|----------------|--|-------|
| 216 | SHUTTER_DRIVE | Shutter drive selection; VNIR channel for nominal use; IR is backup; both together is contingency for stuck shutter; | Software Status | 1 | Integer; 0 = IR side; 1 = VNIR side; 2 = both sides | 1,6 |
| 217 | SCAN_LOG_ENB | Scan platform logging enabling; with this enabled requests for spectra return high-rate scan diagnostic data | Software Status | 1 | Integer; 0 = Disable, 1 = Enable | 1,6 |
| 218 | IR_TEMP_MONITOR | IR temperature monitor enable/disable | Software Status | 1 | Integer; 0 = Off, 1 = On | 1,6 |
| 219 | IR_EXPOSE | IR exposure time parameter; number of 1/480ths of inverse frame rate | Software Status | 3 | Integer; 0 - 480 | 1,6 |
| 220 | IR_RATE | IR frame acquisition rate | Software Status | 1 | Integer; 0 = 1 Hz; 1 = 3.75 Hz; 2 = 5 Hz; 3 = 15 Hz; 4 = 30 Hz | 1,6 |
| 221 | VNIR_TEMP_MONITOR | VNIR temperature monitor enable/disable | Software Status | 1 | Integer; 0 = Off, 1 = On | 1,6 |
| 222 | VNIR_EXPOSE | VNIR exposure time parameter; number of 1/480ths of inverse frame rate | Software Status | 3 | Integer; 0 - 480 | 1,6 |
| 223 | VNIR_RATE | VNIR frame acquisition rate | Software Status | 1 | Integer; 0 = 1 Hz; 1 = 3.75 Hz; 2 = 5 Hz; 3 = 15 Hz; 4 = 30 Hz | 1,6 |
| 224 | IR_FILTER | IR wavelength filter table; which onboard table is used to define which detector rows are recorded | Software Status | 1 | Integer; 0 - 3 | 1,6 |
| 225 | IR_BINNING | IR pixel binning mode | Software Status | 1 | Integer; 0 = 1:1, 1 = 2:1, 2 = 5:1, 3 = 10:1 | 1,6 |
| 226 | IR_LOSSY | IR lossy compression enabled or disabled; 12 to 8 bit look-up table commanded line by line in uploaded data structure | Software Status | 1 | Integer; 0 = Disable, 1 = Enable | 1,6 |
| 227 | IR_FAST | Enable/disable IR Fast compression | Software Status | 1 | Integer; 0 = Disable, 1 = Enable | 1,6 |
| 228 | VNIR_FILTER | VNIR wavelength filter table; which onboard table is used to define which detector rows are recorded | Software Status | 1 | Integer; 0 - 3 | 1,6 |
| 229 | VNIR_BINNING | VNIR pixel binning mode | Software Status | 1 | Integer; 0 = 1:1, 1 = 2:1, 2 = 5:1, 3 = 10:1 | 1,6 |
| 230 | VNIR_LOSSY | VNIR lossy compression enabled or disabled; 12 to 8 bit look-up table commanded line by line in uploaded data structure | Software Status | 1 | Integer; 0 = Disable, 1 = Enable | 1,6 |

| Column | Mnemonic | Description | Source of information | Length (bytes) | Format (and range if applicable) | Notes |
|--------|--------------------------|--|-----------------------|----------------|----------------------------------|-------|
| 231 | VNIR_FAST | Enable/disable Fast compression | Software Status | 1 | Integer; 0 = Disable, 1 = Enable | 1,6 |
| 232 | IR_PIXEL_PROC_CHECKSUM | IR pixel processing table CRC-CCITT checksum; the data structure containing gains offsets and which LUT to use is 480 rows and 3 columns; this is the least significant end of the sum and serves as a fingerprint | Software Status | 5 | Integer | 1,6 |
| 233 | VNIR_PIXEL_PROC_CHECKSUM | VNIR pixel processing table CRC-CCITT checksum; the data structure containing gains offsets and which LUT to use is 480 rows and 3 columns; this is the least significant end of the sum and serves as a fingerprint | Software Status | 5 | Integer | 1,6 |

Notes:

- (1) Source of information describes whether information is a value-added field or part of original instrument housekeeping, and if so, the type of housekeeping represented.
- (2) The added parameters represent values calculated in post-processing that are useful to describe frame-dependent data quality, or approximate geometric, lighting, and atmospheric conditions at the time of the observation that are relevant to post-processing corrections.
- (3) The spectrometer image header describes the instrument configuration relevant to an individual frame of data such as exposure time, frame rate, data editing and compression, etc.
- (4) Analog status represents reading of voltage, current and temperature of different components of the CRISM instrument. Monitors are run by different electronics boards in the instrument. The nomenclature is as follows. DPU_PWR_0 represents the 0th status item monitored by the DPU power board, DPU_PWR_1 the 1st, etc. IR_PWR is the IR power board in the DPU. VNIR_PWR is the VNIR power board in the DPU. COOL_PWR is the cooler power board in the DPU. IR_FP is the IR focal plane electronics board in the base of the OSU. VNIR_FP is the VNIR focal plane electronics board in the base of the OSU.
- (5) Digital status represents on/off settings of the instrument, levels of coolers or calibration lamps, or the source of data reported from each focal plane. The source may be measured data from the detector, or one of several tests patterns stored in the focal plane electronics (for diagnostic purposes).
- (6) Software status represents the status of RAM memory, the frequency of housekeeping reporting, the history of commanding, the history of reporting of alarms, commanded setting of coolers and heaters, and the commanded configuration of the instrument (as opposed to the actual configuration reported in the spectrometer image header).

Table 3-3. Bit mapping of scan motor status word

| Name | Length (bits) | Value | Description |
|-------------|---------------|--------------------------------|---------------------------------------|
| Direction | 1 | 0 = Down 1 = Up | Platform direction |
| Index Latch | 1 | 0 = No index 1 = Index seen | Latched (i.e. sticky) index pulse |
| Limit 2 | 1 | 0 = No limit 1 = Limit seen | Latched (i.e. sticky) limit switch #2 |
| Limit 1 | 1 | 0 = No limit 1 = Limit seen | Latched (i.e. sticky) limit switch #1 |
| Inphase | 1 | 0 – 1 | Raw inphase signal |
| Quadrature | 1 | 0 – 1 | Raw quadrature signal |
| Index | 1 | 0 = No index 1 = Index | Raw index signal |
| Hall Sensor | 3 | 0 – 7 | Hall sensors |
| Encoder | 22 | Signed integer | Encoded scan platform position |

Table 3-4. Bit mapping of scan motor control word

| Name | Length (bits) | Value | Description |
|----------------|---------------|-------------------------------|--|
| Enable Counter | 1 | 0 = Disable 1 = Enable | Enable/disable encoder position counter |
| Reset Counter | 1 | 0 = No operation 1 = Reset | Reset (i.e. zero) encoder position counter |
| Reset Index | 1 | 0 = No operation 1 = Reset | Reset index latch |
| Motor Drive | 1 | 0 = Disable 1 = Enable | Enable/disable motor drive |
| Test Clock | 1 | 0 = Disable 1 = Enable | Enable/disable sending external clock (for ground testing) |
| Index Arm | 1 | 0 = No operation 1 = Index | Arm index latch |
| Hall Latch | 1 | 0 = No operation 1 = Latch | Latch Hall inputs |
| Hall Control | 1 | 0 = Automatic 1 = Computer | Enable/disable computer control of Hall outputs |
| Fine Mode | 1 | 0 = Coarse 1 = Fine | Coarse or fine control of motor drive DAC |
| Reset Limits | 1 | 0 = No operation 1 = Reset | Reset limit latches |
| Hall Outputs | 3 | 0 – 7 | Hall outputs |
| Drive | 12 | Signed integer | Motor drive DAC |

Table 3-5. Alarms coded in housekeeping

| ID | Description | Information |
|-------------|--|--------------------|
| 0 | <i>Unused</i> | |
| 1 | Bad packet | 0 |
| 2 | Out of macro contexts | Macro Id |
| 3 ... 15 | <i>Reserved</i> | |
| 16 | Invalid target id | |
| 17 | Scan platform loss of control | |
| 18 ... 127 | <i>Reserved</i> | |
| 128 ... 169 | Monitored value is too low; see Table 3-6 | Value and limit |
| 170 ... 191 | <i>Reserved</i> | |
| 192 ... 233 | Monitored value is too high; see Table 3-6 | Value and limit |
| 234 ... 255 | <i>Reserved</i> | |

Table 3-6. Alarms for monitored housekeeping and responses to out-of-limits conditions

| Source | Alarm Ids Low / High | | Autonomy Macro Executed | |
|-------------------------------------|-------------------------|-----|-------------------------|----------------|
| | | | Value too Low | Value too High |
| DPU power board temperature | 128 | 192 | | |
| DPU +5 voltage | 129 | 193 | | |
| DPU +5 current | 130 | 194 | | |
| Scan motor current 1 & 2 | 131 | 195 | | 10 |
| IR power board temperature | 132 | 196 | | 5 |
| IR FPU +12 voltage | 133 | 197 | | |
| IR FPU +7 voltage | 134 | 198 | | |
| IR FPU current | 135 | 199 | | 5 |
| Heater 3 & 4 current | 136 | 200 | | 12 |
| VNIR power board temperature | 137 | 201 | | 4 |
| VNIR FPU +12 voltage | 138 | 202 | | |
| VNIR FPU +7 voltage | 139 | 203 | | |
| VNIR FPU current | 140 | 204 | | 4 |
| Heater 1 & 2 current | 141 | 205 | | 11 |
| Cooler power board temperature | 142 | 206 | | 8 |
| Cooler +15 voltage | 143 | 207 | | |
| Cooler current | 144 | 208 | | 8 |
| HOP heater 1 & 2 current | 145 | 209 | | 13 |
| Shutter motor current (IR) | 146 | 210 | | 7 |
| IR detector temperature 1 | 147 | 211 | 8 | |
| IR detector temperature 2 | 148 | 212 | 8 | |
| Cooler temperature 1 | 149 | 213 | | 8 |
| Cooler temperature 2 | 150 | 214 | | 8 |
| Cooler temperature 3 | 151 | 215 | | 8 |
| Shutter motor temperature (IR) | 152 | 216 | | |
| Integrating sphere temperature (IR) | 153 | 217 | | |
| Telescope spider temperature (IR) | 154 | 218 | | |
| Spectral cavity temperature (IR) | 155 | 219 | | |
| OSU cavity temperature (IR) | 156 | 220 | | |
| Sphere lamp current (IR) | 157 | 221 | | 14 |
| IR FPU board temperature | 158 | 222 | | 5 |
| HOP temperature (IR) | 159 | 223 | | 13 |
| Shutter motor current (VNIR) | 160 | 224 | | 6 |
| VNIR detector temperature 1 | 161 | 225 | | 15 |
| VNIR detector temperature 2 | 162 | 226 | | 15 |
| Telescope temperature | 163 | 227 | | |
| Optical bench temperature | 164 | 228 | | |
| Telescope spider temp. (VNIR) | 165 | 229 | | |
| Spectral cavity temperature (VNIR) | 166 | 230 | | |
| OSU cavity temperature (VNIR) | 167 | 231 | | |
| VNIR FPU board temperature | 168 | 232 | | 4 |
| Baffle temperature | 169 | 233 | | |

3.1.2 Label Description

Each CRISM EDR is described by a PDS label stored in a separate text file with an extension ".LBL". A PDS label is object-oriented and describes objects in the data file. The PDS label contains keywords for product identification, along with descriptive information needed to interpret or process the data objects in the file.

PDS labels are written in Object Description Language (ODL) [5]. PDS label statements have the form of "keyword = value". Each label statement is terminated with a carriage return character (ASCII 13) and a line feed character (ASCII 10) sequence to allow the label to be read by many operating systems. Pointer statements with the following format are used to indicate the location of data objects:

^object = location

where the carat character (^, also called a pointer) is followed by the name of the specific data object. The location is the name of the file that contains the data object.

The CRISM EDR label is a combined-detached label (see reference 5) that describes both the image and table files that make up a CRISM EDR. An example EDR label is in Appendix A.

EDR label keywords with CRISM-specific values are listed in Table 3-7.

Table 3-7. CRISM-specific values for EDR label keywords

| Keyword | Valid Values |
|------------------------|---|
| PRODUCT_TYPE | EDR |
| OBSERVATION_TYPE | FRT (Full Resolution Targeted Observation) HRL (Half Resolution Long Targeted Observation) HRS (Half Resolution Short Targeted Observation) EPF (Atmospheric Survey EPF) TOD (Tracking Optical Depth Observation) LMB (Limb Scan Observation) MSS (Multispectral Survey, lossy compressed) MSP (Multispectral Survey, losslessly compressed) HSP (Hyperspectral Survey, losslessly compressed) HSV (Hyperspectral Survey, VNIR only) MSW (Multispectral Window) FFC (Flat-field calibration) CAL (Radiometric Calibration) ICL (Calibration source intercalibration) STO (Star Observation) FUN (Functional test) UNK (no valid EDRs within observation that indicate class type) |
| OBSERVATION_ID | 8-byte hexadecimal integer |
| MRO:OBSERVATION_NUMBER | Counter from product ID, hexadecimal |

| Keyword | Valid Values |
|------------------------------|---|
| MRO:ACTIVITY_ID | Type of measurement and macro ID ####used to execute it, i.e.: BI#### – Bias measurement DF#### – Dark field measurement LP#### – Lamp measurement SP#### – Sphere measurement SC#### – Scene measurement T1#### – Focal plane electronics test pattern 1 T2#### – Focal plane electronics test pattern 1 T3#### – Focal plane electronics test pattern 1 T4#### – Focal plane electronics test pattern 1 T5#### – Focal plane electronics test pattern 1 T6#### – Focal plane electronics test pattern 1 T7#### – Focal plane electronics test pattern 1 UN#### – Instrument configuration does not match macro library |
| MRO:FRAME_RATE | "1", "3.75", "5", "15", or "30" |
| MRO:SENSOR_ID | "S" for VNIR, "L" for IR, or "J" for joint |
| SHUTTER_MODE_ID | "OPEN", "SPHERE", OR "CLOSED" |
| LIGHT_SOURCE_NAME | "NONE", "VNIR LAMP 1", "VNIR LAMP 2", "IR LAMP 1", "IR LAMP 1", "SPHERE LAMP 1", "SPHERE LAMP 2" |
| MRO:CALIBRATION_LAMP_STATUS | "OFF", "OPEN LOOP" or "CLOSED LOOP" (for integrating sphere only) |
| MRO:CALIBRATION_LAMP_LEVEL | Value between 0 and 4095 |
| PIXEL_AVERAGING_WIDTH | 1, 2, 5, or 10 |
| COMPRESSION_TYPE | NONE, or 8_BIT |
| MRO:INSTRUMENT_POINTING_MODE | "DYNAMIC POINTING" if SCAN_MODE (housekeeping file column 213) equals 3 ; else "FIXED POINTING" |
| SCAN_MODE_ID | (If DYNAMIC POINTING): "SHORT" (for full-resolution or half-resolution short central swath or limb scan), "LONG" (for half-resolution long central swath), or "EPF" (for EPF even if part of a different class of observation) |
| SAMPLING_MODE_ID | "HYPERSPSCTRAL" if wavelength filter used returns contiguous rows or "MULTISPECTRAL" if not |
| MRO:EXPOSURE_PARAMETER | The value supplied to the CRISM instrument to command the exposure time. At a given frame rate identified in MRO:FRAME_RATE, there are 480 possible exposure times ranging form 1 to 480. |
| MRO:WAVELENGTH_FILTER | Which of four onboard menus of rows was selected for downlink. The four choices are 0, 1, 2, or 3. |

| Keyword | Valid Values |
|----------------------------|--|
| MRO:WAVELENGTH_FILE_NAME | For an EDR, the wavelength file is a 5-column, 480-row text file. The five elements in each row are the row number and a 0 or 1 for each of MRO:WAVELENGTH_FILTER 0, 1, 2 and 3, indicating whether data from that row of the detector is included in the EDR when that option is selected in MRO:WAVELENGTH_FILTER. For a TRDR, the wavelength file is an image whose value at the location of a detector element is the center wavelength of that element, in nanometers. |
| MRO:PIXEL_PROC_FILE_NAME | For an EDR, the name of the ASCII file giving gain and offset to convert from 14 to 12 bits, and LUT used if lossy 12 to 8 bit compression is enabled (3 columns specified on a line-by-line basis) |
| MRO:LOOKUP_TABLE_FILE_NAME | For an EDR, the name of the ASCII file giving the 8-bit outputs from 12-bit inputs for each of the 8 onboard LUTs (8 columns specified for each 12-bit value 0-4095) |

3.2 DDR

3.2.1 Data Product Structure and Organization

The DDR (Figure 3-8) consists of supporting data needed for the post-processing of a TRDR pointed at Mars' surface. There is a one-for-one spatial correspondence of each spatial pixel in a TRDR to each pixel in the DDR. The DDR for an observation is stored separately from the EDR and TRDR to minimize and streamline data product processing and updating. The EDR does not require highly accurate pointing information to construct, which the DDR does. Thus the EDR can be assembled promptly by having it decoupled from the DDR. A change in instrument calibration - not knowledge of its pointing - would require an update of the contents of the radiance portion of a TRDR but not the contents of the DDR. Thus having the DDR decoupled from the TRDR minimizes the amount of reprocessing necessary when knowledge of instrument radiometric characteristics changes.

The DDR contains one multiple-band image. The size of the multiple-band image varies according to the observation mode but is deterministic given the macro ID. A typical multiple-band image might have XX pixels in the sample (cross-track) dimension, YY pixels in the line (along-track) dimension, and ZZ pixels in the wavelength dimension, where:

- XX=640/binning, where 640 is the number of columns read off the detector, and binning is 1, 2, 5, or 10
- YY=the number of frames of data taken by the macro, and
- ZZ=the number layers in the DDR.

Due to optical distortions present in the EDRs and non-resampled TRDRs, not all wavelengths represent exactly the same spatial location. Therefore the spatial location for a DDR represent those of the VNIR band closest to 610 nm and the IR band closest to 2300 nm. There are separate DDRs for VNIR and IR data.

There are 14 layers in the DDR, all represented as 32-bit real numbers. The files are created at approximately 14 days after transfer of target ID files, when sufficiently accurate pointing information is available.

- Solar incidence angle relative to areoid, at same planetary radius as surface projection of pixel, units degrees
- Emission angle relative to areoid, at same planetary radius as surface projection of pixel, units degrees
- Solar phase angle, units degrees
- Areocentric latitude, units degrees N
- Areocentric longitude, units degrees E
- Solar incidence angle relative to planetary surface as estimated using MOLA shape model, units degrees
- Emission angle relative to planetary surface as estimated using MOLA shape model, units degrees
- Slope magnitude, using MOLA shape model and reference ellipsoid, units degrees
- Slope azimuth, using MOLA shape model and reference ellipsoid, units degrees clockwise from N
- Elevation relative to MOLA datum, units meters
- TES thermal inertia, units $\text{J m}^{-2} \text{K}^{-1} \text{s}^{-0.5}$
- TES bolometric albedo
- Local solar time, hours
- Spare

Once image data are assembled into EDRs and calibrated into TRDRs, DDRs are created for the data. A version 0 DDR represents values based on predicted pointing, and is generated to provide quick-look information. Version 1 and subsequent versions of a DDR are based on actual, reconstructed pointing.

DDR = accompanies 1 shutter-open macro
1 DDR from each focal plane
(label points to following files)

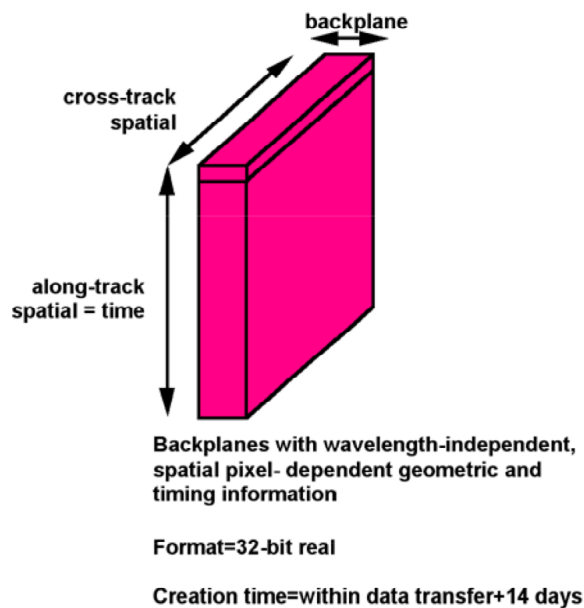


**Figure 3-8. Contents of a CRISM
Derived Data Record (DDR).**

3.2.2 Label Description

See section 2.3.4 for general information on CRISM product labels. A DDR label is detached and points to the single multiband image in the DDR. An example DDR label is in Appendix B.

DDR label keywords with CRISM-specific values are listed in Table 3-9.

Table 3-9. CRISM-specific values for DDR label keywords

| Keyword | Valid Values |
|------------------------------|--|
| PRODUCT_TYPE | DDR |
| OBSERVATION_TYPE | FRT (Full Resolution Targeted Observation) HRL (Half Resolution Long Targeted Observation) HRS (Half Resolution Short Targeted Observation) EPF (Atmospheric Survey EPF) TOD (Tracking Optical Depth Observation) MSS (Multispectral Survey, lossy compressed) MSP (Multispectral Survey, losslessly compressed) HSP (Hyperspectral Survey, losslessly compressed) HSV (Hyperspectral Survey, VNIR only) MSW (Multispectral Window) FFC (Flat-field calibration) |
| OBSERVATION_ID | 8-byte hexadecimal integer |
| MRO:OBSERVATION_NUMBER | Counter from product ID, hexadecimal |
| MRO:ACTIVITY_ID | Only valid value is: DE### – Derived Data |
| MRO:FRAME_RATE | "1", "3.75", "5", "15", or "30" |
| MRO:SENSOR_ID | "S" for VNIR, "L" for IR |
| SHUTTER_MODE_ID | "OPEN" |
| PIXEL_AVERAGING_WIDTH | 1, 2, 5, or 10 |
| MRO:INSTRUMENT_POINTING_MODE | "DYNAMIC POINTING" if SCAN_MODE (housekeeping file column 213) equals 3 ; else "FIXED POINTING" |
| SCAN_MODE_ID | (If DYNAMIC POINTING): "SHORT" (for full-resolution or half-resolution short central swath), "LONG" (for half-resolution long central swath), or "EPF" (for EPF even if part of a different class of observation) |
| BAND_NAME | Brief descriptive name of each layer of data in DDR |

3.3 LDR

3.3.1 Data Product Structure and Organization

The LDR consists of supporting data needed for the post-processing of a TRDR pointed at Mars' limb. The rationale for LDR structure and its geometric relation to a TRDR for a limb scan are similar to that of the DDR. The LDR contains one multiple-band image. The size of the multiple-band image is deterministic given the macro ID and typically the same for all images. A typical multiple-band image might have XX pixels in the sample (cross-track) dimension, YY pixels in the line (along-track) dimension, and ZZ pixels in the wavelength dimension, where:

- XX=640/binning, where 640 is the number of columns read off the detector, and binning is typically 10, for a dimension of 64,
- YY=the number of frames of data taken by the macro, typically 540, and

- ZZ=the number layers in the LDR.

Due to optical distortions present in the EDRs and non-resampled TRDRs, not all wavelengths represent exactly the same spatial location. The spatial location for a LDR represent those of the VNIR band closest to 610 nm and the IR band closest to 2300 nm. There are separate LDRs for VNIR and IR data.

There are 15 layers in the LDR, all represented as 32-bit real numbers. The files are created at approximately 14 days after transfer of target ID files, when sufficiently accurate pointing information is available.

- Solar incidence angle at the areoid, units degrees,
- Emission angle at the areoid, units degrees,
- Phase angle, units degrees,
- Planetocentric latitude at the tangent point of the line of sight, units degrees N,
- Longitude at the tangent point of the line of sight, units degrees E,
- Solar incidence angle at a surface intercept relative to a MOLA shape model, units degrees,
- Emission angle at a surface intercept relative to a MOLA shape model, units degrees,
- Elevation at the tangent point of the line of sight, units meters relative to areoid,
- Elevation at the tangent point of the line of sight, units meters relative to the MOLA shape model,
- Local Solar Time, units hours,
- Ephemeris Time of observation, seconds past noon January 1, 2000"
- Sub-solar planetocentric latitude, units degrees N,
- Sub-solar longitude, units degrees E,
- Sub-spacecraft planetocentric latitude, units degrees N,
- Sub-spacecraft longitude, units degrees E.

Once limb image data are assembled into EDRs, calibrated into TRDRs, and reconstructed pointing is available, LDRs are created for the data. There is no significance to a version 0 or 1.

3.3.2 Label Description

See section 2.3.4 for general information on CRISM product labels. An LDR label is detached and points to the single multiband image in the LDR. An example LDR label is in Appendix H.

DDR label keywords with CRISM-specific values are listed in Table 3-10.

Table 3-10. CRISM-specific values for LDR label keywords

| Keyword | Valid Values |
|------------------------------|---|
| PRODUCT_TYPE | LDR |
| OBSERVATION_TYPE | LMB (Limb Scan Observation) |
| OBSERVATION_ID | 8-byte hexadecimal integer |
| MRO:OBSERVATION_NUMBER | Counter from product ID, hexadecimal |
| MRO:ACTIVITY_ID | Only valid value is: DE### – Derived data |
| MRO:FRAME_RATE | "3.75" |
| MRO:SENSOR_ID | "S" for VNIR, "L" for IR |
| PIXEL_AVERAGING_WIDTH | 10 |
| MRO:INSTRUMENT_POINTING_MODE | "DYNAMIC POINTING" |
| BAND_NAME | Brief descriptive name of each layer of data in LDR |

3.4 Targeted RDR

3.4.1 Data Product Structure and Organization

The TRDR consists of the output of one of the constituent macros associated with a target ID that contains scene data (Mars or other), as shown in Figure 3-11. Not all EDRs are processed to TRDR level; macros containing bias, background, sphere, or calibration lamp data are processed instead to CDRs. Only scene EDRs are processed to the TRDR level.

The TRDR contains one or more multiple-band images (suffix *.IMG). One matches the dimensions of the multiple-band image of raw DN in an EDR, except that the data are in units of radiance. The size of the multiple-band image varies according to the observation mode but is deterministic given the ID of the command macro used to acquire the data. Appended to the multiple-band image is a binary table of the detector rows that were used, as selected by the wavelength filter. This is a one-column table, with each row containing one detector row number expressed as a 16-bit unsigned integer values, most significant bit first.

Other multiple-band images may contain I/F, Lambert albedo, or derived summary products (Table 3-12). The Lambert albedo image, if present, parallels the structure of the I/F image. The summary product image has the same spatial dimensions, but a different dimension in the spectral direction and it lacks the table of row numbers.

The size of the multiple-band image varies according to the observation mode but is deterministic given the macro ID. A typical multiple-band image might have XX pixels in the sample (cross-track) dimension, YY pixels in the line (along-track) dimension, and ZZ pixels in the wavelength dimension, where:

- XX=640/binning, where binning is 1, 2, 5, or 10
- YY=the number of frames of data taken by the macro, and
- ZZ=the number of detector rows (wavelengths) that are retained by the instrument.

The procedure for deriving this multiple-band image from an EDR is discussed in detail in Appendix L.

In addition, beginning with version 3 TRDRs, filtering is applied to the I/F version of the image to reduce effects of propagated noise from ground or inflight calibrations, or from noise in scene measurements (especially those taken later in the mission at higher detector temperatures). The radiance version of the TRDRs is unfiltered for reference. A detailed description of the filtering algorithm will be included in a future version of this document.

The data in a TRDR do not have optical distortions removed. In one column, the projection onto Mars' surface may vary by as much as ± 0.4 not-binned detector elements in the XX dimension depending on position in the FOV (distortions are worst at the edges of the VNIR and IR FOVs). For a single wavelength, its location in the ZZ direction may vary by as much as ± 1 not-binned detector elements depending on wavelength and position in the XX direction (distortions are worst at the short- and long-wavelength ends of the IR detector).

To correct for optical distortions, multiband images may be resampled in the spectral or spatial direction. Three types of resampling may have occurred: (a) resampling in the wavelength direction using nearest-neighbor resampling, as coded in the PS CDR; (b) resampling in the spatial direction, to remove differences in spatial scale with wavelength or band, using the CM CDR; and (c) VNIR data may be rescaled to match the slightly different magnification of the IR spectrometer, also using the CM CDR. A resampled TRDR is distinguished by its label and file name. The label uses local data dictionary keywords to document the type of resampling that has occurred. In the file name, "RTR" for resampled TRDR replaces "TRR."

Components of the TRDR are generated at a different time. The list file can be created nearly as soon as data are received at the SOC; once the approximate spacecraft pointing information, gimbal position, and tables to convert telemetry from digital to physical units are available. The radiance or I/F multiple-band image requires bracketing sphere observations to process and so it might be delayed one day. Construction of the summary product or Lambert albedo multiband images requires coregistered TES and MOLA derived data products and thus accurate, reconstructed spacecraft pointing for the data sets. That information will not be available for up to two weeks.

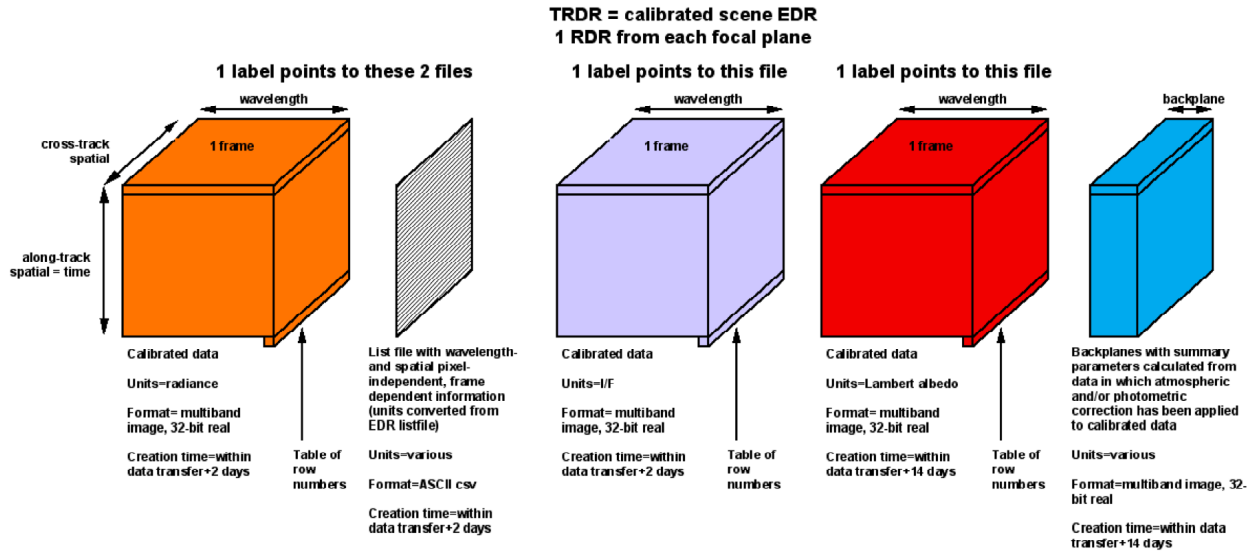


Figure 3-11. Contents of a CRISM Reduced Data Record for a single observation (TRDR).

Table 3-12. Formulation of parameters for summary products

| | NAME | PARAMETER | FORMULATION | RATIONALE | INPUT DATA |
|--------------------------------|------------------------|--|---|--|----------------|
| SURFACE COMPOSITION PARAMETERS | | | | | |
| 1 | R770 | 0.77 micron reflectance | R770 | Rock/dust | Lambert albedo |
| 2 | RBR | Red/blue ratio | R770/R440 | Rock/dust | Lambert albedo |
| 3 | BD530 | 0.53 micron band depth | $1 - (R530 / (a * R709 + b * R440))$ | Crystalline ferric minerals | Lambert albedo |
| 4 | SH600 | 0.6 micron shoulder height | $R600 / (a * R530 + b * R709)$ | Select ferric minerals | Lambert albedo |
| 5 | BD640 | 0.64 micron band depth | $1 - (R648 / (a * R600 + b * R709))$ | Select ferric minerals (esp. maghemite) | Lambert albedo |
| 6 | BD860 | 0.86 micron band depth | $1 - (R860 / (a * R800 + b * R984))$ | Select ferric minerals (esp. hematite) | Lambert albedo |
| 7 | BD920 | 0.92 μ m band depth | $1 - (R920 / (a * R800 + b * R984))$ | Fe mineralogy | Lambert albedo |
| 8 | RPEAK1 * | Reflectance peak 1 | wavelength where 1st derivative=0 of 5th order polynomial fit to R600, R648, R680, R710, R740, R770, R800, R830 | Fe mineralogy | Lambert albedo |
| 9 | BDI1000VIS | 1 micron integrated band depth; VNIR wavelengths | divide R830, R860, R890, R915 by RPEAK1 then integrate over (1 – normalized radiances) to get integrated band depth | Fe mineralogy | Lambert albedo |
| 10 | BDI1000IR | 1 micron integrated band depth; IR wavelengths | divide R1030, R1050, R1080, R1150 by linear fit from peak R (of the 15) between 1.3-1.87 μ m to R2530 extrapolated backwards, then integrate over (1 – normalized radiances) to get integrated band depth | Fe mineralogy; corrected for overlying aerosol induced slope | Lambert albedo |
| 11 | IRA | IR albedo | R1330 | IR albedo | Lambert albedo |
| 12a | OLINDEX (through TRR2) | Olivine index | $(R1695 / (0.1 * R1050 + 0.1 * R1210 + 0.4 * R1330 + 0.4 * R1470)) - 1$ | Olivines will be strongly > 0 | Lambert albedo |

| | NAME | PARAMETER | FORMULATION | RATIONALE | INPUT DATA |
|-----|-----------------------------------|--|---|--|----------------|
| 12b | OLINDEX2 (beginning with TRR3) | Olivine index 2 | $\begin{aligned} &(((RC1054 - R1054)/RC1054) \times 0.1) \\ &+ (((RC1211 - R1211)/(RC1211) \times 0.1) \\ &+ (((RC1329 - R1329)/RC1329) \times 0.4) \\ &+ (((RC1474 - R1474)/RC1474) \times 0.4) \end{aligned}$ where RC#### denotes the value of a point at a wavelength of #### nm along a modeled line that follows the average slope of the spectrum. | Olivines will be strongly > 0 | Lambert albedo |
| 13 | LCPINDEX | LCP index | $\frac{((R1330-R1050)/(R1330+R1050))}{((R1330-R1815)/(R1330+R1815))} *$ | Pyroxene is strongly +; Favours LCP | Lambert albedo |
| 14 | HCPINDEX | Pyroxene index | $\frac{((R1470-R1050)/(R1470+R1050))}{((R1470-R2067)/(R1470+R2067))} *$ | Pyroxene is strongly +; Favours HCP | Lambert albedo |
| 15 | VAR | 1.0-2.3 micron spectral variance | Fit a line from 1-2.3 microns and find variance of observed values from fit values by summing in quadrature over the # intervening wavelengths | Ol & Px will have high values; (to be used w/ OLPXINDEX) | Lambert albedo |
| 16 | ISLOPE1 | Spectral slope 1 | $(R1815-R2530)/(2530-R1815)$ | ferric coating on dark rock | Lambert albedo |
| 17 | BD1435 | 1.435 micron CO2 ice band depth | $1 - (R1430 / (a*R1370+b*R1470))$ | H2O ice | Lambert albedo |
| 18 | BD1500 | 1.5 micron H2O ice band depth | $1 - (((R1510+R1558)*0.5) / (a*R1808+b*R1367))$ | H2O ice | Lambert albedo |
| 19 | ICER1 | CO2 and H2O ice band depth ratio | $R1510 / R1430$ | CO2 H2O ice mixtures; > 1 for more CO2, < 1 for more water | Lambert albedo |
| 20 | BD1750 | 1.7 micron H2O band depth | $1 - ((R1750) / (a*R1557+b*R1815))$ | Gypsum | Lambert albedo |
| 21 | BD1900 | 1.9 micron H2O band depth | $1 - (((R1930+R1985)*0.5) / (a*R1875+b*R2067))$ | H2O | Lambert albedo |
| 22 | BDI2000 | 2 micron integrated band depth | divide R1660, R1811, R2009, R2141, R2206, R2253, R2292, R2318, R2352, R2391, R2431, R2457 by linear fit from peak R (of 15) between 1.3-1.87µm to R2530, then integrate over (1 – normalized radiances) to get integrated band depth | Fe mineralogy | Lambert albedo |
| 23 | BD2100 | 2.1 micron shifted H2O band depth | $1 - (((R2120+R2140)*0.5) / (a*R1930+b*R2250))$ | H2O | Lambert albedo |
| 24 | BD2210 | 2.21 micron Al-OH band depth | $1 - (R2210/(a*R2140+b*R2250))$ | Al-OH minerals | Lambert albedo |
| 25 | BD2290 | 2.3 micron Mg,Fe-OH band depth / 2.292 micron CO2 ice band depth | $1 - (R2290/(a*R2250+b*R2350))$ | Mg,Fe-OH minerals; ALSO CO2 ice | Lambert albedo |
| 26 | D2300 | 2.3 micron dropoff | $1-(R2290+R2330+R2330)/(R2140+R2170+R2210)$ | Hydrated min will be > 1 | Lambert albedo |
| 27 | SINDEX | Detects convexity at 2.29 µm due to absorptions at 1.9/2.1 µm & 2.4 µm | $1 - (R2100 + R2400) / (2 * R2290)$ | Hydrated min (e.g. mono and polyhydrated sulfates) will be > 1 | Lambert albedo |
| 28 | ICER2 | 2.7 micron CO2 ice band | $R2530 / R2600$ | CO2 vs water ice /soil; CO2 will be >>1, water and soil will be ~1 | Lambert albedo |

| | NAME | PARAMETER | FORMULATION | RATIONALE | INPUT DATA |
|--|-----------|---|--|--|--|
| 29 | BDCARB | Carbonate overtone band depth, or metal-OH band | $1 - (\sqrt{(R2330/(a \cdot R2230 + b \cdot R2390)) \cdot (R2530/(c \cdot R2390 + d \cdot R2600))})$ | Carbonates or hydroxylated silicate; both overtones need to be present to increase parameter value | Lambert albedo |
| 30 | BD3000 | 3 micron H2O band depth | $1 - (R3000 / (R2530 \cdot (R2530 / R2210)))$ | bound H2O (accounts for spectral slope) | Lambert albedo |
| 31 | BD3100 | 3.1 micron H2O ice band depth | $1 - (R3120 / (a \cdot R3000 + b \cdot R3250))$ | H2O ice | Lambert albedo |
| 32 | BD3200 | 3.2 micron CO2 ice band depth | $1 - (R3320 / (a \cdot R3250 + b \cdot R3390))$ | CO2 ice | Lambert albedo |
| 33 | BD3400 | 3.4 micron carbonate band depth | $1 - ((a \cdot R3390 + b \cdot R3500) / (c \cdot R3250 + d \cdot R3630))$ | carbonates | Lambert albedo |
| 34 | CINDEX | 3.9 micron carbonate index | $(R3750 + (R3750 - R3630) / (3750 - 3630) \cdot (3950 - 3750)) / R3950 - 1$ | carbonates will be > 'bkgrnd' values > 0 | Lambert albedo |
| ATMOSPHERIC PROPERTIES PARAMETERS | | | | | |
| 35 | R440 | 0.44 micron reflectance | R440 | Clouds/hazes | I/F |
| 36 | IRR1 | IR ratio 1 | R800 / R1020 | Aphelion ice clouds (>1) vs. seasonal or dust(< 1) | I/F |
| 37 | BD1270O2 | 1265 nm O2 emission band | $1 - ((a \cdot R1261 + b \cdot R1268) / (c \cdot R1250 + d \cdot R1280))$ | O2 emission; inversely correlated with high altitude water; signature of ozone | I/F |
| 38 | BD1400H2O | 1.4 micron H2O band depth | $1 - ((a \cdot R1370 + b \cdot R1400) / (c \cdot R1330 + d \cdot R1510))$ | H2O vapor | I/F |
| 39 | BD2000CO2 | 2 micron CO2 band | $1 - (R2010 / (a \cdot R1815 + b \cdot R2170))$ | atmospheric CO2 | I/F |
| 40 | BD2350 | 2.35 micron CO band depth | $1 - ((a \cdot R2320 + b \cdot R2330 + c \cdot R2350) / (d \cdot R2290 + e \cdot R2430))$ | CO | I/F |
| 41 | BD2600 | 2.6 micron H2O band depth | $1 - (R2600 / (a \cdot R2530 + b \cdot R2630))$ | H2O vapor (accounts for spectral slope) | I/F |
| 42 | IRR2 | IR ratio 2 | R2530 / R2210 | aphelion ice clouds vs. seasonal or dust | I/F (or Lambert albedo for GLO browse product) |
| 43 | R2700 | 2.70 micron reflectance | R2694 | high aerosols | I/F |
| 44 | BD2700 | 2.70 micron CO2 band depth | $1 - (R2694 / (R2530 \cdot (R2530 / R2350)))$ | atmospheric structure (accounts for spectral slope) | I/F |
| 45 | IRR3 | IR ratio 3 | R3500 / R3390 | aphelion ice clouds (higher values) vs. seasonal or dust | I/F |

3.4.2 Label Description

See section 2.3.4 for general information on CRISM product labels. A TRDR contains two labels, both detached. One points to both the multiband radiance image and the housekeeping

listfile. A second label points to the multiband summary product image. An example TRDR label is in Appendix C.

TRDR label keywords with CRISM-specific values are listed in Table 3-13.

Table 3-13. CRISM-specific values for TRDR label keywords

| Keyword | Valid Values |
|------------------------------|---|
| PRODUCT_TYPE | TARGETED_RDR |
| OBSERVATION_TYPE | FRT (Full Resolution Targeted Observation) HRL (Half Resolution Long Targeted Observation) HRS (Half Resolution Short Targeted Observation) EPF (Atmospheric Survey EPF) TOD (Tracking Optical Depth Observation) LMB (Limb Scan Observation) MSS (Multispectral Survey, lossy compressed) MSP (Multispectral Survey, losslessly compressed) HSP (Hyperspectral Survey, losslessly compressed) HSV (Hyperspectral Survey, VNIR only) MSW (Multispectral Window) FFC (Flat-field calibration) |
| OBSERVATION_ID | 8-byte hexadecimal integer |
| MRO:OBSERVATION_NUMBER | Counter from product ID, hexadecimal |
| MRO:ACTIVITY_ID | RA### – Radiance IF### – I/F AL### – Lambert albedo SU### – Summary products |
| MRO:FRAME_RATE | "1", "3.75", "5", "15", or "30" |
| MRO:SENSOR_ID | "S" for VNIR, or "L" for IR |
| SHUTTER_MODE_ID | The only valid value is "OPEN" |
| LIGHT_SOURCE_NAME | The only valid value is "NONE" |
| MRO:CALIBRATION_LAMP_STATUS | The only valid value is "OFF" |
| MRO:CALIBRATION_LAMP_LEVEL | The only valid value is 0 |
| PIXEL_AVERAGING_WIDTH | 1, 2, 5, or 10 |
| MRO:INSTRUMENT_POINTING_MODE | "DYNAMIC POINTING" if SCAN_MODE (housekeeping file column 213) equals 3 ; else "FIXED POINTING" |
| SCAN_MODE_ID | (If DYNAMIC POINTING): "SHORT" (for full-resolution or half-resolution short central swath, or limb scan observation), "LONG" (for half-resolution long central swath), or "EPF" (for EPF even if part of a different class of observation) |
| SAMPLING_MODE_ID | "HYPERSPSCTRAL" if wavelength filter used returns contiguous rows or "MULTISPECTRAL" if not |

| Keyword | Valid Values |
|--------------------------------|--|
| MRO:EXPOSURE_PARAMETER | The value supplied to the CRISM instrument to command the exposure time. At a given frame rate identified in MRO:FRAME_RATE, there are 480 possible exposure times ranging from 1 to 480. |
| MRO:WAVELENGTH_FILTER | Which of four onboard menus of rows was selected for downlink. The four choices are 0, 1, 2, or 3. |
| MRO:WAVELENGTH_FILE_NAME | For an EDR, the wavelength file is a 5-column, 480-row text file. The five elements in each row are the row number and a 0 or 1 for each of MRO:WAVELENGTH_FILTER 0, 1, 2 and 3, indicating whether data from that row of the detector is included in the EDR when that option is selected in MRO:WAVELENGTH_FILTER. For a TRDR, the wavelength file is an image whose value at the location of a detector element is the center wavelength of that element, in nanometers. |
| MRO:PIXEL_PROC_FILE_NAME | For a TRDR, the name of the ASCII file giving gain and offset to convert from 14 to 12 bits, and LUT used if lossy 12 to 8 bit compression is enabled (3 columns specified on a line-by-line basis) |
| MRO:INV_LOOKUP_TABLE_FILE_NAME | For a TRDR, the name of the ASCII file giving the inverse translation from 8 to 12 bits if 12 to 8 bit compression was enabled |
| MRO:INVALID_PIXEL_LOCATION | (In v2 and earlier) X,Y,Z locations within a TRDR at which data values are invalid because they represent cosmic ray hits (not currently used) |
| MRO:REPLACED_PIXEL_LOCATION | (In v2 and earlier) X,Y,Z locations within a TRDR at which data values were replaced by interpolating from surrounding pixels, because original data values were affected by cosmic ray hits (not currently used) |
| MRO:ATMO_CORRECTION_FLAG | Whether or not a correction has been performed for photometric and atmospheric effects; "OFF" or "ON" |
| MRO:THERMAL_CORRECTION_MODE | Whether and what type of thermal correction has been performed to calibrated data. Valid values are "OFF", "CLIMATOLOGY;ADR_CL", "EMPIRICAL_MODEL_FROM_SPECTRUM;ALG_M", "PHYSICAL_MODEL;ADR_TE" |
| MRO:PHOTOCLIN_CORRECTION_FLAG | Validity only in the case where the value of keyword MRO:THERMAL_CORRECTION_MODE is PHYSICAL_MODEL;ADR_TE. If MRO:PHOTOCLIN_CORRECTION_FLAG is OFF, then slopes used to calculate temperature come from the companion DDR. If it is ON, then the slopes are calculated using photoclinometry of CRISM data |
| MRO:SPATIAL_SUBSAMPLING_FLAG | If = 1, keystone corrected to 610 or 2300 nm by cubic resampling |

| Keyword | Valid Values |
|--------------------------------|--|
| MRO:SPATIAL_SUBSAMPLING_FILE | If MRO:SPATIAL_SUBSAMPLING_FLAG=1, name of instrument kernel or "CM" CDR used |
| MRO:SPATIAL_RESCALING_FLAG | If =1, VNIR rescaled to IR- 2300 nm - by cubic resampling |
| MRO:SPATIAL_RESCALING_FILE | If MRO:SPATIAL_RESCALING_FLAG=1, names of instrument kernel or "CM" CDR and frames kernel used |
| MRO:SPECTRAL_RESAMPLING_FLAG | If =1, nearest-neighbor spectral resampling has been performed |
| MRO:SPECTRAL_RESAMPLING_FILE | If MRO:SPECTRAL_RESAMPLING_FLAG=1, names of "PS" CDR used |
| MRO:HDF_SOFTWARE_NAME | Name of the CRISM hyperspectral data filter software used to process radiance TRDR data to I/F |
| MRO:HDF_SOFTWARE_VERSION_ID | Version of the software used by the CRISM hyperspectral data filter application |
| MRO:IF_MIN_VALUE | Control parameter for iterative kernel filter (IKF) used to convert IR radiance to I/F; minimum valid value of I/F. Values outside valid range are ignored during preprocessing |
| MRO:IF_MAX_VALUE | Maximum valid value of I/F for IR IKF |
| MRO:TRACE_MIN_VALUE | Control parameter for Ratio Shift Correction (RSC) used to convert VNIR and IR radiance to I/F; minimum valid value of a computed ratio. Values outside of the range are ignored during this processing step |
| MRO:TRACE_MAX_VALUE | Maximum valid value of I/F for RSC |
| MRO:REFZ_MEDIAN_BOX_WIDTH | IKF control parameter; kernel size of a median filter used in the spectral direction in the computation of the reference cube during the preprocessing steps |
| MRO:REFZ_SMOOTH_BOX_WIDTH | IKF control parameter; kernel size of a boxcar smoothing filter used in the spectral direction in the computation of the reference cube during the preprocessing steps |
| MRO:FRAM_STAT_MEDIAN_BOX_WIDTH | IKF control parameter; kernel size of a median filter used on the frame median profile in the computation of bad frames during preprocessing steps |
| MRO:FRAM_STAT_MIN_DEVIATION | IKF control parameter; minimum deviation from the mean of an element of the normalized frame median profile necessary to be classified as a bad frame during preprocessing steps |
| MRO:FRAM_STAT_MEDIAN_CONF_LVL | IKF control parameter; the confidence level for the Grubb's Test used for outlier detection of elements of the normalized median frame profile in the detection of bad frames during preprocessing steps; typical values near 0.95 |

| Keyword | Valid Values |
|--------------------------------|---|
| MRO:FRAM_STAT_IQR_CONF_LVL | IKF control parameter; the confidence level for the Grubb's Test used for outlier detection of elements of the normalized median profile of the frame interquartile range in the detection of bad frames during preprocessing steps; typical values near 0.95 |
| MRO:RSC_REF_XY_MEDIAN_WIDTH | RSC control parameter; kernel size of a median filter used in the XY direction while computing the reference cube during the preprocessing steps |
| MRO:RSC_REF_XY_SMOOTH_WIDTH | RSC control parameter; kernel size of a boxcar smoothing filter used in the XY direction while computing the reference cube during the preprocessing steps |
| MRO:RSC_REF_YZ_MEDIAN_WIDTH | RSC control parameter; kernel size of a median filter used in the YZ direction while computing the reference cube during the preprocessing steps |
| MRO:RSC_REF_YZ_SMOOTH_WIDTH | RSC control parameter; kernel size of a boxcar smoothing filter used in the YZ direction while computing the reference cube during the preprocessing steps |
| MRO:RSC_RATIO_XY_MEDIAN_WIDTH | RSC control parameter; kernel size of a median filter used in the XY direction while computing the ratio cube during preprocessing steps |
| MRO:RSC_RATIO_XY_SMOOTH_WIDTH | RSC control parameter; kernel size of a smoothing boxcar filter used in the XY direction while computing the ratio cube during preprocessing steps |
| MRO:RSC_RES_XY_PLY_ORDER | RSC control parameter; the order of the polynomial used to model low frequency content in the XY direction used as part of the RSC while computing the resolve cube during post processing steps |
| MRO:RSC_RES_XY_PLY_EXTND_WIDTH | RSC control parameter; number of pixels used to extend the trend of the column profiles when computing the polynomial used to model low frequency content in the XY direction used as part of the RSC while computing the resolve cube during the post processing steps |
| MRO:LOG_XFORM_NEG_CLIP_VALUE | IKF control parameter; value used for a negative I/F in the log base10 transform; represents minimum possible output pixel value for IKF procedure |
| MRO:IKF_NUM_REGIONS | IKF control parameter; number of spectral regions for application of IKF procedure |
| MRO:IKF_START_CHANNEL | IKF control parameter; number of first channel in a given spectral region for application of IKF procedure |
| MRO:IKF_STOP_CHANNEL | IKF control parameter; number of last channel in a given spectral region for application of IKF procedure |
| MRO:IKF_CONFIDENCE_LEVEL | IKF control parameter; confidence level for Grubb's Test used for outlier detection of elements of model residuals in IKF procedure; typical values near 0.95 |

| Keyword | Valid Values |
|--------------------------|---|
| MRO:IKF_WEIGHTING_STDDEV | IKF control parameter; weighting parameter for final model evaluation in IKF procedure |
| MRO:IKF_KERNEL_SIZE_X | IKF control parameter; size of the kernel in the X direction used in the IKF procedure |
| MRO:IKF_KERNEL_SIZE_Y | IKF control parameter; size of the kernel in the Y direction used in the IKF procedure |
| MRO:IKF_KERNEL_SIZE_Z | IKF control parameter; size of the kernel in the Z direction used in the IKF procedure |
| MRO:IKF_MODEL_ORDER_X | IKF control parameter; dimensionality of the model in the X direction used in the IKF procedure |
| MRO:IKF_MODEL_ORDER_Y | IKF control parameter; dimensionality of the model in the Y direction used in the IKF procedure |
| MRO:IKF_MODEL_ORDER_Z | IKF control parameter; dimensionality of the model in the Z direction used in the IKF procedure |
| BAND_NAME | Brief descriptive name of each layer of data in the summary product multi-band image |

3.5 Map-Projected Multispectral RDR

3.5.1 Data Product Structure and Organization

An MRDR (Figure 3-14) consists of mosaicked, map-projected multispectral TRDRs. All data are represented as 32-bit real numbers. The files are updated infrequently, when a large amount of new coverage or new processing procedures are available. The multispectral map RDR contains up to five multiple-band images at 256 pixels/degree, and one list file.

The first multiple-band image is map-projected I/F without any further corrections applied, taken directly from the TRDR associated with a strip of multispectral data. Although in the TRDRs there are separate multiple-band images for the VNIR and IR detectors, in this case the data are merged. The size of the multiple-band image varies between map tiles. A typical multiple-band image might have 1280 pixels in the latitude direction, a variable number of pixels in the longitude direction, and approximately 72 pixels in the wavelength dimension, representing each of the selected channels in multispectral mode.

The second multiple-band image is geometrically identical to the map-projected I/F multiple-band image, except that the data have been processed using the ADR binary tables to Lambert albedo (the thermally-corrected estimated surface contribution to reflected I/F, divided by $\cos i$).

The third and fourth multiple-band image contains map-projected data from the DDRs associated with strips of multispectral data, used to derive I/F from radiance. One file corresponds to the I/F image, and one file corresponds to the Lambert albedo image. In each of these, 11 additional layers are specific to individual multispectral strips used to assemble the tile, and are thus not contained in the source DDRs.

- Solar longitude, units degrees
- Solar distance at time of measurement, units AU

- VNIR OBSERVATION_ID of constituent measurement
- IR OBSERVATION_ID of constituent measurement
- The VNIR OBSERVATION_NUMBER carried through from the source scene EDRs;
- The IR OBSERVATION_NUMBER carried through from the source scene EDRs;
- The VNIR LINE_SAMPLE carried through from the temporary TRDR used to populate the MRDR; this identifies the VNIR wavelength calibration at the spatial pixel of the MRDR
- The IR LINE_SAMPLE carried through from the temporary TRDR used to populate the MRDR; this identifies the IR wavelength calibration at the spatial pixel of the MRDR
- The LINE_SAMPLE from the source VNIR TRDR; this together with column number, observation ID, and ordinal counter provides traceability back to a spatial pixel in a source EDR
- The LINE from the source IR TRDR
- The LINE from the source VNIR TRDR

The fifth multiple-band image contains map-projected summary products from the TRDR associated with a strip of multispectral data.

The listfile, in ASCII format, contains wavelengths of each layer in the Lambert albedo and I/F images.

Because of the mosaicked nature of an MRDR, the following protocol is used to select between overlapping TRDRs for inclusion in the MRDR:

- 1) If I/F is available but not Lambert albedo, the TRDR with the lower incidence angle at the areoid is used
- 2) If Lambert albedo is available, then an alternate strategy is available but not implemented:
 - 2a) If both TRDRs have incidence angles $>70^\circ$, the one with the lower incidence angle is used.
 - 2b) If one incidence angle is $>70^\circ$ and one is $<70^\circ$, the TRDR with $i < 70^\circ$ is used.
 - 2c) If both incidence angles are $<70^\circ$, then the TRDR with the lower 440-nm Lambert albedo is used.

3.5.2 Map projection standards

Areocentric latitude and longitude, incidence, emission, and phase angles are derived from spacecraft attitude, gimbal position, pixel location, and MOLA shape model of Mars. The adopted projection convention is planetocentric, positive east, using the 2000 IAU prime meridian and pole of rotation. The projection varies in 5° latitude bands, using EQUIRECTANGULAR equatorward of 87.5° latitude and POLAR STEREOGRAPHIC poleward of that latitude. For the latitude bands projected equirectangularly, the center latitude of

projection is the center of each tile to minimize "distortion." For the latitude band projected polar stereographically, in the north 0° longitude is down, and in the south 0° longitude is up.

For multispectral RDRs, the planet is divided into 1964 non-overlapping, 256 pixel/degree tiles as shown in Figure 2-10. Their longitude width increases poleward to keep tiles approximately the same in area.

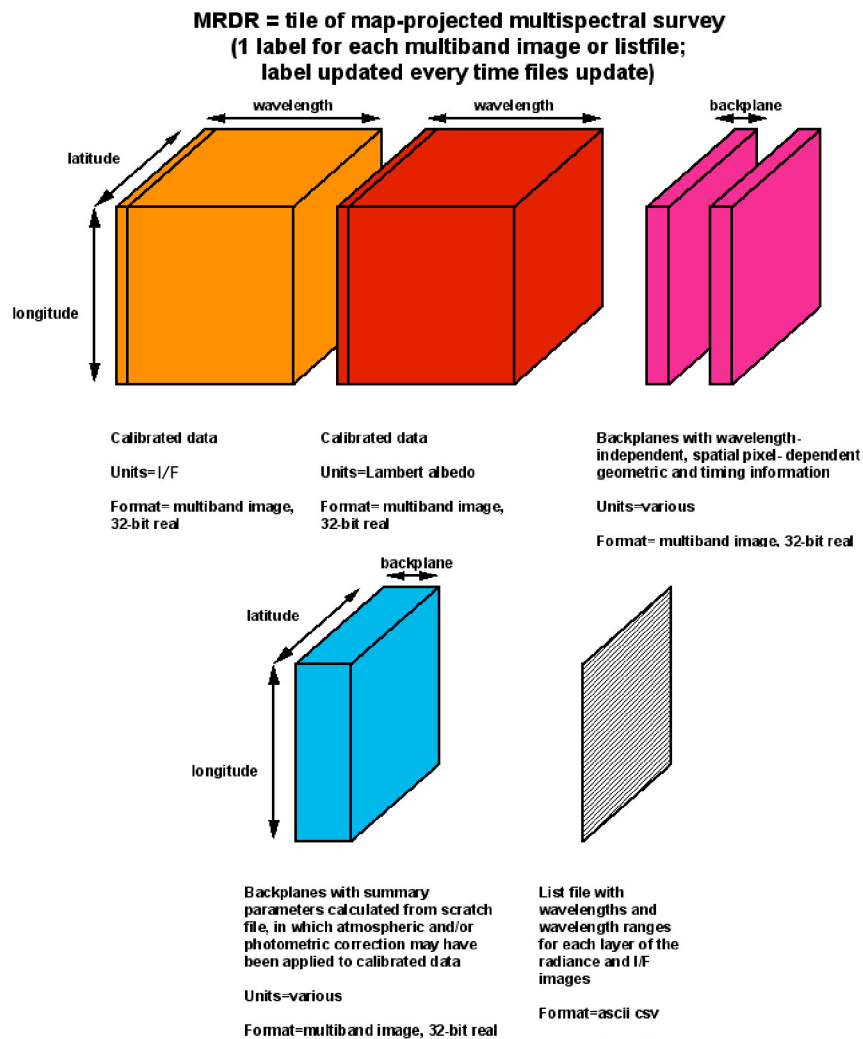


Figure 3-14. Contents of a CRISM Reduced Data Record for a multispectral map tile (MRDR).

3.5.3 Label Description

See section 2.3.4 for general information on CRISM product labels. Each component file of the MRDR has a single label pointing to it. An example MRDR label is in Appendix D.

MRDR label keywords with CRISM-specific values are listed in Table 3-15.

Table 3-15. CRISM-specific values for MRDR label keywords

| Keyword | Valid Values |
|-------------------------------|--|
| PRODUCT_TYPE | MAP_PROJECTED_MULTISPECTRAL_RDR |
| BAND_NAME | Brief descriptive name of each layer of data in the summary product multi-band image or the geometric/timing multi-band image |
| MRO:ATMO_CORRECTION_FLAG | Whether or not a correction has been performed for photometric and atmospheric effects; "OFF" or "ON" |
| MRO:PHOTOCLIN_CORRECTION_FLAG | Validity only in the case where the value of keyword MRO:THERMAL_CORRECTION_MODE is PHYSICAL_MODEL;ADR_TE. If MRO:PHOTOCLIN_CORRECTION_FLAG is OFF, then slopes used to calculate temperature come from the companion DDR. If it is ON, then the slopes are calculated using photoclinometry of CRISM data |
| MRO:THERMAL_CORRECTION_MODE | Whether and what type of thermal correction has been performed to calibrated data. Valid values are "OFF", "CLIMATOLOGY;ADR_CL", "EMPIRICAL_MODEL_FROM_SPECTRUM;ALG_M", "PHYSICAL_MODEL;ADR_TE" |

3.6 Map-Projected Targeted RDR

3.6.1 Data Product Structure and Organization

The map-projected TRDR, or MTRDR (Figure 3-16), contains one TRDR which has been map-projected, and I/F values corrected to a nadir illumination and viewing geometry. Essentially it is a local, high-resolution map tile comparable to an MRDR, but at 12-times higher resolution and with hyperspectral sampling. The MTRDR contains multiple-band images in units of corrected I/F (approximating Lambert albedo) and summary products, and text information that lists the wavelengths present. In either of the multiple-band images, data values are given in 32-bit real numbers.

MTRDRs are generated only for the high-resolution central swath of each targeted observation (Class Type = FRT, HRL, or HRS). The data are map projected, and VNIR and IR are joined into a single multiple-band image. Corrections are applied to remove atmospheric gas absorptions, normalize dust opacity to that at the lowest emission angle present in the image, and normalize brightness to normal illumination assuming Lambertian scattering properties. An additional correction is applied for along-slit optical variations to normalize spectral radiance to that in the center columns of the detector. Finally, wavelength bands with suspect calibration are omitted.

MTRDRs are created external to the SOC by the CRISM science team using the CRISM Analysis Tool, and are delivered to the SOC for archival purposes.

The first multiple-band image is corrected, map-projected I/F. A typical multiple-band image might have XX pixels in the longitude dimension, YY pixels in the latitude dimension, and ZZ pixels in the wavelength dimension, where XX and YY depend on the site(s) and ZZ is the number of channels.

The second multiple-band image is map-projected summary products.

The list file, in ASCII format, contains wavelengths of each layer in the corrected I/F image.

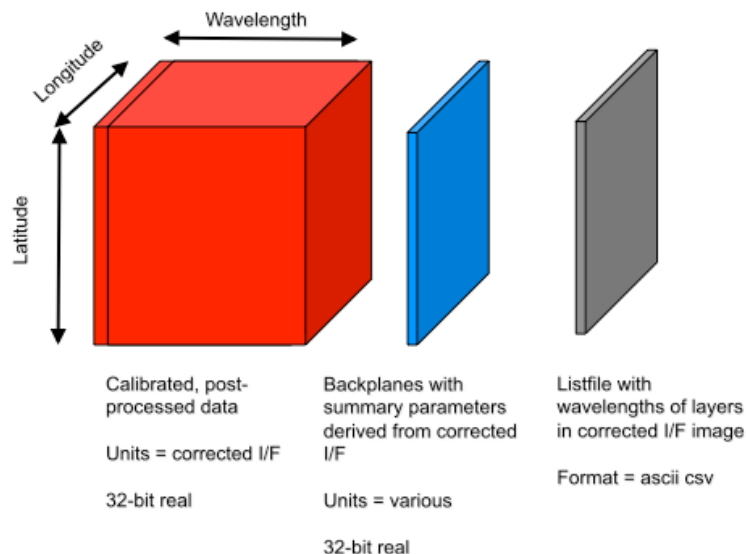


Figure 3-16. Contents of a CRISM Reduced Data Record for a MTRDR

3.6.2 Label Description

See section 2.3.4 for general information on CRISM product labels. An example MTRDR label is in Appendix E.

MTRDR label keywords with CRISM-specific values are listed in Table 3-17.

Table 3-17. CRISM-specific values for MTRDR label keywords

| Keyword | Valid Values |
|-----------------------------|---|
| PRODUCT_TYPE | MAP_PROJECTED_TARGETED_RDR |
| OBSERVATION_TYPE | FRT (Full Resolution Targeted Observation) HRL (Half Resolution Long Targeted Observation) HRS (Half Resolution Short Targeted Observation) |
| OBSERVATION_ID | 8-byte hexadecimal integer |
| MRO:OBSERVATION_NUMBER | Counter from product ID |
| MRO:ACTIVITY_ID | The only valid value is: IF### – Scene measurement |
| MRO:SENSOR_ID | "J" for joined |
| SHUTTER_MODE_ID | The only valid value is "OPEN" |
| LIGHT_SOURCE_NAME | The only valid value is "NONE" |
| MRO:CALIBRATION_LAMP_STATUS | The only valid value is "OFF" |

| Keyword | Valid Values |
|--------------------------------|--|
| MRO:CALIBRATION_LAMP_LEVEL | The only valid value is 0 |
| PIXEL_AVERAGING_WIDTH | 1 or 2 |
| MRO:INSTRUMENT_POINTING_MODE | "DYNAMIC POINTING" |
| SCAN_MODE_ID | "SHORT" (for full-resolution or half-resolution short central swath), "LONG" (for half-resolution long central swath) |
| SCAN_RATE | 3.75 (Hz frame rate) |
| SAMPLING_MODE_ID | "HYPERSPSCTRAL" |
| MRO:EXPOSURE_PARAMETER | The value supplied to the CRISM instrument to command the exposure time. At a given frame rate identified in MRO:FRAME_RATE, there are 480 possible exposure times ranging form 1 to 480. |
| MRO:WAVELENGTH_FILTER | 0 |
| MRO:WAVELENGTH_FILE_NAME | The name of the companion file with the wavelengths of each image band. |
| MRO:PIXEL_PROC_FILE_NAME | For the the source TRDR, the name of the ASCII file giving gain and offset to convert from 14 to 12 bits, and LUT used if lossy 12 to 8 bit compression is enabled (3 columns specified on a line-by-line basis) |
| MRO:INV_LOOKUP_TABLE_FILE_NAME | For a source TRDR, the name of the ASCII file giving the inverse translation from 8 to 12 vits if 12 to 8 bit compression was enabled |
| MRO:ATMO_CORRECTION_FLAG | Whether or not a correction has been performed for photometric and atmospheric effects; "OFF" or "ON" |
| MRO:THERMAL_CORRECTION_MODE | Whether and what type of thermal correction has been performed to calibrated data. Valid values are "OFF", "CLIMATOLOGY;ADR_CL", "EMPIRICAL_MODEL_FROM_SPECTRUM;ALG_M", "PHYSICAL_MODEL;ADR_TE" |
| MRO:PHOTOCLIN_CORRECTION_FLAG | Validity only in the case where the value of keyword MRO:THERMAL_CORRECTION_MODE is PHYSICAL_MODEL;ADR_TE. If MRO:PHOTOCLIN_CORRECTION_FLAG is OFF, then slopes used to calculate temperature come from the companion DDR. If it is ON, then the slopes are calculated using photoclinometry of CRISM data |
| MRO:SPATIAL_SUBSAMPLING_FLAG | If = 1, keystone corrected to 610 or 2300 nm by resampling |
| MRO:SPATIAL_SUBSAMPLING_FILE | If MRO:SPATIAL_SUBSAMPLING_FLAG=1, name of instrument kernel or "CM" CDR used |
| MRO:SPATIAL_RESCALING_FLAG | If =1, VNIR rescaled to IR- 2300 nm by resampling |
| MRO:SPATIAL_RESCALING_FILE | If MRO:SPATIAL_RESCALING_FLAG=1, names of instrument kernel or "CM" CDR and frames kernel used |
| MRO:SPECTRAL_RESAMPLING_FLAG | If =1, nearest-neighbor spectral resampling has been performed |
| MRO:SPECTRAL_RESAMPLING_FILE | If MRO:SPECTRAL_RESAMPLING_FLAG=1, names of "PS" CDR used |

| Keyword | Valid Values |
|--------------------------------|---|
| MRO:HDF_SOFTWARE_NAME | Name of the CRISM hyperspectral data filter software used to process radiance TRDR data to I/F |
| MRO:HDF_SOFTWARE_VERSION_ID | Version of the software used by the CRISM hyperspectral data filter application |
| MRO:IF_MIN_VALUE | Control parameter for iterative kernel filter (IKF) used to convert IR radiance to I/F; minimum valid value of I/F. Values outside valid range are ignored during preprocessing |
| MRO:IF_MAX_VALUE | Maximum valid value of I/F for IR IKF |
| MRO:TRACE_MIN_VALUE | Control parameter for Ratio Shift Correction (RSC) used to convert VNIR and IR radiance to I/F; minimum valid value of a computed ratio. Values outside of the range are ignored during this processing step |
| MRO:TRACE_MAX_VALUE | Maximum valid value of I/F for RSC |
| MRO:REFZ_MEDIAN_BOX_WIDTH | IKF control parameter; kernel size of a median filter used in the spectral direction in the computation of the reference cube during the preprocessing steps |
| MRO:REFZ_SMOOTH_BOX_WIDTH | IKF control parameter; kernel size of a boxcar smoothing filter used in the spectral direction in the computation of the reference cube during the preprocessing steps |
| MRO:FRAM_STAT_MEDIAN_BOX_WIDTH | IKF control parameter; kernel size of a median filter used on the frame median profile in the computation of bad frames during preprocessing steps |
| MRO:FRAM_STAT_MIN_DEVIATION | IKF control parameter; minimum deviation from the mean of an element of the normalized frame median profile necessary to be classified as a bad frame during preprocessing steps |
| MRO:FRAM_STAT_MEDIAN_CONF_LVL | IKF control parameter; the confidence level for the Grubb's Test used for outlier detection of elements of the normalized median frame profile in the detection of bad frames during preprocessing steps; typical values near 0.95 |
| MRO:FRAM_STAT_IQR_CONF_LVL | IKF control parameter; the confidence level for the Grubb's Test used for outlier detection of elements of the normalized median profile of the frame interquartile range in the detection of bad frames during preprocessing steps; typical values near 0.95 |
| MRO:RSC_REF_XY_MEDIAN_WIDTH | RSC control parameter; kernel size of a median filter used in the XY direction while computing the reference cube during the preprocessing steps |
| MRO:RSC_REF_XY_SMOOTH_WIDTH | RSC control parameter; kernel size of a boxcar smoothing filter used in the XY direction while computing the reference cube during the preprocessing steps |

| Keyword | Valid Values |
|--------------------------------|---|
| MRO:RSC_REF_YZ_MEDIAN_WIDTH | RSC control parameter; kernel size of a median filter used in the YZ direction while computing the reference cube during the preprocessing steps |
| MRO:RSC_REF_YZ_SMOOTH_WIDTH | RSC control parameter; kernel size of a boxcar smoothing filter used in the YZ direction while computing the reference cube during the preprocessing steps |
| MRO:RSC_RATIO_XY_MEDIAN_WIDTH | RSC control parameter; kernel size of a median filter used in the XY direction while computing the ratio cube during preprocessing steps |
| MRO:RSC_RATIO_XY_SMOOTH_WIDTH | RSC control parameter; kernel size of a smoothing boxcar filter used in the XY direction while computing the ratio cube during preprocessing steps |
| MRO:RSC_RES_XY_PLY_ORDER | RSC control parameter; the order of the polynomial used to model low frequency content in the XY direction used as part of the RSC while computing the resolve cube during post processing steps |
| MRO:RSC_RES_XY_PLY_EXTND_WIDTH | RSC control parameter; number of pixels used to extend the trend of the column profiles when computing the polynomial used to model low frequency content in the XY direction used as part of the RSC while computing the resolve cube during the post processing steps |
| MRO:LOG_XFORM_NEG_CLIP_VALUE | IKF control parameter; value used for a negative I/F in the log base10 transform; represents minimum possible output pixel value for IKF procedure |
| MRO:IKF_NUM_REGIONS | IKF control parameter; number of spectral regions for application of IKF procedure |
| MRO:IKF_START_CHANNEL | IKF control parameter; number of first channel in a given spectral region for application of IKF procedure |
| MRO:IKF_STOP_CHANNEL | IKF control parameter; number of last channel in a given spectral region for application of IKF procedure |
| MRO:IKF_CONFIDENCE_LEVEL | IKF control parameter; confidence level for Grubb's Test used for outlier detection of elements of model residuals in IKF procedure; typical values near 0.95 |
| MRO:IKF_WEIGHTING_STDDEV | IKF control parameter; weighting parameter for final model evaluation in IKF procedure |
| MRO:IKF_KERNEL_SIZE_X | IKF control parameter; size of the kernel in the X direction used in the IKF procedure |
| MRO:IKF_KERNEL_SIZE_Y | IKF control parameter; size of the kernel in the Y direction used in the IKF procedure |
| MRO:IKF_KERNEL_SIZE_Z | IKF control parameter; size of the kernel in the Z direction used in the IKF procedure |
| MRO:IKF_MODEL_ORDER_X | IKF control parameter; dimensionality of the model in the X direction used in the IKF procedure |

| Keyword | Valid Values |
|-----------------------|---|
| MRO:IKF_MODEL_ORDER_Y | IKF control parameter; dimensionality of the model in the Y direction used in the IKF procedure |
| MRO:IKF_MODEL_ORDER_Z | IKF control parameter; dimensionality of the model in the Z direction used in the IKF procedure |
| BAND_NAME | Brief descriptive name of each layer of data in the summary product multi-band image |

3.7 Level-6 CDR

3.7.1 Data Product Structure and Organization

A level-6 CDR (Figure 3-18) consists of tabulated derived data. Typically it is used for calibration of EDRs to CDRs, radiance or I/F. Derivation of the level-6 CDRs from flight data is described in Appendix M. The different types of calibration-related level-6 CDRs are given in Table 3-19.

The CDR6 format is also used to store operationally significant engineering information that the user may find helpful, but that are beyond the scope of the required elements of the archive. This includes a time ordered history of observations and the characteristics of the sites observed, as well as the configuration-managed history of the hardware and software state of the CRISM instrument. These "operational CDRs" are described in Table 3-20.

File format is comparable to that of EDR and RDR list files. The tables are ASCII comma-separated value (CSV) format.

3.7.2 Label Description

See section 2.3.4 for general information on CRISM product labels. An example level-6 CDR label is in Appendix F.

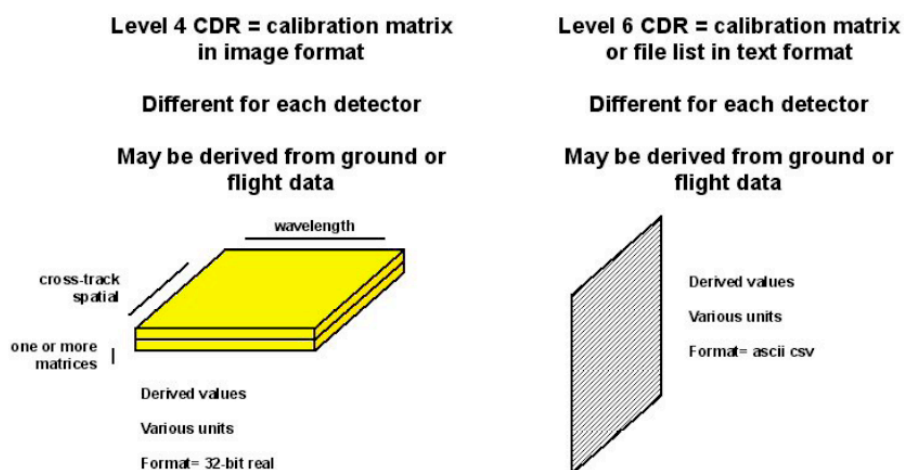


Figure 3-18. Contents of a CRISM Calibration Data Record (CDR). Level 4 is image data; level 6 is text.

Table 3-19. Descriptions of calibration-related level-6 CDRs

| PRODUCTS | FORM FOR EACH FOCAL PLANE | PRODUCT ACRONYM |
|---|--|-----------------|
| INFREQUENTLY UPDATED PRODUCTS | | |
| Coefficients for correcting raw housekeeping for effects of lamps, coolers, frame rate | ASCII table , 11 columns (only one file applicable to both VNIR and IR) | HD |
| Coefficients for calibrating housekeeping from digital to physical units | ASCII table , 5 columns (only one file applicable to both VNIR and IR) | HK |
| Coefficients to convert housekeeping voltages for perturbations due to current | ASCII table , 7 columns (only one file applicable to both VNIR and IR) | HV |
| Gain and offset to use for each row for 12 to 14 bit conversion; 12 to 8 bit lookup tables used for each row | ASCII table, 4 columns, 1 per detector | PP |
| Wavelength tables | ASCII table, 5 columns, 1 per detector | WV |
| Bandwidth for each row (band) in central columns of each detector at which spectral smile and keystone are minimum. | ASCII table, 2 cols VNIR and 11 cols IR, 1 per detector | BW |
| Center wavelength for each row (band) in central columns of each detector at which spectral smile and keystone are minimum. | ASCII table, 2 columns, 1 per detector | SW |
| 12 to 8 bit lookup tables | ASCII table, 1 col. of 12-bit input, 8 cols. of 8-bit output | LK |
| 8 to 12 bit lookup tables (inverse of 12 to 8) | ASCII table, 8 cols. of 8-bit input, 1 col. of 12-bit output | LI |
| Linearity correction | ASCII table, 7 columns, 1 per detector | LC |
| Bias step function as a function of frame rate and quadrant | ASCII table, 3 columns, 1 per detector | BS |
| Additive correction of bias to nominal detector operating temperature | ASCII table, 3 columns, 1 per detector | DB |
| Additive correction of bias to nominal focal plane electronics operating temperature | ASCII table, 3 columns, 1 per detector | EB |
| Interquadrant ghost removal scaling factors | ASCII table, 6 columns, 1 per detector | GH |
| Average Mars spectrum for limiting cases in different operating modes | ASCII table, 6 columns, 1 per detector | AS |
| Saturation limit for each detector quadrant and frame rate | ASCII table, 3 columns, 1 per detector | SL |
| Valid limits for each detector quadrant and frame rate for 14-bit DN level and noise | ASCII table, 5 columns, 1 per detector | VL |
| Atmospheric transmission for each wavelength bin averaged over IR columns 270-369 or VNIR columns 260-359, the part of each detector at which spectral smile and keystone are minimum | ASCII table, 2 columns, 1 per detector | CT |
| FREQUENTLY UPDATED PRODUCTS | | |

| PRODUCTS | FORM FOR EACH FOCAL PLANE | PRODUCT ACRONYM |
|--|----------------------------------|------------------------|
| Standard telemetry file: CRISM low-rate telemetry in raw counts, from the beginning of a UTC calendar day to its end. This is used in preference to the telemetry attached to each image for correction of thermal effects. | ASCII table, 224 columns | ST |
| Predicted EDR processing table: Predicted table of EDRs containing scene data and the corresponding EDRs containing time-dependent calibration measurements. It is constructed from uplinked commands | ASCII table, 21 columns | BTF |
| EDR processing table: Table of EDRs containing scene data and the corresponding EDRs containing time-dependent calibration measurements. Used to process scene EDRs to TRDRs, and calibration EDRs to CDRs. If there is a discrepancy between the actual and predicted EDRs used for calibration, the TRDRs resulting from scene EDRs are quality-flagged. | ASCII table, 6 columns | ATF |

Table 3-20. Descriptions of operational level-6 CDRs

| PRODUCTS | FORM FOR EACH FOCAL PLANE | PRODUCT ACRONYM |
|--|---|------------------------|
| Digital values of alarm limits and instrument parameters. Used for validation of uplinked sequences. | ASCII table with columns of start time of applicability, raw digital value, and comments (only one file applicable to both VNIR and IR) | DR |
| Calibrated physical values of alarm limits. Used for validation of uplinked sequences. | ASCII table with columns of start time of applicability, value as Celsius, volts, or amps, and comments (only one file applicable to both VNIR and IR) | DC |
| Digital values of heater and cooler settings. Used for validation of uplinked sequences. | ASCII table with columns of start time of applicability, raw digital value, and comments (only one file applicable to both VNIR and IR) | SR |
| Calibrated physical values of heater and cooler settings. Used for validation of uplinked sequences. | ASCII table with columns of start time of applicability, value as Celsius, and comments (only one file applicable to both VNIR and IR) | SC |

| PRODUCTS | FORM FOR EACH FOCAL PLANE | PRODUCT ACRONYM |
|--|---|-----------------|
| | and IR) | |
| Expected compression ratio of data in different instrument configurations. Used for management of solid state recorder usage. | ASCII table with columns activity, wavelength filter, binning, lossy compression setup, lossless compression setup, and expected compression ratio of data with that configuration. | CP |
| Mission event log. Includes times of updates to instrument software or settings, command loads, flight tests, or other notable events. | ASCII table with columns of start time and comments (only one file applicable to both VNIR and IR) | EL |

3.8 Level-4 CDR

3.8.1 Data Product Structure and Organization

A level-4 CDR (Figure 3-18) consists of a derived image product needed for calibration to radiance or I/F. Derivation of the level-4 CDRs from flight data is described in Appendix L. The different types of level-4 CDRs are given in Table 3-21. The data may be bitmap or 32-bit real numbers, depending on the product.

A level-4 CDR contains one or more images. The size varies according to pixel binning. The dimensions are XX' pixels in the sample (cross-track) dimension, YY pixels in the wavelength dimension, where:

- $XX' = (640) / \text{binning}$, where 640 is the number of columns read off the detector, and binning is 1, 2, 5, or 10
- $YY =$ the number of rows (wavelength) that are retained by the instrument.

3.8.2 Label Description

See section 2.3.4 for general information on CRISM product labels. An example level-4 CDR label is in Appendix G.

Table 3-21. Descriptions of level-4 CDRs

| PRODUCTS | FORM FOR EACH FOCAL PLANE | VERSIONS FOR DIFFERENT PIXEL BINNING / CHANNEL SELECTION? | VERSIONS FOR DIFFERENT FRAME RATE? | ACRONYM |
|--|-------------------------------|---|------------------------------------|---------|
| GROUND CALIBRATION PRODUCTS | | | | |
| Masks of detector dark columns, scattered light columns, scene columns | 2D matrix per detector, 8 bit | Y | N | DM |

| PRODUCTS | FORM FOR EACH FOCAL PLANE | VERSIONS FOR DIFFERENT PIXEL BINNING / CHANNEL SELECTION? | VERSIONS FOR DIFFERENT FRAME RATE? | ACRONYM |
|--|---|--|---|----------------|
| Nonuniformity file: time-tagged, row-normalized measurement of detector nonuniformity | Two 2D matrices, 32 bit | Y | Y | NU |
| Matrices to remove estimated leaked higher order light | Four 2D matrices per detector, 16 bit integer, row numbers Four 2D matrices per detector, 32 bit, weighting coefficients | Y | N | LL |
| Sphere spectral radiance at set point (pixel by pixel coefficients to a 2nd order polynomial function of optical bench temperature) | Three 2D matrices per detector, 32 bit, for each sphere bulb | Y | N | SS |
| Shutter position reproducibility correction to sphere radiance (pixel by pixel coefficients to a linear function of the ratio of corrected sphere image to sphere spectral radiance model) | 2 2D matrices per detector, 32 bit, for each sphere bulb | Y | N | SH |
| Temperature dependence of detector responsivity (pixel by pixel coefficients to a 2nd order polynomial function of detector temperature) | Three 2D matrices per detector, 32 bit | Y | N | TD |
| Along-slit angle measured from slit center | 2D matrix per detector, 32 bit | Y | N | CM |
| Number of lines by which to shift each column (sample) of an image to minimize the effects of spectral smile | 2D matrix per detector, 32 bit | Y | N | PS |
| Wavelength image (each pixel) determined onground | 2D matrix per detector, 32 bit | Y | N | WA |
| Nearest-neighbor resampled wavelength image (each pixel) determined onground | 2D matrix per detector, 32 bit | Y | N | RW |
| Spectral bandpass, or full width half maximum (each pixel) determined onground | One (VNIR) or ten(IR) 2D matrices per detector, 32 bit | Y | N | SB |
| Solar flux at 1 AU (for each pixel to take into account spectral smile effects) | 2D matrix per detector, 32 bit | Y | N | SF |

| PRODUCTS | FORM FOR EACH FOCAL PLANE | VERSIONS FOR DIFFERENT PIXEL BINNING / CHANNEL SELECTION? | VERSIONS FOR DIFFERENT FRAME RATE? | ACRONYM |
|--|--|---|------------------------------------|---------|
| Nearest-neighbor resampled solar flux at 1 AU (for each pixel to take into account spectral smile effects) | 2D matrix per detector, 32 bit | Y | N | RF |
| Atmospheric transmission as measured from a nadir-pointed hyperspectral scan across Olympus Mons | 2D matrix per detector, 32 bit | Y | N | AT |
| Atmospheric transmission as measured from a nadir-pointed hyperspectral scan across Olympus Mons, nearest-neighbor resampled in the wavelength direction | 2D matrix per detector, 32 bit | Y | N | RT |
| FREQUENTLY UPDATED PRODUCTS | | | | |
| Bad pixel mask: time-tagged bitmap of bad pixels | 2D matrix, 8 bits, per detector | Y | Y | BP |
| Bias file: time-tagged, fitted VNIR and IR images extrapolated to zero exposure time | 2D matrix, 32 bit, per detector | Y | Y | BI |
| Background file: time-tagged, bias- and ghost-subtracted, linearized, averaged VNIR and IR background frames | 2D matrix, 32 bit, per detector | Y | Y | BK |
| Noise file: time-tagged, image of pixel-by-pixel uncertainties in background images | 2D matrix, 32 bit, per detector | Y | Y | UB |
| Processed sphere image in units of DN/ms | 2D matrix, 32 bit, per detector (1 for each sphere bulb) | Y | N | SP |

CDR label keywords with CRISM-specific values are listed in Table 3-22.

Table 3-22. CRISM-specific values for CDR label keywords

| Keyword | Valid Values |
|--------------|--------------|
| PRODUCT_TYPE | CDR |

| Keyword | Valid Values |
|-----------------------------|--|
| OBSERVATION_TYPE | If produced from flight data: FRT (Full Resolution Targeted Observation) HRL (Half Resolution Long Targeted Observation) HRS (Half Resolution Short Targeted Observation) EPF (Atmospheric Survey EPF) TOD (Tracking Optical Depth Observation) MSS (Multispectral Survey, lossy compressed) MSP (Multispectral Survey, losslessly compressed) MSW (Multispectral Window) CAL (Radiometric Calibration) FFC (Flat-field calibration) ICL (Calibration source intercalibration) STO (Star Observation) FUN (Functional test) UNK (no valid EDRs within observation that indicate class type, or ground-derived) |
| OBSERVATION_ID | 10-digit hexadecimal integer (if produced from flight data) |
| MRO:OBSERVATION_NUMBER | Counter from product ID (if produced from flight data) |
| MRO:ACTIVITY_ID | Valid values (if produced from flight data) are: BI#### – Bias measurement DF#### – Dark field measurement LP#### – Lamp measurement SP#### – Sphere measurement SC#### – Scene measurement (for flat-field calibration) |
| SOURCE_PRODUCT_ID | The product ID of the EDR from which a CDR was constructed (if produced from flight data) |
| MRO:EXPOSURE_PARAMETER | The value supplied to the CRISM instrument to command the exposure time. At a given frame rate identified in MRO:FRAME_RATE, there are 480 possible exposure times ranging from 1 to 480. |
| MRO:WAVELENGTH_FILTER | Which of four onboard menus of rows was selected for downlink. The four choices are 0, 1, 2, or 3. |
| MRO:SENSOR_ID | "S" for VNIR, or "L" for IR |
| SHUTTER_MODE_ID | "OPEN", "SPHERE", OR "CLOSED" (if produced from flight data) |
| LIGHT_SOURCE_NAME | "NONE", "VNIR LAMP 1", "VNIR LAMP 2", "IR LAMP 1", "IR LAMP 1", "SPHERE LAMP 1", "SPHERE LAMP 2" |
| MRO:CALIBRATION_LAMP_STATUS | "OFF", "OPEN LOOP" or "CLOSED LOOP" (for integrating sphere only) |
| MRO:CALIBRATION_LAMP_LEVEL | Value between 0 and 4095 |
| PIXEL_AVERAGING_WIDTH | 1, 2, 5, or 10 |

| Keyword | Valid Values |
|-------------------------------|---|
| MRO:DETECTOR_TEMPERATURE | Physical units; used to correct bias or responsivity for detector temperature. On each detector there are two temperature sensors. The primary source of IR detector temperature is IR temperature sensor 1 (column 50 in the EDR list file). The backup source of IR detector temperature is IR temperature sensor 2 (column 51 in the EDR list file). The primary source of VNIR detector temperature is VNIR temperature sensor 2 (column 65 in the EDR list file). The backup source of VNIR detector temperature is VNIR temperature sensor 1 (column 64 in the EDR list file)." |
| MRO:FPE_TEMPERATURE | Physical units; used to correct bias for electronics temperature. The temperature of the IR focal plane electronics (if MRO:SENSOR_ID = "L"), or the VNIR focal plane electronics (if MRO:SENSOR_ID = "S"). |
| MRO:OPTICAL_BENCH_TEMPERATURE | Physical units; backup to correct sphere radiance for sphere temperature |
| MRO:SPHERE_TEMPERATURE | Physical units; used to correct sphere radiance for sphere temperature |
| MRO:SPECTROMETER_HOUSING_TEMP | Physical units; used in backup correction of background for spectrometer housing temperature. The primary source of this temperature is a measurement digitized by the VNIR focal plane electronics, column 58 in the EDR list file. The backup source of this temperature is a measurement digitized by the IR focal plane electronics, column 69 in the EDR list file |
| BAND_NAME | Brief descriptive name of each layer of data in the CDR |

3.9 ADR

An Ancillary Data Record or ADR contains a hyperdimensional binary table of derived values, where the axes of the matrix represent values of a layer of a DDR (e.g., incidence angle, thermal inertia, etc.), the output of another ADR, or a value extracted from a TRDR.

The overall objective of ADRs is to correct I/F in a TRDR for a strip of multispectral survey data for atmospheric, photometric, or thermal effects to isolate the surface-reflected component of I/F as Lambert albedo. There are three types of ADRs:

1. The "CL" ADR is a table of surface temperatures and atmospheric dust and ice opacities, given for a latitude and longitude from the DDR and Ls and local solar time from the TRDR label.
2. The "AC" ADR is a table of correction from I/F to Lambert albedo, for an incidence, emission, and phase angle and surface elevation from the DDR, dust and ice optical depths

and surface temperature from the CL ADR, and observed I/F from a TRDR. There is a separate AC ADR for each wavelength that is corrected; nominal wavelengths are those used in multispectral mapping, in wavelength filter 1.

3. The "TE" ADR is a table of calculated surface temperature for latitude, thermal inertia, elevation, and slope magnitude and azimuth from the DDR, dust and ice opacity from the CL ADR, Ls and local solar time from the TRDR label, and bolometric albedo estimated from Lambert albedo at wavelengths <2300 nm. This supplants surface temperature that is returned from the CL ADR.

ADR contents are described in Tables 3-23 through 3-25.

Table 3-23. LUT for atmospheric opacity (ADR type = CL)

| VARIABLE | RANGE | UNIT |
|---------------------|---------|-----------------------|
| Latitude | -90-90° | degrees |
| Longitude | -90-90° | degrees |
| Ls | 0-360° | degrees |
| Local time | 15 | (assumed local time)r |
| Surface temperature | 180-310 | °K |
| Dust opacity | 0-1.0 | dimensionless opacity |
| Ice opacity | 0-1.0 | dimensionless opacity |

Table 3-24. LUT for predicted atmospheric / photometric / thermal correction (ADR type = AC)

| VARIABLE | RANGE | WAVELENGTH |
|---------------------------|-------------|--------------------------------------|
| Wavelength | 410-3920 nm | (separate table for each wavelength) |
| Incidence angle at areoid | 25-75° | degrees |
| Emission angle at areoid | 0-45° | degrees |
| Phase angle at areoid | 45-135° | degrees |
| Elevation | -8000-26000 | meters |
| Dust optical depth | 0-1 | dimensionless opacity |
| Ice optical depth | 0-0.6 | dimensionless opacity |
| Surface temperature | 140-300 K | °K |
| Observed I/F | 0.03-0.50 | dimensionless |

Table 3-25. LUT for local surface temperature (ADR type = TE)

| VARIABLE | RANGE | UNITS |
|-------------------|-------------|---|
| Latitude | -90-90° | degrees |
| Slope magnitude | 0-10 | degrees |
| Slope azimuth | 0-270 | degrees clockwise from north |
| Elevation | -8000-26000 | meters |
| Thermal inertia | 5-5000 | J m ⁻² K ⁻¹ s ^{-0.5} |
| Dust+ice opacity | 0-1.0 | dimensionless opacity |
| Ls | 0-360° | degrees |
| Local time | 13-17 | (assumed local time)r |
| Bolometric albedo | 0.15-0.35 | dimensionless |

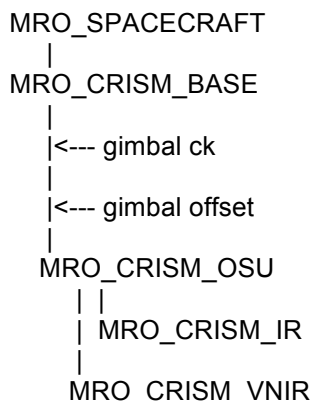
3.10 CRISM-Generated SPICE Files

Four types of SPICE kernels are needed to calculate CRISM's pointing:

1) Frames kernel (FK). This file defines the relationships of the of CRISM's field of view to the spacecraft, with the gimbal at "nadir". These transformations in frames of reference include:

- gimbal base (MRO_CRISM_BASE) -> spacecraft (MRO_SPACECRAFT)
- optical axis at gimbal "nadir" (MRO_CRISM_OSU) -> gimbal base (MRO_CRISM_BASE)
- (the gimbal C kernel defines the relationship of optic axis at a gimbal position to the gimbal nadir)
- (the gimbal offset defines the software offset between commanded nadir and physical nadir)
- IR zero position for IK (MRO_CRISM_IR) -> optical axis (MRO_CRISM_OSU); nominal there two are coaligned and offsets of the IR FOV from the optical axis are entirely accounted for in the IK
- VNIR zero position for IK (MRO_CRISM_VNIR) -> optical axis (MRO_CRISM_OSU); nominal there two are coaligned and offsets of the VNIR FOV from the optical axis are entirely accounted for in the IK

Graphically, this is:



The CRISM frames kernel is delivered to NAIF and is incorporated into the MRO frames kernel.

2) Instrument kernel (IK). This file describes the relationship of position of each detector element (at a row or wavelength and spatial or column position) to a zero position within the field of view. Nominally, that is in the VNIR row closest to 610 nm or the IR row closest to 2300 nm, at the column position closest to the optical axis. Due to keystone distortion, there is a different relationship for every row number of either detector.

The CRISM instrument kernel is delivered to NAIF.

3) Gimbal C kernel. This file gives a time history of the angle of the gimbal within the gimbal plane, relative to its commanded nadir. It is constructed from gimbal attitude measurements in image headers, i.e., from the TAB file part of an EDR. One file covers a 2-week time span of CRISM data.

CRISM gimbal C kernels are delivered to NAIF.

4) Metakernel. This file gives, for any time span covered by a gimbal C kernel, the MRO and CRISM SPICE kernels used to create DDRs for observations occurring during that time period. Note that kernels are loaded in the order listed., so the highest priority kernel is listed last.

3.11 Browse Products

Browse products are synoptic versions of data products to help identify products of interest. There are browse products for EDRs, MTRDRs, and MRDRs.

3.11.1 EDR Browse Products

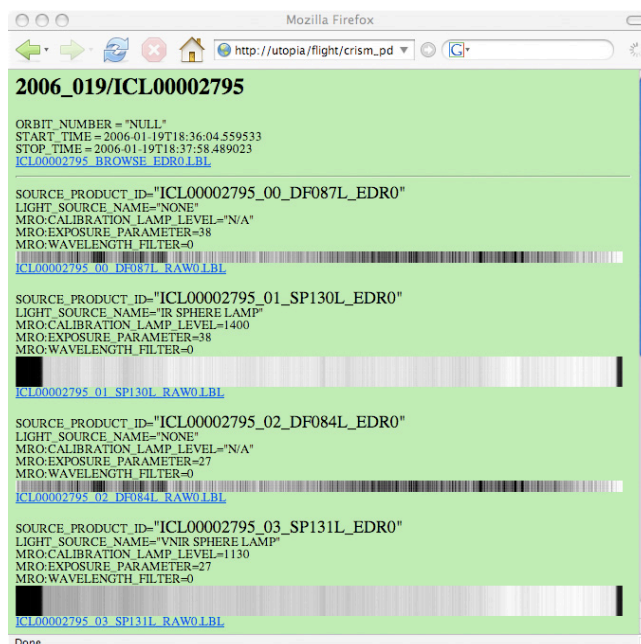
There are two types of products. One is an HTML file that gives the key parameters of the component EDRs for each observation, and links to PNG files for each EDR in the observation. A detached label to the HTML file describes the observation at a high level.

The browse product for each EDR is a scaled (0-255), median DN value from selected wavelengths for each spatial element in an EDR multiband image, stored in PNG format. The dimensions of the PNG file, XX pixels in the sample (cross-track) dimension and YY pixels in the line (along-track) dimension, match the spatial dimensions of the source EDR. A detached label to the PNG file describes the source EDR and the scaling between its raw data values and the PNG file.

Figure 3-26 shows an example EDR HTML browse product, linking to the PNG files for the component EDRs and to all of the associated labels.

An example set of EDR browse product labels is in Appendix I.

Figure 3-26. Example EDR browse product



3.11.2 MTRDR Browse Products

There are two types of MTRDR browse products. One is an HTML file that contains the key parameters of the source MTRDR, and links to PNG files for each TRDR in that observation. A detached label to the HTML file describes the observation at a high level.

There are up to four PNG browse product images for each VNIR MTRDR, and up to eleven PNG browse product images for each IR TRDR. The dimensions of each PNG file, XX pixels in the sample (cross-track) dimension and YY pixels in the line (along-track) dimension, match the spatial dimensions of the source MTRDR. A detached label to each PNG file describes the source MTRDR and the scaling between its raw data values and the PNG file.

The first VNIR browse product (browse product type TRU) is an enhanced true color representation of the scene, derived from I/F after correction for atmospheric or photometric effects:

red= 600-nm I/F

green = 530-nm I/F

blue = 440-nm I/F

The second VNIR browse product (type VNA) shows I/F at 770 nm, (derived from summary product R770), after correction for atmospheric and photometric effects.

The third VNIR browse product (type FEM) shows information related to Fe minerals. It is derived from the spectral parameters stored in summary products that have been corrected for atmospheric and photometric effects:

red= 530-nm band depth (derived from summary product BD530, highlighting some ferric minerals including hematite)

green = 600-nm shoulder (derived from summary product SH600, highlighting coatings and olivine)

blue = 1-micron band depth (derived from summary product BDI1000VIS, highlighting a variety of Fe minerals)

The fourth VNIR browse product (type FM2) shows complementary information related to Fe minerals. It is derived from the spectral parameters stored in summary products that have been corrected for atmospheric and photometric effects:

red= 530-nm band depth (derived from summary product BD530, highlighting some ferric minerals including hematite)

green = 920-nm band depth (derived from summary product SH600, highlighting crystalline ferric minerals or lo-Ca pyroxene)

blue = 1-micron band depth (derived from summary product BDI1000VIS, highlighting a variety of Fe minerals)

The first IR browse product (type IRA) shows I/F at 1330 nm, (derived from summary product IRA), after correction for atmospheric and photometric effects.

The second IR browse product (browse product type FAL) is an infrared false color representation of the scene, derived from I/F after correction for atmospheric or photometric effects. The wavelengths chosen highlight differences between key mineral groups:

red= 2529-nm I/F

green = 1506-nm I/F

blue = 1080-nm I/F

The third IR browse product (type MAF) shows information related to mafic mineralogy. It is derived from the spectral parameters stored in summary products that have been corrected for atmospheric and photometric effects:

red= scaled olivine index (derived from summary product OLINDEX2, highlighting olivine or iron phyllosilicates)

green = scaled LCP index (derived from summary product LCPINDEX, highlighting low-Ca pyroxene)

blue = scaled HCP index (derived from summary product HCPINDEX, highlighting high-Ca pyroxene)

The fourth IR browse product (type HYD) shows information related to bound water in minerals. It is also derived from the spectral parameters stored in summary products that have been corrected for atmospheric and photometric effects:

red = strength of bands due to bound water (derived from summary product SINDEXX, highlighting water-containing minerals or water ice)

green = 2.1 micron H₂O band depth (derived from summary product BD2100, highlighting monohydrated sulfates or water ice)

blue = 1.9 micron H₂O band depth (derived from summary products BD1900, highlighting hydrated sulfates, clays, glass, carbonate or water ice)

The fifth IR browse product (type PHY) shows information related to hydroxylated minerals including phyllosilicate. It is also derived from the spectral parameters stored in summary products that have been corrected for atmospheric and photometric effects:

red = 2.29 micron band depth (derived from summary product D2300 , highlighting Fe/Mg phyllosilicate or Mg-carbonate)

green = 2.21 micron band depth (derived from summary product BD2210, highlighting Al-phyllosilicate or hydrated silica)

blue = 1.9 micron H₂O band depth (derived from summary products BD1900, highlighting hydrated sulfates, clays, glass, carbonate or water ice)

The sixth IR browse product (type PH2) shows information related to cation composition of hydroxylated minerals including phyllosilicate. It is also derived from the spectral parameters stored in summary products that have been corrected for atmospheric and photometric effects:

red = 2.35 micron band depth (derived from summary products BD2350, highlighting chlorite, prehnite, or Ca/Fe carbonate)

green = 2.29 micron band depth (derived from summary product D2300 , highlighting Fe/Mg phyllosilicate or Mg-carbonate)

blue = 2.21 micron band depth (derived from summary product BD2210, highlighting Al-phyllosilicate or hydrated silica)

The seventh IR browse product (type ICE) shows information related to water or carbon dioxide frost or ice. It is also derived from the spectral parameters stored in summary products that have been corrected for atmospheric and photometric effects:

red = 1.9 micron H₂O band depth (derived from summary product BD1900, highlighting hydrated sulfates, clays, glass, carbonate or water ice)

green = 1.5 micron H₂O band depth (derived from summary product BD1500, highlighting water ice)

blue = 1.435 micron CO₂ ice band depth (derived from summary product BD1435, highlighting CO₂ ice)

The eighth IR browse product (type IC2) shows complementary information related to water or carbon dioxide frost or ice. It is also derived from a combination of I/F and spectral parameters stored in summary products that have both been corrected for atmospheric and photometric effects:

red= 3920-nm I/F, highlighting warm ice-free surfaces

green = 1.5 micron H₂O band depth (derived from summary product BD1500, highlighting water ice)

blue = 1.435 micron CO₂ ice band depth (derived from summary product BD1435, highlighting CO₂ ice)

The ninth IR browse product (type GLO) shows information related to putative chloride deposits in THEMIS "glowing terrain", and to spatially associated hydrated mineral deposits. It is derived from spectral parameters stored in summary products that have both been corrected for atmospheric and photometric effects. The combination of parameters highlights chlorides (blue) and hydrated minerals (yellow-green).

red = slope of the IR continuum (derived from summary product ISLOPE)

green = 3.0 micron H₂O band depth (derived from summary product BD3000, highlighting molecular water)

blue = spectral slope at 2.2-2.5 microns (derived from summary product IRR2)

The tenth IR browse product (type CAR) shows information related to Mg carbonate minerals. It is derived from spectral parameters stored in summary products that have both been corrected for atmospheric and photometric effects. The combination of parameters highlights Mg carbonates in bluish white:

red = 2.29 micron band depth (derived from summary product D2300 , highlighting Fe/Mg phyllosilicate or Mg-carbonate)

green = 2.5 micron carbonate band depth (derived from a non-standard summary product BD2500H which can be derived from CRISM hyperspectral but not multispectral data)

blue = 1.9 micron H₂O band depth (derived from summary products BD1900, highlighting hydrated sulfates, clays, glass, carbonate or water ice)

The eleventh IR browse product (type CR2) shows information related to Fe/Ca carbonate minerals. It is derived from spectral parameters stored in summary products that have both been corrected for atmospheric and photometric effects. The combination of parameters highlights Fe/Ca carbonates in white:

red = 2.29 micron band depth (derived from summary product D2300 , highlighting Fe/Mg phyllosilicate or carbonate)

green = 2.35 and 2.55 micron carbonate band depth (derived from summary product BDCARB , highlighting Fe/Ca carbonate)

blue = 3.9 micron carbonate band depth (derived from summary products CINDEX, highlighting Fe/Ca carbonate)

An example set of TRDR browse product labels is in Appendix J.

3.11.3 MRDR Browse Products

There are 11 browse products for MRDRs, a subset of the browse products created for MTRDRs. The product types IC2, GLO, CAR, and CR2 are not generated due to one of several reasons: lack of necessary wavelengths, lack of widespread deposits to be highlighted; or occurrence of artifacts between strips of data that would obscure real surface spectral variations. Formulations of the remaining products (TRU, VNA, FEM, FM2, FAL, IRA, MAF, PHY, PH2, HYD, ICE) are identical to those for MTRDR browse products, and a detached label to the PNG file describes the source MRDR and the scaling between its raw data values and the PNG file.

A detached label to each PNG file describes the source MRDR and the scaling between its raw data values and the PNG file.

An example set of MTRDR browse product labels is in Appendix K.

3.12 Extra Products

The detailed contents of operational CDR6's are described in Table 3-19.

Among the observation tracking tables, the format of only the OBS_ID table is well defined at this time. This table is used to provide a synopsis of the disposition and quality of CRISM observations that have actually been commanded to the instrument. Its contents are described in Table 3-27. There is one row per commanded EDR.

Table 3-27. Contents of OBS_ID Table.

| Information | Description |
|---------------------------|---|
| REQUEST_ID | May be null if it is not site-related, such as calibration or functional test (class = FUN or CAL). |
| PARTICIPATING_INSTRUMENTS | Any combination of the characters CHX to indicate instruments planning to participate. |
| COORDINATED_TARGET | 1 if true |
| MEP_TARGET | 1 if true |

| Information | Description |
|----------------------------|---|
| RIDEALONG | 1 if true |
| OBSERVATION_ID | 8-byte hexadecimal integer, if in integrated target list. |
| OBSERVATION_TYPE | FRT, HRL, HRS, EPF, TOD, MSW, MSS, MSP, CAL, FFC, ICL, STO, or FUN |
| ACTIVITY_ID | AC### where AC is a 2-letter designation of the type of measurement made, and ### as a 3-numeral designation of the instrument command macro that was executed to acquire the data. Macro numbers are in the range 0-255. BI is measurement of detector bias, DF is a measurement of background including dark current and thermal background, LP is measurement of a focal plane lamp, SP is measurement of the internal integrating sphere, and SC is measurement of an external scene. TP indicates that the EDR contains any test pattern produced by instrument electronics. T1 through T7 specify the test pattern, test pattern 1 through test pattern 7. UN indicates data in which housekeeping does not match the commanded instrument configuration. |
| PLAN_OBSERVATION_NUMBER | Monotonically increasing ordinal counter of the EDRs generated from one spectrometer for a single OBSERVATION_ID. |
| PLAN_SENSOR_ID | Spectrometer identifier. 0 = IR; 1 = VNIR. |
| PLAN_LINES | Number of frames |
| PLAN_BANDS | Number of wavelengths |
| PLAN_BINNING | Spatial pixel binning mode; specified separately for each detector; 0 = 1:1; 1 = 2:1; 2 = 5:1; 3 = 10:1 |
| PLAN_RATE | Rate of frame acquisition; 0 = 1 Hz; 1 = 3.75 Hz; 2 = 5 Hz; 3 = 15 Hz; 4 = 30 Hz; specified separately for each detector |
| PLAN_EXPOSURE_PARAMETER | At a given frame rate there are 480 possible exposure times ranging from 1 to 480. An exposure parameter of 480 yields an exposure time equal to the inverse of the frame rate. An exposure time parameter of 1 yields an exposure time 1/480 as large. |
| PLAN_SHUTTER_POS | Shutter position from 0 to 32; nominal open is 3; viewing sphere is 17; closed is 32. |
| PLAN_FILTER | Wavelength filter table; which of uploadable tables 0-3; specified separately for each detector |
| PLAN_FAST | Lossless Fast compression enabled or disabled; specified separately for each detector; 0 = disabled; 1 = enabled |
| PLAN_LOSSY | Lossy compression enabled or disabled; 12 to 8 bit look-up table commanded line by line in uploaded data structure; specified separately for each detector; 0 = disabled; 1 = enabled |
| PLAN_IR_FLOOD1_PWR | IR flood lamp 1 power (IR); 0 = off; 1 = on. |
| PLAN_IR_FLOOD1_LEVEL | IR flood lamp 1 level 0-4095. |
| PLAN_IR_FLOOD2_PWR | IR flood lamp 2 power (IR); 0 = off; 1 = on. |
| PLAN_IR_FLOOD2_LEVEL | IR flood lamp 2 level 0-4095. |
| PLAN_IR_SPHERE_PWR | IR sphere lamp power; 0 = off; 1 = on. |
| PLAN_IR_SPHERE_GOAL | Closed-loop goal, 0-4095. |
| PLAN_VNIR_FLOOD1_PWR | VNIR flood lamp 1 power (VNIR); 0 = off; 1 = on. |
| PLAN_VNIR_FLOOD1_LEVEL | VNIR flood lamp 1 level 0-4095. |
| PLAN_VNIR_FLOOD2_PWR | VNIR flood lamp 2 power (VNIR); 0 = off; 1 = on. |
| PLAN_VNIR_FLOOD2_LEVEL | VNIR flood lamp 2 level 0-4095. |
| PLAN_VNIR_SPHERE_PWR | VNIR sphere lamp power; 0 = off; 1 = on. |
| PLAN_VNIR_SPHERE_GOAL | Closed-loop goal, 0-4095. |
| PLAN_COMPRESSION_RATIO | Compression ratio used to model data volume. |
| PLAN_CLOSEST_APPROACH_TIME | yyyy-mm-ddThh:mm:ss.sss, ISO UTC time format |

| Information | Description |
|----------------------------|--|
| PLAN_START_TIME | yyyy-mm-ddThh:mm:ss.sss, ISO UTC time format |
| PLAN_STOP_TIME | yyyy-mm-ddThh:mm:ss.sss, ISO UTC time format |
| PLAN_LOWER_RIGHT_LATITUDE | Planned latitude of the surface point at the edge of the FOV on the antisunward (right-hand) side of the groundtrack at the observation start. |
| PLAN_LOWER_RIGHT_LONGITUDE | Planned longitude of the surface point at the edge of the FOV on the antisunward (right-hand) side of the groundtrack at the observation start. |
| PLAN_LOWER_LEFT_LATITUDE | Planned latitude of the surface point at the edge of the FOV on the sunward (left-hand) side of the groundtrack at the observation start. |
| PLAN_LOWER_LEFT_LONGITUDE | Planned longitude of the surface point at the edge of the FOV on the sunward (left-hand) side of the groundtrack at the observation start. |
| PLAN_UPPER_RIGHT_LATITUDE | Planned latitude of the surface point at the edge of the FOV on the antisunward (right-hand) side of the groundtrack at the observation end. |
| PLAN_UPPER_RIGHT_LONGITUDE | Planned longitude of the surface point at the edge of the FOV on the antisunward (right-hand) side of the groundtrack at the observation end. |
| PLAN_UPPER_LEFT_LATITUDE | Planned latitude of the surface point at the edge of the FOV on the sunward (left-hand) side of the groundtrack at the observation end. |
| PLAN_UPPER_LEFT_LONGITUDE | Planned longitude of the surface point at the edge of the FOV on the sunward (left-hand) side of the groundtrack at the observation end. |
| RECEIPT | Received on ground; 0 = no, 1 = partially received with no gap filled, 2 = partially received with gap filled, 3 = received. |
| PRODUCT_ID | CCCNNNNNNNN_XX_AAAAAS_EDRV where CCC = OBSERVATION_TYPE, NNNNNNNN = OBSERVATION_ID as a hexadecimal number, XX = OBSERVATION_NUMBER, AAAAA = ACTIVITY_ID, S = SENSOR_ID S or L, V = Product version number |
| ENCODING_COMPRESSION_RATIO | Actual compression ratio of data. |
| CLOSEST_APPROACH_TIME | yyyy-mm-ddThh:mm:ss.sss, ISO UTC time format |
| START_TIME | yyyy-mm-ddThh:mm:ss.sss, ISO UTC time format |
| STOP_TIME | yyyy-mm-ddThh:mm:ss.sss, ISO UTC time format |
| LOWER_RIGHT_LATITUDE | Actual latitude of the surface point at the edge of the FOV on the antisunward (right-hand) side of the groundtrack at the observation start. |
| LOWER_RIGHT_LONGITUDE | Actual longitude of the surface point at the edge of the FOV on the antisunward (right-hand) side of the groundtrack at the observation start. |
| LOWER_LEFT_LATITUDE | Actual latitude of the surface point at the edge of the FOV on the sunward (left-hand) side of the groundtrack at the observation start. |
| LOWER_LEFT_LONGITUDE | Actual longitude of the surface point at the edge of the FOV on the sunward (left-hand) side of the groundtrack at the observation start. |
| UPPER_RIGHT_LATITUDE | Actual latitude of the surface point at the edge of the FOV on the antisunward (right-hand) side of the groundtrack at the observation end. |

| Information | Description |
|-------------------------|--|
| UPPER_RIGHT_LONGITUDE | Actual longitude of the surface point at the edge of the FOV on the antisunward (right-hand) side of the groundtrack at the observation end. |
| UPPER_LEFT_LATITUDE | Actual latitude of the surface point at the edge of the FOV on the sunward (left-hand) side of the groundtrack at the observation end. |
| UPPER_LEFT_LONGITUDE | Actual longitude of the surface point at the edge of the FOV on the sunward (left-hand) side of the groundtrack at the observation end. |
| DATA_QUALITY_INDEX | See description in section 2.5.2 |
| FILE_SPECIFICATION_NAME | Pathname of image EDR in data directory, e.g., EDR/2006_350/FRT00001270/FRT00001270_01_SC001S_EDR 0.IMG |
| LINES | Number of frames |
| COMMENT | Text string describing nature of observation |

4. APPLICABLE SOFTWARE

4.1 Utility Programs

To facilitate timely and consistent analysis of CRISM data, the CRISM Analysis Tool (CAT) has been developed under the direction of Co-I Mustard. The Science Team has also developed a spectral library of well-characterized Mars analog materials, measured under dry N₂-purged conditions over CRISM's wavelength range and convolved with the CRISM's slit function. This special measurement environment is necessary because many lithologies of interest adsorb water strongly and under ambient conditions are spectrally dissimilar to their state on Mars.

The spectral library is documented separately; the reference is listed in section 1.2.

The CAT is based on the commercially available ENVI software package which requires IDL to run. Both CAT and the spectral library are available at the PDS Geosciences Node web site, <http://pds-geoscience.wustl.edu/>, along with tutorial information to operate the CAT.

Key data-reduction and management capabilities of the CRISM analysis tool (CAT) include:

- The CAT has the ability to read EDRs, TRDRs, DDRs, MRDRs, and CDRs, plus MTRDRs once available.
- The CAT has the ability to map-project data following the conventions given in section 3.4.2.
- The CAT has the ability to access the SOC and to download and apply current CDRs for correction of atmospheric and photometric effects.
- The CAT has the ability to create site-specific browse products.
- The CAT also has the ability to apply all of the extensive analysis capabilities already built into ENVI, including classification (e.g. spectral angle mapping), mixture modeling, principal components analysis, and techniques that use the spectral library as input.

4.2 Applicable PDS Software Tools

PDS-labeled images and tables can be viewed with the program NASAView, developed by the PDS and available for a variety of computer platforms from the PDS web site <http://pds.nasa.gov/tools>.

APPENDIX A. EDR LABEL

```

PDS_VERSION_ID          = PDS3
LABEL_REVISION_NOTE = "2003-11-19, S. Slavney (GEO);
                      2005-02-01, C. Hash (ACT);
                      2006-01-04, C. Hash (ACT);"

/* EDR Identification */

DATA_SET_ID              = "MRO-M-CRISM-2-EDR-V1.0"
PRODUCT_ID               = "FRT00004ECA_07_SC166L_EDR0"
/* cccnnnnnnnn_xx_ooaaas_EDRv          */
/* ccc = Class Type                    */
/* nnnnnnnn = Observation ID (hex)      */
/* xx = counter within observation (hex) */
/* ooaaa = obs type, macro number      */
/* s = sensor ID (S or L)              */
/* v = version number                  */

INSTRUMENT_HOST_NAME = "MARS RECONNAISSANCE ORBITER"
SPACECRAFT_ID        = MRO
INSTRUMENT_NAME      = "COMPACT RECONNAISSANCE IMAGING
                      SPECTROMETER FOR MARS"
INSTRUMENT_ID        = CRISM
TARGET_NAME          = MARS
PRODUCT_TYPE         = EDR
PRODUCT_CREATION_TIME = 2007-04-06T16:41:28
START_TIME           = 2007-03-23T03:02:31.910417
STOP_TIME            = 2007-03-23T03:04:39.644669
SPACECRAFT_CLOCK_START_COUNT = "2/0859086170.55396"
SPACECRAFT_CLOCK_STOP_COUNT = "2/0859086298.37980"
ORBIT_NUMBER         = "NULL"
OBSERVATION_TYPE     = "FRT"
OBSERVATION_ID       = "16#00004ECA#"
MRO:OBSERVATION_NUMBER = 16#07#
MRO:ACTIVITY_ID       = "SC166"
MRO:SENSOR_ID        = "L"
PRODUCT_VERSION_ID   = "0"
PRODUCER_INSTITUTION_NAME = "JOHNS HOPKINS UNIVERSITY
                          APPLIED PHYSICS LABORATORY"
SOFTWARE_NAME        = "pipe_edrslice"
SOFTWARE_VERSION_ID  = "4.3"

/* EDR Instrument and Observation Parameters */
/* for first frame */
TARGET_CENTER_DISTANCE = NULL <KM>
SOLAR_DISTANCE         = NULL <KM>
SHUTTER_MODE_ID        = OPEN
LIGHT_SOURCE_NAME      = "NONE"
MRO:CALIBRATION_LAMP_STATUS = "OFF"
MRO:CALIBRATION_LAMP_LEVEL = "N/A"
PIXEL_AVERAGING_WIDTH  = 1
MRO:INSTRUMENT_POINTING_MODE = "DYNAMIC POINTING"
SCAN_MODE_ID           = SHORT
MRO:FRAME_RATE         = 3.75 <HZ>
MRO:EXPOSURE_PARAMETER = 301
SAMPLING_MODE_ID       = "HYPERSPEC"
COMPRESSION_TYPE       = "NONE"
MRO:WAVELENGTH_FILTER  = 0
MRO:WAVELENGTH_FILE_NAME = "CDR6_1_0000000000_WV_L_1.TAB"
MRO:PIXEL_PROC_FILE_NAME = "CDR6_1_0000000000_PP_L_1.TAB"

```

```

MRO:LOOKUP_TABLE_FILE_NAME = "CDR6_1_0000000000_LK_J_0.TAB"

/* This EDR label describes two data files. The first file contains */
/* the first two objects and the second file contains the third: */
/* 1. A multiple-band image file containing uncalibrated EDR data, */
/* 2. A binary table of selected image row numbers from detector, */
/* 3. A table of ancillary and housekeeping data. */
/* Description of EDR IMAGE file */

OBJECT = FILE
  ^IMAGE      = "FRT00004ECA_07_SC166L_EDR0.IMG"
  ^ROWNUM_TABLE = ("FRT00004ECA_07_SC166L_EDR0.IMG", 210241)
  RECORD_TYPE  = FIXED_LENGTH
  RECORD_BYTES = 1280
  FILE_RECORDS = 210241

OBJECT = IMAGE
  LINES          = 480
  LINE_SAMPLES   = 640
  SAMPLE_TYPE    = MSB_UNSIGNED_INTEGER
  SAMPLE_BITS    = 16
  BANDS          = 438
  BAND_STORAGE_TYPE = LINE_INTERLEAVED
  MISSING_CONSTANT = 65535
  CHECKSUM       = "NULL"
END_OBJECT = IMAGE

OBJECT = ROWNUM_TABLE
  NAME          = "SELECTED ROWS FROM DETECTOR"
  INTERCHANGE_FORMAT = "BINARY"
  ROWS          = 438
  COLUMNS      = 1
  ROW_BYTES     = 2
  DESCRIPTION   = "The detector is subsampled in the spectral direction
                    by selecting specific rows to be downlinked. This
                    table provides a list of the rows selected for all
                    frames in this multidimensional image cube."

OBJECT = COLUMN
  NAME          = DETECTOR_ROW_NUMBER
  DATA_TYPE    = MSB_UNSIGNED_INTEGER
  BIT_MASK      = 2#0000000111111111#
  START_BYTE    = 1
  BYTES         = 2
  MISSING_CONSTANT = 65535
  DESCRIPTION   = "Detector row number from which the data was taken."
END_OBJECT = COLUMN

END_OBJECT = ROWNUM_TABLE

END_OBJECT = FILE

/* Description of EDR HOUSEKEEPING TABLE file */

OBJECT = FILE
  ^EDR_HK_TABLE = "FRT00004ECA_07_SC166L_HKP0.TAB"
  RECORD_TYPE    = FIXED_LENGTH
  RECORD_BYTES   = 1038
  FILE_RECORDS   = 480

OBJECT = EDR_HK_TABLE
  NAME          = "EDR HOUSEKEEPING TABLE"
  INTERCHANGE_FORMAT = "ASCII"
  ROWS          = 480
  COLUMNS      = 233

```

```
ROW_BYTES          = 1038

/* Columns in the table are described in this external file: */
^STRUCTURE         = "EDRHK.FMT"

END_OBJECT = EDR_HK_TABLE

END_OBJECT = FILE
END
```

APPENDIX B. DDR LABEL

```

PDS_VERSION_ID          = PDS3
LABEL_REVISION_NOTE     = "2004-11-22, S. Slavney (GEO);
                          2006-04-05, S. Murchie (JHU/APL);"

/* DDR Identification */

DATA_SET_ID              = "MRO-M-CRISM-6-DDR-V1.0"
PRODUCT_ID               = "FRT00004ECA_07_DE166L_DDR1"
/* cccnnnnnnnn_xx_ooaaas_DDRv          */
/* ccc = Class Type                    */
/* nnnnnnnn = Observation ID (hex)     */
/* xx = counter this observation (hex) */
/* ooaaa = obs type, macro number      */
/* s = sensor ID (S or L)              */
/* v = version number                  */

INSTRUMENT_HOST_NAME     = "MARS RECONNAISSANCE ORBITER"
SPACECRAFT_ID            = MRO
INSTRUMENT_NAME          = "COMPACT RECONNAISSANCE IMAGING
                          SPECTROMETER FOR MARS"

INSTRUMENT_ID            = CRISM
TARGET_NAME              = MARS
PRODUCT_TYPE             = DDR
PRODUCT_CREATION_TIME    = 2007-04-07T07:48:44
START_TIME               = 2007-03-23T03:02:31.499
STOP_TIME                = 2007-03-23T03:04:39.233
SPACECRAFT_CLOCK_START_COUNT = "2/859086170:55396"
SPACECRAFT_CLOCK_STOP_COUNT = "2/859086298:37980"

ORBIT_NUMBER             = 0
OBSERVATION_TYPE         = "FRT"
OBSERVATION_ID           = "16#00004ECA#"
MRO:OBSERVATION_NUMBER   = 16#07#
MRO:ACTIVITY_ID          = "DE166"
MRO:SENSOR_ID            = "L"
PRODUCT_VERSION_ID       = "1"
SOURCE_PRODUCT_ID        = {
    "MRO_SCLKSCET.00021.65536.tsc",
    "mro_v08.tf",
    "MRO_CRISM_FK_0000_000_N_1.TF",
    "MRO_CRISM_IK_0000_000_N_1.TI",
    "naif0008.tls",
    "pck00008.tpc",
    "mro_sc_psp_070313_070319.bc",
    "mro_sc_psp_070320_070326.bc",
    "mro_sc_2007-03-27.bc",
    "mro_sc_2007-03-28.bc",
    "spck_2007_081_r_1.bc",
    "spck_2007_082_r_1.bc",
    "spck_2007_083_r_1.bc",
    "spck_2007_084_r_1.bc",
    "spck_2007_085_r_1.bc",
    "spck_2007_086_r_1.bc",
    "de410.bsp",
    "mro_cruise.bsp",
    "mro_ab.bsp",
    "mro_psp.bsp",
    "mro_psp_rec.bsp"
}

```

```

PRODUCER_INSTITUTION_NAME    = "APPLIED PHYSICS LABORATORY"
SOFTWARE_NAME                 = "crism_ddr"
SOFTWARE_VERSION_ID           = "1.9"

/* DDR Instrument and Observation Parameters */

TARGET_CENTER_DISTANCE        = 3675.164588 <KM>
                               /* distance to Mars center at first frame */
SOLAR_DISTANCE                 = 212137794.935710 <KM>
SOLAR_LONGITUDE                = 205.303815 <DEGREES>
MRO:FRAME_RATE                 = 3.75 <HZ>
PIXEL_AVERAGING_WIDTH         = 1
MRO:INSTRUMENT_POINTING_MODE  = "DYNAMIC POINTING"
SCAN_MODE_ID                   = "LONG"

/* This DDR label describes one data file: */
/* 1. A multiple-band backplane image file with wavelength-independent, */
/* spatial pixel-dependent geometric and timing information. */

/* See the CRISM Data Products SIS for more detailed description. */

OBJECT                        = FILE
  ^IMAGE                      = "FRT00004ECA_07_DE166L_DDR1.IMG"
  RECORD_TYPE                 = FIXED_LENGTH
  RECORD_BYTES                 = 2560
  FILE_RECORDS                 = 6720

  OBJECT                      = IMAGE
    LINES                     = 480
    LINE_SAMPLES               = 640
    SAMPLE_TYPE                = PC_REAL
    SAMPLE_BITS                = 32
    BANDS                      = 14
    BAND_STORAGE_TYPE          = BAND_SEQUENTIAL
    BAND_NAME                   = ("INA at areoid, deg",
                                   "EMA at areoid, deg",
                                   "Phase angle, deg",
                                   "Latitude, areocentric, deg N",
                                   "Longitude, areocentric, deg E",
                                   "INA at surface from MOLA, deg",
                                   "EMA at surface from MOLA, deg",
                                   "Slope magnitude from MOLA, deg",
                                   "MOLA slope azimuth, deg clkwise from N",
                                   "Elevation, meters relative to MOLA",
                                   "Thermal inertia, J m^-2 K^-1 s^-0.5",
                                   "Bolometric albedo",
                                   "Local solar time, hours",
                                   "Spare")

  END_OBJECT                  = IMAGE

END_OBJECT                    = FILE

END

```


APPENDIX C1. TRDR LABEL (RADIANCE IMAGE + LISTFILE)

```

PDS_VERSION_ID          = PDS3
LABEL_REVISION_NOTE     = "2004-11-22, S. Slavney (GEO);
                           2005-12-20, H. Taylor (JHU/APL);
                           2006-04-05, S. Murchie (JHU/APL);
                           2006-09-18, P. Cavender (JHU/APL);
                           2007-04-30, P. Cavender (JHU/APL);
                           Version 1, Improved SS CDRs and
                           added post-processing bad pixel
                           correction
                           2007-09-13, D. Humm (JHU/APL);
                           Version 2, Improved calibration
                           motivated by Deimos observation
                           2010-06-01, D. Humm (JHU/APL);
                           Version 3, shutter mirror correction
                           and other calibration tweaks
                           2010-10-12, C. Hash (ACT);
                           Version 3, Added data filter control
                           parameters"

DATA_SET_ID              = "MRO-M-CRISM-3-RDR-TARGETED-V1.0"
PRODUCT_ID               = "FRT00004ECA_07_RA166L_TRR3"

/* cccnnnnnnnnn_xx_ooaaas_TRRv          */
/* ccc = Class Type                      */
/* nnnnnnnnn = Observation ID, hexadecimal */
/* ooaaa = Image type, Macro number       */
/* s = Sensor ID (S or L)                 */
/* v = Version number                     */

INSTRUMENT_HOST_NAME     = "MARS RECONNAISSANCE ORBITER"
SPACECRAFT_ID            = "MRO"
INSTRUMENT_NAME          = "COMPACT RECONNAISSANCE IMAGING
                           SPECTROMETER FOR MARS"

INSTRUMENT_ID            = "CRISM"
TARGET_NAME              = "MARS"
PRODUCT_TYPE             = "TARGETED_RDR"
PRODUCT_CREATION_TIME    = "2010-11-09T00:34:29"
START_TIME               = "2007-03-23T03:02:31.499"
STOP_TIME                = "2007-03-23T03:04:39.233"
SPACECRAFT_CLOCK_START_COUNT = "2/0859086170.55396"
SPACECRAFT_CLOCK_STOP_COUNT  = "2/0859086298.37980"
ORBIT_NUMBER             = "NULL"
OBSERVATION_TYPE         = "FRT"
OBSERVATION_ID           = "16#00004ECA#"
MRO:OBSERVATION_NUMBER   = "16#07#"
MRO:ACTIVITY_ID          = "RA166"
MRO:SENSOR_ID            = "L"
MRO:DETECTOR_TEMPERATURE = -165.838
MRO:OPTICAL_BENCH_TEMPERATURE = -48.411
MRO:SPECTROMETER_HOUSING_TEMP = -72.699
MRO:SPHERE_TEMPERATURE   = -48.064
MRO:FPE_TEMPERATURE      = 0.812
PRODUCT_VERSION_ID       = "3"
SOURCE_PRODUCT_ID = {
    "CDR410000000000_DM0000000L_3",
    "CDR410000000000_LL0000000L_4",
    "CDR410000000000_SH0000001L_4",
    "CDR410000000000_SS0000001L_6",
    "CDR410000000000_TD0000000S_2",
    "CDR410803692813_SF0000000L_4",
    "CDR420847411200_NU1000001L_5",

```

```

"CDR420859086160_BK1030100L_3",
"CDR420859086162_BP1000000L_3",
"CDR420859086162_UB1030100L_3",
"CDR420859086234_BP1000000L_3",
"CDR420859086302_BK1030100L_3",
"CDR420859086303_BP1000000L_3",
"CDR420859086303_UB1030100L_3",
"CDR420859087293_BK0003800L_3",
"CDR420859087299_UB0003800L_3",
"CDR420859087333_SP0003801L_3",
"CDR420859087333_SP0042501S_3",
"CDR420859087355_BK0003800L_3",
"CDR420859087361_UB0003800L_3",
"CDR420859127820_BI1000000L_3",
"CDR420861470430_BI0000000L_3",
"CDR6_1_0000000000_AS_L_0",

"CDR6_1_0000000000_BS_L_0",
"CDR6_1_0000000000_DB_L_0",
"CDR6_1_0000000000_EB_L_0",
"CDR6_1_0000000000_GH_L_2",
"CDR6_1_0000000000_HD_J_1",
"CDR6_1_0000000000_HK_J_1",
"CDR6_1_0000000000_HV_J_1",
"CDR6_1_0000000000_LC_L_1",
"CDR6_1_0000000000_LI_J_0",
"CDR6_1_0000000000_VL_L_0",
"CDR6_2_0835294537_PP_L_0",
"CDR6_2_0859075219_ST_J_0",
"FRT00004ECA_07_SC166L_EDR0"
}
MRO:INVALID_PIXEL_LOCATION = {
}
PRODUCER_INSTITUTION_NAME      = "JOHNS HOPKINS UNIVERSITY
                                   APPLIED PHYSICS LABORATORY"
SOFTWARE_NAME                    = "crism_imagecal"
SOFTWARE_VERSION_ID              = "2.5.3"

/* Targeted RDR Instrument and Observation Parameters */

TARGET_CENTER_DISTANCE          = "NULL" <KM>
SOLAR_DISTANCE                  = 212139419.063420 <KM>
SOLAR_LONGITUDE                 = 205.304261
SHUTTER_MODE_ID                 = "OPEN"
LIGHT_SOURCE_NAME                = "NONE"
MRO:CALIBRATION_LAMP_STATUS     = "OFF"
MRO:CALIBRATION_LAMP_LEVEL      = "N/A"
PIXEL_AVERAGING_WIDTH           = 1
MRO:INSTRUMENT_POINTING_MODE    = "DYNAMIC POINTING"
SCAN_MODE_ID                    = "SHORT"
MRO:FRAME_RATE                  = 3.75 <HZ>
MRO:EXPOSURE_PARAMETER          = 301
SAMPLING_MODE_ID                = "HYPERSPEC"
COMPRESSION_TYPE                = "NONE"
MRO:WAVELENGTH_FILTER           = "0"
MRO:WAVELENGTH_FILE_NAME        = "CDR410803692813_WA0000000L_3.IMG"
MRO:PIXEL_PROC_FILE_NAME        = "CDR6_2_0835294537_PP_L_0.TAB"
MRO:INV_LOOKUP_TABLE_FILE_NAME  = "CDR6_1_0000000000_LI_J_0.TAB"
MRO:ATMO_CORRECTION_FLAG        = "OFF"
MRO:THERMAL_CORRECTION_MODE     = "OFF"
MRO:PHOTOCLIN_CORRECTION_FLAG  = "OFF"
MRO:SPATIAL_RESAMPLING_FLAG     = "OFF"
MRO:SPATIAL_RESAMPLING_FILE     = "N/A"

MRO:SPATIAL_RESCALING_FLAG      = "OFF"

```

```

MRO:SPATIAL_RESCALING_FILE      = "N/A"
MRO:SPECTRAL_RESAMPLING_FLAG    = "OFF"
MRO:SPECTRAL_RESAMPLING_FILE    = "N/A"

/* Hyperspectral Data Filter Control Parameters */

MRO:HDF_SOFTWARE_NAME           = "N/A"

MRO:HDF_SOFTWARE_VERSION_ID     = "N/A"
MRO:IF_MIN_VALUE                = "N/A"
MRO:IF_MAX_VALUE                = "N/A"
MRO:TRACE_MIN_VALUE             = "N/A"
MRO:TRACE_MAX_VALUE             = "N/A"
MRO:REFZ_MEDIAN_BOX_WIDTH       = "N/A"
MRO:REFZ_SMOOTH_BOX_WIDTH       = "N/A"
MRO:FRAM_STAT_MEDIAN_BOX_WIDTH  = "N/A"
MRO:FRAM_STAT_MIN_DEVIATION     = "N/A"
MRO:FRAM_STAT_MEDIAN_CONF_LVL   = "N/A"
MRO:FRAM_STAT_IQR_CONF_LVL     = "N/A"
MRO:RSC_REF_XY_MEDIAN_WIDTH     = "N/A"
MRO:RSC_REF_XY_SMOOTH_WIDTH     = "N/A"
MRO:RSC_REF_YZ_MEDIAN_WIDTH     = "N/A"
MRO:RSC_REF_YZ_SMOOTH_WIDTH     = "N/A"
MRO:RSC_RATIO_XY_MEDIAN_WIDTH   = "N/A"
MRO:RSC_RATIO_XY_SMOOTH_WIDTH   = "N/A"
MRO:RSC_RES_XY_PLY_ORDER        = "N/A"
MRO:RSC_RES_XY_PLY_EXTND_WIDTH  = "N/A"
MRO:LOG_XFORM_NEG_CLIP_VALUE    = "N/A"
MRO:IKF_NUM_REGIONS             = "N/A"
MRO:IKF_START_CHANNEL           = ("N/A", "N/A")
MRO:IKF_STOP_CHANNEL            = ("N/A", "N/A")
MRO:IKF_CONFIDENCE_LEVEL        = ("N/A", "N/A")
MRO:IKF_WEIGHTING_STDDEV        = ("N/A", "N/A")
MRO:IKF_KERNEL_SIZE_X           = ("N/A", "N/A")
MRO:IKF_KERNEL_SIZE_Y           = ("N/A", "N/A")
MRO:IKF_KERNEL_SIZE_Z           = ("N/A", "N/A")
MRO:IKF_MODEL_ORDER_X           = ("N/A", "N/A")
MRO:IKF_MODEL_ORDER_Y           = ("N/A", "N/A")
MRO:IKF_MODEL_ORDER_Z           = ("N/A", "N/A")

/* This Targeted RDR label describes two data files.  The first file */
/* contains the first two objects and the second file contains the   */
/* third:                                                              */
/* 1. A multiple-band image file containing calibrated RDR data,      */
/*    in units of radiance,                                           */
/* 2. A binary table of selected image row numbers from detector,     */
/* 3. A table of ancillary and housekeeping data converted to        */
/*    engineering units.                                              */

OBJECT      = FILE
^IMAGE      = "FRT00004ECA_07_RA166L_TRR3.IMG"
^ROWNUM_TABLE = ("FRT00004ECA_07_RA166L_TRR3.IMG", 210241 )
RECORD_TYPE = FIXED_LENGTH
RECORD_BYTES = 2560
FILE_RECORDS = 210241

OBJECT      = IMAGE
  LINES      = 480
  LINE_SAMPLES = 640
  SAMPLE_TYPE = PC_REAL
  SAMPLE_BITS = 32
  UNIT        = "W / (m**2 micrometer sr)"
  BANDS       = 438
  BAND_STORAGE_TYPE = LINE_INTERLEAVED
END_OBJECT = IMAGE

```

```

OBJECT          = ROWNUM_TABLE
  NAME          = "SELECTED ROWS FROM DETECTOR"
  INTERCHANGE_FORMAT = "BINARY"
  ROWS          = 438
  COLUMNS      = 1
  ROW_BYTES     = 2
  DESCRIPTION   = "The detector is subsampled in the spectral direction
                  by selecting specific rows to be downlinked. This
                  table provides a list of the rows selected for all
                  frames in this multidimensional image cube."

  OBJECT = COLUMN
    NAME          = DETECTOR_ROW_NUMBER
    DATA_TYPE     = MSB_UNSIGNED_INTEGER
    COLUMN_NUMBER  = 1
    BIT_MASK       = 2#0000000111111111#
    START_BYTE     = 1
    BYTES          = 2
    DESCRIPTION    = "Detector row number from which the data was taken."
  END_OBJECT = COLUMN
END_OBJECT      = ROWNUM_TABLE

END_OBJECT = FILE

OBJECT = FILE
  ^TRDR_HK_TABLE = "FRT00004ECA_07_RA166L_HKP3.TAB"
  RECORD_TYPE    = FIXED_LENGTH
  RECORD_BYTES   = 1221
  FILE_RECORDS   = 480
  OBJECT         = TRDR_HK_TABLE
  NAME          = "TARGETED RDR HOUSEKEEPING TABLE"
  INTERCHANGE_FORMAT = ASCII
  ROWS          = 480
  COLUMNS      = 233
  ROW_BYTES     = 1221
  ^STRUCTURE     = "TRDRHK.FMT"
  END_OBJECT     = TRDR_HK_TABLE
END_OBJECT = FILE
END

```

APPENDIX C2. TRDR LABEL (I/F IMAGE)

```

PDS_VERSION_ID          = PDS3
LABEL_REVISION_NOTE     = "2004-11-22, S. Slavney (GEO);
                           2005-12-20, H. Taylor (JHU/APL);
                           2006-04-05, S. Murchie (JHU/APL);
                           2006-09-18, P. Cavender (JHU/APL);
                           2007-04-30, P. Cavender (JHU/APL);
                           Version 1, Improved SS CDRs and
                           added post-processing bad pixel
                           correction
                           2007-09-13, D. Humm (JHU/APL);
                           Version 2, Improved calibration
                           motivated by Deimos observation
                           2010-06-01, D. Humm (JHU/APL);
                           Version 3, shutter mirror correction
                           and other calibration tweaks
                           2010-10-12, C. Hash (ACT);
                           Version 3, Added data filter control
                           parameters"

DATA_SET_ID              = "MRO-M-CRISM-3-RDR-TARGETED-V1.0"
PRODUCT_ID               = "FRT00004ECA_07_IF166L_TRR3"

/* cccnnnnnnnnn_xx_ooaaas_TRRv          */
/* ccc = Class Type                      */
/* nnnnnnnnn = Observation ID, hexadecimal */
/* ooaaa = Image type, Macro number       */
/* s = Sensor ID (S or L)                */
/* v = Version number                    */

INSTRUMENT_HOST_NAME     = "MARS RECONNAISSANCE ORBITER"
SPACECRAFT_ID            = "MRO"
INSTRUMENT_NAME          = "COMPACT RECONNAISSANCE IMAGING
                           SPECTROMETER FOR MARS"

INSTRUMENT_ID            = "CRISM"
TARGET_NAME              = "MARS"
PRODUCT_TYPE             = "TARGETED_RDR"
PRODUCT_CREATION_TIME    = "2010-11-11T04:21:39"
START_TIME               = "2007-03-23T03:02:31.499"
STOP_TIME                = "2007-03-23T03:04:39.233"
SPACECRAFT_CLOCK_START_COUNT = "2/0859086170.55396"
SPACECRAFT_CLOCK_STOP_COUNT = "2/0859086298.37980"
ORBIT_NUMBER             = "NULL"
OBSERVATION_TYPE         = "FRT"
OBSERVATION_ID           = "16#00004ECA#"
MRO:OBSERVATION_NUMBER   = "16#07#"
MRO:ACTIVITY_ID          = "IF166"
MRO:SENSOR_ID            = "L"
MRO:DETECTOR_TEMPERATURE = -165.838
MRO:OPTICAL_BENCH_TEMPERATURE = -48.411
MRO:SPECTROMETER_HOUSING_TEMP = -72.699
MRO:SPHERE_TEMPERATURE   = -48.064
MRO:FPE_TEMPERATURE      = 0.812
PRODUCT_VERSION_ID       = "3"
SOURCE_PRODUCT_ID = {
    "CDR410000000000_DM0000000L_3",
    "CDR410000000000_LL0000000L_4",
    "CDR410000000000_SH0000001L_4",
    "CDR410000000000_SS0000001L_6",
    "CDR410000000000_TD0000000S_2",
    "CDR410803692813_SF0000000L_4",
    "CDR420847411200_NU1000001L_5",

```

```

"CDR420859086160_BK1030100L_3",
"CDR420859086162_BP1000000L_3",
"CDR420859086162_UB1030100L_3",
"CDR420859086234_BP1000000L_3",
"CDR420859086302_BK1030100L_3",
"CDR420859086303_BP1000000L_3",
"CDR420859086303_UB1030100L_3",
"CDR420859087293_BK0003800L_3",
"CDR420859087299_UB0003800L_3",
"CDR420859087333_SP0003801L_3",
"CDR420859087333_SP0042501S_3",
"CDR420859087355_BK0003800L_3",
"CDR420859087361_UB0003800L_3",
"CDR420859127820_BI1000000L_3",
"CDR420861470430_BI0000000L_3",
"CDR6_1_0000000000_AS_L_0",

"CDR6_1_0000000000_BS_L_0",
"CDR6_1_0000000000_DB_L_0",
"CDR6_1_0000000000_EB_L_0",
"CDR6_1_0000000000_GH_L_2",
"CDR6_1_0000000000_HD_J_1",
"CDR6_1_0000000000_HK_J_1",
"CDR6_1_0000000000_HV_J_1",
"CDR6_1_0000000000_LC_L_1",
"CDR6_1_0000000000_LI_J_0",
"CDR6_1_0000000000_VL_L_0",
"CDR6_2_0835294537_PP_L_0",
"CDR6_2_0859075219_ST_J_0",
"FRT00004ECA_07_SC166L_EDR0"
}
MRO:INVALID_PIXEL_LOCATION = {
}
PRODUCER_INSTITUTION_NAME      = "JOHNS HOPKINS UNIVERSITY
                                   APPLIED PHYSICS LABORATORY"
SOFTWARE_NAME                   = "crism_imagecal"
SOFTWARE_VERSION_ID             = "2.5.3"

/* Targeted RDR Instrument and Observation Parameters */

TARGET_CENTER_DISTANCE          = "NULL" <KM>
SOLAR_DISTANCE                  = 212139419.063420 <KM>
SOLAR_LONGITUDE                 = 205.304261
SHUTTER_MODE_ID                 = "OPEN"
LIGHT_SOURCE_NAME               = "NONE"
MRO:CALIBRATION_LAMP_STATUS     = "OFF"
MRO:CALIBRATION_LAMP_LEVEL     = "N/A"
PIXEL_AVERAGING_WIDTH          = 1
MRO:INSTRUMENT_POINTING_MODE    = "DYNAMIC POINTING"
SCAN_MODE_ID                   = "SHORT"
MRO:FRAME_RATE                  = 3.75 <HZ>
MRO:EXPOSURE_PARAMETER          = 301
SAMPLING_MODE_ID               = "HYPERSPEC"
COMPRESSION_TYPE                = "NONE"
MRO:WAVELENGTH_FILTER           = "0"
MRO:WAVELENGTH_FILE_NAME       = "CDR410803692813_WA0000000L_3.IMG"
MRO:PIXEL_PROC_FILE_NAME       = "CDR6_2_0835294537_PP_L_0.TAB"
MRO:INV_LOOKUP_TABLE_FILE_NAME = "CDR6_1_0000000000_LI_J_0.TAB"
MRO:ATMO_CORRECTION_FLAG       = "OFF"
MRO:THERMAL_CORRECTION_MODE     = "OFF"
MRO:PHOTOCLIN_CORRECTION_FLAG  = "OFF"
MRO:SPATIAL_RESAMPLING_FLAG    = "OFF"
MRO:SPATIAL_RESAMPLING_FILE    = "N/A"

```

```

MRO:SPATIAL_RESCALING_FLAG      = "OFF"
MRO:SPATIAL_RESCALING_FILE      = "N/A"
MRO:SPECTRAL_RESAMPLING_FLAG    = "OFF"
MRO:SPECTRAL_RESAMPLING_FILE    = "N/A"

/* Hyperspectral Data Filter Control Parameters */

MRO:HDF_SOFTWARE_NAME           = "crismhdf"
MRO:HDF_SOFTWARE_VERSION_ID     = "1.0.4"
MRO:IF_MIN_VALUE                = 0.000000
MRO:IF_MAX_VALUE                = 1.000000
MRO:TRACE_MIN_VALUE             = 0.01
MRO:TRACE_MAX_VALUE             = 100.00
MRO:REFZ_MEDIAN_BOX_WIDTH       = 35
MRO:REFZ_SMOOTH_BOX_WIDTH       = 9
MRO:FRAM_STAT_MEDIAN_BOX_WIDTH  = 5
MRO:FRAM_STAT_MIN_DEVIATION     = 0.00500000
MRO:FRAM_STAT_MEDIAN_CONF_LVL   = 0.99999900
MRO:FRAM_STAT_IQR_CONF_LVL      = 0.99999900
MRO:RSC_REF_XY_MEDIAN_WIDTH     = 15
MRO:RSC_REF_XY_SMOOTH_WIDTH     = 5
MRO:RSC_REF_YZ_MEDIAN_WIDTH     = 15
MRO:RSC_REF_YZ_SMOOTH_WIDTH     = 5
MRO:RSC_RATIO_XY_MEDIAN_WIDTH   = 25
MRO:RSC_RATIO_XY_SMOOTH_WIDTH   = 13
MRO:RSC_RES_XY_PLY_ORDER        = 5
MRO:RSC_RES_XY_PLY_EXTND_WIDTH  = 38
MRO:LOG_XFORM_NEG_CLIP_VALUE    = 0.00000100
MRO:IKF_NUM_REGIONS             = 2
MRO:IKF_START_CHANNEL           = ( 0, 179 )
MRO:IKF_STOP_CHANNEL            = ( 178, 437 )
MRO:IKF_CONFIDENCE_LEVEL        = ( 0.900, 0.900 )
MRO:IKF_WEIGHTING_STDDEV        = ( 1.500, 1.250 )
MRO:IKF_KERNEL_SIZE_X           = ( 5, 5 )
MRO:IKF_KERNEL_SIZE_Y           = ( 3, 3 )
MRO:IKF_KERNEL_SIZE_Z           = ( 5, 5 )
MRO:IKF_MODEL_ORDER_X           = ( 1, 1 )
MRO:IKF_MODEL_ORDER_Y           = ( 1, 1 )
MRO:IKF_MODEL_ORDER_Z           = ( 1, 4 )

/* This Targeted RDR label describes two data files.  The first file */
/* contains the first two objects and the second file contains the */
/* third:                                                              */
/* 1. A multiple-band image file containing calibrated RDR data,      */
/*    in units of radiance,                                           */
/* 2. A binary table of selected image row numbers from detector,     */
/* 3. A table of ancillary and housekeeping data converted to        */
/*    engineering units.                                              */

OBJECT      = FILE
^IMAGE      = "FRT00004ECA_07_IF166L_TRR3.IMG"
^ROWNUM_TABLE = ("FRT00004ECA_07_IF166L_TRR3.IMG", 210241 )
RECORD_TYPE = FIXED_LENGTH
RECORD_BYTES = 2560
FILE_RECORDS = 210241

OBJECT      = IMAGE
  LINES      = 480
  LINE_SAMPLES = 640
  SAMPLE_TYPE = PC_REAL
  SAMPLE_BITS = 32
  UNIT        = "I_OVER_F"
  BANDS       = 438
  BAND_STORAGE_TYPE = LINE_INTERLEAVED
END_OBJECT = IMAGE

```

```

OBJECT          = ROWNUM_TABLE
  NAME           = "SELECTED ROWS FROM DETECTOR"
  INTERCHANGE_FORMAT = "BINARY"
  ROWS           = 438
  COLUMNS       = 1
  ROW_BYTES      = 2
  DESCRIPTION    = "The detector is subsampled in the spectral direction
                    by selecting specific rows to be downlinked. This
                    table provides a list of the rows selected for all
                    frames in this multidimensional image cube."

  OBJECT = COLUMN
    NAME           = DETECTOR_ROW_NUMBER
    DATA_TYPE      = MSB_UNSIGNED_INTEGER
    COLUMN_NUMBER   = 1
    BIT_MASK        = 2#0000000111111111#
    START_BYTE      = 1
    BYTES           = 2
    DESCRIPTION     = "Detector row number from which the data was taken."
  END_OBJECT = COLUMN
END_OBJECT      = ROWNUM_TABLE

END_OBJECT = FILE

OBJECT = FILE
  ^TRDR_HK_TABLE   = "FRT00004ECA_07_RA166L_HKP3.TAB"
  RECORD_TYPE      = FIXED_LENGTH
  RECORD_BYTES     = 1221
  FILE_RECORDS     = 480
  OBJECT           = TRDR_HK_TABLE
  NAME             = "TARGETED RDR HOUSEKEEPING TABLE"
  INTERCHANGE_FORMAT = ASCII
  ROWS             = 480
  COLUMNS         = 233
  ROW_BYTES        = 1221
  ^STRUCTURE       = "TRDRHK.FMT"
  END_OBJECT       = TRDR_HK_TABLE
END_OBJECT = FILE
END

```


APPENDIX D1. MRDR LABEL (I/F IMAGE)

```

PDS_VERSION_ID          = PDS3
RECORD_TYPE              = FIXED_LENGTH
RECORD_BYTES             = 4544
FILE_RECORDS             = 92160
LABEL_REVISION_NOTE      = "2003-11-19, S. Slavney (GEO);
                           2005-09-25, S. Murchie (JHU/APL);
                           2007-03-09, E. Malaret (ACT Corp.);
                           2007-09-14, C. Hash (ACT Corp)"

^IMAGE                   = "T1396_MRRIF_30N088_0256_1.IMG"

/* Map-projected Multispectral RDR Identification */

DATA_SET_ID              = "MRO-M-CRISM-5-RDR-MULTISPECTRAL-V1.0"
PRODUCT_ID               = "T1396_MRRIF_30N088_0256_1"
/*( TNNNN MRRss_yydxrr_v                                     )*/
/*( NNNN = tile number                                       )*/
/*( ss = subtype of image product                           )*/
/*( yy = latitude of upper left corner                       )*/
/*( d = N or S for north or south latitude                  )*/
/*( xxx = east longitude of upper left corner                )*/
/*( rrrr = resolution in pixels/degree                       )*/
/*( v = version number                                       )*/

INSTRUMENT_HOST_NAME     = "MARS RECONNAISSANCE ORBITER"
SPACECRAFT_ID            = MRO
INSTRUMENT_NAME           = "COMPACT RECONNAISSANCE IMAGING
                           SPECTROMETER FOR MARS"

INSTRUMENT_ID            = CRISM
TARGET_NAME              = MARS
PRODUCT_TYPE             = MAP_PROJECTED_MULTISPECTRAL_RDR
PRODUCT_CREATION_TIME     = 2008-12-09T07:58:41.208
START_TIME                = "N/A"
STOP_TIME                 = "N/A"
SPACECRAFT_CLOCK_START_COUNT = "N/A"
SPACECRAFT_CLOCK_STOP_COUNT = "N/A"
PRODUCT_VERSION_ID       = "1"
PRODUCER_INSTITUTION_NAME = "APPLIED PHYSICS LABORATORY"
SOFTWARE_NAME             = "PIPE_create_crism_mrdr_product"
SOFTWARE_VERSION_ID       = "12.05.08"
MRO:WAVELENGTH_FILE_NAME = "T1396_MRRWV_30N088_0256_1.TAB"

/* This Map Projected Multispectral RDR label describes one data file: */
/* 1. A multiple-band image file of calibrated RDR data in radiance, */
/* This RDR represents one latitude-longitude bin in a global map. */
/* See the Map Projection Object below for bin coordinates and resolution.*/
/* See the CRISM Data Products SIS for more detailed description. */

/* Description of MAP PROJECTED MULTISPECTRAL RDR RADIANCE IMAGE file */

OBJECT                    = IMAGE
  LINES                   = 1280
  LINE_SAMPLES            = 1136
  SAMPLE_TYPE             = PC_REAL
  SAMPLE_BITS             = 32
  UNIT                    = "I over F"
  BANDS                   = 72
  BAND_STORAGE_TYPE       = BAND_SEQUENTIAL
END_OBJECT                = IMAGE

```

```

/* Map projection information about this RDR is in the IMAGE_MAP_PROJECTION */
/* object below. */

```

```

OBJECT                = IMAGE_MAP_PROJECTION
  ^DATA_SET_MAP_PROJECTION = "MRR_MAP.CAT"
  MAP_PROJECTION_TYPE      = "EQUIRECTANGULAR"
  A_AXIS_RADIUS            = 3396 <KM>
  B_AXIS_RADIUS            = 3396 <KM>
  C_AXIS_RADIUS            = 3396 <KM>
  FIRST_STANDARD_PARALLEL  = "N/A"
  SECOND_STANDARD_PARALLEL = "N/A"
  POSITIVE_LONGITUDE_DIRECTION = "EAST"
  CENTER_LATITUDE          = 27.50000 <DEGREE>
  CENTER_LONGITUDE         = 87.50000 <DEGREE>
  REFERENCE_LATITUDE       = "N/A"
  REFERENCE_LONGITUDE      = "N/A"
  LINE_FIRST_PIXEL         = 1 /* North edge */
  LINE_LAST_PIXEL          = 1280 /* South edge */
  SAMPLE_FIRST_PIXEL       = 1 /* West edge */
  SAMPLE_LAST_PIXEL        = 1136 /* East edge */
  MAP_PROJECTION_ROTATION  = 0.0
  MAP_RESOLUTION           = 256 <PIXEL/DEGREE>
  MAP_SCALE                = 0.231528833585 <KM/PIXEL>
  MAXIMUM_LATITUDE         = 32.50000 <DEGREE>
  MINIMUM_LATITUDE         = 27.50000 <DEGREE>
  WESTERNMOST_LONGITUDE    = 85.00000 <DEGREE>
  EASTERNMOST_LONGITUDE    = 90.00000 <DEGREE>
  LINE_PROJECTION_OFFSET   = 8320.000
  SAMPLE_PROJECTION_OFFSET = 640.000
  COORDINATE_SYSTEM_TYPE   = "BODY-FIXED ROTATING"
  COORDINATE_SYSTEM_NAME   = "PLANETOCENTRIC"
END_OBJECT              = IMAGE_MAP_PROJECTION

```

```

END

```

APPENDIX D2. MRDR LABEL (DERIVED DATA IMAGE)

```

PDS_VERSION_ID          = PDS3
RECORD_TYPE              = FIXED_LENGTH
RECORD_BYTES            = 4544
FILE_RECORDS            = 30720
LABEL_REVISION_NOTE     = "2003-11-19, S. Slavney (GEO);
                           2005-09-25, S. Murchie (JHU/APL);
                           2007-03-09, E. Malaret (ACT Corp.);
                           2007-09-14, C. Hash (ACT Corp)"

^IMAGE                  = "T1396_MRRDE_30N088_0256_1.IMG"

/* Map-projected Multispectral RDR Identification */

DATA_SET_ID              = "MRO-M-CRISM-5-RDR-MULTISPECTRAL-V1.0"
PRODUCT_ID               = "T1396_MRRDE_30N088_0256_1"
/*( TNNNN_MRRss_yydxrrrr_v                                     )*/
/*( NNNN = tile number                                         )*/
/*( ss = subtype of image product                             )*/
/*( yy = latitude of upper left corner                         )*/
/*( d = N or S for north or south latitude                    )*/
/*( xxx = east longitude of upper left corner                 )*/
/*( rrrr = resolution in pixels/degree                        )*/
/*( v = version number                                         )*/

INSTRUMENT_HOST_NAME     = "MARS RECONNAISSANCE ORBITER"
SPACECRAFT_ID            = MRO
INSTRUMENT_NAME          = "COMPACT RECONNAISSANCE IMAGING
                           SPECTROMETER FOR MARS"

INSTRUMENT_ID            = CRISM
TARGET_NAME              = MARS
PRODUCT_TYPE             = MAP_PROJECTED_MULTISPECTRAL_RDR
PRODUCT_CREATION_TIME    = 2008-12-09T07:58:41.208
START_TIME               = "N/A"
STOP_TIME                = "N/A"
SPACECRAFT_CLOCK_START_COUNT = "N/A"
SPACECRAFT_CLOCK_STOP_COUNT = "N/A"
PRODUCT_VERSION_ID       = "1"
PRODUCER_INSTITUTION_NAME = "APPLIED PHYSICS LABORATORY"
SOFTWARE_NAME            = "PIPE_create_crism_mrdr_product"
SOFTWARE_VERSION_ID       = "12.05.08"
MRO:WAVELENGTH_FILE_NAME = "T1396_MRRWV_30N088_0256_1.TAB"

/* This Map Projected Multispectral RDR label describes one data file: */
/* 1. A multiple-band image file of calibrated RDR data in radiance, */
/* This RDR represents one latitude-longitude bin in a global map. */
/* See the Map Projection Object below for bin coordinates and resolution.*/
/* See the CRISM Data Products SIS for more detailed description. */

/* Description of MAP PROJECTED MULTISPECTRAL RDR RADIANCE IMAGE file */

OBJECT                  = IMAGE
  LINES                 = 1280
  LINE_SAMPLES          = 1136
  SAMPLE_TYPE           = PC_REAL
  SAMPLE_BITS           = 32

  BANDS                 = 24
  BAND_STORAGE_TYPE     = BAND_SEQUENTIAL
  BAND_NAME             = ("Solar longitude, deg",
                           "Solar distance, AU",

```

```

        "Observation ID, VNIR",
        "Observation ID, IR",
        "Ordinal counter, VNIR",
        "Ordinal counter, IR",
        "Column number, VNIR",
        "Column number, IR",
        "Line, or frame number, VNIR",
        "Line, or frame number, IR",
        "INA at areoid, deg",
        "EMA at areoid, deg",
        "Phase angle, deg",
        "Latitude, areocentric, deg N",
        "Longitude, areocentric, deg E",
        "INA at surface from MOLA, deg",
        "EMA at surface from MOLA, deg",
        "Slope magnitude from MOLA, deg",
        "MOLA slope azimuth, deg clkwise from N",
        "Elevation, meters relative to MOLA",
        "Thermal inertia, J m-2 K-1 s-0.5",
        "Bolometric albedo",
        "Local solar time, hours",
        "Spare")
END_OBJECT = IMAGE

/* Map projection information about this RDR is in the IMAGE_MAP_PROJECTION */
/* object below. */

OBJECT = IMAGE_MAP_PROJECTION
  ^DATA SET MAP_PROJECTION = "MRR_MAP.CAT"
  MAP_PROJECTION_TYPE = "EQUIRECTANGULAR"
  A_AXIS_RADIUS = 3396 <KM>
  B_AXIS_RADIUS = 3396 <KM>
  C_AXIS_RADIUS = 3396 <KM>
  FIRST_STANDARD_PARALLEL = "N/A"
  SECOND_STANDARD_PARALLEL = "N/A"
  POSITIVE_LONGITUDE_DIRECTION = "EAST"
  CENTER_LATITUDE = 27.50000 <DEGREE>
  CENTER_LONGITUDE = 87.50000 <DEGREE>
  REFERENCE_LATITUDE = "N/A"
  REFERENCE_LONGITUDE = "N/A"
  LINE_FIRST_PIXEL = 1 /* North edge */
  LINE_LAST_PIXEL = 1280 /* South edge */
  SAMPLE_FIRST_PIXEL = 1 /* West edge */
  SAMPLE_LAST_PIXEL = 1136 /* East edge */
  MAP_PROJECTION_ROTATION = 0.0
  MAP_RESOLUTION = 256 <PIXEL/DEGREE>
  MAP_SCALE = 0.231528833585 <KM/PIXEL>
  MAXIMUM_LATITUDE = 32.50000 <DEGREE>
  MINIMUM_LATITUDE = 27.50000 <DEGREE>
  WESTERNMOST_LONGITUDE = 85.00000 <DEGREE>
  EASTERNMOST_LONGITUDE = 90.00000 <DEGREE>
  LINE_PROJECTION_OFFSET = 8320.000
  SAMPLE_PROJECTION_OFFSET = 640.000
  COORDINATE_SYSTEM_TYPE = "BODY-FIXED ROTATING"
  COORDINATE_SYSTEM_NAME = "PLANETOCENTRIC"
END_OBJECT = IMAGE_MAP_PROJECTION

END

```

APPENDIX D3. MRDR LABEL (SUMMARY PRODUCT IMAGE)

```

PDS_VERSION_ID          = PDS3
RECORD_TYPE              = FIXED_LENGTH
RECORD_BYTES            = 4544
FILE_RECORDS            = 57600
LABEL_REVISION_NOTE     = "2003-11-19, S. Slavney (GEO);
                           2005-09-25, S. Murchie (JHU/APL);
                           2007-03-09, E. Malaret (ACT Corp.);
                           2007-09-14, C. Hash (ACT Corp)"

^IMAGE                  = "T1396_MRRSU_30N088_0256_1.IMG"

/* Map-projected Multispectral RDR Identification */

DATA_SET_ID             = "MRO-M-CRISM-5-RDR-MULTISPECTRAL-V1.0"
PRODUCT_ID              = "T1396_MRRSU_30N088_0256_1"
/*( TNNNN_MRRss_yydxrr_v                                     )*/
/*( NNNN = tile number                                       )*/
/*( ss = subtype of image product                           )*/
/*( yy = latitude of upper left corner                       )*/
/*( d = N or S for north or south latitude                  )*/
/*( xxx = east longitude of upper left corner               )*/
/*( rrrr = resolution in pixels/degree                      )*/
/*( v = version number                                       )*/

INSTRUMENT_HOST_NAME    = "MARS RECONNAISSANCE ORBITER"
SPACECRAFT_ID           = MRO
INSTRUMENT_NAME         = "COMPACT RECONNAISSANCE IMAGING
                           SPECTROMETER FOR MARS"

INSTRUMENT_ID           = CRISM
TARGET_NAME             = MARS
PRODUCT_TYPE            = MAP_PROJECTED_MULTISPECTRAL_RDR
PRODUCT_CREATION_TIME   = 2008-08-03T11:32:50.342
START_TIME              = "N/A"
STOP_TIME               = "N/A"
SPACECRAFT_CLOCK_START_COUNT = "N/A"
SPACECRAFT_CLOCK_STOP_COUNT = "N/A"
PRODUCT_VERSION_ID      = "1"
PRODUCER_INSTITUTION_NAME = "APPLIED PHYSICS LABORATORY"
SOFTWARE_NAME           = "PIPE_create_crism_mrdr_product"
SOFTWARE_VERSION_ID     = "04.21.08"
MRO:WAVELENGTH_FILE_NAME = "N/A"

/* This Map Projected Multispectral RDR label describes one data file: */
/* 1. A multiple-band image file of calibrated RDR data in radiance, */
/* This RDR represents one latitude-longitude bin in a global map. */
/* See the Map Projection Object below for bin coordinates and resolution.*/
/* See the CRISM Data Products SIS for more detailed description. */

/* Description of MAP PROJECTED MULTISPECTRAL RDR RADIANCE IMAGE file */

OBJECT                  = IMAGE
  LINES                 = 1280
  LINE_SAMPLES          = 1136
  SAMPLE_TYPE           = PC_REAL
  SAMPLE_BITS           = 32

BANDS                  = 45
BAND_STORAGE_TYPE      = BAND_SEQUENTIAL
BAND_NAME              = ("R770",

```

```

        "RBR",
        "BD530",
        "SH600",
        "BD640",
        "BD860",
        "BD920",
        "RPEAK1",
        "BDI1000VIS",
        "BDI1000IR",
        "IRAC",
        "OLINDEX",
        "LCPINDEX",
        "HCPXINDEX",
        "VAR",
        "ISLOPE1",
        "BD1435",
        "BD1500",
        "ICER1",
        "BD1750",
        "BD1900",
        "BDI2000",
        "BD2100",
        "BD2210",
        "BD2290",
        "D2300",
        "SINDEX",
        "ICER2",
        "BDCARB",
        "BD3000",
        "BD3100",
        "BD3200",
        "BD3400",
        "CINDEX",
        "R440",
        "IRR1",
        "BD1270O2",
        "BD1400H2O",
        "BD2000CO2",
        "BD2350",
        "BD2600",
        "IRR2",
        "R2700",
        "BD2700",
        "IRR3")
END_OBJECT = IMAGE

/* Map projection information about this RDR is in the IMAGE_MAP_PROJECTION */
/* object below. */

OBJECT = IMAGE_MAP_PROJECTION
^DATA_SET_MAP_PROJECTION = "MRR_MAP.CAT"
MAP_PROJECTION_TYPE = "EQUIRECTANGULAR"
A_AXIS_RADIUS = 3396 <KM>
B_AXIS_RADIUS = 3396 <KM>
C_AXIS_RADIUS = 3396 <KM>
FIRST_STANDARD_PARALLEL = "N/A"
SECOND_STANDARD_PARALLEL = "N/A"
POSITIVE_LONGITUDE_DIRECTION = "EAST"
CENTER_LATITUDE = 27.50000 <DEGREE>
CENTER_LONGITUDE = 87.50000 <DEGREE>
REFERENCE_LATITUDE = "N/A"
REFERENCE_LONGITUDE = "N/A"
LINE_FIRST_PIXEL = 1 /* North edge */
LINE_LAST_PIXEL = 1280 /* South edge */
SAMPLE_FIRST_PIXEL = 1 /* West edge */

```

```

SAMPLE_LAST_PIXEL      = 1136      /* East edge */
MAP_PROJECTION_ROTATION = 0.0
MAP_RESOLUTION         = 256 <PIXEL/DEGREE>
MAP_SCALE              = 0.231528833585 <KM/PIXEL>
MAXIMUM_LATITUDE       = 32.50000 <DEGREE>
MINIMUM_LATITUDE       = 27.50000 <DEGREE>
WESTERNMOST_LONGITUDE  = 85.00000 <DEGREE>
EASTERNMOST_LONGITUDE  = 90.00000 <DEGREE>
LINE_PROJECTION_OFFSET = 8320.000
SAMPLE_PROJECTION_OFFSET = 640.000
COORDINATE_SYSTEM_TYPE = "BODY-FIXED ROTATING"
COORDINATE_SYSTEM_NAME = "PLANETOCENTRIC"
END_OBJECT             = IMAGE_MAP_PROJECTION

END

```

APPENDIX D4. MRDR LABEL (WAVELENGTH FILE)

```

PDS_VERSION_ID          = PDS3
RECORD_TYPE              = FIXED_LENGTH
RECORD_BYTES            = 16
FILE_RECORDS             = 72
LABEL_REVISION_NOTE     = "2003-11-19, S. Slavney (GEO);
                          2006-09-25, S. Murchie (JHU/APL)
                          2006-09-27, S. Murchie (JHU/APL)
                          2007-09-14, C. Hash (ACT Corp)"

^TABLE                  = "T1396_MRRWV_30N088_0256_1.TAB"

/* Map-projected Multispectral RDR Identification */
DATA_SET_ID              = "MRO-M-CRISM-5-RDR-MULTISPECTRAL-V1.0"
PRODUCT_ID               = "T1396_MRRWV_30N088_0256_1"
                          /*( Tnnnn_MRRss_xxdyyy_rrrr_v                      )*/
                          /*( nnnn = tile number                            )*/
                          /*( ss = subtype of image product                  )*/
                          /*( xx = latitude of tile center                   )*/
                          /*( d = N or S for north or south latitude         )*/
                          /*( yyy = east longitude of tile center            )*/
                          /*( rrrr = resolution in pixels/degree             )*/
                          /*( v = version number                            )*/
INSTRUMENT_HOST_NAME     = "MARS RECONNAISSANCE ORBITER"
SPACECRAFT_ID            = MRO
INSTRUMENT_NAME          = "COMPACT RECONNAISSANCE IMAGING
                          SPECTROMETER FOR MARS"
INSTRUMENT_ID            = CRISM
TARGET_NAME              = MARS
PRODUCT_TYPE             = MAP_PROJECTED_MULTISPECTRAL_RDR
PRODUCT_CREATION_TIME    = 2008-12-09T08:00:39.178
START_TIME               = "N/A"
STOP_TIME                = "N/A"
SPACECRAFT_CLOCK_START_COUNT = "N/A"
SPACECRAFT_CLOCK_STOP_COUNT = "N/A"
PRODUCT_VERSION_ID       = "1"
PRODUCER_INSTITUTION_NAME = "APPLIED PHYSICS LABORATORY"
SOFTWARE_NAME            = "PIPE_create_crism_tile_wv"
SOFTWARE_VERSION_ID      = "12.05.08"

/* This Map Projected Multispectral RDR label describes four data files: */
/* 6. A listfile including detector row numbers and wavelengths in the */
/* I.F and Lambert albedo images. */
/* This RDR represents one latitude-longitude bin in a global map. */
/* See the Map Projection Object below for bin coordinates and resolution.*/
/* See the CRISM Data Products SIS for more detailed description. */
/* Description of MAP PROJECTED MULTISPECTRAL RDR LISTFILE */

OBJECT                  = TABLE
NAME                    = "CRISM MRDR WAVELENGTH TABLE"
INTERCHANGE_FORMAT      = "ASCII"
ROWS                    = 72
COLUMNS                = 3
ROW_BYTES               = 14
DESCRIPTION              = "CRISM MRDR wavelength table "
OBJECT                  = COLUMN
COLUMN_NUMBER           = 1
NAME                    = SPECT_ID
DATA_TYPE               = ASCII_INTEGER

```



```

        START_BYTE      = 214
        BYTES            = 1
        DESCRIPTION      = "Spectrometer identifier; 0 = IR; 1 = VNIR"
    END_OBJECT          = COLUMN
    OBJECT              = COLUMN
        COLUMN_NUMBER    = 2
        NAME              = ROWNUM
        DATA_TYPE        = ASCII_INTEGER
        START_BYTE        = 3
        BYTES             = 3
        DESCRIPTION       = "detector row number (0-479)"
    END_OBJECT          = COLUMN
    OBJECT              = COLUMN
        COLUMN_NUMBER    = 3
        NAME              = SAMPL_WAV
        DATA_TYPE        = ASCII_REAL
        START_BYTE        = 7
        BYTES             = 8
        DESCRIPTION       = "Standard sampling center wavelength in nm"
        UNIT              = "NM"
    END_OBJECT          = COLUMN
END_OBJECT            = TABLE
END

```

APPENDIX E. MTRDR LABEL (CORRECTED I/F FILE)

```

PDS_VERSION_ID          = PDS3
LABEL_REVISION_NOTE     = "2010-11-29, S. Murchie (APL)"
DATA_SET_ID             = "MRO-M-CRISM-5-RDR-MPTARGETED-V1.0"
PRODUCT_ID              = "FRT00004ECA_07_IF166J_MTR0"

/* cccnnnnnnnn_xx_ooaaas_TRRv          */
/* ccc = Class Type                    */
/* nnnnnnnnn = Observation ID, hexadecimal */
/* ooaaa = Image type, Macro number      */
/* s = Sensor ID (S or L)               */
/* v = Version number                   */

INSTRUMENT_HOST_NAME     = "MARS RECONNAISSANCE ORBITER"
SPACECRAFT_ID            = "MRO"
INSTRUMENT_NAME          = "COMPACT RECONNAISSANCE IMAGING
                           SPECTROMETER FOR MARS"
INSTRUMENT_ID            = "CRISM"
TARGET_NAME              = "MARS"
PRODUCT_TYPE             = "MPTARGETED_RDR"
PRODUCT_CREATION_TIME    = "N/A"
START_TIME               = "2007-03-23T03:02:31.499"
STOP_TIME                = "2007-03-23T03:04:39.233"
SPACECRAFT_CLOCK_START_COUNT = "2/0859086170.55396"
SPACECRAFT_CLOCK_STOP_COUNT  = "2/0859086298.37980"
ORBIT_NUMBER             = "NULL"
OBSERVATION_TYPE         = "FRT"
OBSERVATION_ID           = "16#00004ECA#"
MRO:OBSERVATION_NUMBER   = "16#07#"
MRO:ACTIVITY_ID          = "IF166"
MRO:SENSOR_ID            = "J"

/* Detector and FPE temperature refer to IR component of observation */

MRO:DETECTOR_TEMPERATURE = -165.838
MRO:OPTICAL_BENCH_TEMPERATURE = -48.411
MRO:SPECTROMETER_HOUSING_TEMP = -72.699
MRO:SPHERE_TEMPERATURE    = -48.064
MRO:FPE_TEMPERATURE       = 0.812
PRODUCT_VERSION_ID        = "0"
SOURCE_PRODUCT_ID = {
    "FRT00004ECA_07_IF166L_TRR3",
    "FRT00004ECA_07_DE166L_DDR1"
}
PRODUCER_INSTITUTION_NAME = "JOHNS HOPKINS UNIVERSITY
                           APPLIED PHYSICS LABORATORY"
SOFTWARE_NAME              = "N/A"
SOFTWARE_VERSION_ID        = "N/A"

/* Targeted RDR Instrument and Observation Parameters */

TARGET_CENTER_DISTANCE    = "NULL" <KM>
SOLAR_DISTANCE            = 212139419.063420 <KM>
SOLAR_LONGITUDE           = 205.304261
SHUTTER_MODE_ID           = "OPEN"
LIGHT_SOURCE_NAME         = "NONE"
MRO:CALIBRATION_LAMP_STATUS = "OFF"
MRO:CALIBRATION_LAMP_LEVEL = "N/A"
PIXEL_AVERAGING_WIDTH     = 1
MRO:INSTRUMENT_POINTING_MODE = "DYNAMIC POINTING"
SCAN_MODE_ID              = "SHORT"

```

```

MRO:FRAME_RATE              = 3.75 <HZ>
MRO:EXPOSURE_PARAMETER      = 301
SAMPLING_MODE_ID            = "HYPERSPEC"
COMPRESSION_TYPE             = "NONE"
MRO:WAVELENGTH_FILTER       = "0"
MRO:WAVELENGTH_FILE_NAME    = "FRT00004ECA_07_WV166J_MTR0.TAB"
MRO:ATMO_CORRECTION_FLAG    = "ON"
MRO:THERMAL_CORRECTION_MODE = "OFF"
MRO:PHOTOCLIN_CORRECTION_FLAG = "OFF"
MRO:SPATIAL_RESAMPLING_FLAG = "OFF"
MRO:SPATIAL_RESAMPLING_FILE = "N/A"

MRO:SPATIAL_RESCALING_FLAG  = "ON"
MRO:SPATIAL_RESCALING_FILE  = "N/A"
MRO:SPECTRAL_RESAMPLING_FLAG = "ON"
MRO:SPECTRAL_RESAMPLING_FILE = "N/A"

/* This Map-Projected Targeted RDR label describes one file.      */
/* 1. A multiple-band image file containing calibrated, corrected */
/* TRDR data, in units of I/F.                                     */

OBJECT                      = IMAGE
  LINES                     = 761
  LINE_SAMPLES              = 806
  SAMPLE_TYPE               = PC_REAL
  SAMPLE_BITS               = 32
  UNIT                      = "I over F"
  BANDS                     = 450
  BAND_STORAGE_TYPE         = BAND_SEQUENTIAL
END_OBJECT                  = IMAGE

/* Map projection information about this RDR is in the IMAGE_MAP_PROJECTION */
/* object below.                                                         */

OBJECT                      = IMAGE_MAP_PROJECTION
  ^DATA_SET_MAP_PROJECTION  = "MTR_MAP.CAT"
  MAP_PROJECTION_TYPE       = "EQUIRECTANGULAR"
  A_AXIS_RADIUS             = 3396 <KM>
  B_AXIS_RADIUS             = 3396 <KM>
  C_AXIS_RADIUS             = 3396 <KM>
  FIRST_STANDARD_PARALLEL   = "N/A"
  SECOND_STANDARD_PARALLEL  = "N/A"
  POSITIVE_LONGITUDE_DIRECTION = "EAST"
  CENTER_LATITUDE           = 20.00000 <DEGREE>
  CENTER_LONGITUDE          = "N/A"
  REFERENCE_LATITUDE        = "N/A"
  REFERENCE_LONGITUDE       = "N/A"
  LINE_FIRST_PIXEL          = 1 /* North edge */
  LINE_LAST_PIXEL           = 761 /* South edge */
  SAMPLE_FIRST_PIXEL        = 1 /* West edge */
  SAMPLE_LAST_PIXEL         = 806 /* East edge */
  MAP_PROJECTION_ROTATION   = 0.0
  MAP_RESOLUTION            = 3072 <PIXEL/DEGREE>
  MAP_SCALE                 = 0.019294069 <KM/PIXEL>
  MAXIMUM_LATITUDE          = 25.0631 <DEGREE>
  MINIMUM_LATITUDE          = 24.8155 <DEGREE>
  WESTERNMOST_LONGITUDE     = -19.9259 <DEGREE>
  EASTERNMOST_LONGITUDE     = -19.6388 <DEGREE>
  LINE_PROJECTION_OFFSET    = 76233.216
  SAMPLE_PROJECTION_OFFSET  = -60330.394
  COORDINATE_SYSTEM_TYPE    = "BODY-FIXED ROTATING"
  COORDINATE_SYSTEM_NAME    = "PLANETOCENTRIC"
END_OBJECT                  = IMAGE_MAP_PROJECTION
END

```

2. APPENDIX F. LEVEL 6 CDR LABEL

```

PDS_VERSION_ID          = PDS3
LABEL_REVISION_NOTE     = "2005-12-22, P. Cavender;
                           2006-09-18, MRO CRISM:HWT line length fix;
                           2009-04-03, Scott Murchie; modified
                           table 2 to contain hyperspectral survey,
                           and put old table 2 into table 3
                           2009-08-07, C. Hash; modified table 2
                           to be a superset of table 1."

/* Level 6 CDR (Calibration Data Record) Identification */
DATA_SET_ID              = "MRO-M-CRISM-4/6-CDR-V1.0"
PRODUCT_ID               = "CDR6_9_0947778566_WV_L_0"
PRODUCT_TYPE             = CDR
SPACECRAFT_ID            = MRO
INSTRUMENT_ID            = CRISM
START_TIME               = 2010-01-12T15:48:55
STOP_TIME                = NULL
SPACECRAFT_CLOCK_START_COUNT = "9/0947778566"
SPACECRAFT_CLOCK_STOP_COUNT = NULL
PRODUCT_CREATION_TIME    = 2010-02-19T18:58:00
MRO:SENSOR_ID            = "L"
PRODUCT_VERSION_ID       = "0"

/* Description of CDR6 TABLE file */

OBJECT                   = FILE
  ^TABLE                 = "CDR6_9_0947778566_WV_L_0.TAB"
  RECORD_TYPE            = FIXED_LENGTH
  RECORD_BYTES           = 13
  FILE_RECORDS           = 480

OBJECT                   = TABLE
  NAME                   = "WAVELENGTH TABLE"
  INTERCHANGE_FORMAT     = "ASCII"
  ROWS                   = 4804
  COLUMNS               = 5
  ROW_BYTES              = 13
  DESCRIPTION            = "Wavelength Table"

OBJECT                   = COLUMN
  COLUMN_NUMBER          = 1
  NAME                   = IR_ROW
  DATA_TYPE             = ASCII_INTEGER
  START_BYTE             = 1
  BYTES                  = 3
  DESCRIPTION            = "IR detector row; low numbers are at the long
                           wavelength end"
END_OBJECT               = COLUMN

OBJECT                   = COLUMN
  COLUMN_NUMBER          = 2
  NAME                   = IR_FILTER_0
  DATA_TYPE             = ASCII_INTEGER
  START_BYTE             = 5
  BYTES                  = 1
  DESCRIPTION            = "IR wavelength table 0; in housekeeping file
                           when SPECT_ID=0 this column is applicable
                           when FILTER=0; if value is 0 then data from
                           that row of the detector is not returned; if

```

```

value is 1 then data from that row of the
detector is returned"

END_OBJECT          = COLUMN

OBJECT              = COLUMN
  COLUMN_NUMBER     = 3
  NAME              = IR_FILTER_1
  DATA_TYPE        = ASCII_INTEGER
  START_BYTE        = 7
  BYTES             = 1
  DESCRIPTION       = "IR wavelength table 1; in housekeeping file
                      when SPECT_ID=0 this column is applicable
                      when FILTER=1; if value is 0 then data from
                      that row of the detector is not returned; if
                      value is 1 then data from that row of the
                      detector is returned"

END_OBJECT          = COLUMN

OBJECT              = COLUMN
  COLUMN_NUMBER     = 4
  NAME              = IR_FILTER_2
  DATA_TYPE        = ASCII_INTEGER
  START_BYTE        = 9
  BYTES             = 1
  DESCRIPTION       = "IR wavelength table 2; in housekeeping file
                      when SPECT_ID=0 this column is applicable
                      when FILTER=2; if value is 0 then data from
                      that row of the detector is not returned; if
                      value is 1 then data from that row of the
                      detector is returned"

END_OBJECT          = COLUMN

OBJECT              = COLUMN
  COLUMN_NUMBER     = 5
  NAME              = IR_FILTER_3
  DATA_TYPE        = ASCII_INTEGER
  START_BYTE        = 11
  BYTES             = 1
  DESCRIPTION       = "IR wavelength table 3; in housekeeping file
                      when SPECT_ID=0 this column is applicable
                      when FILTER=3; if value is 0 then data from
                      that row of the detector is not returned; if
                      value is 1 then data from that row of the
                      detector is returned"

END_OBJECT          = COLUMN

END_OBJECT          = TABLE

END_OBJECT          = FILE

END

```

APPENDIX G. LEVEL 4 CDR LABEL

```

PDS_VERSION_ID          = PDS3
LABEL_REVISION_NOTE     = "2006-04-11 D. Humm (APL), modified;
                           version 0 prelim Rob Green cal <2500 nm
                           and 5x5 >2500 nm; version 1 D. Humm,

                           replace all non-scene with 65535.;
                           version 2 2006-09-21 D. Humm,
                           final ground Rob Green cal
                           <2500 nm and 5x5 >2500 nm;
                           version 3 2007-01-23 D. Humm,
                           adjust by 1.5-3 nm wavelength
                           shift as a function of column #
                           supplied by Rob Green 2007-01-03"

/*( NOTE: Comments in this label that are delimited with parentheses,      )*/
/*( for example:                                                            )*/
/*(   /*( comment )*/                                                       )*/
/*( are notes to the data provider. These comments should be removed       )*/
/*( from the final label. Comments without parentheses, for example:       )*/
/*(   /* comment */                                                         )*/
/*( are intended to be part of the final label.                             )*/

/* Level 4 CDR (Calibration Data Record) Identification */

DATA_SET_ID              = "MRO-M-CRISM-4/6-CDR-V1.0"
PRODUCT_ID               = "CDR410803692813_WA0000000L_3"

                           /*( CDR4Ptttttttttt_pprbeewsn_v                )*/
                           /*( P = partition of sclk time                  )*/
                           /*( tttttttttt = s/c start or mean time         )*/
                           /*( pp = calib. type from SIS table 2-8         )*/
                           /*( r = frame rate identifier, 0-4              )*/
                           /*( b = binning identifier, 0-3                 )*/
                           /*( eee = exposure time parameter, 0-480       )*/
                           /*( w = wavelength filter, 0-3                 )*/
                           /*( s = side: 1 or 2, or 0 if N/A               )*/
                           /*( n = sensor ID: S, L, or J                   )*/
                           /*( v = version                                 )*/

PRODUCT_TYPE              = CDR
SPACECRAFT_ID             = MRO
INSTRUMENT_ID             = CRISM
START_TIME                = 2005-06-19T23:59:59.999
STOP_TIME                 = NULL
SPACECRAFT_CLOCK_START_COUNT = "1/0803692813"
SPACECRAFT_CLOCK_STOP_COUNT = NULL
OBSERVATION_TIME          = NULL
PRODUCT_CREATION_TIME     = 2007-01-23T23:26:00

OBSERVATION_TYPE          = NULL
OBSERVATION_ID            = NULL
MRO:OBSERVATION_NUMBER    = NULL
MRO:ACTIVITY_ID           = NULL
SOURCE_PRODUCT_ID         = NULL
MRO:SENSOR_ID             = "L"
PRODUCT_VERSION_ID        = "3"

/* CDR Instrument and Observation Parameters */

SAMPLING_MODE_ID          = "HYPERSPEC"

```

```

MRO:WAVELENGTH_FILE_NAME      = "CDR410803692813_WA0000000L_3.IMG"
MRO:DETECTOR_TEMPERATURE      = NULL
MRO:OPTICAL_BENCH_TEMPERATURE = NULL
MRO:SPECTROMETER_HOUSING_TEMP = NULL
MRO:SPHERE_TEMPERATURE        = NULL
SHUTTER_MODE_ID               = "OPEN"
LIGHT_SOURCE_NAME              = "NONE"
MRO:CALIBRATION_LAMP_STATUS    = "OFF"
MRO:CALIBRATION_LAMP_LEVEL     = 0
MRO:FRAME_RATE                 = NULL
PIXEL_AVERAGING_WIDTH          = 1 /*( pixel bin size, across track ) */
MRO:EXPOSURE_PARAMETER         = NULL
MRO:WAVELENGTH_FILTER          = "0"

/* This Level 4 CDR label describes one calibration data file. The file */
/* is a mutiple-band, single-frame image file derived from ground data. */
/* It consists of a binary image followed by a list of row numbers      */
/* corresponding to the wavelength filter.                               */

/* The WA level 4 CDR gives the center wavelength in nm of each pixel, */
/* assuming a given spatial binning and wavelength filter.              */

/* Description of CDR IMAGE file */

OBJECT                          = FILE
  ^IMAGE                        = "CDR410803692813_WA0000000L_3.IMG"

/* offset is in file records, which is just (imgbands*imglines) + 1 */
^ROWNUM_TABLE = ("CDR410803692813_WA0000000L_3.IMG",439 )

RECORD_TYPE    = FIXED_LENGTH
RECORD_BYTES   = 2560 /* one row now, not one frame to save space in table */
FILE_RECORDS   = 439 /* compute by ROUND ((imgbands * imglines *
/*                                     line_samples * samplebits/8 +
/*                                     tablerows * tablerowbytes) /
/*                                     record_bytes + 0.5 )
/*

OBJECT          = IMAGE
  LINES          = 1
  LINE_SAMPLES   = 640
  SAMPLE_TYPE    = PC_REAL
  SAMPLE_BITS    = 32
  BANDS          = 438
  BAND_NAME      = NULL
  BAND_STORAGE_TYPE = LINE_INTERLEAVED
  DESCRIPTION     = "Center wavelength in nm for each
                    detector pixel"
  UNIT           = "NM"
END_OBJECT       = IMAGE

/* be sure to pad this object to a full record (2560/bin bytes here) */
OBJECT = ROWNUM_TABLE
  NAME          = "SELECTED ROWS FROM DETECTOR"
  INTERCHANGE_FORMAT = "BINARY"
  ROWS          = 438
  COLUMNS      = 1
  ROW_BYTES     = 2
  DESCRIPTION    = "The detector is subsampled in the spectral direction
                    by selecting specific rows to be downlinked. This
                    table provides a list of the rows selected for all
                    frames in this multidimensional image cube."

OBJECT = COLUMN
  NAME          = DETECTOR_ROW_NUMBER
  DATA_TYPE    = MSB_UNSIGNED_INTEGER
  BIT_MASK      = 2#0000000111111111#

```

```
        START_BYTE      = 1
        BYTES            = 2
        DESCRIPTION      = "Detector row number from which the data was taken."
        END_OBJECT = COLUMN

        END_OBJECT = ROWNUM_TABLE

END_OBJECT              = FILE

END
```


APPENDIX H. LDR LABEL

```

PDS_VERSION_ID          = PDS3
LABEL_REVISION_NOTE     = "2009-04-07, S. Murchie (JHU/APL);"

/* LDR Identification */

DATA_SET_ID              = "MRO-M-CRISM-6-LDR-V1.0"
PRODUCT_ID               = "LMB00002B61_0B_DE227S_LDR0"
/* cccnnnnnnnnn_xx_ooaaas_LDRv          */
/* ccc = Class Type                    */
/* nnnnnnnnn = Observation ID (hex)     */
/* xx = counter this observation (hex)  */
/* ooaaa = obs type, macro number       */
/* s = sensor ID (S or L)              */
/* v = version number                  */

INSTRUMENT_HOST_NAME     = "MARS RECONNAISSANCE ORBITER"
SPACECRAFT_ID            = "MRO"
INSTRUMENT_NAME          = "COMPACT RECONNAISSANCE IMAGING
                           SPECTROMETER FOR MARS"

INSTRUMENT_ID            = "CRISM"
TARGET_NAME              = "MARS"
PRODUCT_TYPE             = "LDR"
PRODUCT_CREATION_TIME    = "2009-09-03T19:50:25"
START_TIME               = "2009-07-11T09:12:06.267"
STOP_TIME                = "2009-07-11T09:14:30.001"
SPACECRAFT_CLOCK_START_COUNT = "6/931770748:44476"
SPACECRAFT_CLOCK_STOP_COUNT = "6/931770892:27045"

ORBIT_NUMBER             = 0
OBSERVATION_TYPE         = "LMB"
OBSERVATION_ID           = "16#00002B61#"
MRO:OBSERVATION_NUMBER   = "16#0B#"
MRO:ACTIVITY_ID          = "DE227"
MRO:SENSOR_ID            = "S"
PRODUCT_VERSION_ID       = "0"
SOURCE_PRODUCT_ID        = {
    "mro.tsc",
    "mro_v14.tf",
    "MRO_CRISM_FK_0000_000_N_01.TF",
    "MRO_CRISM_IK_0000_000_N_10.TI",
    "naif0009.tls",
    "pck00008.tpc",
    "mro_sc_psp_090707_090713.bc",
    "spck_2009_191_r_1.bc",
    "spck_2009_192_r_1.bc",
    "de410.bsp",
    "mro_cruise.bsp",
    "mro_ab.bsp",
    "mro_psp.bsp",
    "mro_psp1.bsp",
    "mro_psp2.bsp",
    "mro_psp_rec.bsp"
}

PRODUCER_INSTITUTION_NAME = "APPLIED PHYSICS LABORATORY"
SOFTWARE_NAME              = "crism_ldr"
SOFTWARE_VERSION_ID        = "1.0"

/* LDR Instrument and Observation Parameters */

SOLAR_DISTANCE             = 213229293.617318 <KM>

```

```

SOLAR_LONGITUDE          = 301.331137 <DEGREES>
MRO:FRAME_RATE           = 3.75 <HZ>
PIXEL_AVERAGING_WIDTH    = 10
MRO:INSTRUMENT_POINTING_MODE = "DYNAMIC POINTING"

/* This LDR label describes one data file: */
/* 1. A multiple-band backplane image file with wavelength-independent, */
/* spatial pixel-dependent geometric and timing information. */

/* See the CRISM Data Products SIS for more detailed description. */

OBJECT                    = FILE
  ^IMAGE                  = "LMB00002B61_0B_DE227S_LDR0.IMG"
  RECORD_TYPE             = FIXED_LENGTH
  RECORD_BYTES            = 256
  FILE_RECORDS            = 8100

OBJECT                    = IMAGE
  LINES                   = 540
  LINE_SAMPLES            = 64
  SAMPLE_TYPE             = PC_REAL
  SAMPLE_BITS             = 32
  BANDS                   = 15
  BAND_STORAGE_TYPE       = BAND_SEQUENTIAL
  BAND_NAME               = ("INA at areoid, deg",
                             "EMA at areoid, deg",
                             "Phase angle, deg",
                             "Latitude, areocentric, deg N",
                             "Longitude, areocentric, deg E",
                             "INA at surface from MOLA, deg",
                             "EMA at surface from MOLA, deg",
                             "Elevation, meters relative to areoid",
                             "Elevation, meters relative to MOLA",
                             "Local Solar Time, hours",
                             "Ephemeris Time of observation, seconds past noon
January 1, 2000",
                             "Sub-Solar Latitude, areocentric, deg N",
                             "Sub-Solar Longitude, areocentric, deg E",
                             "Sub-Spacecraft Latitude, areocentric, deg N",
                             "Sub-Spacecraft Longitude, areocentric, deg E)"

  END_OBJECT              = IMAGE
END_OBJECT                = FILE
END

```

APPENDIX I1. EDR BROWSE PRODUCT HTML FILE LABEL

```

PDS_VERSION_ID      = PDS3
LABEL_REVISION_NOTE = "2006-02-25, S.Murchie (APL)"

/* This browse product provides an overview of the MRO CRISM EDRs */
/* from a single observation */

^HTML_DOCUMENT      = "FRT00004ECA_BROWSE_EDR0.HTML"

DATA_SET_ID         = "MRO-M-CRISM-2-EDR-V1.0"
PRODUCT_ID          = "FRT00004ECA_BROWSE_EDR0"
/* EDR browse product */
/* cccnnnnnnnnn_BROWSE_EDRv */
/* ccc = Class Type */
/* nnnnnnnn = Observation ID (hex) */
/* v = Version number */

INSTRUMENT_HOST_NAME = "MARS RECONNAISSANCE ORBITER"
SPACECRAFT_ID        = MRO
INSTRUMENT_NAME       = "COMPACT RECONNAISSANCE IMAGING
                        SPECTROMETER FOR MARS"
INSTRUMENT_ID         = CRISM
TARGET_NAME           = MARS
PRODUCT_TYPE          = BROWSE
PRODUCT_CREATION_TIME = 2007-04-25T11:17:50.529
PRODUCER_INSTITUTION_NAME = "JOHNS HOPKINS UNIVERSITY
                            APPLIED PHYSICS LABORATORY"
SOFTWARE_NAME         = "pipe_crism_create_browse"
SOFTWARE_VERSION_ID   = "1.0"

/* The following information is relevant to an entire observation */

ORBIT_NUMBER          = NULL
OBSERVATION_TYPE      = "FRT"
OBSERVATION_ID        = "16#00004ECA#"
PRODUCT_VERSION_ID    = "0"
SOLAR_DISTANCE        = NULL <KM>

/* These times are from the beginning of the first EDR of the observation */
/* to the end of the last EDR of the observation */

START_TIME            = 2007-03-23T02:59:55.113681
STOP_TIME              = 2007-03-23T03:06:55.910109
SPACECRAFT_CLOCK_START_COUNT = "2/0859086014.03181"
SPACECRAFT_CLOCK_STOP_COUNT  = "2/0859086434.55376"

OBJECT                = HTML_DOCUMENT
  DOCUMENT_NAME        = "EDR BROWSE OVERVIEW"
  RECORD_TYPE          = UNDEFINED
  PUBLICATION_DATE     = 2007-04-25
  DOCUMENT_TOPIC_TYPE  = "HTML NAVIGATION"
  INTERCHANGE_FORMAT   = ASCII
  DOCUMENT_FORMAT      = HTML
  DESCRIPTION          = "This document provides an overview of the MRO
                        CRISM EDRs from a single observation."
END_OBJECT            = HTML_DOCUMENT

END

```

APPENDIX I2. EDR BROWSE PRODUCT PNG FILE LABEL

```

PDS_VERSION_ID          = PDS3
LABEL_REVISION_NOTE = "2003-11-19, S. Slavney (GEO);
                        2005-02-01, C. Hash (ACT);
                        2006-01-04, C. Hash (ACT);"

/* EDR Identification */

DATA_SET_ID              = "MRO-M-CRISM-2-EDR-V1.0"
PRODUCT_ID               = "FRT00004ECA_07_SC166L_RAW0"
/* cccnnnnnnnn_xx_ooaaas_RAWv */
/* ccc = Class Type */
/* nnnnnnnnn = Observation ID (hex) */
/* xx = counter within observation (hex) */
/* ooaaa = obs type, macro number */
/* s = sensor ID (S or L) */
/* v = version number */

INSTRUMENT_HOST_NAME = "MARS RECONNAISSANCE ORBITER"
SPACECRAFT_ID        = MRO
INSTRUMENT_NAME      = "COMPACT RECONNAISSANCE IMAGING
                        SPECTROMETER FOR MARS"
INSTRUMENT_ID        = CRISM
TARGET_NAME          = MARS
PRODUCT_TYPE         = BROWSE
PRODUCT_CREATION_TIME = 2007-04-06T13:22:26
START_TIME           = 2007-03-23T03:02:31.910417
STOP_TIME            = 2007-03-23T03:04:39.644669
SPACECRAFT_CLOCK_START_COUNT = "2/0859086170.55396"
SPACECRAFT_CLOCK_STOP_COUNT = "2/0859086298.37980"
ORBIT_NUMBER         = "NULL"
OBSERVATION_TYPE     = "FRT"
OBSERVATION_ID       = "16#00004ECA#"
MRO:OBSERVATION_NUMBER = 16#07#
MRO:ACTIVITY_ID       = "SC166"
MRO:SENSOR_ID        = "L"
PRODUCT_VERSION_ID   = "0"
PRODUCER_INSTITUTION_NAME = "JOHNS HOPKINS UNIVERSITY
                            APPLIED PHYSICS LABORATORY"
SOFTWARE_NAME        = "pipe_edrslice"
SOFTWARE_VERSION_ID   = "4.3"

/* EDR Instrument and Observation Parameters */
/* for first frame */
TARGET_CENTER_DISTANCE = NULL <KM>
SOLAR_DISTANCE         = NULL <KM>
SHUTTER_MODE_ID        = OPEN
LIGHT_SOURCE_NAME      = "NONE"
MRO:CALIBRATION_LAMP_STATUS = "OFF"
MRO:CALIBRATION_LAMP_LEVEL = "N/A"
PIXEL_AVERAGING_WIDTH  = 1
MRO:INSTRUMENT_POINTING_MODE = "DYNAMIC POINTING"
SCAN_MODE_ID           = SHORT
MRO:FRAME_RATE         = 3.75 <HZ>
MRO:EXPOSURE_PARAMETER = 301
SAMPLING_MODE_ID       = "HYPERSPEC"
COMPRESSION_TYPE       = "NONE"
MRO:WAVELENGTH_FILTER  = 0
MRO:WAVELENGTH_FILE_NAME = "CDR6_1_0000000000_WV_L_1.TAB"
MRO:PIXEL_PROC_FILE_NAME = "CDR6_1_0000000000_PP_L_1.TAB"

```

```

MRO:LOOKUP_TABLE_FILE_NAME = "CDR6_1_0000000000_LK_J_0.TAB"

/* These parameters describe the browse image as a PDS document. */

^DOCUMENT          = "FRT00004ECA_07_SC166L_RAW0.PNG"
OBJECT             = DOCUMENT
  DOCUMENT_NAME    = "FRT00004ECA_07_SC166L_RAW0"
  DOCUMENT_FORMAT  = PNG
  DOCUMENT_TOPIC_TYPE = "BROWSE IMAGE"
  INTERCHANGE_FORMAT = BINARY
  PUBLICATION_DATE  = 2007-04-06
  SOURCE_PRODUCT_ID = "FRT00004ECA_07_SC166L_EDR0"
  LINES            = 480
  LINE_SAMPLES     = 640
  SAMPLE_TYPE      = MSB_UNSIGNED_INTEGER
  SAMPLE_BITS      = 8
  DERIVED_MINIMUM  = 0
  DERIVED_MAXIMUM  = 250
  OFFSET           = -145.522
  SCALING_FACTOR   = 0.299
  MISSING_CONSTANT = 255
  DESCRIPTION      = "This file is a scaled median image of raw DN level
                     in a CRISM EDR. The x-y coordinates of the image
                     are spatial and in sensor space (not map-
                     projected), where x = detector column and y = frame
                     number within an EDR. The encoded 8-bit value at
                     each x-y location is the scaled median of the
                     values at all wavelengths."
END_OBJECT         = DOCUMENT
END

```

APPENDIX J. MTRDR BROWSE PRODUCT 'TRU' PNG FILE LABEL

```

PDS_VERSION_ID          = PDS3
RECORD_TYPE              = UNDEFINED
LABEL_REVISION_NOTE     = "2010-11-29, S. Murchie (APL)"
DATA_SET_ID             = "MRO-M-CRISM-5-RDR-MPTARGETED-V1.0"
PRODUCT_ID              = "FRT00004ECA_07_TRU166J_MTR0"
INSTRUMENT_HOST_NAME    = "MARS RECONNAISSANCE ORBITER"
SPACECRAFT_ID           = MRO
INSTRUMENT_NAME         = "COMPACT RECONNAISSANCE IMAGING
                        SPECTROMETER FOR MARS"

INSTRUMENT_ID           = CRISM
TARGET_NAME             = MARS
PRODUCT_TYPE            = MPTARGETED_RDR
PRODUCT_CREATION_TIME   = "N/A"
START_TIME              = 2007-03-23T03:02:31.499
STOP_TIME               = 2007-03-23T03:04:39.233
SPACECRAFT_CLOCK_START_COUNT = "2/0859086170.55396"
SPACECRAFT_CLOCK_STOP_COUNT  = "2/0859086298.37980"
ORBIT_NUMBER            = "NULL"
OBSERVATION_TYPE        = "FRT"
OBSERVATION_ID          = "16#00004ECA#"
MRO:OBSERVATION_NUMBER  = 16#07#
MRO:ACTIVITY_ID         = "IF166"
MRO:SENSOR_ID           = "J"

/* Detector and FPE temperature refer to IR component of observation */

MRO:DETECTOR_TEMPERATURE = -165.838
MRO:OPTICAL_BENCH_TEMPERATURE = -48.411
MRO:SPECTROMETER_HOUSING_TEMP = -72.699
MRO:SPHERE_TEMPERATURE    = -48.064
MRO:FPE_TEMPERATURE       = 0.812
PRODUCT_VERSION_ID        = "0"
SOURCE_PRODUCT_ID         = {"FRT00004ECA_07_IF166J_MTR3"}
PRODUCER_INSTITUTION_NAME = "JOHNS HOPKINS UNIVERSITY
                        APPLIED PHYSICS LABORATORY"
SOFTWARE_NAME             = "N/A"
SOFTWARE_VERSION_ID       = "N/A"

/* MPTargeted RDR Instrument and Observation Parameters */

TARGET_CENTER_DISTANCE    = "NULL" <KM>
SOLAR_DISTANCE            = 212139419.063420 <KM>
SOLAR_LONGITUDE           = 205.304261
SHUTTER_MODE_ID           = "OPEN"
LIGHT_SOURCE_NAME         = "NONE"
MRO:CALIBRATION_LAMP_STATUS = "OFF"
MRO:CALIBRATION_LAMP_LEVEL = "N/A"
PIXEL_AVERAGING_WIDTH     = 1
MRO:INSTRUMENT_POINTING_MODE = "DYNAMIC POINTING"
SCAN_MODE_ID              = "SHORT"
MRO:FRAME_RATE            = 3.75 <HZ>
MRO:EXPOSURE_PARAMETER    = 301
SAMPLING_MODE_ID          = "HYPERSPEC"
COMPRESSION_TYPE          = "NONE"
MRO:WAVELENGTH_FILTER     = "0"
MRO:WAVELENGTH_FILE_NAME  = "FRT00004ECA_07_WV166J_MTR0.TAB"
MRO:ATMO_CORRECTION_FLAG  = "ON"
MRO:THERMAL_CORRECTION_MODE = "OFF"
MRO:PHOTOCLIN_CORRECTION_FLAG = "OFF"

```

```

MRO:SPATIAL_RESAMPLING_FLAG      = "OFF"
MRO:SPATIAL_RESAMPLING_FILE      = "N/A"

MRO:SPATIAL_RESCALING_FLAG       = "ON"
MRO:SPATIAL_RESCALING_FILE       = "N/A"
MRO:SPECTRAL_RESAMPLING_FLAG     = "ON"
MRO:SPECTRAL_RESAMPLING_FILE     = "N/A"

/* These parameters describe the browse image as a PDS document. */

^PNG_DOCUMENT                     = " FRT00004ECA_07_TRU166J_MTR0.PNG"
OBJECT                           = PNG_DOCUMENT
  DOCUMENT_NAME                   = " FRT00004ECA_07_TRU166J_MTR0"
  DOCUMENT_FORMAT                 = PNG
  DOCUMENT_TOPIC_TYPE             = "BROWSE IMAGE"
  INTERCHANGE_FORMAT              = BINARY
  PUBLICATION_DATE                = 2009-12-02
  SOURCE_PRODUCT_ID               = "FRT00004ECA_07_IF166J_MTR0"
  SAMPLE_TYPE                    = LSB_UNSIGNED_INTEGER
  SAMPLE_BITS                    = 8
  BANDS                          = 3
  BAND_SEQUENCE                   = ("RED", "GREEN", "BLUE")
  BAND_NAME                      = ("598 nm", "533 nm", "442 nm")

/* The following information to scale from real numbers to an */
/* 8-bit integer is hard-coded for this type of browse image. */

DERIVED_MINIMUM                  = (0,0,0)
DERIVED_MAXIMUM                  = (250,250,250)
OFFSET                          = (0.00000,0.00000,0.00000)
SCALING_FACTOR                   = (0.00120,0.00120,0.00120)
MISSING_CONSTANT                 = (255,255,255)
DESCRIPTION                      = "This file is a true color VNIR image assembled
                                  from calibrated radiance, solar distance, and
                                  solar flux as sampled in the wavelength filter
                                  and binning state being used: radiance_factor =
                                  I*D^2/(pi*F) where I = spectral radiance,
                                  D = solar distance in AU, and F = solar flux at
                                  1 AU. Subsequently a correction was made for
                                  atmospheric and photometric effects."
END_OBJECT                      = PNG_DOCUMENT

/* Map projection information about this RDR is in the IMAGE_MAP_PROJECTION */
/* object below.                                                         */

OBJECT                           = IMAGE_MAP_PROJECTION
  ^DATA_SET_MAP_PROJECTION        = "MTR_MAP.CAT"
  MAP_PROJECTION_TYPE             = "EQUIRECTANGULAR"
  A_AXIS_RADIUS                   = 3396 <KM>
  B_AXIS_RADIUS                   = 3396 <KM>
  C_AXIS_RADIUS                   = 3396 <KM>
  FIRST_STANDARD_PARALLEL         = "N/A"
  SECOND_STANDARD_PARALLEL        = "N/A"
  POSITIVE_LONGITUDE_DIRECTION   = "EAST"
  CENTER_LATITUDE                 = 20.00000 <DEGREE>
  CENTER_LONGITUDE                = "N/A"
  REFERENCE_LATITUDE              = "N/A"
  REFERENCE_LONGITUDE             = "N/A"
  LINE_FIRST_PIXEL                = 1 /* North edge */
  LINE_LAST_PIXEL                 = 761 /* South edge */
  SAMPLE_FIRST_PIXEL              = 1 /* West edge */
  SAMPLE_LAST_PIXEL               = 806 /* East edge */
  MAP_PROJECTION_ROTATION         = 0.0
  MAP_RESOLUTION                  = 3072 <PIXEL/DEGREE>

```

```

MAP_SCALE                = 0.019294069 <KM/PIXEL>
MAXIMUM_LATITUDE         = 25.0631 <DEGREE>
MINIMUM_LATITUDE         = 24.8155 <DEGREE>
WESTERNMOST_LONGITUDE    = -19.9259 <DEGREE>
EASTERNMOST_LONGITUDE    = -19.6388 <DEGREE>
LINE_PROJECTION_OFFSET   = 76233.216
SAMPLE_PROJECTION_OFFSET = -60330.394
COORDINATE_SYSTEM_TYPE   = "BODY-FIXED ROTATING"
COORDINATE_SYSTEM_NAME   = "PLANETOCENTRIC"
END_OBJECT               = IMAGE_MAP_PROJECTION
END

```


APPENDIX K. MRDR BROWSE PRODUCT 'TRU' PNG FILE LABEL

```

PDS_VERSION_ID          = PDS3
RECORD_TYPE              = UNDEFINED
LABEL_REVISION_NOTE     = "2003-11-19, S. Slavney (GEO);
                          2005-09-25, S. Murchie (JHU/APL);
                          2007-09-14, C. Hash (ACT Corp)"

/* Map-projected Multispectral RDR Identification */
DATA_SET_ID              = "MRO-M-CRISM-5-RDR-MULTISPECTRAL-V1.0"
PRODUCT_ID               = "T1396_MRRTRU_30N088_0256_2"
                          /*( Tnnnn_MRRsss_xxdyyy_rrrr_v                )*/
                          /*( nnnn = tile number                        )*/
                          /*( sss = subtype of browse product          )*/
                          /*( xx = latitude of tile center              )*/
                          /*( d = N or S for north or south latitude    )*/
                          /*( yyy = east longitude of tile center        )*/
                          /*( rrrr = resolution in pixels/degree         )*/
                          /*( v = version number                        )*/

INSTRUMENT_HOST_NAME     = "MARS RECONNAISSANCE ORBITER"
SPACECRAFT_ID            = MRO
INSTRUMENT_NAME           = "COMPACT RECONNAISSANCE IMAGING
                          SPECTROMETER FOR MARS"

INSTRUMENT_ID            = CRISM
TARGET_NAME              = MARS
PRODUCT_TYPE             = BROWSE
PRODUCT_CREATION_TIME    = 2009-12-02T16:48:56
START_TIME               = "N/A"
STOP_TIME                = "N/A"
SPACECRAFT_CLOCK_START_COUNT = "N/A"
SPACECRAFT_CLOCK_STOP_COUNT = "N/A"
PRODUCT_VERSION_ID       = "2"
PRODUCER_INSTITUTION_NAME = "APPLIED PHYSICS LABORATORY"
SOFTWARE_NAME            = "PIPE_create_crism_mrdr_browse"
SOFTWARE_VERSION_ID      = "09.01.09"
MRO:WAVELENGTH_FILE_NAME = "N/A"

/* These parameters describe the browse image as a PDS document. */
^PNG_DOCUMENT            = "T1396_MRRTRU_30N088_0256_2.PNG"
OBJECT                   = PNG_DOCUMENT
  DOCUMENT_NAME          = "T1396_MRRTRU_30N088_0256_2"
  DOCUMENT_FORMAT         = PNG
  DOCUMENT_TOPIC_TYPE     = "BROWSE IMAGE"
  INTERCHANGE_FORMAT      = BINARY
  PUBLICATION_DATE        = 2009-12-02
  SOURCE_PRODUCT_ID       = "T1396_MRRAL_30N088_0256_2"
  SAMPLE_TYPE             = LSB_UNSIGNED_INTEGER
  SAMPLE_BITS             = 8
  BANDS                   = 3
  BAND_SEQUENCE           = ("RED", "GREEN", "BLUE")
  BAND_NAME               = ("598 nm", "533 nm", "442 nm")
/* The following information to scale from real numbers to an */
/* 8-bit integer is hard-coded for this type of browse image. */
  DERIVED_MINIMUM         = (0,0,0)
  DERIVED_MAXIMUM         = (250,250,250)
  OFFSET                  = (0.000000,0.000000,0.000000)
  SCALING_FACTOR          = (0.00120,0.00120,0.00120)
  MISSING_CONSTANT        = (255,255,255)
  DESCRIPTION              = "This file is a true color VNIR image assembled
                          from calibrated radiance, solar distance, and
                          solar flux as sampled in the wavelength filter
                          and binning state being used: radiance_factor =
                          I*D^2/(pi*F) where I = spectral radiance,

```

```

D = solar distance in AU, and F = solar flux at
1 AU. Subsequently a correction was made for
atmospheric and photometric effects either
predictively from climatology or after the fact
from CRISM measurements."
END_OBJECT = PNG_DOCUMENT
/* Map projection information about this RDR is in the IMAGE_MAP_PROJECTION */
/* object below. */
OBJECT = IMAGE_MAP_PROJECTION
^DATA_SET_MAP_PROJECTION = "MRR_MAP.CAT"
MAP_PROJECTION_TYPE = "EQUIRECTANGULAR"
A_AXIS_RADIUS = 3396 <KM>
B_AXIS_RADIUS = 3396 <KM>
C_AXIS_RADIUS = 3396 <KM>
FIRST_STANDARD_PARALLEL = "N/A"
SECOND_STANDARD_PARALLEL = "N/A"
POSITIVE_LONGITUDE_DIRECTION = "EAST"
CENTER_LATITUDE = 27.50000 <DEGREE>
CENTER_LONGITUDE = 87.50000 <DEGREE>
REFERENCE_LATITUDE = "N/A"
REFERENCE_LONGITUDE = "N/A"
LINE_FIRST_PIXEL = 1
LINE_LAST_PIXEL = 1280
SAMPLE_FIRST_PIXEL = 1
SAMPLE_LAST_PIXEL = 1136
MAP_PROJECTION_ROTATION = 0.0
MAP_RESOLUTION = 256 <PIXEL/DEG>
MAP_SCALE = 0.231528833585 <KM/PIXEL>
MAXIMUM_LATITUDE = 32.50000 <DEGREE>
MINIMUM_LATITUDE = 27.50000 <DEGREE>
WESTERNMOST_LONGITUDE = 85.00000 <DEGREE>
EASTERNMOST_LONGITUDE = 90.00000 <DEGREE>
LINE_PROJECTION_OFFSET = 1280.000
SAMPLE_PROJECTION_OFFSET = 640.000
COORDINATE_SYSTEM_TYPE = "BODY-FIXED ROTATING"
COORDINATE_SYSTEM_NAME = "PLANETOCENTRIC"
END_OBJECT = IMAGE_MAP_PROJECTION
END

```

APPENDIX L. DATA PROCESSING DETAILS

Dave Humm and Scott Murchie

1/28/2009

(Describes the TRDR calibration pipeline, v2)

1. CALIBRATION OVERVIEW

1.1 Collection of calibration data in flight

Darks will be taken bracketing every targeted measurement as part of the macro for that targeted measurement. Darks will be taken every 5 minutes in mapping mode.

Onboard integrating sphere calibration data will be taken with the IR lamp at nominally fixed intervals in time. The plan is to take sphere calibrations once every 1.5 orbits, bracketing scene observations with a dayside and nightside sphere observation. The idea is that the IR detector will be relatively warm (by a degree or so, maybe much less) on the dayside and relatively cool on the nightside. To correct the radiometric calibration for detector temperature, we interpolate in indicated detector temperature between the dayside and nightside sphere calibrations. In some cases, we will skip an extra orbit or two between the dayside and nightside due to restrictions on scheduling. The primary sphere lamp is lamp 1, the IR-controlled “cross-slit” lamp, and these data are used for all calibrations (as of 12/16/2008). Integrating sphere data with lamp 2, the VNIR-controlled “along-slit” lamp, will be taken on the same schedule for redundancy.

Bias calibration data, darks with multiple integration times, will be taken at nominally fixed intervals for the IR detector only. Currently, the default is to take a bias set with every integrating sphere calibration measurement. There is a specific macro for the bias calibration.

Focal plane lamp data are taken occasionally. The focal plane lamp data are not used in the calibration algorithm, so this is just for verification and engineering checkout. There is a specific macro for the focal plane lamp calibration.

A nadir-pointed hyperspectral swath of a featureless region of Mars is taken at a nominally fixed interval. Currently, the plan is to take these data monthly. These data will be used to flat-field the VNIR detector at all wavelengths and the IR detector at wavelengths where there are no sharp atmospheric spectral features.

1.2 Reduction of flight target image data using calibration data

0. Use pixel processing table and LUT tables to convert 8-bit data to 12-bit if data are 8-bit. Section 2.2.
1. Use pixel processing table to convert 12-bit data to 14-bit data. Section 2.2.
2. Subtract bias calculated from nearest available flight bias calibration data set. For IR only. Apply to scene images and darks. Sections 2.3 and 3.1.
3. Subtract median of masked pixels in each image frame. Sections 2.3 and 3.1.

4. Subtract darks from scene images. For VNIR only. Use a weighted average of darks taken before and after the target image, with the weighting factors derived from the relative time at which each dark was taken with respect to the scene image. Sections 2.3 and 3.2.
5. Make detector quadrant ghost correction applying coefficients from ground calibration to each quadrant within each image. For IR, apply to darks as well. Section 2.4. Replace saturated pixels with 65535.
6. Apply a priori bad pixel mask to all images, replacing bad pixels with a linear spatial nearest-neighbor interpolation. For VNIR there's a single dead pixel only in full-resolution images, defined by a CDR. For IR, we calculate the bad pixel mask for each image using the set of associated dark and bias images. Sections 2.5 and 2.6.
7. Apply overall detector nonlinearity correction to scene images. For IR, apply to darks as well. Section 2.7.
8. Divide by integration time to get counts/millisecond. Section 2.8
9. Subtract processed darks from processed scene images. Use a weighted average of darks taken before and after the scene image, with the weighting factors derived from the relative time at which each dark was taken with respect to the scene image. For IR only. Sections 2.9 and 3.2.
10. Apply stray light subtraction using stray light pixels within each image. VNIR only. For IR, the sphere radiance is adjusted to account for stray light and there is no explicit correction. The formula for the VNIR correction is complex. Section 2.10.
11. Apply subtraction of 2nd order leaked light in Zone 3 of IR detector using Zone 1 and 2 counts from same image and ground-derived coefficients. For IR only. Section 2.11.
12. Apply shutter mirror nonrepeatability correction to ground integrating sphere radiance. This corrects the ground-measured radiance of the integrating sphere to the shutter mirror position in the flight calibration sphere data. Uses flight calibration sphere data to correct ground sphere radiance. No effect on flight scene or calibration images, but it does use data from the flight calibration image, so it must be performed in sequence after the previous calibration steps. Section 3.4. As of 1/28/2009, this correction is in the software but the associated CDR is zeroed out so the correction is not applied. Instead, the sphere radiance in the CDR has a one-time correction for flight versus ground already applied.
13. Calculate spectroradiometric responsivity using nearest available flight integrating sphere data and ground sphere radiance. This spectrum is a function of wavelength pixel and spatial pixel. For VNIR detector rows 185-215 (short wavelengths), the responsivity is simply read from a CDR, not calculated from a sphere image, because the sphere is too dim. Section 3.5.
14. Apply binning to responsivity for the different modes. Section 2.13.
15. Divide corrected counts/second in the scene images by the binned responsivity to get radiance at the instrument aperture. Note that before the radiance is calculated, the scene data sets should be processed using steps 1-13 above. Section 2.14.
16. Divide radiance image by image of external flat field. Section 2.14.
17. Apply ex post facto bad pixel removal algorithm to scene images. Section 2.15.
18. Replace non-scene pixels with the value 65535. Section 2.15.

2. CALIBRATION DESCRIPTION

2.1 Overview of calibration equation

Radiometric calibration to units of radiance follows the equation

$$RD_{x,\lambda,r} = M_{x,\lambda,HZ} ((K_{x,\lambda,HZ} (D14_{\lambda} (DN_{x,\lambda,TaV,TaW,TaI,TaJ,Ta2,HZ,t,r}) - BiaT_{x,\lambda,TaV,TaW,TaI,TaJ,HZ,t}) / t - Bkgd_{x,\lambda,TaI,Ta2,HZ} - Scat_{x,\lambda,TaV,TaI,Ta2,HZ,r}) / (RST_{x,\lambda,TaV,TaI,Ta2} * FF_{x,\lambda,HZ}))$$

Diffuse spectral reflectivity (I/F) is calculated by

$$IF_{x,\lambda} = \pi \cdot RD_{x,\lambda,r} / (SF_{x,\lambda} / r^2)$$

Subscripts include:

- x, **spatial position** in a row on the focal plane, in detector elements
- λ , **wavelength** in spectral direction on the focal plane, in detector elements or nm
- Hz, **frame rate, wavelength table, and binning mode**
- T_{aI} , **IR detector temperature** in K for scene measurement
- T_{aV} , **VNIR detector temperature** in K for scene measurement
- T_{a2} , **spectrometer housing temperature** in K
- T_{c3} , **temperature of the integrating sphere** in K for flight calibration measurement
- T_{aJ} , **IR focal plane board temperature** in K for scene measurement
- T_{aW} , **VNIR focal plane board temperature** in K for scene measurement
- t, **integration time** in seconds
- s, **choice of sphere bulb**, side 1 or 2

Temperatures are given for scene measurements, bias measurements, calibration measurements, or first and second dark measurements according to the lowercase subscripts a, b, c, d, and e respectively. So, for example, T_{aI} would be the IR detector temperature for the scene image, T_{dI} would be the IR detector temperature for the “before” dark image, T_{eI} for the “after” dark image, T_{cI} would be the IR detector temperature for the associated flight calibration images, and T_{bI} would be the IR detector temperature for the associated bias measurement. The algorithm uses temperatures from the low-rate telemetry. The temperatures are taken once per second and a 10-point median smoothing is applied.

Subscripts indicate which terms in the equation are dependent on which parameters. This includes both explicit and implicit dependence, and excludes when an implicit dependence has been explicitly subtracted out. For example, the $Bkgd_{x,\lambda,TaI,Ta2,HZ}$ term includes background from the IR glow of the inside walls of the spectrometer, so it depends on the spectrometer temperature T_{a2} . $Bkgd_{x,\lambda,TaI,Ta2,HZ}$ is calculated from dark images with spectrometer temperatures T_{d2} and T_{e2} , but the calculation is designed to give the level of the background for the target measurement spectrometer temperature T_{a2} . The explicit dependence on T_{d2} and T_{e2} has been subtracted out, leaving an implicit dependence on T_{a2} , so T_{a2} is in the subscript.

Description of the terms of the equation:

D14_i() converts from raw DN to 14-bit DN.

BiaT_{x,λ,TaV,TaW,TaI,TaJ,HZ,t} is the detector bias (DN at zero integration time).

K_{x,λ,HZ}() flags saturated pixels and applies the detector ghost, initial bad pixel, and detector nonlinearity corrections.

Bkgd_{x,λ,TaI,Ta2,HZ} is the dark subtraction term calculated from shutter-closed measurements.

Scat_{x,λ,TaV,TaI,Ta2,HZ,r} is the stray light subtraction, including uniform glare and 2nd order light.

RST_{x,λ,TaV,TaI,Ta2} is the responsivity calculated from flight onboard sphere calibration images.

M_{x,λ,HZ}() applies the detector mask and the final scene bad pixel correction.

FF_{x,λ,HZ} is the flat field.

RD_{x,λ,r} is the observed spectral radiance in W/(m² micrometer sr) at the instrument aperture.

SF_{x,λ} is solar spectral irradiance for a normally illuminated surface 1 AU from the Sun, convolved to the CRISM spectral profiles.

r is the distance of Mars from the Sun in astronomical units.

IF_{x,λ} is the I/F of the scene (unitless), a measure of diffuse reflectivity.

Definition of the terms of the equation:

The value 65535 is treated as a flag and any pixel with that value does not receive any further processing at any step of the calibration. The value of 65535 is just passed on to the next step.

$$D14_i(DN_{x,\lambda,TaV,TaI,Ta2,HZ,t,r}) = Offset_i + Gain_i \cdot ILUT_i(DN_{x,\lambda,TaV,TaI,Ta2,HZ,t,r})$$

This is conversion from raw DN (raw DN has fast lossless compression undone) to 14-bit DN. See section 2.2.

$$\begin{aligned} BiaT_{x,\lambda,TaI,TaJ,HZ,t} = & Bias_{x,\lambda,TbI,TbJ,HZ} - a0_I \cdot Hv(row_i+1-(502/480) \cdot (480-integ(t))) \\ & + \beta_{I,HZ} \cdot (T_{aI} - T_{bI}) - \beta_{J,HZ} \cdot (T_{aJ} - T_{bJ}) \\ & + median_{x,\lambda}(DN14_{x1...xn,\lambda,TaI,TaJ,Ta2,HZ,t,r}) \end{aligned}$$

for IR and

$$\begin{aligned} BiaT_{x,\lambda,TaV,TaW,HZ,t} = & (\alpha_{ea} \cdot Bias_{x,\lambda,TdV,TdW,HZ,t} + \alpha_{ad} \cdot Bias_{x,\lambda,TeV,TeW,HZ,t}) / (\alpha_{ad} + \alpha_{ea}) \\ & + \beta_{V,HZ} \cdot [\alpha_{ea} \cdot (T_{aV} - T_{dV}) + \alpha_{ad} \cdot (T_{eV} - T_{aV})] / (\alpha_{ad} + \alpha_{ea}) \\ & + \beta_{W,HZ} \cdot [\alpha_{ea} \cdot (T_{aW} - T_{dW}) + \alpha_{ad} \cdot (T_{eW} - T_{aW})] / (\alpha_{ad} + \alpha_{ea}) \\ & + median_{x,\lambda}(DN14_{x1...xn,\lambda,TaV,TaW,HZ,t,r}) \end{aligned}$$

for VNIR is the temperature-corrected bias subtraction. The masked pixel subtraction renders the detector temperature correction redundant, but it is still performed. See section 2.3 and section 3.1.

K_{x,λ,HZ}() = F_{HZ}(B_{x,λ,HZ}(S(H())))) applies the detector ghost correction, flags saturated pixels, applies the a priori bad pixel correction, and applies the detector nonlinearity correction. See sections 2.4 through 2.7.

$$H(DN14^a_{x,\lambda,TaV,TaI,Ta2,HZ,t,r}) = DN14^a_{x,\lambda,TaV,TaI,Ta2,HZ,t,r} - \sum_{n=0}^{n=3} G(DN14^a_{x0+n-\lambda,\lambda,TaV,TaI,Ta2,HZ,t,r})$$

applies the detector quadrant ghost correction. See section 2.4.

$S(DN14_{x,\lambda,TaV,TaI,Ta2,HZ,t,r}^b) = 65565$ if $DN14_{x,\lambda,TaV,TaI,Ta2,HZ,t,r}^a > DN14_{maxI}^a$ for IR or $DN14_{maxV}^a$ for VNIR. See section 2.5.

$B_{x,\lambda,HZ}()$ is the a priori bad pixel removal function. See section 2.5.

$F_{HZ}()$ is the detector average nonlinearity function. See section 2.7.

$Bkgd_{x,\lambda,TaI,Ta2,HZ} = Bkgd_{x,\lambda,TdI,TeI,Td2,Te2,HZ,taI,tdI,teI}$ is the dark-subtraction term. It is zero for VNIR. The parameters in the subscripts on the right-hand side are explicitly used to calculate a value of the background that should be implicitly dependent only on the parameters in the subscripts on the left-hand side. See section 2.9.

$Scat_{x,\lambda,TaI,Ta2,HZ,r} = \sum_{n=1}^{n=6} \kappa_{x,\lambda,n,HZ} \cdot RT14_{x,\lambda',yn,HZ,TaI,Ta2,HZ,r}^i$
for IR comprises the stray light correction for second order. See section 2.11.
 $Scat_{x,\lambda,TaI,Ta2,HZ,r} = <RT14_{x1...xn,\lambda,TaV,TaI,Ta2,HZ,r}^h> \cdot SW_{x,TaV,TaI,Ta2,HZ}^h$ for $\lambda < 563$ nm and
 $<RT14_{x1...xn,\lambda,TaV,TaI,Ta2,HZ,r}^h> \cdot CS_{x,\lambda,TaV,TaI,Ta2,HZ}^h$ for $\lambda > 563$ nm
for VNIR comprises the stray light correction for scattered light. See section 2.10.

$RST_{x,\lambda,TaI,Ta2} = (RSP_{x,\lambda,TcI,Tc2}^j \cdot (T_{aI} - T_{fl}) + RSP_{x,\lambda,Tfl,Tf2}^j \cdot (T_{cI} - T_{aI})) / (T_{cI} - T_{fl})$
for IR, where T_{cI} and T_{fl} are the IR detector temperatures for the dayside and nightside sphere calibrations respectively. As of 12/30/2008, this capability is in the code but is not being utilized. We just use the nearest IR flight integrating sphere data twice.

$RST_{x,\lambda,TaV,Ta2} = RSP_{x,\lambda,TcV,Tc2}^j \cdot (\mu_{x,\lambda} + \nu_{x,\lambda} \cdot TaV + \pi_{x,\lambda} \cdot TaV^2) / (\mu_{x,\lambda} + \nu_{x,\lambda} \cdot T_{cV} + \pi_{x,\lambda} \cdot T_{cV}^2)$
for VNIR is the temperature-corrected CRISM responsivity calculated from the flight onboard sphere calibration measurements. As of 12/30/2008, $\mu=1$, $\nu=0$, and $\pi=0$, so the correction is not applied. See section 3.4, section 3.5, and section 2.12.

$FF_{x,\lambda,HZ} = FL_{x,\lambda,HZ} + EP_{x,\lambda,HZ} \cdot \log(RT_{x,\lambda,TaV,TaI,Ta2,HZ,r}^j / RSP_{x,\lambda,TaV,TaI,Ta2,HZ}^l)$
where $FL_{x,\lambda,HZ}$ is the radiance image of an external flat field scene, run through the whole calibration pipeline and then normalized so the scene pixels in each row average to 1. See section 3.3 and section 2.14. As of 1/28/2009, $EP_{x,\lambda}$ is zero, so it is a straight flat field with no allowance for pixel-dependent nonlinearity.

$M_{x,\lambda,HZ}()$ replaces non-scene pixels with the value 65535. For IR, it also applies the ex post facto bad pixel correction. See section 2.15.

$RD_{x,\lambda,r}$ is the observed spectral radiance in $W/(m^2 \text{ micrometer sr})$ at the instrument aperture for scene or EPF measurements. See section 2.14.

$IF_{x,\lambda}$ is I/F, a measure of the observed diffuse reflectivity of the Martian surface as a function of wavelength. The normalization is such that the I/F of a normally illuminated perfect white Lambertian surface is 1. See section 2.17.

2.2 Uncompression and conversion to 14-bit DN

Before any calibration steps are taken, the lossless fast compression is undone, yielding **raw DN**.

The first term in the calibration equation, $DN_{x,\lambda,H_z,t}$, is **raw DN** for some column x and row λ , taken at some frame rate H_z with exposure time t . Raw DN levels are in EDRs named according to the convention `ccnnnnnnnnn_xx_aaaaas_EDRv.IMG` where `ccc`=class of observation (targeted, multispectral windows, etc.), `nnnnnnnnn`=observation ID in hex, `xx`=counter of EDRs within that observation, `aaaaa`=activity type, `s`=sensor ID, and `v`=version number.

Some raw DN values may be 65535. These are unphysical values used as flags for data dropout pixels. For later steps in the calibration algorithm, the value 65535 will be used to flag saturated and non-scene pixels. Whenever the value of 65535 is encountered at this or any other step, the calibration algorithm assumes it is a flag, not a true DN, and simply passes the value through rather than applying the calibration calculation to that pixel.

- Although raw DN has the lossless fast compression undone, it is still always written to an EDR compressed from a 14-bit state. This compression is performed in the DPU before lossless fast compression. Raw DN is restored to 14 bits using a pixel processing table which has one line per detector row, with 3 elements per line. This step occurs after the EDRs are generated, as part of the conversion of the EDRs to radiance units.

The conversion needs to know:

- Which one of 8 look-up tables was used to convert 12 to 8 bits on that line, if the data are 8 bits
- An inverted version of the lookup table used for each line, to convert back to 12 bits
- A gain, by which the 12-bit DN should be divided
- An offset, which should be added to the gain-corrected DN

For 8-bit raw DN (lossy compression on), there are two steps to the conversion, converting raw DN to 12-bit DN12, and converting 12-bit DN12 to 14-bit DN14. For 12-bit raw DN (lossy compression off), the first step is skipped.

The formula for generating 12-bit DN12 is

$$DN12_{x,\lambda,TaV,TaW,TaI,TaJ,Ta2,H_z,t,r} = ILUT_{\lambda} (DN_{x,\lambda,TaV,TaW,TaI,TaJ,Ta2,H_z,t,r})$$

for 8-bit raw DN, and

$$DN12_{x,\lambda,TaV,TaW,TaI,TaJ,Ta2,H_z,t,r} = DN_{x,\lambda,TaV,TaW,TaI,TaJ,Ta2,H_z,t,r}$$

for 12-bit raw DN. $ILUT_{\lambda}$ is the inverse of the original look-up table used by the flight DPU to perform the lossy compression. In addition to the above formulas, the values of 65535 in the data drop-out pixels are simply passed forward as always.

The formula for converting 12-bit DN12 to 14-bit DN14 is

$$DN14_{x,\lambda,TaV,TaW,TaI,TaJ,Ta2,HZ,t,r} = Offset_{\lambda} + Gain_{\lambda} \cdot DN12_{x,\lambda,TaV,TaW,TaI,TaJ,Ta2,HZ,t,r}$$

The offset, gain, and lookup tables are all given row-by-row, and tables are valid over specified time ranges.

Which LUTs were used for each row is maintained as the last column in the level 6 pixel processing CDR, named CDR6_#_#####_PP_n_v.TAB, where #=spacecraft time SCLK partition at the beginning time of validity of the CDR, #####=spacecraft time SCLK at the beginning time of validity of the CDR, n=sensor ID and v=version number. The LUTs themselves are maintained as CDR6_1_0000000000_LK_n_v.TAB, and the conversion back to 14 bits uses the inverse lookup table, maintained as CDR6_1_0000000000_LI_n_v.TAB. The gains are maintained as the second column of the level 6 pixel processing CDR, and the offsets are maintained as the third column of the level 6 pixel processing CDR.

2.3 Remove bias

Next the bias is removed from the data. The bias subtraction formula for the IR is

$$DN14^a_{x,\lambda,TaI,Ta2,HZ,t,r} = DN14_{x,\lambda,TaJ,Ta2,HZ,t,r} - Bias_{x,\lambda,TbI,TbJ,HZ} \\ + a0_I \cdot Hv(row_{\lambda}+1-(502/480) \cdot (480-integ(t))) - \beta_{I,HZ} \cdot (T_{aI} - T_{bI}) - \beta_{J,HZ} \cdot (T_{aJ} - T_{bJ}) \\ - median(DN14_{x1...xn,\lambda0...,\lambda S,TaI,TaJ,Ta2,HZ,t,r})$$

The superscript “a” indicates the first step in the calibration algorithm has been applied, and we continue through the alphabet for subsequent steps of the calibration algorithm. As discussed earlier, any values of 65535 are treated as flags and simply passed through with no calculation performed on them.

Bias is different and more complicated for the IR detector as compared to the VNIR detector. Bias is the DN level extrapolated to zero exposure time, in image form, taken at a particular frame rate. This represents an electronics bias added to the measured signal, to prevent near-zero DNs from going negative (and being clipped) due to superimposed noise. In detector-level testing it was found that bias has a nearly fixed pattern pixel to pixel, but that its magnitude varies weakly with temperature and strongly with frame rate.

In flight, bias for the IR detector is derived from a dedicated calibration, performed periodically, in which, at each frame rate, a burst of 10 images is taken with the shutter closed at each of several short exposure times. These data are taken at IR detector temperature T_{bI} . After making a correction for a step in the bias that is a function of integration time parameter, the DN values are fit linearly on a pixel-by-pixel basis and the exposure time=0 y-intercept image is used as the bias estimate. This process is described in section 3.1.

The IR bias images $Bias_{x,\lambda,TbI,TbJ,HZ}$ are corrected for the step function $-a0_I \cdot Hv(row_{\lambda}+1-(502/480) \cdot (480-integ(t)))$. This term results from details of the readout of the image in the electronics. It

is entirely predetermined, and contains the entire dependence of the bias on the integration time. The constant a_0 is determined from ground calibration data, $H_v()$ is the Heaviside function, row_x is the detector row number (counting from zero), and $integ(t)$ is the integration time parameter. The value of t in ms is calculated from the integration time parameter $integ$ using the formula $t = 1000 \cdot (502 - \text{floor}((502/480) \cdot (480 - integ)) / (502 \cdot \text{rate}))$, where $\text{floor}()$ is the function that creates an integer from a real number by rounding down. Since the bias images $Bias_{x,\lambda,T_{bl},T_{bj},Hz}$ do not include the step function, it is subtracted explicitly in the equation above.

The IR bias images $Bias_{x,\lambda,T_{bl},T_{bj},Hz}$ are stored as level 4 calibration data records (CDRs) named $CDR4\#_tttttttt_BIrbeeewsL_v.IMG$, where $\#$ =spacecraft SCLK partition for the mean time at which that bias data was taken, $tttttttt$ =mean spacecraft time SCLK for that bias data, r =frame rate, b =binning, eee =exposure time parameter, w =wavelength filter, $s=0$, L =detector (IR), and v =version number. The calibration software uses the partition $\#$ and the mean SCLK $tttttttt$ to calculate encoded SCLK for the bias measurement. It uses the SCLK given in the .TAB list file that goes with each frame of the EDR along with a partition $\#$ from the .LBL file that goes with that EDR to calculate encoded SCLK for that EDR. It then uses the CDR4 file with the value of encoded SCLK that is closest to the value of encoded SCLK for the scene measurement.

The bias calibration may be taken at an IR detector temperature T_{bl} different from that of the data being corrected, T_{al} . The term $\beta_{l,HZ} \cdot (T_{al} - T_{bl})$ represents the scalar difference between two modeled values of averaged, temperature-dependent bias. This scalar value is intended to correct the bias image for small temperature differences between the time of its acquisition and the time of the data being corrected. The coefficients $\beta_{l,HZ}$ are given in a level 6 CDR named $CDR6_ \#_0000000000_DB_L_v.TAB$. Separate coefficients are defined for the 4 detector quadrants, but as of this writing (11/4/2005) the values are the same for all the quadrants so there is no subscript to represent the quadrant dependence.

The bias calibration may be taken at an IR focal plane electronics board temperature T_{bj} different from that of the data being corrected, T_{aj} . The term $\beta_{j,HZ} \cdot (T_{aj} - T_{bj})$ represents the scalar difference between two modeled values of averaged, temperature-dependent bias. This scalar value is intended to correct the bias image for small temperature differences between the time of its acquisition and the time of the data being corrected. The coefficients $\beta_{j,HZ}$ are given in a level 6 CDR named $CDR6_ \#_0000000000_EB_L_v.TAB$. Separate coefficients are defined for the 4 detector quadrants, but as of this writing (11/4/2005) the values are the same for all the quadrants so there is no subscript to represent the quadrant dependence.

After the temperature corrections were implemented, it was determined that there was an image-to-image noise in the bias that generated horizontal lines in the image. This noise could not be modeled. The only way to eliminate it was to subtract the median of a set of detector pixels covered by a physical mask and therefore completely unilluminated, even by scattered light. The median is taken over a set of columns $x \dots x_n$ along the edge of the detector, and over all detector wavelengths $\lambda \dots \lambda_s$. The columns used for masked pixel subtraction for a given pixel binning b and wavelength table w are specified in the DM level 4 CDR $CDR410000000000_BI0b000w0L_v.IMG$. In addition to removing the image-to-image noise, the masked pixel subtraction would also effectively remove the temperature dependence. The temperature correction steps are left in but are redundant and have no significant effect on the

images.

For the VNIR images, the dark current and thermal photons are nil, so the bias is directly measured when the shutter is closed (the dark measurements taken before and after a scene or calibration image). For the IR, a separate bias subtraction is necessary because there is background due to dark current and thermal photons, and it is necessary to separate that background from the bias in order to make an accurate linearity correction.

The bias subtraction formula for VNIR is

$$\begin{aligned} \text{DN14}_{x,\lambda,\text{TaV,HZ,t,r}}^a &= \text{DN14}_{x,\lambda,\text{Hz,TaV,TaW,t,r}} \\ &- (\alpha_{\text{ea}} \cdot \text{Bias}_{x,\lambda,\text{TdV,TdW,HZ,t}} + \alpha_{\text{ad}} \cdot \text{Bias}_{x,\lambda,\text{TeV,TeW,HZ,t}}) / (\alpha_{\text{ad}} + \alpha_{\text{ea}}) \\ &- \beta_{\text{V,HZ}} \cdot [\alpha_{\text{ea}} \cdot (T_{\text{aV}} - T_{\text{dV}}) + \alpha_{\text{ad}} \cdot (T_{\text{eV}} - T_{\text{aV}})] / (\alpha_{\text{ad}} + \alpha_{\text{ea}}) \\ &- \beta_{\text{W,HZ}} \cdot [\alpha_{\text{ea}} \cdot (T_{\text{aW}} - T_{\text{dW}}) + \alpha_{\text{ad}} \cdot (T_{\text{eW}} - T_{\text{aW}})] / (\alpha_{\text{ad}} + \alpha_{\text{ea}}) \\ &- \text{median}(\text{DN14}_{x1 \dots xn, \lambda 0 \dots \lambda s, \text{TaV,TaW,HZ,t,r}}) \end{aligned}$$

The α coefficients in the VNIR equation are time-weighting coefficients. The two VNIR bias images are linearly interpolated in time to the time of the scene image. The variable t represents integration time, not clock time, so a new variable, t_{a1} indicates clock time. The value of t_{a1} is the mean value of encoded SCLK for that image specifically. It is derived from the instrument timetag value in the header of each image, calculated by the CRISM instrument clock, frequently updated by the spacecraft clock, and corrected using the partition number to be encoded SCLK instead of just SCLK. Calculations on a local computer may not have the SPICE information available to convert SCLK to encoded SCLK. One may use SCLK for this calculation as long as the partition number does not change. Just like for the temperatures, t_{a1} indicates timetag for the scene image, t_{d1} and t_{e1} the dark images, t_{b1} the bias images, and t_{c1} the calibration images.

$$\alpha_{\text{ad}} = t_{\text{a1}} - t_{\text{d1}} \text{ and } \alpha_{\text{ea}} = t_{\text{e1}} - t_{\text{a1}}$$

The VNIR bias images $\text{Bias}_{x,\lambda,\text{TdV,TdW,HZ,t}}$ and $\text{Bias}_{x,\lambda,\text{TeV,TeW,HZ,t}}$ are calculated from the VNIR bias EDRs by taking the mean DN value in each detector element across all the images in an EDR, with the two largest and two smallest DN values thrown out. The results are stored as level 4 calibration data records (CDRs) named `CDR4#ttttttttt_BIrbeeewsS_v.IMG`, where # = spacecraft SCLK partition for the beginning of time of validity of the data product, tttttttt = spacecraft time SCLK for the beginning of time of validity of the data product, r = frame rate, b = binning, eee = exposure time parameter, w = wavelength filter, s = 0, S = detector (VNIR), and v = version number. The calibration software uses the partition # and the mean SCLK to calculate encoded SCLK for the bias measurement. It uses the SCLK given in the .TAB list file that goes with each frame of the EDR along with a partition # given in the .LBL file that goes with that EDR to calculate encoded SCLK for that EDR. It then uses the CDR4 file with the value of encoded SCLK that is closest to the value of encoded SCLK for the scene measurement. A description of the calculation of $\text{Bias}_{x,\lambda,\text{TdV,TdW,HZ,t}}$ and $\text{Bias}_{x,\lambda,\text{TeV,TeW,HZ,t}}$ is given in section 3.2.

The VNIR coefficients $\beta_{\text{V,HZ}}$ are given in `CDR6_#_0000000000_DB_n_v.TAB`, and the VNIR coefficients $\beta_{\text{W,HZ}}$ are given in `CDR6_#_0000000000_EB_n_v.TAB`. The VNIR temperature correction is with respect to the temperatures T_{dV} , T_{eV} of the VNIR detector and T_{dW} , T_{eW} of the

VNIR focal plane electronics board during the before and after darks respectively.

After the temperature corrections were implemented, it was determined that there was an image-to-image noise in the bias that generated horizontal lines in the image. This noise could not be modeled. The only way to eliminate it was to subtract the median of a set of detector pixels covered by a physical mask and therefore completely unilluminated, even by scattered light. The median is taken over a set of columns $x \dots xn$ along the edge of the detector, and over all detector wavelengths $l \dots ls$. The columns used for masked pixel subtraction for a given pixel binning b and wavelength table w are specified in the DM level 4 CDR CDR410000000000_BI0b000w0S_v.IMG. In addition to removing the image-to-image noise, the masked pixel subtraction would also effectively remove the temperature dependence. The temperature correction steps are left in but are redundant and have no significant effect on the images.

The above description of the bias correction applies to the scene images, which have temperatures T_{aI} , T_{aJ} and T_{aV} , T_{aW} . The bias correction is also applied to dark images for the IR, and the formula is the same except T_{aI} , T_{aJ} are replaced by T_{dI} , T_{dJ} . It is also applied to the calibration images for both IR and VNIR, and likewise T_{aI} , T_{aJ} are replaced by T_{cI} , T_{cJ} and T_{aV} , T_{aW} by T_{cV} , T_{cW} .

2.4 Remove detector quadrant electronics ghost

Next, electronics ghosts are removed from the data. There are two types of ghosts, each at the percent level, that add to the measured DN but do not represent real signal.

The first type of electronics ghost is a weak, negative image of any one of the four 160-column wide quadrants in each other quadrant.



Weak electronics ghost negative images of the quadrant 4 signal in each other quadrant.

Each quadrant produces the same ghost image in all 4 quadrants. We include the self-ghosting because it makes the subsequent nonlinearity correction smaller. For VNIR, the ghost is a nonlinear function of the signal. For IR, the ghost is a linear function of the signal, but with a nonzero intercept when extrapolated to zero signal indicating that the ghost would be nonlinear at small signal levels if we had data there. For VNIR or IR, the ghost has the same function $G(DN)$ for all 4 quadrants whether one changes the quadrant in which the source is located or the quadrant in which the ghost appears.

To remove the detector quadrant ghost, we subtract the ghost calculated from the signal in each of the 4 quadrants from each pixel. The quadrant the pixel itself is in is included, so the self-ghosting is subtracted.

$$DN14^b_{x,\lambda,TaV,HZ,t,r} = DN14^a_{x,\lambda,TaV,HZ,t,r} - \sum_{n=0}^{n=3} G_V(DN14^a_{x0+n\cdot\delta,\lambda,TaV,HZ,t,r})$$

for VNIR and

$$DN14^b_{x,\lambda,TaI,Ta2,HZ,t,r} = DN14^a_{x,\lambda,TaI,Ta2,HZ,t,r} - \sum_{n=0}^{n=3} G_I(DN14^a_{x0+n\cdot\delta,\lambda,TaI,Ta2,HZ,t,r})$$

for IR, where δ = the width of a quadrant (160 for full resolution images), and $x0 = x$ modulo δ , the position in the first quadrant corresponding to the position of x in the current quadrant. $G()$ is the ghost function, which is different for VNIR and IR but does not depend on frame rate or any other parameter. The coefficients in the ghost function $G()$ are given in a level 6 CDR named: CDR6_#_0000000000_GH_n_v.TAB.

The above functions define the ghost removal function $H()$, so that

$$DN14^b_{x,\lambda,TaV,HZ,t,r} = H(DN14^a_{x,\lambda,TaV,HZ,t,r}) \text{ for VNIR and}$$

$$DN14^b_{x,\lambda,TaI,Ta2,HZ,t,r} = H(DN14^a_{x,\lambda,TaI,Ta2,HZ,t,r}) \text{ for IR.}$$

Treatment of pixels flagged with 65535 in ghost removal correction:

As always, these pixels are passed on to the next step in the calibration algorithm with no processing. For the right hand side of the equation above, $DN14^a_{x0+n\cdot\delta,\lambda,TaI,Ta2,HZ,t,r}$ is set equal to zero, so these pixels have zero contribution.

2.5 Flag saturated pixels

Saturated pixels do not represent accurate data values, so we intended to flag them by replacing them with the value 65535. The saturated pixels are processed up to the level of the detector electronics ghost, because it is more accurate to apply the saturated value to the ghost correction than to apply zero.

The algorithm goes back to the raw images $DN_{x,\lambda,TaV,TaW,TaI,TaJ,Ta2,HZ,t,r}$ from the EDR and identifies any saturated pixel values. For those pixel coordinates (x, λ) , it then replaces the pixel value in $DN14^b_{x,\lambda,TaV,TaI,Ta2,HZ,t,r}$, the output of the detector quadrant ghost correction, with 65535. The algorithm is basically:

If ($DN_{x,\lambda,TaV,TaW,TaI,TaJ,Ta2,HZ,t,r}$ eq 4095) then $DN14^b_{x,\lambda,TaV,TaI,Ta2,HZ,t,r} = 65535$
 For 8-bit raw DN, use 255 instead of 4095. We call these “digital saturated pixels”.

In addition to the pixels with raw DN values pegged at 4095 (255 for 8-bit raw DN), some pixels with a smaller (but still high) value of raw DN are in a strongly nonlinear range of detector response. We call these “analog saturated pixels”. Again we have to go back to earlier data to correct current data. The analog saturated pixel criterion is based on bias-subtracted DN, so we

go back to the $DN14^a_{x,\lambda,TaV,TaI,Ta2,HZ,t,r}$ values to evaluate it, and we flag the $DN14^b_{x,\lambda,TaV,TaI,Ta2,HZ,t,r}$ values.

The analog saturated pixel removal function replaces $DN14^b_{x,\lambda,TaV,HZ,t,r}$ with the value 65535 if $DN14^a_{x,\lambda,TaV,HZ,t,r} > DN14^a_{\max V,x,HZ}$ for VNIR, and replaces $DN14^b_{x,\lambda,TaI,Ta2,HZ,t,r}$ with the value 65535 if $DN14^a_{x,\lambda,TaI,Ta2,HZ,t,r} > DN14^a_{\max I,x,HZ}$ for IR. The values $DN14^a_{\max V,x,HZ}$ and $DN14^a_{\max I,x,HZ}$ are given in the level 6 CDR named CDR6_1_0000000000_VL_n_v.TAB, where n=detector and v=version number. There are different values for different detector quadrants and frame rates, but the values are close for a given detector.

Note 4/14/2006: We have reviewed the analog saturated pixel values and determined the digital saturated pixel removal is redundant. Any digital saturated pixels will be removed by the analog saturated pixel step anyway. Since the digital saturated pixel removal step requires going back to the 12-bit or 8-bit DN, it is somewhat awkward to implement at this point in the algorithm and we have decided to drop it.

The function S() is defined as the function that flags the saturated pixels as described above.

$$DN14^c_{x,\lambda,TaI,Ta2,HZ,t,r} = S(DN14^b_{x,\lambda,TaV,TaI,Ta2,HZ,t,r}, DN14^a_{x,\lambda,TaV,TaI,Ta2,HZ,t,r}, DN_{x,\lambda,TaV,TaW,TaI,TaJ,Ta2,HZ,t,r})$$

Any pixels flagged with 65535 are not processed by any subsequent step in the calibration algorithm, but just passed on to the next step unchanged.

2.6 Apply a priori bad pixel mask to all images

The a priori bad pixel mask uses the bias, sphere, and background flight calibration images to calculate pixels that are potentially saturated in the scene or sphere image, dead, or excessively noisy in the scene or sphere image. These pixels are replaced by linear spatial interpolation from neighboring good pixels at the same wavelength.

The a priori bad pixel mask for each scene image is calculated entirely from calibration images and scene brightness models. In addition, at the end of the calibration an ex post facto bad pixel mask is calculated from the calibrated scene radiance image and applied to it. See section 2.15.

1. Noisy pixels. For each detector element (“pixel” for the current discussion, but this is a column and wavelength bin on the detector, *not* a spatial pixel on Mars which has multiple wavelengths), we take the standard deviation of the DN value in multiple nominally identical images, with the largest two and smallest two DN values thrown out. If that standard deviation is greater than 15 DN, the pixel is “bad”. This is calculated for each pixel within each EDR for all bias EDRs (multiple integration times for IR) including the sphere bias EDRs, and for all IR background EDRs, including those for the sphere EDRs. If a pixel is bad in even one of these EDRs, it is included in the bad pixel mask. Note the “bad pixel bias” EDRs are *not* used to calculate noisy pixels.
2. Dead pixels. Bias and background subtract are applied to sphere calibration images, and

any pixel that is <5% (this criterion is given in the VL CDR CDR6_1_0000000000_VL_n_0.TAB) of the median of its wavelength band is deemed “dead” and added to the bad pixel mask.

3. Potentially saturated pixels. The AS CDR CDR6_1_0000000000_AS_n_0.TAB contains a model of the maximum DN level expected from any scene image, and the same for any sphere calibration image. This was derived from models of the scene radiance, sphere radiance, and instrument responsivity, allowing for the integration times used in the different types of images. For sphere and scene, bias and dark current (for VNIR, dark current is assumed to be zero) calculated from the “bad pixel bias” EDRs is added to the AS CDR value. If the result exceeds 93% of the saturation value of the detector (the 93% criterion and the saturation values are given in the VL CDR), then that pixel is declared bad and added to the bad pixel mask. In practice, this is always due to excessive bias or dark current in a single pixel or a few pixels, not an excessively bright scene, and so applying the dark mask by replacing bad pixels with values interpolated from good neighboring pixels is appropriate.

Binning:

Noisy pixels are usually calculated from images with the same spatial binning as the scene. In cases where the noisy pixels are calculated from higher spatial resolution images (sphere biases, for example), the binned pixel is bad if any of the individual pixels are bad (“OR binning”). When dead pixels are binned, the binned pixel is bad only if all the individual pixels are bad (“AND binning”). Potentially saturated pixels are always calculated at the full spatial resolution of 640 columns. They are always OR binned. This is why a special “bad pixel bias” EDR or set of EDRs is defined, to ensure the potentially saturated pixels are always calculated at full resolution. The binning done in the CRISM electronics is at the digital level, and the binned pixel will have an inaccurate DN value if any of the sub-pixels are saturated. A detail: The “binning” done in the CRISM electronics is averaging, not summing.

The bad pixel masks are stored as images for each frame rate in the files named CDR4#ttttttttt_BPrbeewsn_v.IMG. The file CDR6_#_0000000000_PD_n_v.TAB contains a list of the bad pixel mask image CDR4 filenames. The bad pixel mask CDR for a scene image contains bad pixels for the ex post facto bad pixel correction as well as the a priori bad pixel correction.

In addition to the BP CDR written for the scene image, BP CDRs are also written for the bias, sphere, and background images that are written to the BI, SP, and BK CDRs respectively. They can be distinguished by the spacecraft clock value tttttttt in the filename. The value put in the BP CDR filename is the spacecraft clock value at the time the bias, sphere, or background EDR was taken. For the IR bias, there are several EDRs, and we use the midpoint of the EDRs for the spacecraft clock value. The bias BP CDRs flag only the noisy pixels for the given bias EDRs. The sphere BP CDRs flag the noisy, dead, and potentially saturated (for that sphere image, not for the scene) pixels for a given SP CDR. The BP CDRs written for the IR background images include all the a priori bad pixels for the scene image, except if there are noisy pixels in one background image that are not in the other, they will be in only one of the background BK CDRs. The set of pixels that are bad pixels in one or the other of the two BP CDRs for the background images that go with a scene gives the full set of a priori bad pixels applied to that

scene. Note this includes scene bias and scene background noisy pixels, dead pixels, and potentially saturated scene pixels. It does not include noisy and potentially saturated sphere pixels, which have been corrected in the sphere image, and the corrected values have been used to calibrate the scene image. If one wants to look at just the a priori bad pixel mask for the IR, one must use the background BP CDRs. The BP CDR for the scene itself also contains many bad pixels from the IR ex post facto bad pixel correction, described in section 2.15.

The a priori bad pixel mask is applied to an image by replacing each bad pixel with the average of the two pixels in adjacent columns (spatial pixels) in the same row (wavelength pixel). If two or more pixels in the same row and adjacent columns are bad, they are replaced using a linear interpolation of the two nearest good pixels in that row. The bad pixel mask is applied after bias subtraction and detector ghost removal.

Special cases:

1. When the bad pixel is the first or last column of the scene mask, so that the nearest neighbor on one side is not a scene pixel, the bad pixel will be replaced by the neighboring pixel in the adjacent column that is part of the scene, and the neighboring pixel not part of the scene will not be used. If two or more pixels in the same row and adjacent columns are bad, including the first or last column, they will be replaced by the nearest good pixel in that row.
2. When the bad pixel is in the stray light mask, it will not be used. If all of the stray light pixels in a given row are bad, then they are replaced by a linear interpolation of the two pixels in adjacent rows in the same column. If two or more stray light pixels in adjacent rows are bad, they will be replaced using a linear interpolation of the two nearest good pixels in that column. See section 2.10.

In the above rules, a “good” pixel is one not in the bad pixel mask and also with a value not equal to 65535.

The stray light mask defines columns close enough to the edge of the detector to be outside the image of the spectrometer entrance slit but far enough away from the edges of the detector to be unmasked. They sample any stray light that is uniform in character. The stray light pixels are defined as columns $x_1 \dots x_n$ and the values are as follows: 8-27, 4-13, 2-4, and 1 for the IR detector with 1x, 2x, 5x, and 10x binning respectively. For VNIR, there are stray light columns on both sides of the detector: 12-23 and 627-639 for 1x binning, 6-11 and 314-319 for 2x binning, 3 and 126-127 for 5x binning, and 1 and 63 for 10x binning. The values are given in a level 4 calibration data record (CDR) named CDR410000000000_DM0b000w0n_v.IMG, where b=binning, w=wavelength filter, n=detector, and v=version number.

Applying the calculations described in the calculation above is defined as $B()$, the bad pixel removal function, so we have

$$DN14^d_{x,\lambda,TaV,TaI,Ta2,HZ,t,r} = B_{x,\lambda,HZ}(DN14^c_{x,\lambda,TaV,TaI,Ta2,HZ,t,r})$$

The bad pixel mask is not applied to bias images written to the BI CDRs, because it is calculated from the bias images and applied after the bias subtraction. However, the sphere bad pixel mask, including noisy, dead, and saturated pixels, is applied to the sphere calibration images before the SP CDR is written. Likewise, the IR background bad pixel mask, including almost all the scene bad pixels, is applied to the background image before the BK CDR is written.

Each RDR generated from an EDR will have ancillary information that includes the name of the bad pixel mask CDR4 file used as part of the generation of that RDR, so users who wish to reject the bad pixels entirely have the information to do so. All of the bad pixels are flagged by this method. However, the calibration algorithm will replace the bad pixels with interpolated values, not reject them.

2.7 Detector average nonlinearity correction

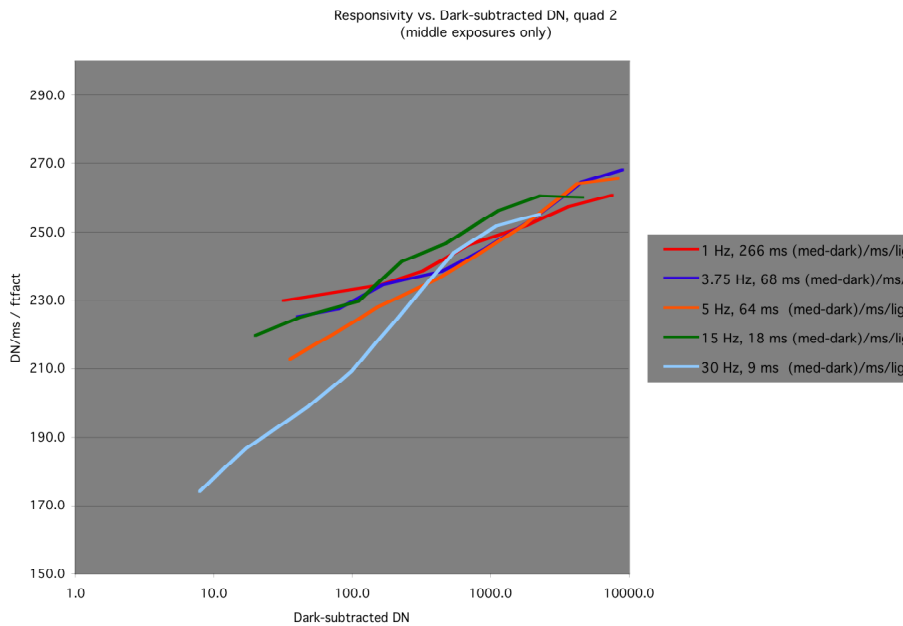
We use an empirical model of the detector nonlinearity to correct 14-bit DN to a signal related linearly to the sum of contributions from dark current, thermal background, scattered light, and scene imaged through the slit. This is a correction for nonlinearity in the responsivity of the instrument. The source of this nonlinearity is in the detector electronics, as part of the conversion of electrons to DN. We correct for the fact that conversion efficiency of electrons to DN increases with DN. The value of DN is converted back to what it would be in an idealized case with a constant number of electrons per DN. In detector level testing it was found that, on average, conversion efficiency varies nearly linearly with the logarithm of bias-corrected DN, and that the relationship differs slightly between frame rates. This gives the following model.

$$\text{Eff} = \text{DN} / (\text{Rate} \cdot t) = \varepsilon \cdot \log(\text{DN}) + \phi$$

where Eff is the detector conversion efficiency (DN/electrons) and Rate is the total rate of production of electrons, including source photons, background photons, and detector dark current but not including detector bias. The function $\log()$ is the natural or base-e logarithm. We calculate ε and ϕ from DN_{crs} , from images taken during spacecraft cruise before arrival at Mars. We used the spectrometer focal plane lamps as sources. We used different exposure times (t), and different lamp currents to give different electron production rates (Rate). The exposure times were known to high accuracy, and by comparing image DN for different exposure times and lamp currents, we were able to determine the relative value of (Rate) for each lamp current. Then, we used a linear fit to $y = \varepsilon \cdot x + \phi$ with $y = \text{DN}_{\text{crs}} / (\text{Rate} \cdot t)$ and $x = \log(\text{DN}_{\text{crs}})$ to give the nonlinearity parameters ε and ϕ .

The parameters ε and ϕ are calculated as averages over the whole detector and applied to the DN level on a pixel by pixel basis. Typically, we use benchtop detector data and DN_{gnd} is an average over a region with constant filter performance and constant illumination to sample constant DN. We can also use DN_{gnd} from data taken with the detector in the instrument, in which case it is generally an average over a row or a few rows to sample fairly constant DN. We assume that variations in the nonlinearity parameters from pixel to pixel within a row are small enough to be addressed in the flat field correction, as long as the flat field DN is roughly similar to the scene DN.

Note the calibration pipeline software does have the ability to assign different values of ϵ and ϕ for each pixel. For ϕ , this is equivalent to the standard flat field, which scales the image for each pixel. For ϵ , the flat field FF CDR has a second layer that includes values of ϵ that may be chosen independently for each pixel. As of 1/28/2009, the second layer of the FF CDR is all zeroes, and the only nonlinearity correction uses the same ϵ over the whole image. The flat field correction is described in more detail in Section 2.14.



Nonlinear relationship of responsivity to radiance level for VNIR, measured during detector-level testing.

Then, we use the values of ϵ and ϕ from the fit to convert our flight DN back to an idealized DN which would result from a linear response. That linearized DN is proportional to $(\text{Rad} \cdot t)$, so we solve for $(\text{Rad} \cdot t)$ in the model and our correction equation becomes

$$\text{DN14}^g_{x,\lambda,\text{TaI},\text{Ta2},\text{TaV},\text{Hz},t,r} = F_{\text{Hz}}(\text{DN14}^e_{x,\lambda,\text{TaI},\text{Ta2},\text{TaV},\text{Hz},t,r})$$

$$F_{\text{Hz}}(\text{DN14}^e_{x,\lambda,\text{TaI},\text{Ta2},\text{TaV},\text{Hz},t,r}) = \text{DN14}^e_{x,\lambda,\text{TaI},\text{Ta2},\text{TaV},\text{Hz},t,r} / (\epsilon_{\text{Hz}} \cdot \log(\text{DN14}^e_{x,\lambda,\text{TaI},\text{Ta2},\text{TaV},\text{Hz},t,r}) + \phi_{\text{Hz}})$$

where $\text{DN14}^f_{x,\lambda,\text{TaI},\text{Ta2},\text{TaV},\text{Hz},t,r}$ is the linearized DN for our actual flight data. The function $\log()$ is the natural or base-e logarithm. As shown, ϵ and ϕ are a function of frame rate. They are proportional to $(\text{Rate} \cdot t)$ but there's an arbitrary scaling factor. We scale them so that $F(1000)=1$. The coefficients ϵ and ϕ are given in a level 6 CDR named `CDR6_#_000000000000_LC_n_v.TAB` where n =sensor ID and v =version number.

2.8 Divide by integration time to get counts/second

$$\text{RT14}^g_{x,\lambda,\text{TaI},\text{Ta2},\text{TaV},\text{Hz},r} = \text{DN14}^g_{x,\lambda,\text{TaI},\text{Ta2},\text{TaV},\text{Hz},t,r} / t$$

The nomenclature RT denotes rate instead of DN for data number, and the integration time is omitted to indicate that the images are nominally independent of integration time, but the rest of the subscripts are kept the same. We use t in milliseconds, so the units of RT are counts/ms.

2.9 Background subtraction

The IR detector has dark current and is sensitive to IR background from the walls of the spectrometer. Now that the DN are bias-subtracted and linearized, this background must be subtracted before the scene images may be calibrated. The VNIR detector has no sensitivity to IR glow from the walls of the spectrometer, and at the -60° C operating temperature there is no significant dark current, so no background subtraction is necessary for the VNIR channel.

The background is most strongly influenced by changes in the temperature of the IR detector. A spectrometer housing temperature only 0.02° C different from the data being corrected, at relatively warm housing temperatures near -78° C, may result in a background at the longest IR wavelengths that is different by the noise-equivalent radiance. Originally, we had planned to interpolate the dark measurements using the measured spectrometer housing temperatures, but we do not expect the temperature sensors to be accurate enough. Therefore, the dark measurements are interpolated based on the time each was taken and the time of the image being background corrected. The value of t_{a1} is the mean value of encoded SCLK for that image specifically. It is derived from the instrument timetag value in the header of each image, calculated by the CRISM instrument clock, frequently updated by the spacecraft clock, and corrected using the partition number to be encoded SCLK instead of just SCLK. Calculations on a local computer may not have the SPICE information available to convert SCLK to encoded SCLK. One may use SCLK for this calculation as long as the partition number does not change. Just like for the temperatures, t_{a1} indicates timetag for the scene image, t_{d1} and t_{e1} the dark images, t_{b1} the bias images, and t_{c1} the calibration images.

The equation for background subtraction is

$$RT14_{x,\lambda,TaI,Ta2,HZ,r}^h = RT14_{x,\lambda,TaI,Ta2,HZ,ta1,r}^g - Bkgd_{x,\lambda,TdI,TeI,Td2,Te2,HZ,ta1,td1,te1}$$

with

$$Bkgd_{x,\lambda,TdI,TeI,Td2,Te2,HZ,ta1,td1,te1} = \left[1 / (t_{e1} - t_{d1}) \right] \cdot \left[RTD14_{x,\lambda,TdI,Td2,HZ,td1}^g \cdot (t_{e1} - t_{a1}) + RTD14_{x,\lambda,TeI,Te2,HZ,te1}^g \cdot (t_{a1} - t_{d1}) \right]$$

$$\text{and } RTD14_{x,\lambda,TdI,Td2,HZ,td1}^g = DND14_{x,\lambda,TdI,Td2,HZ,td}^g / t_d$$

for IR. The term $Bkgd_{x,\lambda,TdI,TeI,Td2,Te2,HZ,ta1,td1,te1}$ is simply an average of the dark measurements taken before and after the given scene measurement, weighted by the inverse of the time difference between each dark measurement and the given scene measurement.

The term $RTD14_{x,\lambda,TdI,Td2,HZ,td1}^g$ is simply the 14-bit DN/second for the dark measurement taken

before the measurement being background-subtracted, the superscript g indicating that it has gone through the same set of corrections as the measurement being background-subtracted. The variable t_d is the integration time for that particular dark measurement.

The images $DND14^g_{x,\lambda,TdI,Td2,HZ,t_d}$ are stored as level 4 calibration data records (CDRs) named $CDR4\#tttttttt_BKrbeeewsl_v.IMG$, where $\#$ =spacecraft time SCLK partition at the beginning of validity of the CDR, $tttttttt$ =spacecraft time SCLK at the beginning of validity of the CDR, r =frame rate, b =binning, eee =exposure time parameter, w =wavelength filter, $s=0$, L =detector (IR), and v =version number. The integration time t_d , used to calculate $RTD14^g_{x,\lambda,TdI,Td2,HZ,t_d}$ from $DND14^g_{x,\lambda,TdI,Td2,HZ,t_d}$, may be calculated from the integration time parameter in the label file $CDR4\#tttttttt_BKrbeeewsl_v.LBL$ that goes with the .IMG file containing the $DND14^g_{x,\lambda,TdI,Td2,HZ,t_d}$ images.

For VNIR, there's no background correction, so it's just

$$RT14^h_{x,\lambda,TaV,HZ,r} = RT14^g_{x,\lambda,TaV,HZ,r}$$

2.10 Scattered light correction

CRISM has two known significant sources of optical stray light that must be removed during the correction of spectrally dispersed light, that is, an integrating sphere measurement to a responsivity correction or a Mars scene to radiance:

- Scatter from optical elements in the spectrometer scatters light and the spatial direction x and the wavelength direction λ . This is measured directly by the unmasked pixels to the side of the slit image. The contribution to scattered light resembles glare and is not in focus. This scattered light is stronger at shorter wavelengths, and an explicit correction is made only for VNIR. For IR, a small correction is included implicitly in the radiance calibration SS CDR.
- Second order light (source wavelength $\lambda/2$) leaks through zone 3 of the order sorting filter at $\lambda=2760-3960$ nm, and an apparent optical ghost with source wavelength near $\lambda/1.8$ occurs in a narrow range of λ near 2400 nm. The optical ghost is small, and it has not been detected in flight data, only in laboratory data. It is not corrected. The second order light occurs only in the IR, and an explicit correction is made.

The scattered light pixels are columns close enough to the edge of the detector to be outside the image of the spectrometer entrance slit but far enough away from the edges of the detector to be unmasked. They sample any stray light that is uniform in character. The stray light pixels are defined as columns $x_1 \dots x_n$ and the values are as follows: 8-27, 4-13, 2-4, and 1 for the IR detector with 1x, 2x, 5x, and 10x binning respectively. Note the IR stray light pixels are not used in the calibration algorithm. For VNIR, there were originally stray light columns on both sides of the detector, but only one side is used: 630-639 for 1x binning, 315-319 for 2x binning, 126-127 for 5x binning, and 63 for 10x binning. The VNIR stray light pixels are used in the calibration algorithm. These values are given in a level 4 calibration data record (CDR) named $CDR4\#0000000000_DMrbeeewsn_v.IMG$, where $\#$ =spacecraft time SCLK partition at the

beginning of validity of the CDR, tttttttt=spacecraft time, r=frame rate, b=binning, eee=exposure time parameter, w=wavelength filter s=0, n=detector, and v=version number.

The scattered light is corrected for a VNIR pixel by estimating the scattered light from the other pixels in the same frame (note a frame is column x wavelength for a single line of the Mars image) and subtracting that estimated scattered light.

There are several possible straightforward methods to estimate the VNIR scattered light:

1. Simply take an average value in the stray light pixels for each wavelength band in a frame and subtract it from the pixel in every column for that wavelength band in that frame. This technique would be accurate in theory if the scattered light were perfectly uniform with radiance independent of angle, like a Lambertian surface. In this case the stray light pixels would accurately monitor the same amount of scattered light as the pixels in the image at each wavelength. However, in practice this method is inaccurate because scattered light is peaked with scattering angle. The function varies but usually is close to an inverse power of the scattering angle, often the inverse square of the scattering angle. This causes two problems with just subtracting the stray light pixel.
 - a. The scene is not uniform with column number, and pixels with other bright pixels nearby have more scattered light than pixels with only dim pixels nearby. One scattered light value for a wavelength bin can't cover all the columns.
 - b. The scattered light pixels are on the edge of the detector and so they only get scattered light from one side, while scene pixels near the center of the detector get scattered light from both sides. In practice, for a uniformly bright scene, all scene pixels except those very close to the edge of the detector have scattered light of more than twice that recorded by the stray light pixels. Whether it's 2x, 2.5x, or 3x depends on how many stray light pixels are included in the average. The stray light pixels further away from the illuminated scene and closer to the edge of the detector have lower signal and a larger factor must be used if they are included.
2. The VNIR bands go down to very short wavelength, where the already dim direct signal is further reduced by a cut-on order sorting filter, leaving only the scattered light coming from longer wavelengths. The nominal wavelength of VNIR band 0 for CRISM multispectral mapping images (band 2 for hyperspectral images) is 378 nm. The short-wavelength CRISM VNIR order sorting filter is made of Schott glass GG375, with nominal cut-on longward of 375 nm. For each CRISM frame, one can simply take the multispectral band 0 value (or the mean of bands 1-3 for hyperspectral images) and subtract it from all the pixels in that frame in the same column. This method samples the variation in stray light with column number. However, it suffers from the following problems.
 - a. The stray light varies with wavelength, because the image brightness varies with wavelength and the stray light is locally peaked. Therefore, the scattered light sampled by multispectral band 0 is generally smaller overall than the scattered light in the rest of the frame.
 - b. Different parts of the scene can have considerably different spectra. For example, dust and rocks are reddish and ice is white. For frames with some columns of ice and some columns of rock, even the relative values of the scattered light in

different columns of multispectral band 0 don't accurately measure the relative values of the scattered light in different columns of the longer wavelengths.

3. Except for the very edges of the detector, the source of the scattered light in a frame is well sampled by the frame itself, because the scattered light is locally peaked. One could simply model the scattered light by convolving each single VNIR CRISM frame with a scattering function, derived from lab data, representing the approximately inverse theta squared dependence of the scattered light for large scattering angle theta. The scattering function would have an approximately inverse lambda squared dependence on the source wavelength. Because the CRISM dichroic beamsplitter is an important source of scattered light and it's tilted, the scattering function may be anamorphic (have a different scaling in the spatial direction and wavelength direction). The scattering function would be smoothed and capped at small values of theta corresponding to just a few pixels away from the pixel being corrected, because the purpose of the correction is to correct scattered light, not alter the point spread function of the instrument. This method is accurate in theory, and does not require the scattered light pixels. However, we were concerned about the following possible problems.
 - a. If the scattering function is not accurate, artifacts might be generated in the scene images. For example, if the scattered light is overcorrected at smaller angles and undercorrected at larger angles, one might see a dark and then bright band next to a bright/dark boundary in a scene. Note that such an artifact would be introduced only in the cross-track direction in a Mars image, because the correction is applied independently to each detector frame, corresponding to a single line in the Mars image.
 - b. This method uses all the pixels in a given frame to calculate one pixel, so it is more computationally intensive than other calculations in the calibration algorithm.

The production scattered light subtraction algorithm incorporates elements of method 3, but we did not try the straightforward and naïve method 3 as described above. It might be interesting to do a trial with method 3 to see if the VNIR scattered light subtraction algorithm could be simplified, but the existing method, although complicated, works very well.

We started with method 1, simple subtraction of the stray light pixel. Then, discovering the scattered light was undersubtracted, we scaled it by a factor of 2. Then, it became clear the subtraction was inaccurate for nonuniform scenes, and we scaled the value in the stray light pixel for each band with the signal in multispectral band 0 (bands 1-3 for hyperspectral) relative to the stray light pixel in multispectral band 0.

This hybrid version of methods 1 and 2 was not working for scenes that had both rock and ice and it didn't account well for spectral smile, so for longer wavelength bands the scattered light function for each band was further scaled to a convolution of an empirical scattering function, optimized to minimize artifacts in nonuniform Mars scenes, with the brightness of the pixels in the columns of that band (approximating the brightness of the source of scattered light). This differs from method 3 in that it's just a one-dimensional convolution, limited to the pixels in a single band, rather than using the pixels in the entire frame. Although multispectral band 0 was still explicitly in the algorithm, for the longer wavelength bands the scaling effectively replaced

it with the convolution of the band being corrected with the one-dimensional scattering function.

The resulting method was fairly effective, but in scenes that had ice near the stray light pixels, the spectrum of the scattered light subtraction was the spectrum of the ice, which was not appropriate for the rock areas of scenes with mixed ice and rock. Therefore, the stray light pixels were corrected by dividing by the mean of scene pixels near the edge where the stray light pixels were located. This resulted in realistic VNIR spectra of both rock and ice, even in mixed ice-rock scenes, and the spectra were insensitive to whether there was rock or ice near the stray light pixel. Obvious artifacts were dramatically reduced from uncorrected spectra.

The VNIR scattered light algorithm explicitly uses the following data:

- A. The scattered light pixels in each band
- B. Multispectral band 0 (bands 1-3 for hyperspectral)
- C. The scene pixels in each band convolved with a one-dimensional scattering function
- D. Scene pixels near the edge of the detector close to the scattered light pixel in each band

The exact parameters of the algorithm were determined by much empirical optimization on CRISM target mode and mapping mode scenes, but there was not much analysis of the meaning of layering the different corrections on top of each other. The algorithm as implemented is effectively method 2 scaled with wavelength by method 1 at the short wavelengths, and it is my feeling (D. Humm, 12/23/2008) that it is effectively method 3 at the long wavelengths, except it uses a 1-dimensional scattering function instead of the actual 2-dimensional scattering function. At the long wavelengths, the scattered light pixel wavelength dependence is effectively canceled out by ratioing it to the average of nearby scene pixels, and the multispectral band 0 spatial function is effectively canceled out by scaling it to the convolved scene pixels in the band being corrected. Although the relative wavelength and spatial dependence of methods 1 and 2 are canceled out, they still contribute an overall scaling factor to the calculated scattered light.

The equation for VNIR scattered light correction is different for short and long wavelengths. Note the brackets $\langle \rangle$ in the equations below all refer to taking a simple mean over some range of columns.

For detector rows 185-215 (roughly, $\lambda < 563$ nm)

$$RT14^i_{x,\lambda,TaV,TaI,Ta2,HZ,r} = RT14^h_{x,\lambda,TaV,TaI,Ta2,HZ,r} - \langle RT14^h_{x1 \dots xn,\lambda,TaV,TaI,Ta2,HZ,r} \rangle \cdot SW^h_{x,\lambda,TaV,TaI,Ta2,HZ}$$

$$where \quad SW^h_{x,\lambda,TaV,TaI,Ta2,HZ} = RT14^h_{x,\lambda_0,TaV,TaI,Ta2,HZ,r} / \langle RT14^h_{x1 \dots xn,\lambda_0,TaV,TaI,Ta2,HZ,r} \rangle$$

with λ_0 corresponding to detector row 187 (roughly $\lambda = 378$ nm) and $x_1 \dots x_n$ the stray light columns (630-639 for 1x binning, 315-319 for 2x binning, 126-127 for 5x binning, and 63 for 10x binning, given in the DM CDR). Note that for hyperspectral images, a mean of the stray light columns in detector rows 186, 187, and 188 is taken instead of just row 187.

This is the hybrid of methods 1 and 2, taking the scattered light function from a short-wavelength row and scaling it to the value of the scattered light pixel in the row being corrected.

For detector rows 216-291 (roughly, $\lambda > 563$ nm)

$$RT14^i_{x,\lambda,TaV,TaI,Ta2,HZ,r} = RT14^h_{x,\lambda,TaV,TaI,Ta2,HZ,r} - \langle RT14^h_{x1 \dots xn,\lambda,TaV,TaI,Ta2,HZ,r} \rangle \cdot CS^h_{x,\lambda,TaV,TaI,Ta2,HZ}$$

where

$$CS_{x,\lambda,TaV,TaI,Ta2,HZ}^h = SW_{x,TaV,TaI,Ta2,HZ}^h \cdot (CB_{x,\lambda,TaV,TaI,Ta2,HZ,r}^h / CB_{x,\lambda_0,TaV,TaI,Ta2,HZ,r}^h) \cdot (<SW_{x1\dots xm,TaV,TaI,Ta2,HZ,r}^h> / <RT14_{x1\dots xm,\lambda,TaV,TaI,Ta2,HZ,r}^h>)$$

and

$$CB_{x,\lambda,TaV,TaI,Ta2,HZ,r}^h = \sum_k RT14_{xk,\lambda,TaV,TaI,Ta2,HZ,r}^h \cdot B_x / (1 + ((x-x_k) / 10)^2)$$

with

$$B_x = 1 / (\sum_k 1 / (1 + ((x-x_k) \cdot \text{binning} / 10)^2))$$

$CB_{x,\lambda,TaV,TaI,Ta2,HZ,r}^h$ is just the convolution of a single band in a single frame with the function $1 / (1 + ((x-x_k) \cdot \text{binning} / 10)^2)$, and B_x is the normalization factor for that function. The columns $x_1 \dots x_m$ are the scene full-resolution columns 540-619 (columns 270-309 for 2x binning, 108-123 for 5x, and 54-61 for 10x) near the stray light pixels, and $[(x-x_k) \cdot \text{binning}]$ is the number of columns from x_k to x in full-resolution, unbinned pixel units. The symbol \sum_k indicates a sum over scene columns only, not including the extra stray light and dark columns at the edge of the detector. Note the normalization factor B_x depends on x because it depends on how close x is to the edge of the scene.

This is the more complex correction that attempts to mimic method 3 without having to use all the detector rows of a frame to correct just one row. The factor $(CB_{x,\lambda,TaV,TaI,Ta2,HZ,r}^h / CB_{x,\lambda_0,TaV,TaI,Ta2,HZ,r}^h)$ changes the relative value of the scattered light subtraction from the $SW_{x,TaV,TaI,Ta2,HZ,r}^h$ value valid at short wavelengths to the $CB_{x,\lambda,TaV,TaI,Ta2,HZ,r}^h$ value valid at long wavelengths. The factor $(<SW_{x1\dots xm,TaV,TaI,Ta2,HZ,r}^h> / <RT14_{x1\dots xm,\lambda,TaV,TaI,Ta2,HZ,r}^h>)$ then more or less divides out the wavelength dependence of the stray light pixel, using the scene pixels near the stray light pixel as a proxy for the stray light pixel. The resulting relative spatial and spectral function for scattered light subtraction at long wavelengths pretty much all derives from $CB_{x,\lambda,TaV,TaI,Ta2,HZ,r}^h$, and the $<RT14_{x1\dots xn,\lambda,TaV,TaI,Ta2,HZ,r}^h> \cdot SW_{x,TaV,TaI,Ta2,HZ,r}^h$ factor used at short wavelengths only affects the overall scale of the correction at long wavelengths.

A special case:

Multispectral images with spacecraft clock SCLK<850327000 (transition orbit and earlier) were taken with a different wavelength table, and those images do not have detector row 187. In that case,

$$SW_{x,TaV,TaI,Ta2,HZ}^h = SW_x^h$$

where SW_x^h gives the ratio of response of detector row 187 to response of the mean of the stray light pixels in detector row 187 for a uniform scene. SW_x^h is read from the level 4 calibration data record (CDR) named CDR410000000000_SCRb000wsS_v.IMG, where r=frame rate, b=binning, w=wavelength filter s=0, and v=version number. For detector rows 216-291, the formula for scattered light subtraction is unchanged. One just substitutes the new value of $SW_{x,TaV,TaI,Ta2,HZ}^h$. This algorithm isn't very sensitive to $SW_{x,TaV,TaI,Ta2,HZ}^h$ anyway, except for overall normalization. For detector rows 185-215, the algorithm changes to one similar to that used at longer wavelengths.

For multispectral images with SCLK<85032700, detector rows 185-216 (roughly, $\lambda < 563$ nm), the scattered light subtraction formula is

$$RT14_{x,\lambda,TaV,TaI,Ta2,HZ,r}^h = RT14_{x,\lambda,TaV,TaI,Ta2,HZ,r}^h - <RT14_{x1\dots xn,\lambda,TaV,TaI,Ta2,HZ,r}^h> \cdot CS_{x,TaV,TaI,Ta2,HZ}^h$$

where

$$CS_{x,TaV,TaI,Ta2,HZ}^h = SW_{x,TaV,TaI,Ta2,HZ}^h \cdot (CB_{x,\lambda,TaV,TaI,Ta2,HZ,r}^h / CB_{x,\lambda_0,TaV,TaI,Ta2,HZ,r}^h)$$

$$\cdot (\langle \text{SW}^h_{x1 \dots xm, \text{TaV}, \text{TaI}, \text{Ta2}, \text{Hz}, r} \rangle / \langle \text{RT14}^h_{x1 \dots xm, \lambda_1, \text{TaV}, \text{TaI}, \text{Ta2}, \text{Hz}, r} \rangle)$$

This is the same as used at longer wavelengths, except CS is no longer a function of wavelength λ , because CB and RT14 are evaluated at wavelength band λ_1 instead of λ . Wavelength band λ_1 is defined as the shortest wavelength (smallest detector row number) greater than or equal to detector row 216, the first detector row that uses the long wavelength scattered light subtraction formula. This is the wavelength where the short and long wavelength scattered light subtraction methods match most closely, so it's the best place to estimate the value of the short wavelength scattered light when we are missing detector row 187. Typically, detector row 221 (approx 599 nm) is the shortest multispectral wavelength matching this criterion.

The fact that the above procedure works, with CS independent of wavelength at shorter wavelengths and a function of wavelength at longer wavelengths gives a window into why there are two different wavelength regions of scattered light behavior for the VNIR. The scattered light function is peaked and the source is much brighter at longer wavelengths. At short wavelengths, the spatial shape of the scattered light function is relatively independent of wavelength because the scattered light is mostly coming from the slowly varying tails of functions that are peaked at long wavelengths. At long wavelengths, the spatial shape of the scattered light function changes with wavelength because the scattered light is mostly coming from nearby wavelengths and one is close to the peak of the scattered light function. This tends to bring out changes in the spatial shape of scattered light due to scene nonuniformity and spectral smile.

If a pixel in one of the scattered light columns has the value 65535, is in the bad pixel mask, or is identified as one of the cosmic ray pixels, that pixel is not used. If all the scattered light columns in a given row are bad, the scattered light column value is filled in by linear interpolation of the nearest good rows.

2.11 Subtraction of second-order stray light

The CRISM IR channel has considerable second order light (source wavelength $\lambda/2$) from the grating at $\lambda=2760\text{-}3960$ nm. This stray light is sampled by detector pixels inside the focal plane at the source wavelengths for a given frame of (x, λ) , so it is subtracted just by defining a matrix containing the row number of the source of second order light for each detector row that contains scattered light, and another matrix defining the ratio of second order stray light signal to source signal. That ratio is measured using a monochromator in ground calibration. Interpolated values are used for columns not illuminated in that test. The second order light in a single pixel should come from at most two pixels near $\lambda/2$, but to be safe we define 6 row numbers which might all contribute to the stray light for a given pixel. We assume the second order light is translated directly along the columns of the detector, which is not exactly correct (there is some keystone which moves the second order light slightly from the source column) but should be good enough for stray light subtraction. The row number images $y_{x, \lambda, n, \text{Hz}}$ with $n=1\text{-}6$ give the detector row numbers of the 6 rows that are second order light sources for each detector pixel. The coefficient images $\kappa_{x, \lambda, n, \text{Hz}}$ with $n=1\text{-}6$ give the fraction of the direct signal from detector pixel $(x, y_{x, \lambda, n, \text{Hz}})$ contributed to detector pixel (x, λ) . Then, the stray light is subtracted by the formula

$$RT14_{x,\lambda,TaI,Ta2,HZ,r}^i = RT14_{x,\lambda,TaI,Ta2,HZ,r}^i - \sum_{n=1}^{n=6} \kappa_{x,\lambda,n,HZ} \cdot RT14_{x,\lambda',yn,HZ,TaI,Ta2,HZ,r}^i$$

for the IR. For the VNIR, this correction is not necessary, and the formula is just

$$RT14_{x,\lambda,TaV,HZ,r}^i = RT14_{x,\lambda,TaV,HZ,r}^i$$

The calculation of the y images is to use only the closest wavelengths shorter and longer than $\lambda/2$, calculated from the production WA CDRs. Detector rows 332-355 (wavelengths approximately 1744-1592 nm) are excluded as source rows because the zone 1/zone 2 order sorting filter boundary causes them to be inaccurately sampled. Note that for wavelengths in hyperspectral images outside this range (3184-3488 nm for the pixels being corrected), the wavelengths are densely sampled near $\lambda/2$. For the multispectral images and the hyperspectral images 3184-3488 nm, the wavelengths may be sparsely sampled near $\lambda/2$, and the correction will not be as accurate.

The κ values are derived from laboratory monochromator data on the second-order light contamination. The coefficient values are weighted to apply linear interpolation in wavelength between the detector rows with closest wavelength shorter and longer than $\lambda/2$, as given in the y images, to an effective value at $\lambda/2$.

These images are stored as level 4 calibration data records (CDRs) named CDR4#0000000000_LLrbeeewsn_v.IMG, where r=frame rate, b=binning, eee=exposure time parameter, w=wavelength filter, s=1 or 2 depending on whether side 1 or 2 lamps are used, n=detector, and v=version number. The LL CDRs have the 6 y images and the 6 κ images interleaved, starting with the n=1 y image, then the n=1 κ image, then the n=2 y image, etc.

If any pixels in the sum $\sum_{n=1}^{n=4} \kappa_{x,\lambda,n,HZ} \cdot RT14_{x,\lambda',yn,HZ,TaI,Ta2,HZ,r}^i$ have the value 65535.0, they are treated as being zero for the purposes of this calculation.

2.12 Correction of instrument responsivity for detector temperature

Responsivity as a function of wavelength results from three effects:

- The instrument design including telescope design, efficiency of optical elements, and quantum efficiency of the detectors.
- Variations in detector responsivity as a function of detector temperature. The main effects are a shift in the long wavelength edge for the VNIR detector, and a movement in the interference fringes that appear on the long wavelength end of the IR detector.
- Accumulation of absorbing contaminants on optical surface. The major expected contaminant is water ice on the detector.

CRISM's responsivity is tracked in flight using the internal integrating sphere, run under closed

loop control, using either bulb. This provides a field- and aperture-filling source with stable radiance. The current plan is to take sphere calibration measurements with one lamp within a few minutes of every scene measurement, and take calibration measurements with the other lamp once a month to check the first lamp. The sphere calibration may also be checked with images from Deimos when available. The calibration is not expected to be a function of integration time or frame rate, and all of the sphere calibration images are taken at 1 Hz.

The instrument responsivity is the ratio of the DN from the in-flight sphere data, corrected for bias, background, nonlinearity, stray light etc. in the same way the as scene data, to the sphere radiance, measured on the ground and corrected to a value appropriate to the in-flight sphere data. The calculation of instrument responsivity at the time and temperatures of the in-flight sphere radiometric calibration is described in Section 3.5. The responsivity in DN/ms/(W/(m² micrometer sr)) is $RSP_{x,\lambda,TcV,TcI,Tc2}^j$.

To apply that responsivity to a scene image to calculate radiance at the instrument aperture, we must first correct it for the instrument temperatures in effect during the scene measurement. The algorithm includes corrections for the detector temperatures T_{aV} and T_{aI} . It is possible the spectrometer temperature T_{a2} could also affect the responsivity by shifting the beamsplitter reflectivity and transmission in wavelength. In Section 3.4, this is discussed regarding the radiometric calibration itself, and we believe we will be taking radiometric calibration data close enough in time to the scene data that this effect will be the same in both. In other words, $T_{a2}=T_{c2}$ to the accuracy required by the beamsplitter effect.

As of 12/30/2008, the responsivity correction for detector temperature is not applied either for VNIR or IR images. In both cases, the calibration software does the calculation, but the correction is zero.

The equation to correct the responsivity for detector temperature is

$$RSP_{x,\lambda,TaV,Ta2}^k = RSP_{x,\lambda,TcV,Tc2}^j \cdot (\mu_{x,\lambda} + \nu_{x,\lambda} \cdot T_{aV} + \pi_{x,\lambda} \cdot T_{aV}^2) / (\mu_{x,\lambda} + \nu_{x,\lambda} \cdot T_{cV} + \pi_{x,\lambda} \cdot T_{cV}^2)$$

for VNIR, where $(\mu_{x,\lambda} + \nu_{x,\lambda} \cdot T_{aV} + \pi_{x,\lambda} \cdot T_{aV}^2)$ is a model of relative responsivity at each element x,λ as a function of detector temperature T_{aV} . The quadratic functions are sufficiently accurate over the range of temperatures expected, about 2° C for the VNIR detector. If the temperature ranges are larger, they could be replaced with more descriptive functions, which would probably be $(1+\tanh())$ for the VNIR.

The coefficient matrices $\mu_{x,\lambda}$, $\nu_{x,\lambda}$, and $\pi_{x,\lambda}$ are stored as a level 4 calibration data record (CDR) named CDR4#0000000000_TDrbeewsS_v.IMG, where r=frame rate=0, b=binning=0, eee=exposure time parameter, w=wavelength filter, s=0, S=VNIR detector, and v=version number. Note that as of 12/30/2008, $\mu_{x,\lambda}=1$, $\nu_{x,\lambda}=0$, and $\pi_{x,\lambda}=0$ in the TD CDR, so no correction is applied.

For IR, instead of explicitly temperature correcting a single responsivity measurement, we calculate the responsivity twice using two flight sphere calibration measurements, one dayside and one nightside. We then linearly interpolate in IR detector temperature between those two

responsivity images to get the temperature-corrected IR responsivity. For IR

$$RSP_{x,\lambda,Ta1,Ta2}^k = (RSP_{x,\lambda,Tcl,Tc2}^j \cdot (T_{a1} - T_{fl}) + RSP_{x,\lambda,Tfl,Tf2}^j \cdot (T_{cl} - T_{a1})) / (T_{cl} - T_{fl})$$

where T_{cl} and T_{fl} are the IR detector temperatures for the dayside and nightside sphere calibrations respectively. IR detector temperature 2 is the sensor specified in the software. As of 12/30/2008, the “dayside” and “nightside” sphere calibration measurements specified in the calibration pipeline are always the same sphere image, generally the one closest in time to the scene image, so the detector temperature interpolation is not applied.

As of 12/30/2008, the responsivity correction for detector temperature is not applied for either VNIR or IR images. In both cases, the calibration software does the calculation, but the correction is zero. For the VNIR, the relevant values in the TD CDR were zero. It was determined that the correction was small and the values obtained from ground calibration not highly accurate, so we decided not to apply the correction. For IR, two sphere calibrations are specified in the software, but the tables generated always use just the single sphere calibration closest in time twice, so the interpolation with detector temperature does not get applied. It is possible the use of two sphere calibrations as described below might reduce Fabry-Perot fringing at long wavelengths of the detector, but we were concerned about introducing additional noise by using the second sphere calibration.

2.13 Apply binning and detector masks to responsivity

This step is trivial, because we do not expect binning to affect the responsivity. For pixels defined as “scene” pixels in the detector mask CDR, the responsivity of a binned pixel is just the mean of the responsivity of the detector elements in that bin.

Pixels not defined as “scene” pixels in the detector mask CDR have their values replaced by 65535 at this point. This includes dark and scattered light pixels. The number of columns in the responsivity image after this step is 640/binning, where binning is 1, 2, 5, or 10. At this point, we also apply the wavelength table to the responsivity, by simply selecting out the responsivity values at each wavelength present in the table and throwing away the rest. The number of rows in the responsivity image after this step is just the number of active rows in the wavelength table.

The binned responsivity is called $RSP_{x,\lambda,TaV,Ta1,Ta2,HZ}^l$.

The detector masks are given in level 4 calibration data records (CDRs) named CDR4#0000000000_DMrbeewsn_v.IMG, where r=frame rate, b=binning, eee=0, w=wavelength filter, s=0, n=detector, and v=version number. Each detector mask consists of an image of 8-bit integers, with the individual bits set equal to 1 for different masks. Bits 0,1,2,3,4,5,6,7 represent no data, scene, dark, dark/scatter transition, scattered light, scatter/scene transition, scene/dark transition, and row 0 respectively. For example, when bit 1 is 1, the pixel is a scene pixel, and when bit 1 is 0, the pixel is not a scene pixel.

The wavelength tables are implicit in the detector masks, because scene pixels in rows that are

used have bit 1 set equal to 1 while all pixels in rows that are not used have bit 0 set equal to 1. However, the wavelength tables are also given in the level 6 CDR named CDR6_0000000000_WV_n_v.TAB, where n=sensor ID and v=version number. In these tables, a 1 indicates the row is used, and a 0 indicates the row is not used.

2.14 Calculate scene radiance at instrument aperture and divide by flat field

Again this is trivial now that we have gone through all the correction steps. The spectral radiance $RD_{x,\lambda,r}^m$ is just the count rate divided by the instrument responsivity and the flat field $FF_{x,\lambda}$. The flat field is just the image of an external flat field with the scene pixels in each row normalized to average to 1.

$$RD_{x,\lambda,r}^m = RT_{x,\lambda,TaV,TaI,Ta2,HZ,r}^j / (FF_{x,\lambda,HZ} \cdot RSP_{x,\lambda,TaV,TaI,Ta2,HZ}^l)$$

$$FF_{x,\lambda,HZ} = FL_{x,\lambda,HZ} + EP_{x,\lambda,HZ} \cdot \log(RT_{x,\lambda,TaV,TaI,Ta2,HZ,r}^j / RSP_{x,\lambda,TaV,TaI,Ta2,HZ}^l)$$

The units of $RD_{x,\lambda,r}^m$ are W/(m² micrometer sr). As of 1/28/2009, $EP_{x,\lambda,HZ}$ is zero, so it is a straight flat field with no allowance for pixel-dependent nonlinearity.

The flat field $FL_{x,\lambda,HZ}$ is given in layer 0 of the flight level 4 calibration data records (CDRs) named CDR4#ttttttttt_NUrbeewsd_v.IMG, where #=spacecraft time SCLK partition at the beginning of validity of the CDR, tttttttt=spacecraft time SCLK at the beginning of validity of the CDR, r=frame rate, b=binning, eee=exposure time parameter, w=wavelength filter, s=sphere lamp used to calibrate the flat field scenes (see section 3.3), d=detector, and v=version number. Unlike the rest of the flight CDR4s, which are generated automatically by the pipeline software, the NU CDR is generated periodically by the science team, based on averages of images of a featureless area of Mars. The IR flat fields are set equal to 1 in some bands, where the interaction of sharp atmospheric features with instrument smile makes the flat-fielding unreliable. The generation of the NU CDRs is described in section 3.3.

The pixel-dependent nonlinearity parameter $EP_{x,\lambda,HZ}$ is given in layer 1 of the NU CDRs. This allows one to apply a different linearizing function for different pixels, using the same form of the nonlinearity as applied to the entire detector using average values of the nonlinearity parameters in Section 2.7. Instead of pixel-dependent nonlinearity, one could equally well call this a brightness-dependent flat field. The function log() is the natural or base-e logarithm. As of 1/28/2009, $EP_{x,\lambda,HZ}$ is always zero in all the NU CDRs, so the pixel-dependent nonlinearity correction is not applied.

2.15 Ex post facto bad pixel removal and apply detector masks

VNIR images generally have no bad pixels except for a single dead detector pixel in the full-resolution, hyperspectral mode.

IR image cubes, on the other hand, have many noisy pixels. Some detector pixels are always

noisy, some are noisy for a time encompassing several image cubes, and some are noisy for a time period within an image cube. It's useful to assign bad detector pixels from the bias images (generally taken within a week of the scene) to filter out pixels that are saturated or always noisy, and bad pixels from the dark images (taken within 5 minutes of a scene) to filter out pixels that are noisy for several minutes. However, pixels that become noisy after the first dark calibration image is taken and before the start of the second dark calibration image aren't captured by this "a priori" bad pixel mask. Also, the "a priori" mask throws out the brightest two and dimmest two values when it calculates standard deviations on nominally identical images. A pixel has to be **really** noisy to be included in the "a priori" mask.

The result is that the IR image cubes still have many noisy pixels even after the "a priori" bad pixel mask is applied. The images benefit greatly from identification of bad pixels using the processed image itself, and interpolation over those bad pixels. This is an "ex post facto" bad pixel removal, because it uses only the scene image cube itself to identify bad pixels, which are then interpolated over in the scene image cube. The "a priori" bad pixel algorithm used only calibration images to identify bad pixels, which are then interpolated over in the scene image cube.

The ex post facto bad pixel map is calculated entirely from a single frame equal to the mean of all the lines in the image cube. A frame has spatial columns as the x coordinate and wavelength bands as the y coordinate. For this purpose, the content of the image cube in the spacecraft downtrack direction is averaged out. Now, construct a "filtered mean frame" by filtering each wavelength band of that frame with a moving 7-element median in the spatial (i.e. crosstrack or column) direction. The 7-element median is used for full resolution images. For half-resolution images, we use a 5-element median. We use a 3-element median for 5x and 10x binned images. Now, define the "difference frame" as the difference of the mean frame and the filtered mean frame. For each wavelength band of the difference frame, calculate the standard deviation over the entire crosstrack scene. If the absolute value of a pixel of the difference frame is greater than 2.4 times the standard deviation for that pixel's band, then that pixel is "ex post facto" bad. Bad pixels are replaced by linear interpolation from nearest neighbor columns just like for the "a priori" bad pixel map. The BP CDR for the scene includes all the "a priori" bad pixels and all the "ex post facto" bad pixels. See section 2.6.

The bad pixels have now been replaced by interpolation. In addition, pixels from the edge of the detector ("non-scene" pixels) do not correctly represent the scene and are replaced with the value 65535 in this last step. The function $M_{x,\lambda,HZ}()$ applies the IR ex post facto bad pixel correction described above, and also replaces the non-scene pixels with 65535.

$$RD_{x,\lambda,r}^n = M_{x,\lambda,HZ}(RD_{x,\lambda,r}^m)$$

The detector masks are given in level 4 calibration data records (CDRs) named CDR4#0000000000_DMrbeewsn_v.IMG, where r=frame rate, b=binning, eee=0, w=wavelength filter, s=0, n=detector, and v=version number. Each detector mask consists of an image of 8-bit integers, with the individual bits set equal to 1 for different masks. Bits 0,1,2,3,4,5,6,7 represent no data, scene, dark, dark/scatter transition, scattered light, scatter/scene transition, scene/dark transition, and row 0 respectively. For example, when bit 1 is 1, the pixel

is a scene pixel, and when bit 1 is 0, the pixel is not a scene pixel.

The radiance $RD_{x,\lambda,r}^n$ for each scene image is saved in a targeted radiance data record (TRDR) named CCC#####_XX_SCmmmn_TRRv.TAB, where CCC describes the observation (target mode, multispectral survey or multispectral windows mode, etc.), ##### is the observation ID in hex, XX is the counter within the observation, mmm is the macro ID, n is the detector number 1 or 2, and v is the software version number.

TRDRs are saved in both target mode and mapping mode. The use of the word “targeted” in TRDR has nothing to do with target mode versus mapping mode. Rather, “targeted” in this application is synonymous with “scene”.

In addition to the scene radiance for every image, the TRDR also contains a smaller cube with summary products. The summary products are designed to isolate surface and atmospheric spectral features of scientific interest. Typically, they are formulae based on ratios of radiances in defined wavelength channels, but sometimes they are just the radiance of a given channel. Generally, the atmospheric summary products are calculated directly from the radiance $RD_{x,\lambda,r}^n$, while the surface summary products are calculated from radiances with further atmospheric corrections applied. The summary parameters are beyond the scope of this report, which deals only with generating calibrated radiance images.

The science team will monitor the TRDR files for saturated pixels and adjust the choice of integration time or bad pixel algorithm as necessary. As of 12/30/2008, no adjustments have been necessary.

2.16 Measurement uncertainties due to nonrepeatability

Four sources of nonrepeatability contribute to uncertainty in $RD_{x,\lambda,r}^n$.

(1) Shot noise, from photon-counting statistics in the signal, is given as

$$\text{sqrt}(DN14_{x,\lambda,Ta1,Ta2,TaV,HZ,t,r}^g \cdot \text{gain}) / \text{gain}$$

where gain is approximately $80e^-/\text{DN}$ for each detector.

(2) Dark noise, which contains both read noise, shot noise due to dark current and thermal background, and effects of any systematic detector noise. This is calculated with each set of dark data

$$\text{Noise}_{x,\lambda,HZ} = \sigma(DND14_{m=0\dots m_{tot},x,\lambda,Td1,Td2,HZ,t,r})$$

The $\text{Noise}_{x,\lambda,HZ}$ read noise images are stored as a level 4 calibration data record (CDR) named CDR4#0000000000_UBrbeewsn_v.IMG, where r=frame rate=0, b=binning=0, eee=exposure time parameter, w=wavelength filter, n=detector, and v=version number. A time ordered list of these files is also maintained as a level 6 CDR, named CDR6_#_0000000000_UD_n_v.TAB,

where n=sensor ID and v=version number.

(3) Variations in throughput of the optics due to differences in the exact position of the shutter and what fraction of the beam of light it occludes. This would be the variations in sphere radiance after the shutter mirror correction has been made as described in section 3.4

(4) Variations in the sphere radiance each time the sphere is measured, as a function of any inaccuracy in the closed loop control system. Again, this is after the corrections for sphere temperature and shutter mirror position described in section 3.4 are made.

Note that all of the errors in the list above are either random errors or some other form of nonrepeatability. Currently, the uncertainty tables do not include any allowance for systematic error such as errors in the calibration of the reference source used on the ground or aging of the sphere lamps over the course of the mission.

Another error term that would be important for zone 3 of the IR spectrometer is error due to subtraction of the 2nd order stray light. This would include a random term due to noise in the scene data at the source wavelength, and a systematic term accounting for errors in the ground measurement of the stray light matrix.

2.17 Processing from radiance to I/F

The I/F is the ratio of the radiance observed from a surface to that of a perfect white Lambertian surface illuminated by the same light but at normal incidence. The formula is

$$IF_{x,\lambda} = \pi \cdot RD_{x,\lambda,r}^n / (SF_{x,\lambda} / r^2)$$

The solar flux $SF_{x,\lambda}$ is solar spectral irradiance as seen by a normally illuminated surface 1 AU from the Sun. $SF_{x,\lambda}$ is evaluated at the wavelengths corresponding to the CRISM spectral calibration and convolved to the CRISM spectral profile functions. The variable r is the distance of Mars from the Sun in AU for that particular observation.

The array $SF_{x,\lambda}$ is stored as a level 4 calibration data record (CDR) named CDR4#####_SFrbceewsn_v.IMG, where #=spacecraft time SCLK partition at the beginning of validity of the CDR, #####=spacecraft time for start of applicability of the file, r=frame rate, b=binning, eee=exposure time parameter, w=wavelength filter, s=lamp=0, n=detector, and v=version number.

The I/F will have a dependence on incident (illumination) angle and emission (reflection) angle. Incidence and emission angles relative to a model of the Martian surface are given in a derived data record (DDR) file that is associated with each TRDR file. The name of the DDR file is CCC#####_XX_SCmmmn_DDRv.TAB, where CCC describes the observation (target mode, multispectral survey or multispectral windows mode, etc.), ##### is the observation ID in hex, XX is the counter within the observation, mmm is the macro ID, n is the detector number 1 or 2, and v is the software version number. The variable r is the value of the keyword

SOLAR_DISTANCE in the label file CCC#####_XX_SCmmmn_DDRv.LBL that accompanies each DDR file and describes its contents.

Interpretation of I/F. In optics, we often use BRDF, the ratio of the observed radiance from a surface area to the irradiance incident on that surface area. The quantity $I/F = \text{BRDF} \cdot \pi \cdot \cos\theta$, where θ is the angle of incidence of the light from the Sun on the surface of Mars. The BRDF of a perfect Lambertian surface is a constant $1/\pi$, which gives the factor of π at $\theta=0$. The factor of $\cos\theta$ comes from the fact that the solar flux is the energy per unit area per unit time incident on a normally illuminated surface, while the irradiance is the energy per unit area per unit time incident on the actual surface given the incidence angle of the light coming from the Sun. We prefer to leave in the dependence on $\cos\theta$ rather than dividing it out because θ depends on the local topography of the surface, so the user may decide to use different values depending on the preferred model of the local topography. The factor of π makes I/F more intuitive in terms of energy absorbed and reflected. If the surface has some absorption but its reflections are diffuse with a Lambertian distribution, then the value of I/F for normal incidence light at a given wavelength is just the total reflectivity, the total light energy reflected at that wavelength divided by the total light energy incident at that wavelength.

3. ADDITIONAL MINI-PIPELINES FOR GENERATING CALIBRATION TABLES FROM FLIGHT CALIBRATION DATA

3.1 Calculation of IR bias images

Bias is the DN level extrapolated to zero exposure time, in image form, taken at a particular frame rate. This represents an electronics bias added to the measured signal, to prevent near-zero DNs from going negative (and being clipped) due to superimposed noise. In detector-level testing it was found that bias has a nearly fixed pattern pixel to pixel, but that its magnitude varies weakly with temperature and strongly with frame rate.

In flight, bias for the IR detector is derived from a dedicated calibration, performed periodically, in which, at each frame rate, a burst of 12 images is taken with the shutter closed at each of several short exposure times. These data are taken at IR detector temperature T_{bl} . After making a correction for a step in the bias that is a function of integration time parameter, the DN values are fit linearly on a pixel-by-pixel basis and the exposure time=0 y-intercept image is used as the bias estimate.

Processing of the bias image cubes $\text{DNB}_{n,x,\lambda,TbI,TbJ,Tb2,HZ,t}$ before bias $\text{Bias}_{x,\lambda,TbI,TbJ,HZ}$ is calculated. See sections 2.2 and 2.6 for details.

$\text{DNB}_{m,x,\lambda,TbI,TbJ,Tb2,HZ,t}$ is raw DN after fast lossless compression is undone. The subscript m runs from 0 to 11 and represents image number within a burst of identical images.

Lossy compression will never be used on bias measurements, so there is no 8-bit to 12-bit conversion.

$$\begin{aligned}
\text{DNB12}_{m,x,\lambda,\text{TbI},\text{TbJ},\text{Tb2},\text{Hz},t} &= \text{DNB}_{m,x,\lambda,\text{TbI},\text{TbJ},\text{Tb2},\text{Hz},t} \\
\text{DNB14}_{m,x,\lambda,\text{TbI},\text{TbJ},\text{Tb2},\text{Hz},t} &= \text{Offset}_k + \text{Gain}_k \cdot \text{DNB12}_{m,x,\lambda,\text{TbI},\text{TbJ},\text{Tb2},\text{Hz},t} \\
\text{DNB14}_{x,\lambda,\text{TbI},\text{TbJ},\text{Tb2},\text{Hz},t}^a &= \text{mean}_{2,2}(\text{DNB14}_{m,x,\lambda,\text{TbI},\text{TbJ},\text{Tb2},\text{Hz},t})
\end{aligned}$$

The function $\text{mean}_{2,2}()$ is the per-pixel mean of the 12 bias frames with the two highest and two lowest values thrown out for each pixel. This removes cosmic rays and reduces noise.

At a single frame rate, each pixel of the set of bias images at different integration rates are fit to the following equation.

$$\text{DNB14}_{x,\lambda,\text{TbI},\text{TbJ},\text{Tb2},\text{Hz},t}^a = c0_{x,\lambda,\text{TbI},\text{TbJ},\text{Hz}} + c1_{x,\lambda,\text{TbI},\text{Tb2},\text{Hz}} \cdot t - a0_I \cdot \text{Hv}(\text{row}_k + 1 - (502/480)) \cdot (480 - \text{integ}(t))$$

Note that $c0$ corresponds to the bias for that frame rate, and $c1 \cdot t$ corresponds to the background signal for that frame rate. The third term is a step function resulting from details of the readout of the image in the electronics. It is entirely predetermined. The constant $a0$ is determined from ground calibration data, $\text{Hv}()$ is the Heaviside function, and $\text{integ}(t)$ is the integration parameter. The value of t in ms is calculated from the integration time parameter integ using the formula $t = 1000 \cdot (502 - \text{floor}((502/480) \cdot (480 - \text{integ}))) / (502 \cdot \text{rate})$, where $\text{floor}()$ is a function that creates an integer from a real number by rounding down.

To calculate $c0$ and $c1$, DNB is corrected for the third term and a linear fit is performed for each pixel. The fit is $y = mx + b$, where $y = \text{DNB14}_{x,\lambda,\text{TbI},\text{TbJ},\text{Tb2},\text{Hz},t}^a + a0_I \cdot \text{Hv}(\text{row}_k + 1 - (502/480)) \cdot (480 - \text{integ}(t))$, $m = c1$, $x = t$, and $b = c0$. Then,

$$\text{Bias}_{x,\lambda,\text{TbI},\text{TbJ},\text{Hz}} = B_{x,\lambda,\text{Hz}}(c0_{x,\lambda,\text{TbI},\text{TbJ},\text{Hz}})$$

The function $B()$ is the bad pixel removal algorithm (see section 2.6). Bias frames $\text{Bias}_{x,\lambda,\text{TbI},\text{TbJ},\text{Hz}}$ are stored as level 4 calibration data records (CDRs) named $\text{CDR4}\#\text{tttttttt_BIrbeeewsL_v.IMG}$, where $\# = \text{spacecraft time SCLK partition at the beginning of validity of the CDR}$, $\text{tttttttt} = \text{spacecraft time SCLK at the beginning of validity of the CDR}$, $r = \text{frame rate}$, $b = \text{binning}$, $eee = \text{exposure time parameter}$, $w = \text{wavelength filter}$, $s = 0$, $L = \text{detector (IR)}$, and $v = \text{version number}$. The $\text{tttttttt} = \text{spacecraft time SCLK at the beginning of validity of the CDR}$ tells the software which bias measurement to use for a given scene measurement. The calibration software uses the CDR4 file with the largest value of tttttttt that is smaller than the value of SCLK for the scene measurement.

The constants $a0_I$ for IR and $a0_V$ for VNIR are calculated from ground calibration data and given in the level 6 CDR named $\text{CDR6}__\text{0000000000_BS_n_v.TAB}$, where $\# = \text{spacecraft time SCLK partition at the beginning time of validity of the CDR}$, $0000000000 = \text{spacecraft time SCLK at the beginning time of validity of the CDR}$, $n = \text{detector}$, and $v = \text{version number}$.

3.2 Mini-pipeline for IR background and VNIR bias images (darks)

Shutter-closed image cubes (darks) are taken with every scene and calibration measurement to subtract instrumental background. They are taken at the same set of frame rates, integration times, wavelength tables, and binning as the associated scene or calibration measurement. For the VNIR, there is no dark current or IR thermal background and this represents just detector bias, the DN level at zero integration time. For the IR, the bias is subtracted separately so that the nonlinearity correction may be applied before the dark current and IR thermal background subtraction. The shutter-closed images are then used in the IR background subtraction step.

Pipeline for VNIR darks:

$DND_{m,x,\lambda,TdV,HZ,t}$ is raw DN after fast lossless compression is undone. The subscript m represents line number within a burst of identical frames. The subscript d on the temperatures indicates temperatures for the dark image taken before the scene image. The pipeline is exactly the same for the dark image taken after the scene image, which is given the subscript e in the main pipeline.

Lossy compression will never be used on dark measurements, so there is no 8-bit to 12-bit conversion.

$$\begin{aligned} DND12_{m,x,\lambda,TdV,TdW,HZ,t} &= DND_{m,x,\lambda,TdV,TdW,HZ,t} \\ DND14_{m,x,\lambda,TdV,TdW,HZ,t} &= Offset_{\lambda} + Gain_{\lambda} \cdot DND12_{m,x,\lambda,TdV,TdW,HZ,t} \\ Bias_{x,\lambda,TdV,TdW,HZ,t} &= mean_{2,2}(B_{x,\lambda,HZ}(DND14_{m,x,\lambda,TdV,TdW,HZ,t})) \end{aligned}$$

VNIR bias frames will have to be binned in ground processing for use with scene images that are EPFs and have 10x binning at 3.75 Hz.

The function B() is the bad pixel removal algorithm (see section 2.6), and DND14 is the 14-bit DN for the dark images. The frames within the burst are averaged, throwing out the two as part of the cosmic ray removal algorithm, so the subscript m disappears at that point. The dark image taken before has VNIR detector temperature T_{dV} , and the dark image taken after has VNIR detector temperature T_{eV} .

The VNIR bias images $Bias_{x,\lambda,TdV,TdW,HZ,t}$ are stored as level 4 calibration data records (CDRs) named CDR4#ttttttttt_BIrbeeewS_v.IMG, where #=spacecraft time SCLK partition at the beginning of validity of the CDR, tttttttt=spacecraft time SCLK at the beginning of validity of the CDR, r=frame rate, b=binning, eee=exposure time parameter, w=wavelength filter, s=0, S=detector (VNIR), and v=version number. The calibration software uses the CDR4 file with the largest value of tttttttt that is smaller than the value of SCLK for the scene measurement.

Pipeline for IR darks:

$DND_{m,x,\lambda,TdI,TdJ,Td2,HZ,t}$ is raw DN after fast lossless compression is undone. The subscript m represents image number within a burst of identical images. The subscript d on the temperatures indicates temperatures for the dark image taken before the scene image. The pipeline is exactly

the same for the dark image taken after the scene image, which is given the subscript e in the main pipeline.

Lossy compression will never be used on dark measurements, so there is no 8-bit to 12-bit conversion.

$$\begin{aligned}
DND12_{m,x,\lambda,TdI,TdJ,Td2,HZ,t} &= DND_{m,x,\lambda,TdI,TdJ,Td2,HZ,t} \\
DND14_{m,x,\lambda,TdI,TdJ,Td2,HZ,t} &= Offset_{\lambda} + Gain_{\lambda} \cdot DND12_{m,x,\lambda,TdI,TdJ,Td2,HZ,t} \\
DND14^a_{m,x,\lambda,TdI,Td2,HZ,t} &= DND14_{m,x,\lambda,TdI,TdJ,Td2,HZ,t} - Bias_{x,\lambda,TbI,TbJ,HZ} \\
&\quad + a0_I \cdot Hv(row_{\lambda}+1-(502/480) \cdot (480-integ(t))) - \beta_{I,HZ} \cdot (T_{dI} - T_{bI}) - \beta_{J,HZ} \cdot (T_{dJ} - T_{bJ}) \\
DND14^b_{m,x,\lambda,TdI,Td2,HZ,t} &= DND14^a_{m,x,\lambda,TdI,Td2,HZ,t} - \sum_{n=0}^{n=3} G_I(DND14^a_{m,x0+n\lambda,TdI,Td2,HZ,t}) \\
DND14^c_{m,x,\lambda,TdI,Td2,HZ,t} &= \\
&\quad S(DND14^b_{m,x,\lambda,TdI,Td2,HZ,t}, DND14^a_{m,x,\lambda,TdI,Td2,HZ,t}, DND_{m,x,\lambda,TdI,TdJ,Td2,HZ,t}) \\
DND14^d_{m,x,\lambda,TdI,Td2,HZ,t} &= B_{x,\lambda,HZ}(DND14^c_{m,x,\lambda,TdI,Td2,HZ,t}) \\
DND14^e_{x,\lambda,TdI,Td2,HZ,t} &= mean_{2,2}(DND14^d_{m,x,\lambda,TdI,Td2,HZ,t}) \\
DND14^g_{x,\lambda,TdI,Td2,HZ,t} &= DND14^e_{x,\lambda,TdI,Td2,HZ,t} / (\epsilon_{HZ} \cdot \log(DND14^e_{x,\lambda,TdI,Td2,HZ,t}) + \phi_{HZ}) \\
RTD14^g_{x,\lambda,TdI,Td2,HZ,t} &= DND14^g_{x,\lambda,TdI,Td2,HZ,t} / t
\end{aligned}$$

IR darks will have to be binned in ground processing for use with scene images that are EPFs and have 10x binning at a given frame rate 3.75 Hz.

The steps above follow the steps of correcting the scene images up to the point of the IR background subtraction. Those steps are described in sections 2.2-2.8.

Background images $DND14^g_{x,\lambda,TdI,Td2,HZ,t}$ are stored as level 4 calibration data records (CDRs) named CDR4#ttttttttt_BKrbceewsL_v.IMG, where #=spacecraft time SCLK partition at the beginning of validity of the CDR, tttttttt=spacecraft time SCLK at the beginning of validity of the CDR, r=frame rate, b=binning, eee=exposure time parameter, w=wavelength filter, s=0, L=detector (IR), and v=version number. The integration time t, used to calculate $RTD14^g_{x,\lambda,TdI,Td2,HZ,t}$ from $DND14^g_{x,\lambda,TdI,Td2,HZ,t}$, may be calculated from the integration time parameter in the label file CDR4#ttttttttt_BKrbceewsL_v.LBL that goes with the .IMG file containing the $DND14^g_{x,\lambda,TdI,Td2,HZ,t}$ images.

The IR background rate $RTD14^g_{x,\lambda,TdI,Td2,HZ,t}$ is an input to section 2.9 of the main pipeline, where the dark images are interpolated to the time of the scene or calibration measurement.

3.3 Generation of the flat fields

The flat field $FF_{x,\lambda,HZ}$ is just an average of many images of a featureless region of Mars, with the scene pixels in each row normalized so they average to 1. The EDRs are sent through the entire calibration pipeline to make radiance images, and then averaged. A slight correction has to be made to the averaged images to account for the fact that the featureless scene spectral radiance varies with wavelength and the spectrometer has smile. Then, each row is normalized so that the scene pixels in that row average to 1.

Some of the IR flat field bands are set equal to 1. These are wavelengths near sharp atmospheric features, where the interaction between sharp spectral feature and instrument smile makes the flat field inaccurate.

The flat field $FF_{x,y,H\lambda}$ is given in layer 0 of the flight level 4 calibration data records (CDRs) named CDR4#ttttttttt_NUrbeeewsd_v.IMG, where #=spacecraft time SCLK partition at the beginning of validity of the CDR, tttttttt=spacecraft time SCLK at the beginning of validity of the CDR, r=frame rate, b=binning, eee=exposure time parameter, w=wavelength filter, s=0, d=detector, and v=version number. Unlike the rest of the flight CDR4s, which are generated automatically by the pipeline software, the NU CDR is generated periodically by the science team, based on averages of images of a featureless area of Mars.

3.4 Calculating sphere radiance including sphere temperature and shutter mirror position

Note as of 12/30/2008: The corrections described in this section are implemented in the software, but the CDRs are zeroed out so that the correction is not performed. Instead, the lab-to-flight differences in integrating sphere temperature and shutter mirror position have been included in the SS CDR.

The sphere radiance was measured in ground calibration with respect to known external sources. The most useful ones were a Spectralon plate illuminated by a NIST standard lamp and a cavity radiation source imaged through a collimator. The sphere radiance measured on the ground is then corrected to a value appropriate for a given calibration source measurement in flight. There are two corrections currently planned:

1. A correction for the temperature of the integrating sphere in flight. The current in the sphere is controlled by a silicon photodiode through a closed loop. The long-wavelength edge of the sensitivity of that photodiode is temperature-dependent, which causes the lamp current and sphere output to be temperature-dependent. From the ground calibration data, we have images taken at different sphere temperatures and we can estimate this effect. This also corrects for variations in the thermal emission of the sphere, which may have a small effect at long wavelengths. In addition, the temperature of the beamsplitter tracks the temperature of the optical bench to some extent, and the temperature of the optical bench tracks the temperature of the integrating sphere. As an unintended side effect, the correction of the sphere radiance for the integrating sphere temperature will also give a partial correction for any dependence of the instrument response on the beamsplitter temperature.
2. A correction for the exact angle of the shutter mirror for the sphere measurement in flight. The shadow of the mask at the boundary of the VNIR order-sorting filter is compared between the flight measurement and the ground measurement, and a correction is made to the ground radiance to give the radiance expected for that flight measurement. This correction changes every time the shutter mirror is moved.

It is possible that other effects such as the temperature of the focal plane board controlling the sphere lamp have an effect on sphere radiance, but as of this writing (10/19/2005) we have not yet investigated the repeatability of the sphere images with changes in the temperature of the focal plane boards.

First, the calculation of sphere radiance at the temperature of the flight sphere images.

The ground measured sphere radiance as a function of temperature is found in level 4 calibration data record CDR4#ttttttttt_SSrbeeewsn_v.IMG, where #=spacecraft time SCLK partition at the beginning of validity of the CDR, tttttttt=spacecraft time, r=frame rate=0, b=binning, eee=exposure time parameter, w=wavelength filter, s=1 or 2 depending on whether side 1 (IRFPE-controlled, cross-slit) or 2 (VNIRFPE-controlled, along-slit) lamp is used, n=detector, and v=version number. It consists of 3 images that are polynomial coefficients for the sphere radiance at each pixel as a function of temperature in degrees C. The sphere radiance is

$$\theta_{s,x,\lambda} + \sigma_{s,x,\lambda} \cdot T_{c3} + \tau_{s,x,\lambda} \cdot T_{c3}^2$$

The units of sphere radiance are W/(m² micrometer sr). Note: As of 12/30/2008, we are using values $\theta=1$, $\sigma=0$, and $\tau=0$, so the correction is not explicitly applied.

Second, the correction of the sphere radiance for shutter mirror position nonrepeatability.

Rows 223-247 of the VNIR sphere images have DN levels sensitive to the shutter mirror position because they are on the edges of the VNIR filter zone boundary mask, and the shadow of the mask moves with the shutter mirror. The mirror parameter MP_s, a single value for each set of calibration images taken without moving the shutter mirror, measures the microscopic difference between the shutter mirror angle for the flight radiance calibration and the ground radiance calibration. A different definition of MP_s is used for s=1 (IRFPE controlled, cross-slit lamp) and s=2 (VNIRFPE-controlled, along-slit lamp).

$$MP_1 = \sum_{s=1, x=0 \dots 639, \lambda=232 \dots 234, T_{c3}} RTS14^j / RGSB_{s=1, T_{c3}}^j - \sum_{s=1, x=0 \dots 639, \lambda=223 \dots 225, T_{c3}} RTS14^j / RGS_{s=1, T_{c3}}^j$$

$$MP_2 = \sum_{s=2, x=0 \dots 639, \lambda=235 \dots 237, T_{c3}} RTS14^j / RGSB_{s=2, T_{c3}}^j - \sum_{s=2, x=0 \dots 639, \lambda=245 \dots 247, T_{c3}} RTS14^j / RGS_{s=2, T_{c3}}^j$$

with

$$RGSB_{s=1, T_{c3}}^j = \sum_{x=0 \dots 639, \lambda=232 \dots 234} RGS14_{s=1, x, \lambda, T_{c3}}^j \cdot (\theta_{s=1, x, \lambda} + \sigma_{s=1, x, \lambda} \cdot T_{c3} + \tau_{s=1, x, \lambda} \cdot T_{c3}^2) / (\theta_{s=1, x, \lambda} + \sigma_{s=1, x, \lambda} \cdot T_{c3} + \tau_{s=1, x, \lambda} \cdot T_{c3}^2)$$

$$RGS_{s=1, T_{c3}}^j = \sum_{x=0 \dots 639, \lambda=223 \dots 225} RGS14_{s=1, x, \lambda, T_{c3}}^j \cdot (\theta_{s=1, x, \lambda} + \sigma_{s=1, x, \lambda} \cdot T_{c3} + \tau_{s=1, x, \lambda} \cdot T_{c3}^2) / (\theta_{s=1, x, \lambda} + \sigma_{s=1, x, \lambda} \cdot T_{c3} + \tau_{s=1, x, \lambda} \cdot T_{c3}^2)$$

$$RGSB_{s=2, T_{c3}}^j = \sum_{x=0 \dots 639, \lambda=235 \dots 237} RGS14_{s=2, x, \lambda, T_{c3}}^j \cdot (\theta_{s=2, x, \lambda} + \sigma_{s=2, x, \lambda} \cdot T_{c3} + \tau_{s=2, x, \lambda} \cdot T_{c3}^2) / (\theta_{s=2, x, \lambda} + \sigma_{s=2, x, \lambda} \cdot T_{c3} + \tau_{s=2, x, \lambda} \cdot T_{c3}^2)$$

$$\text{RGSA}_{s=2, T_{c3}}^j = \sum_{x=0 \dots 639, \lambda=245 \dots 247} \text{RGS14}_{s=2, x, \lambda, T_{gV}, T_{g3}}^j \cdot (\theta_{s=2, x, \lambda} + \sigma_{s=2, x, \lambda} \cdot T_{c3} + \tau_{s=2, x, \lambda} \cdot T_{c3}^2) / (\theta_{s=2, x, \lambda} + \sigma_{s=2, x, \lambda} \cdot T_{g3} + \tau_{s=2, x, \lambda} \cdot T_{g3}^2)$$

RTS14 is count rate observed with the onboard sphere as a source, and RGSA, RGSB are the total count rates from sample rows in a given column of the ground data from which the sphere radiance CDR is derived, corrected from T_{g3} , the integrating sphere temperature for the ground calibration, to T_{c3} , the integrating sphere temperature for the flight calibration. Rows 223-247 of the VNIR have responsivity insensitive to detector temperature, so RTS14, RGSA, and RGSB are not functions of T_{cV} or T_{gV} . RTS14^j and RGS14^j have the full set of corrections for bias, detector ghosts, bad pixel and cosmic ray removal, detector nonlinearity, background subtraction, and stray light subtraction. A detailed description of these corrections is given in section 3.5, and also in the main data pipeline in sections 2.2 to 2.11.

RGS14^j_{s,x,λ,TgV,Tg3} is the count rate for the ground sphere radiance measurement. It is calculated from DGS14^j_{s,x,λ,TgV,Tg3,t}, the counts in the ground sphere radiance measurement, using the equation $\text{RGS14}_{s,x,\lambda,T_{gV},T_{g3}}^j = \text{DGS14}_{s,x,\lambda,T_{gV},T_{g3},t}^j / t$. The counts DGS14^j_{s,x,λ,TgV,Tg3,t} are given in the level 4 calibration data record CDR4#ttttttttt_SHrbeeewsn_v.IMG described at the end of this chapter. The integration time t for the ground measurement may be calculated from the integration time parameter for the ground measurement, which is given in the label file CDR4#ttttttttt_SHrbeeewsn_v.LBL. The integrating sphere temperature T_{g3} for the ground measurement is also given in the label file CDR4#ttttttttt_SHrbeeewsn_v.LBL.

The movement of the shutter mirror causes the signal to increase in one set of rows and decrease in the other. Subtracting the ratios in the two sets of rows makes the parameter MP_s insensitive to small changes in the brightness of the sphere lamps. MP_s is derived from just the VNIR image, but it is used to correct both VNIR and IR images.

The formula for sphere radiance $SR_{s,x,\lambda,T_{c3}}$ including the shutter mirror nonrepeatability correction simply comes from the assumption that the correction is linearly dependent on the shutter movement parameter MP_s . This should be a good assumption if the correction is small, and in ground data it appears to be 5% or less so far.

$$SR_{s,x,\lambda,T_{c3}} = (\theta_{s,x,\lambda} + \sigma_{s,x,\lambda} \cdot T_{c3} + \tau_{s,x,\lambda} \cdot T_{c3}^2) / (1 + MP_s \cdot SC_{s,x,\lambda})$$

The shutter correction $SC_{s,x,\lambda}$ image is derived by taking ratios of images, subtracting 1, and dividing by the value of MP_s for each image ratio. This may be done with ground or flight images, and the correction is proven valid by the fact that the correction image thus derived is pretty much the same for all image pairs for which the shutter mirror has moved enough that the correction is significant. In practice, $SC_{s,x,\lambda}$ is an average of values calculated from multiple ground images. Note: the images ratioed to calculate $SC_{s,x,\lambda}$ as part of the analysis of the ground calibration data not only have all the data pipeline corrections from sections 2.2 to 2.11, but also are corrected for the detector temperature as described in section 2.12, a later step. This is just a detail of how the relevant ground CDR4 is generated, and it does not affect the flight data pipeline.

MP_s itself will depend on which sphere lamp is used, but the correction for shutter mirror

position should be the same for either sphere lamp if the mirror is not moved between one sphere lamp measurement and the other.

The shutter correction image $SC_{s,x,\lambda}$ is kept in layer 1 of the level 4 calibration data record $CDR4\#tttttttt_SHrbeeewsn_v.IMG$, where $\#$ =spacecraft time SCLK partition at the beginning of validity of the CDR, $tttttttt$ =spacecraft time, r =frame rate=0, b =binning=0, eee =exposure time parameter, w =wavelength filter=0, $s=1$ or 2 depending on whether side 1 (IRFPE-controlled, cross-slit) or 2 (VNIRFPE-controlled, along-slit) lamp is used, n =detector, and v =version number. The image $DGS14^j_{s,x,\lambda,TgV,Tg3,t}$ is kept in layer 0 of the level 4 calibration data record $CDR4\#tttttttt_SHrbeeewsn_v.IMG$, where $\#$ =spacecraft time SCLK partition at the beginning of validity of the CDR, $tttttttt$ =spacecraft time, r =frame rate=0, b =binning=0, eee =exposure time parameter, w =wavelength filter=0, $s=1$ or 2 depending on whether side 1 (IRFPE-controlled, cross-slit) or 2 (VNIRFPE-controlled, along-slit) lamp is used, n =detector, and v =version number. The image $DGS14^j_{s,x,\lambda,TgV,Tg3,t}$ is simply the counts for the VNIR ground sphere radiance measurement, converted to 14-bits and with all corrections applied that are applied to the RT^j flight data except the division by integration time t is not applied. The counts from the VNIR ground sphere radiance measurement are necessary in order to calculate the shutter movement parameter MP_s from the flight VNIR calibration image. That calculation also requires the sphere temperature T_{g3} for the ground sphere radiance measurement. T_{g3} is listed in the label file $CDR4\#tttttttt_SHrbeeewsn_v.LBL$. The integration time parameter is listed in the label file $CDR4\#tttttttt_SHrbeeewsn_v.LBL$, and the integration time t may be calculated from the integration time parameter.

As of 12/30/2008, layer 1 of the SH CDR is zero, so the shutter mirror correction is zero. The SS CDR is adjusted to account for the difference in shutter mirror correction between lab calibration and flight, and the shutter mirror has been highly repeatable in flight, so the more complex correction has not been needed.

3.5 Calculation of instrument responsivity from sphere radiance

Responsivity as a function of wavelength results from three effects:

- The instrument design including telescope design, optical efficiency, and detector performance.
- Variations in detector responsivity as a function of detector temperature. The main effects are a shift in the long wavelength edge for the VNIR detector, and a movement in the interference fringes that appear on the long wavelength end of the IR detector.
- Accumulation of absorbing contaminants on optical surface. The major expected contaminant is water ice on the detector.

CRISM's responsivity is tracked in flight using the internal integrating sphere, run under closed loop control, using either bulb. This provides a field- and aperture-filling source with stable radiance. The current plan is to take sphere calibration measurements with one lamp within a

few minutes of every scene measurement, and take calibration measurements with the other lamp once a month to check the first lamp. The sphere calibration may also be checked with images from Diemos when available.

The calculation of sphere radiance $SR_{s,x,\lambda,Tc3}$ is described in Section 3.4, including the correction for shutter mirror position.

The pipeline processing for the onboard integrating sphere images before they are used to calculate the responsivity.

$DNS_{m,s,x,\lambda,TcV,TcI,Tc2,Tc3,t}$ is raw DN after fast lossless compression is undone. The subscript m represents image number within a burst of identical images. The subscript s represents choice of sphere lamp, 1 or 2. The subscript c on the temperatures indicates temperatures for the calibration images. Note the sphere radiance depends on the sphere temperature $Tc3$, so there's an implicit dependence of DNS on $Tc3$ that is shown. Also, all sphere images are taken at 1 Hz with no binning and the largest wavelength tables, so the Hz subscript is omitted. The results are binned and the wavelength tables applied in section 2.13 of the main pipeline.

Lossy compression will never be used on sphere measurements, so there is no 8-bit to 12-bit conversion.

$$\begin{aligned}
 DNS12_{m,s,x,\lambda,TcV,TcW,TcI,TcJ,Tc2,Tc3,t} &= DNS_{m,s,x,\lambda,TcV,TcW,TcI,TcJ,Tc2,Tc3,t} \\
 DNS14_{m,s,x,\lambda,TcV,TcW,TcI,TcJ,Tc2,Tc3,t} &= Offset_{\lambda} + Gain_{\lambda} \cdot DNS12_{m,s,x,\lambda,TcV,TcW,TcI,TcJ,Tc2,Tc3,t} \\
 DNS14^a_{m,s,x,\lambda,TcI,Tc2,Tc3,t} &= DNS14_{m,s,x,\lambda,TcI,TcJ,Tc2,Tc3,t} - Bias_{x,\lambda,TbI,TbJ,HZ=1} \\
 &+ a_{0I} \cdot Hv(row_{\lambda}+1-(502/480) \cdot (480-integ(t))) - \beta_{I,HZ=1} \cdot (T_{cI} - T_{bI}) - \beta_{J,HZ=1} \cdot (T_{cJ} - T_{bJ}) \\
 &- median_{x,\lambda}(DN14_{x1...xn,\lambda,TaI,TaJ,Ta2,HZ,t,r}) \text{ for the IR and} \\
 DNS14^a_{m,s,x,\lambda,TcV,t} &= DNS14_{m,s,x,\lambda,TcV,TcW,t} - (\alpha_{ec} \cdot Bias_{x,\lambda,TdV,TdW,t} + \alpha_{cd} \cdot Bias_{x,\lambda,TeV,TeW,t}) / (\alpha_{cd} + \alpha_{ec}) \\
 &- \beta_{V,HZ=1} \cdot [\alpha_{ec} \cdot (T_{cV} - T_{dV}) + \alpha_{cd} \cdot (T_{eV} - T_{cV})] / (\alpha_{cd} + \alpha_{ec}) \\
 &- \beta_{W,HZ=1} \cdot [\alpha_{ec} \cdot (T_{cW} - T_{dW}) + \alpha_{cd} \cdot (T_{eW} - T_{cW})] / (\alpha_{cd} + \alpha_{ec}) \\
 &- median_{x,\lambda}(DN14_{x1...xn,\lambda,TaV,TaW,HZ,t,r}) \text{ for VNIR.} \\
 DNS14^b_{m,s,x,\lambda,TcV,t} &= DNS14^a_{m,s,x,\lambda,TcV,t} - \sum_{n=0}^{n=3} G_V(DNS14^a_{m,s,x0+n,\lambda,TcV,t}) \text{ for VNIR and} \\
 DNS14^b_{m,s,x,\lambda,TcI,Tc2,Tc3,t} &= DNS14^a_{m,s,x,\lambda,TcI,Tc2,Tc3,t} - \sum_{n=0}^{n=3} G_I(DNS14^a_{m,s,x0+n,\lambda,TcI,Tc2,Tc3,t}) \text{ for IR} \\
 DNS14^c_{m,s,x,\lambda,TcV,TcI,Tc2,Tc3,t} &= \\
 &S(DNS14^b_{m,s,x,\lambda,TcV,TcI,Tc2,Tc3,t}, DNS14^a_{m,s,x,\lambda,TcV,TcI,Tc2,Tc3,t}, DNS_{m,s,x,\lambda,TcV,TcW,TcI,TcJ,Tc2,Tc3,t}) \\
 DNS14^d_{m,s,x,\lambda,TcV,TcI,Tc2,Tc3,t} &= B_{x,\lambda,HZ}(DNS14^c_{m,s,x,\lambda,TcV,TcI,Tc2,Tc3,t}) \\
 DNS14^e_{s,x,\lambda,TcV,TcI,Tc2,Tc3,t} &= mean_{2,2}(DNS14^d_{m,s,x,\lambda,TcV,TcI,Tc2,Tc3,t}) \\
 DNS14^g_{s,x,\lambda,TcI,Tc2,Tc3,Taf,t} &= DNS14^e_{s,x,\lambda,TcI,Tc2,Tc3,TeV,t} / (\epsilon_{Hz} \cdot \log(DNS14^e_{s,x,\lambda,TcI,Tc2,Tc3,TeV,t}) + \phi_{Hz}) \\
 RTS14^g_{s,x,\lambda,TcI,Tc2,Tc3,TeV} &= DNS14^g_{s,x,\lambda,TcI,Tc2,Tc3,TeV,t} / t \\
 RTS14^h_{s,x,\lambda,TcI,Tc2,Tc3} &= RTS14^g_{s,x,\lambda,TcI,Tc2,Tc3,tal} - Bkgd_{x,\lambda,TdI,TdJ,Td2,Td3,tal,td1,td2} \text{ for IR and} \\
 RTS14^h_{s,x,\lambda,TcV,Tc3} &= RTS14^g_{s,x,\lambda,TcV,Tc3} \text{ for VNIR} \\
 RTS14^i_{s,x,\lambda,TcV,TcI,Tc2,Tc3,HZ} &= RTS14^h_{s,x,\lambda,TcV,TcI,Tc2,Tc3} - \sum_{n=1}^{n=6} \kappa_{x,\lambda,n,HZ} \cdot RTS14^h_{x,\lambda',yn,HZ,TaI,Ta2,HZ} \\
 &\text{for IR and} \\
 RTS14^i_{s,x,\lambda,TcV,TcI,Tc2,Tc3,HZ} &= RTS14^h_{s,x,\lambda,TcV,TcI,Tc2,Tc3} - \langle RTS14^h_{x1...xn,\lambda,TaV,TaI,Ta2,HZ} \rangle \cdot
 \end{aligned}$$

$SW_{x,TaV,TaI,Ta2,HZ}^h$ for $\lambda < 563$ nm, - $\langle RTS14_{x1 \dots xn, \lambda, TaV, TaI, Ta2, HZ}^h \rangle \cdot CS_{x, \lambda, TaV, TaI, Ta2, HZ}^h$ for $\lambda > 563$ nm for VNIR.

The steps above follow the steps of correcting the scene images up to the point of the subtraction of second-order stray light. Those steps are described in sections 2.2 to 2.11.

For VNIR detector rows 185-215, the sphere is too dim to be used to calibrate the images, and the SS CDR values in those rows are just instrument responsivity calculated from the laboratory calibration.

The sphere count rate images $RTS14_{s,x,\lambda,TcI,Tc2,Tc3}^i$ are written to level 4 calibration data records (CDRs) named CDR4#ttttttttt_SPrbeeewsn_v.IMG, where # = spacecraft time SCLK partition at the beginning of validity of the CDR, tttttttt = spacecraft time SCLK at the beginning of validity of the CDR, r = frame rate, b = binning, eee = exposure time parameter, w = wavelength filter, s = 0, n = detector, and v = version number.

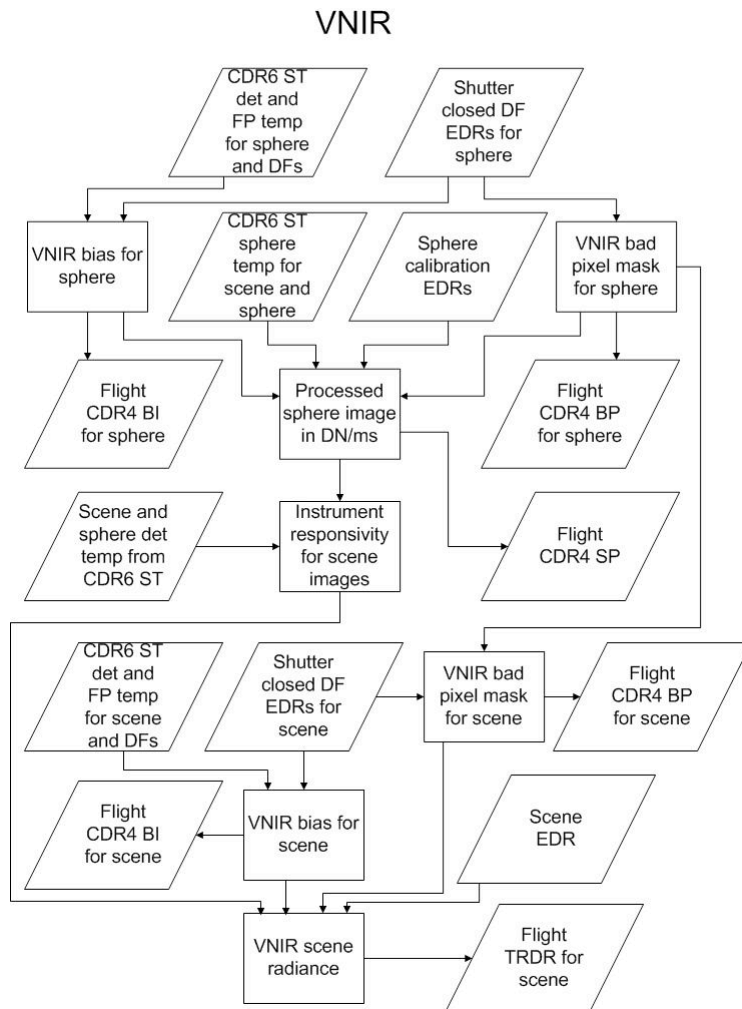
The calculation of responsivity $RSP_{x,\lambda,TcI,Tc2}^i$ is then very simple. It's just counts/radiance.

$$RSP_{x,\lambda,TcI,Tc2}^i = RTS14_{s,x,\lambda,TcV,TcI,Tc2,Tc3}^i / SR_{s,x,\lambda,Tc3}$$

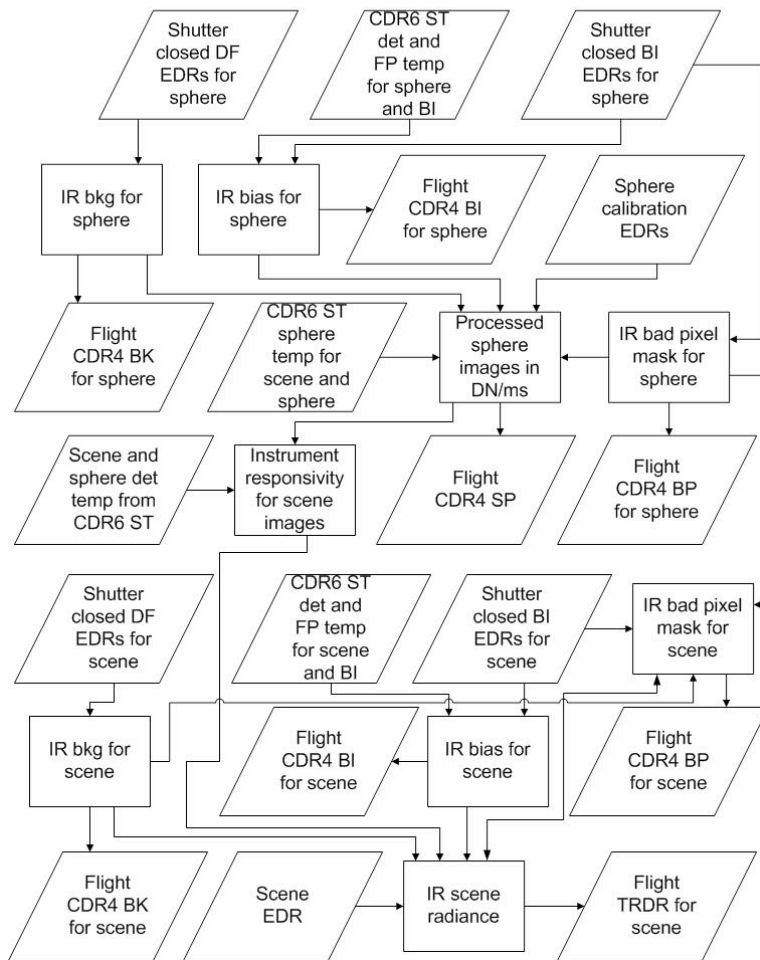
The corrections to the responsivity for detector temperature are made in the main data pipeline in section 2.12. The responsivity is not saved as a calibration data record. It is calculated each time from the flight sphere images and the ground sphere radiance. Normally, the responsivity is calculated using data from the primary sphere lamp, which is s=2 (the VNIRFPE-controlled, cross-slit lamp) as of 10/28/2005. Measurements with the secondary lamp are taken during monthly engineering checkouts. The responsivity should be the same calculated with either lamp, and this is a useful in-flight check on the accuracy of the onboard calibration system. The units of responsivity are DN/ms/(W/(m² micrometer sr)).

4. IMPLEMENTATION IN PIPE

4.1 Data flow of flight calibration and scene EDRs to flight CDR4s and TRDRs



IR



4.2 Logic for choosing specific flight calibration EDRs to use with a given scene EDR

The ATF table is a special CDR used to list the calibration EDRs to be used to calibrate each scene EDR. It is located in the `crism_pds_archive/edr/CDR/yyyy_doy/ATF` directory of the PDS archive. The first column of the ATF table lists every scene EDR with `START_TIME` in that day. The remaining columns of each row list the calibration EDRs to use for the scene EDR given in the first column of that row. The ATF table consists only of EDRs that have actually been received. These are the ones used in calibration. There is a similar BTF table that gives the calibration EDRs that were planned for use with each scene EDR. The BTF table is generated for comparison with the ATF table, in case some of the calibration EDRs are not downlinked and the algorithm was forced to use a substitute.

VNIR

There are 2 types of calibration EDRs to be searched for, the shutter-closed DFs (for VNIR these are for the bias calculation) and the sphere calibration SP EDRs. The SP EDRs have their own DFs for calculating the bias for sphere measurements.

Note that any downlinked EDRs with a “UN” macro descriptor in the filename should be rejected as calibration EDRs. This will filter out any problem EDRs caused when the instrument occasionally reverts back to default state 2 frames before the end of a mapping mode observation.

- I. Logic for determining desired calibration EDRs from predicted EDRs in initial observation tracking table for a given measurement (BTF table)
 - a. Shutter closed DF EDRs for bias for scene or sphere EDR
 - i. Select latest (in encoded SCLK) DF EDR that is earlier than the scene or sphere EDR and has the same frame rate, exposure, and binning as the scene or sphere EDR, and acceptable wavelength filter for the scene or sphere EDR
 - ii. Select earliest (in encoded SCLK) DF EDR that is later than the scene or sphere EDR and has the same frame rate, exposure, and binning as the scene or sphere EDR, and acceptable wavelength filter for the scene or sphere EDR
 - iii. Definition of “acceptable wavelength filter for the scene or sphere EDR”
 1. Filter 0 DF is acceptable for filters 0, 1, 2, and 3 SP or SC
 2. Filter 1 DF is acceptable for filter 1 SP or SC
 3. Filter 2 DF is acceptable for filters 1, 2, and 3 SP or SC
 4. Filter 3 DF is acceptable for filters 1 and 3 SP or SC
 - b. Sphere calibration SP SC EDR for radiometric calibration
 - i. Select closest (in encoded SCLK) SP EDR that is has acceptable binning and wavelength filter to go with the scene EDR
 - ii. Select shutter closed DF EDRs to go with the SP EDR by following (a) above
 - iii. Definition of “acceptable binning to go with the scene EDR”

1. For 10x binning scene EDR, any binning is OK for the SP EDR
2. For 5x binning scene EDR, 1x or 5x are OK for the SP EDR
3. For 2x binning scene EDR, 1x or 2x are OK for the SP EDR
4. For 1x binning scene EDR, 1x is OK for the SP EDR
- c. Shutter closed DF EDR for bad pixel mask
 - i. Select closest (in encoded SCLK) DF EDR with 1x binning, 1Hz frame rate, integ time parameter 425, and hyperspectral wavelength filter
- II. Logic for determining calibration EDRs to use from the list of valid downlinked calibration EDRs (ATF table), and what to do if some of them are invalid
 - a. Shutter closed DF EDRs for bias for scene or sphere EDR
 - i. Select latest (in encoded SCLK) existing valid DF EDR that is earlier than the scene or sphere EDR and has the same frame rate, exposure, and binning as the scene or sphere EDR, and acceptable wavelength filter for the scene or sphere EDR
 - ii. Select earliest (in encoded SCLK) existing valid DF EDR that is later than the scene or sphere EDR and has the same frame rate, exposure, and binning as the scene or sphere EDR, and acceptable wavelength filter for the scene or sphere EDR
 - iii. If unexpected DF EDRs are selected
 1. If the early DF EDR is more than 6 hours earlier than the scene EDR, do not select that EDR but instead select the late DF EDR twice
 2. If the late DF EDR is more than 6 hours later than the scene EDR, do not select that EDR but instead select the early DF EDR twice
 3. If both DF EDRs differ from the scene EDR by more than 6 hours, select the one that is closest in time to the scene EDR twice
 4. If either of the DF EDRs selected is different from that predicted in the early observation tracking table (note this part of the logic is implemented by the C++ program, while the rest is implemented in PIPE)
 - a. For scene measurements, set the flag in the data quality indicator in the TRDR but otherwise continue normally
 - b. For DF EDRs to be used with SP EDRs, declare that SP EDR invalid, do not generate an SP flight CDR4 from that SP EDR, and go back to PIPE to get another SP EDR
 - b. Sphere calibration SP EDR for radiometric calibration
 - i. For VNIR, detector temperature is thermostatically controlled and effect on responsivity is forward modeled, so we use only one SP EDR
 - ii. Select closest (in encoded SCLK) SP EDR that has acceptable binning and wavelength filter to go with the scene EDR
 - iii. Select shutter closed DF EDRs to go with the SP EDR by following (a) above
 - iv. If unexpected SP EDRs are selected
 1. There is no time limit on whether SP EDRs are acceptable, just use the closest in time of the valid ones

2. If the SP EDR selected is different from that predicted in the early observation tracking table, set the flag in the data quality indicator in the TRDR but otherwise continue normally (note this part of the logic is implemented by the C++ program, while the rest is implemented in PIPE)
- c. Shutter closed DF EDR for bad pixel mask
 - i. Select closest (in encoded SCLK) DF EDR with 1x binning, 1 Hz frame rate, integ time parameter 425, and hyperspectral wavelength filter

IR

There are 3 types of calibration EDRs to be searched for, the shutter-closed DFs (for IR these are used for background subtraction), the shutter-closed BIs (for IR these are used for bias subtraction), and the sphere calibration SP EDRs. The SP EDRs have their own DF EDRs for calculating the background for sphere measurements.

Note that any downlinked EDRs with a “UN” macro descriptor in the filename should be rejected as calibration EDRs. This will filter out any problem EDRs caused when the instrument occasionally reverts back to default state 2 frames before the end of a mapping mode observation.

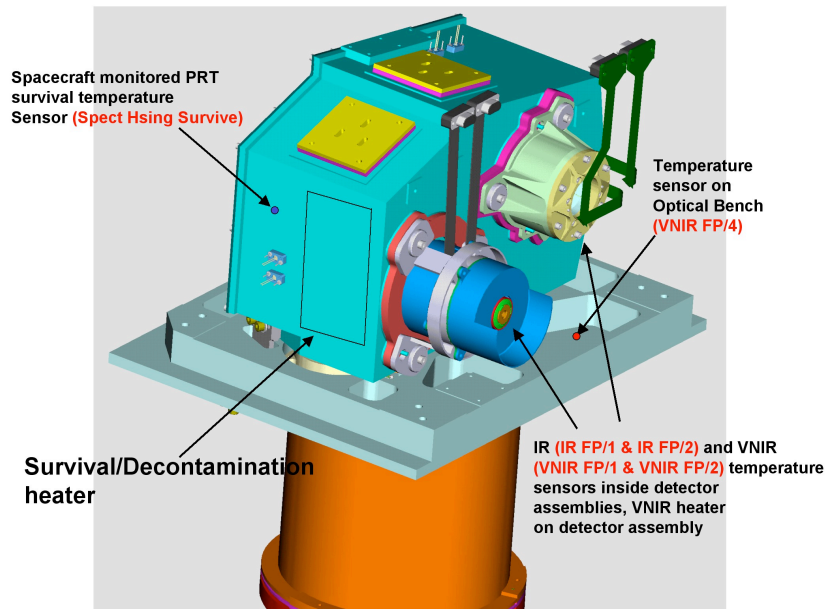
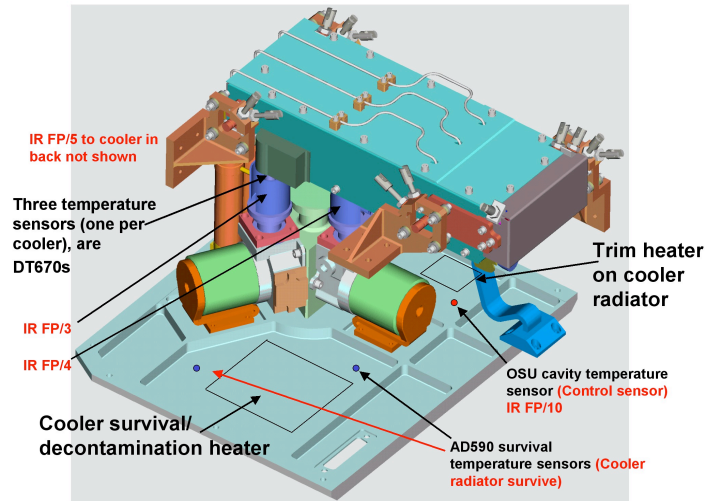
- I. Logic for determining desired calibration EDRs from predicted EDRs in initial observation tracking table for a given measurement (BTF table)
 - a. Shutter closed DF EDRs for background for scene or sphere EDR
 - ii. Select latest (in encoded SCLK) DF EDR that is earlier than the scene or sphere EDR and has the same frame rate, exposure, and binning as the scene or sphere EDR, and acceptable wavelength filter for the scene or sphere EDR
 - iii. Select earliest (in encoded SCLK) DF EDR that is later than the scene or sphere EDR and has the same frame rate, exposure, and binning as the scene or sphere EDR, and acceptable wavelength filter for the scene or sphere EDR
 - b. Shutter closed BI EDRs for bias for scene or sphere EDR
 - iv. Find closest (in encoded SCLK) set of BI EDRs and select all EDRs from that set that have the same frame rate and binning as the scene or sphere measurement regardless of exposure, and acceptable wavelength filter for the scene or sphere EDR
 - c. Sphere calibration SP EDRs for radiometric calibration
 - i. Select closest (in encoded SCLK) nightside SP EDR that has acceptable binning and wavelength filter to go with the scene EDR (note as of 12/30/2008, nightside or dayside is acceptable)
 - ii. Select closest (in encoded SCLK) dayside SP EDR that has acceptable binning and wavelength filter to go with the scene EDR (note as of 12/30/2008, it finds the same sphere as i, nightside or dayside)
 - iii. If either SP EDR differs from the scene EDR by more than 24 hours, replace the errant SP EDR by a dummy EDR name to force the C++

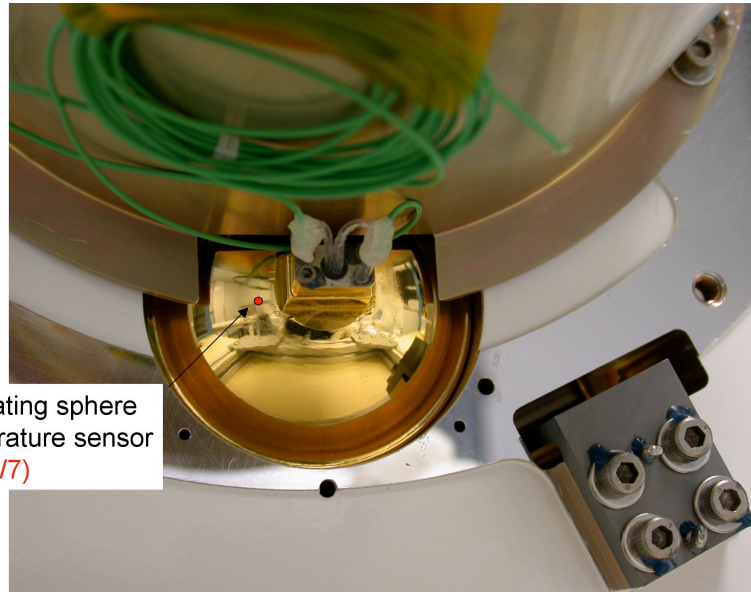
- program to set the data quality flag in the TRDR no matter what SP EDR it actually ends up using
 - iv. Select shutter closed DF EDRs to go with each sphere EDR by following (a) above
 - v. Select shutter closed BI EDRs to go with each sphere EDR by following (b) above
 - d. Shutter closed BI EDRs for bad pixel mask
 - i. Select closest (in encoded SCLK) set of BI EDRs with 1x binning and hyperspectral wavelength filter
- II. Logic for determining calibration EDRs to use from the list of valid downlinked calibration EDRs (ATF table), and what to do if some of them are invalid
 - a. Shutter closed DF EDRs for background for scene or sphere EDR
 - ii. Find latest (in encoded SCLK) existing valid DF EDR that is earlier than the scene or sphere EDR and has the same frame rate, exposure, and binning as the scene or sphere EDR, and acceptable wavelength filter for the scene or sphere EDR
 - i. Find earliest (in encoded SCLK) existing valid DF EDR that is later than the scene or sphere EDR and has the same frame rate, exposure, and binning as the scene or sphere EDR, and acceptable wavelength filter for the scene or sphere EDR
 - ii. If unexpected DF EDRs are selected
 - 1. If the early DF EDR is more than 6 hours earlier than the scene EDR, do not select that EDR but instead select the late DF EDR twice
 - 2. If the late DF EDR is more than 6 hours earlier than the scene EDR, do not select that EDR but instead select the early DF EDR twice
 - 3. If both DF EDRs differ from the scene EDR by more than 6 hours, select the one that is closest in time to the scene EDR twice
 - 4. If either of the DF EDRs selected is different from that predicted in the early observation tracking table (note this part of the logic is implemented by the C++ program, while the rest is implemented in PIPE)
 - a. For scene measurements, set the flag in the data quality indicator in the TRDR but otherwise continue normally
 - b. For DF EDRs to be used with SP EDRs, declare that SP EDR invalid, do not generate an SP flight CDR4 from that SP EDR, and go back to PIPE to get another SP EDR
 - b. Shutter closed BI EDRs for bias for scene or sphere EDR
 - i. Find closest (in encoded SCLK) set of BI EDRs and choose all EDRs from that set that have the same frame rate and binning as the scene or sphere measurement regardless of exposure, and acceptable wavelength filter for the scene or sphere EDR
 - ii. If unexpected BI EDRs are selected (note this part of the logic is implemented by the C++ program, while the rest is implemented in PIPE)

1. There is no time limit on whether BI EDRs are acceptable, just use the closest in time of the valid ones
 2. If the BI EDR selected is different from that predicted in the early observation tracking table, set the flag in the data quality indicator in the TRDR but otherwise continue normally
 3. For BI EDRs to be used with SP EDRs, declare that SP EDR invalid, do not generate an SP flight CDR4 from that SP EDR, and go back to PIPE to get another SP EDR
- c. Sphere calibration SP EDRs for radiometric calibration
- i. Select closest (in encoded SCLK) nightside SP EDR that has acceptable binning and wavelength filter to go with the scene EDR (note as of 12/30/2008, nightside or dayside is acceptable)
 - ii. Select closest (in encoded SCLK) dayside SP EDR that has acceptable binning and wavelength filter to go with the scene EDR (note as of 12/30/2008, it finds the same sphere as i, nightside or dayside)
 - iii. Ensure the IR detector temperature for the scene EDR does not fall too far outside the range of the dayside and nightside SP EDRs
 1. Let T , T_d , and T_n be the median IR detector temperatures for the frames of each of the scene, dayside SP, and nightside SP EDRs respectively
 2. If $T_d \leq T_n$, replace the dayside SP EDR with the one closest (in encoded SCLK) to the scene EDR with $T_d > T_n$
 3. If $(T - T_d) > 0.5 * (T_d - T_n)$, replace the currently selected dayside SP EDR with the one closest (in encoded SCLK) to the scene EDR with $(T - T_d) < 0.5 * (T_d - T_n)$
 4. If $(T_n - T) > 0.5 * (T_d - T_n)$, replace the nightside SP EDR with the one closest (in encoded SCLK) to the scene EDR with $(T_n - T) < 0.5 * (T_d - T_n)$
 - iv. Find shutter closed DF EDRs to go with each sphere EDR by following (a) above
 - v. Find shutter closed BI EDRs to go with each sphere EDR by following (b) above
 - vi. If unexpected SP EDRs are selected
 1. If either SP EDR differs from the scene EDR by more than 24 hours, generate an error and ask for human intervention to select the proper pair of SP EDRs to use in generating the TRDR for the given scene EDR
 2. If either of the SP EDRs selected is different from that predicted in the early observation tracking table, set the flag in the data quality indicator in the TRDR but otherwise continue normally (note this part of the logic is implemented by the C++ program, while the rest is implemented in PIPE)
- e. Shutter closed BI EDRs for bad pixel mask
- i. Select closest (in encoded SCLK) set of BI EDRs with 1x binning and hyperspectral wavelength filter

APPENDIX M. TEMPERATURE SENSOR AND HEATER LOCATIONS

Locations of the reported temperatures, as well as locations of heaters whose current is reported in housekeeping, are shown in the following graphics

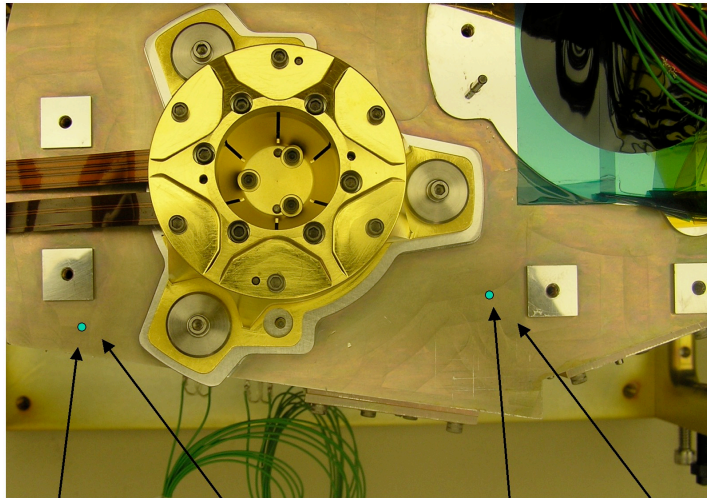




Integrating sphere
temperature sensor
(IR FP/7)

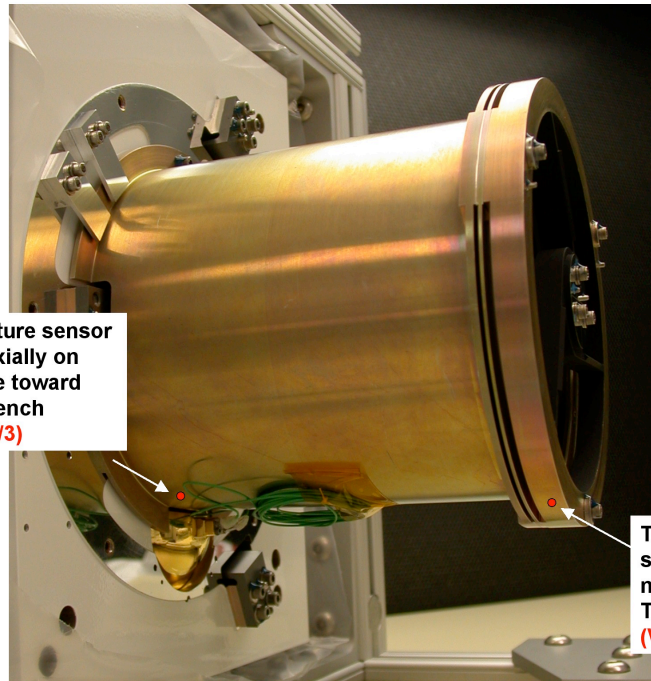


Shutter motor
temperature
Sensor (IR FP/6)



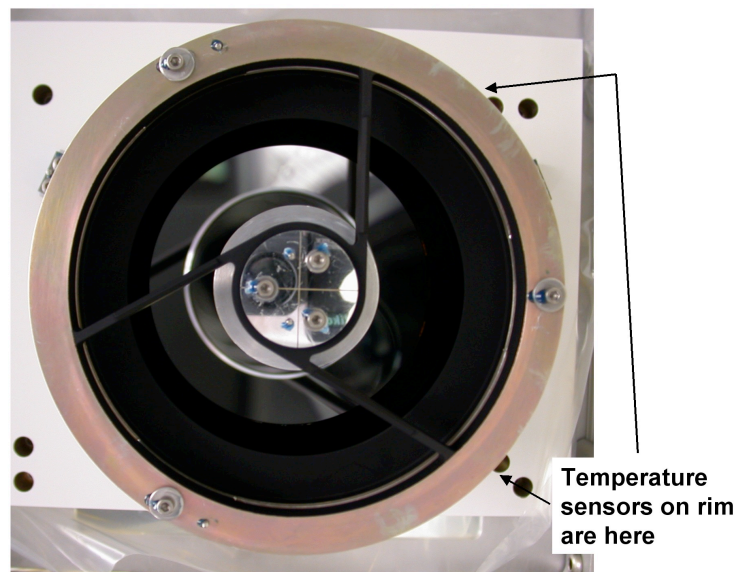
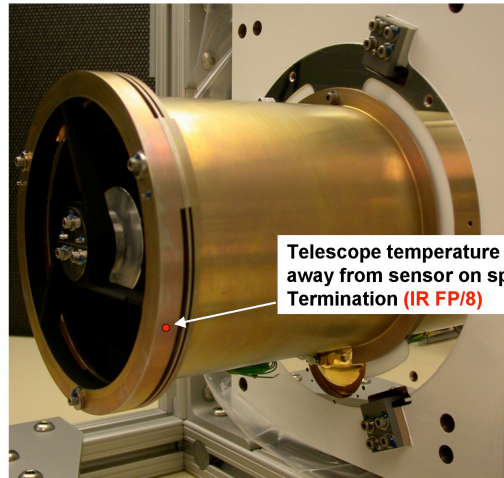
Spectral cavity temperature sensors (these will be the SD (rectangular) package, not the CU package (with hole in it))

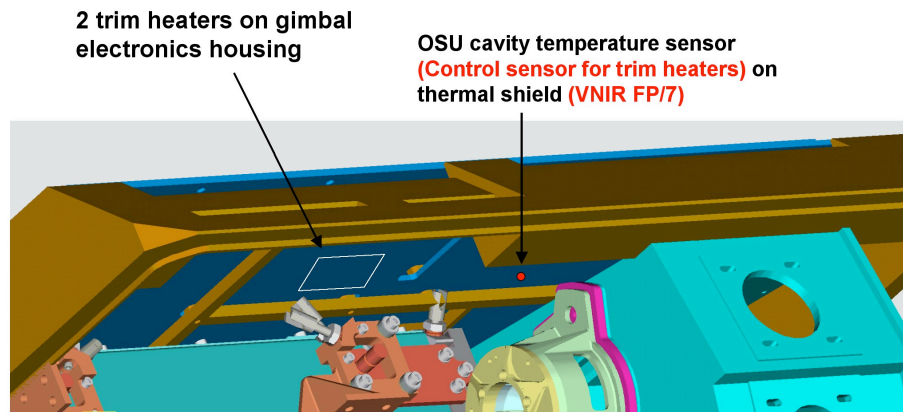
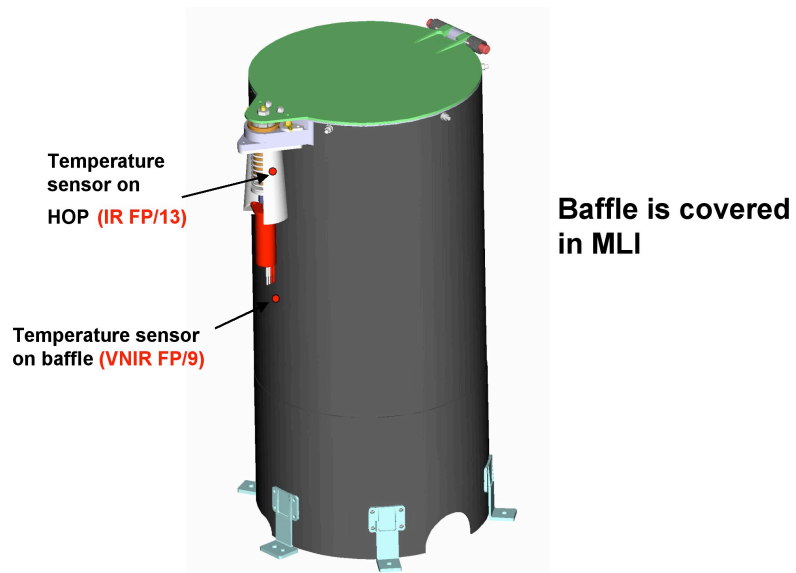
IR FP/9 (control temp sensor for the trim heater) VNIR FP/6



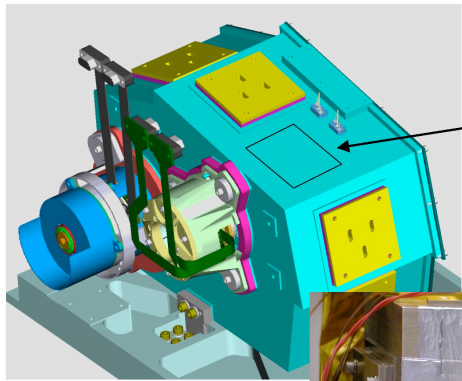
Temperature sensor moved axially on telescope toward optical bench
(VNIR FP/3)

Temperature sensor on rim near spider Termination
(VNIR FP/5)

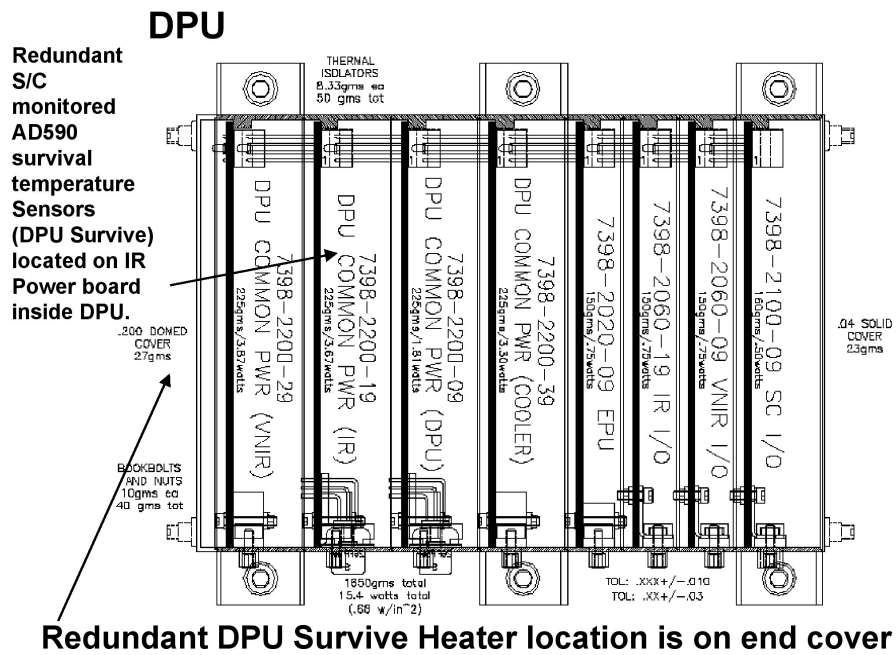
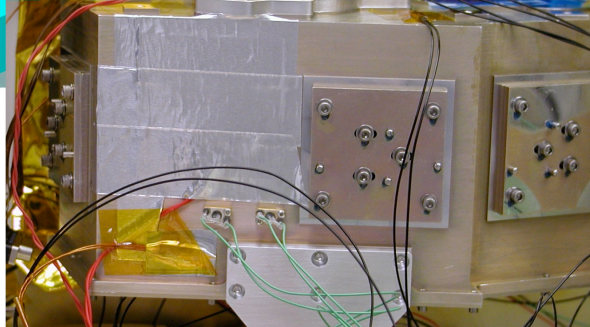




IR (IR FP/11) and VNIR (VNIR FP/8) FPU board temperature sensors on boards



Trim heater on spectrometer housing - similar to OCF calibration configuration (seen in picture below) (IR FP/9 is the control)



APPENDIX N. DESCRIPTION OF TRR3 FILTERING

CRISM Hyperspectral Data Filter

PDS SIS Appendix - 02/02/2011

F. Seelos

Compact Reconnaissance Imaging Spectrometer for Mars (CRISM) TRR3 I/F full and half resolution hyperspectral data products (e.g. FRT0000C202_07_IF165L_TRR3.IMG shown in Figure N-8) have been processed with a custom filtering procedure prior to PDS delivery (Figure N-1) [1,2]. The corresponding PDS delivered radiance on sensor spectral data products (e.g. FRT0000C202_07_RA165L_TRR3.IMG) have not been filtered, allowing for the recovery of unmodified reflectance spectra (Figure N-2). Over the course of the Mars Reconnaissance Orbiter (MRO) mission, CRISM has operated with an IR detector temperature between ~ 107 K and ~ 127 K. IR observations acquired at higher detector temperatures exhibit an increase in systematic and stochastic noise (e.g. Figure N-2, Figure N-4). The primary systematic noise component in both CRISM IR and VNIR data appears as along track column-oriented striping. This is addressed by the Ratio Shift Correction (RSC) - a scene-dependent multiplicative correction frame developed through the serial evaluation of channel-specific inter-column ratio statistics. The dominant CRISM IR stochastic noise components appear as isolated data spikes or column-oriented groups of pixels with erroneous values. Non-systematic noise in IR data is identified and corrected through the application of an Iterative Kernel Filter (IKF), which employs a formal statistical outlier test as the iteration control and recursion termination criterion. This allows the filtering procedure to make a statistically supported distinction between high frequency (spatial/spectral) signal and high frequency noise based on the information content of a given multidimensional data kernel. To illustrate the end-to-end hyperspectral filtering process each data processing procedure shown in Figure 1 is briefly described with the corresponding resulting data products shown in Figures N-2 through N-9.

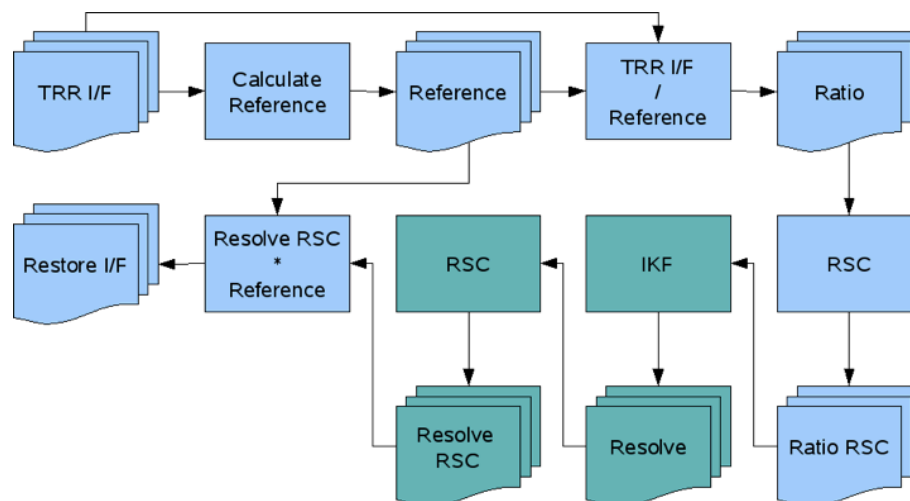


Figure N-1: CRISM hyperspectral data filter processing flow chart. Boxes represent data processing steps; Stacks represent CRISM image cubes. All procedures and intermediate products are employed in the filtering of IR data. The elements shown in green are bypassed by the VNIR filtering process.

Data Processing Overview – The CRISM hyperspectral data filtering process takes as input a three dimensional (x, t, λ) CRISM VNIR or IR I/F image cube (Figure N-1: TRR I/F) and generates a filtered version of the input data (Restore I/F) with the same dimensions – there is a 1:1 correspondence between a given input and output pixel (x_0, t_0, λ_0). The two main data filtering procedures – RSC and IKF – are optimally performed on continuum-normalized spectral data, so the initial data processing steps are the calculation of a reference image cube (Calculate Reference) and the subsequent calculation of a ratio image cube using the reference image cube as the denominator (TRR I/F / Reference). In this referenced-normalized ratio space, the filtering procedures to be applied depend on the wavelength range of the input image cube. CRISM VNIR data does not exhibit the non-systematic or stochastic noise the IKF procedure is designed to address, so only a single application of the RSC procedure is required. The noise structure in CRISM IR data is more complex, and requires the use of the RSC procedure as a pre- and post-processing step relative to the application of the IKF procedure. The image cube resulting from the ratio space data processing (VNIR: Ratio RSC; IR: Resolve RSC) is then recombined with the previously calculated reference cube (Resolve RSC * Reference) to transform the data back to I/F. The image cubes used are described further below.

TRR I/F - PDS deliverable radiance on sensor image cube (e.g. FRT0000C202_07_RA165L_TRR3.IMG) transformed to I/F (Figure N-2).

Reference Cube - The reference cube is a low spectral frequency / high spatial frequency representation of the input image cube (Figure N-3). The spectrum for each spatial pixel is processed with a series of boxcar filters and tuned implementations of the RSC procedure to produce a 'pristine' reference spectrum for each pixel. Any residual noise in the reference cube will be propagated into the final result.

Ratio Cube - The reference cube is used to normalize the input image cube to produce a ratio cube (Figure N-4). High frequency spatial variability is normalized out of the ratio, while high frequency spectral variability (signal and noise) is retained. All subsequent data processing occurs in ratio space or a space resulting from further transformations of the ratio cube.

Ratio Shift Correction (RSC) - The RSC procedure is applied to the normalized spectral data as both a pre-processing (Figure N-5) and post-processing (Figure N-7) step relative to the application of the IKF procedure for IR data, or as the dominant filtering process for VNIR data. Within a given spectral band, a spatial column corresponds to a single detector pixel. The Ratio Shift Correction characterizes residual bias of each detector pixel through the evaluation of inter-column (or cross-track shifted) ratio statistics relative to an appropriate cross track model. Modifying the complexity of the underlying cross track model allows the RSC procedure to address high frequency column striping (Figure N-4 to Figure N-5) or low frequency banding (Figure 6 to Figure 7), while retaining real scene cross-track variability.

Iterative Kernel Filter (IKF) - The IKF procedure is a kernel based filtering algorithm that models the information content of a given three dimensional (x, t, λ) normalized data kernel as a multidimensional polynomial. The model residuals are treated as a sample set and examined for outliers using the Grubbs test. If an outlier is detected, the corresponding pixel is removed from consideration and the kernel model is iterated. Model iteration is terminated when no further

outliers are detected. The filtered value for the target pixel at the center of the input kernel is then given by a proximity weighted model of the kernel elements that were not marked as outliers. The confidence level threshold for the Grubbs test is conservative so the filter retains some marginal noise (Figure N-6) rather than erroneously removing real spectral structure.

Restore I/F - The result of the ratio space data processing (Figure N-7) is multiplied by the reference cube (Figure 3) to transform the filtered data back to I/F (Figure N-8). Figure N-9 shows the effect of the CRISM hyperspectral filtering process on the example image cube.

References -

- [1] Seelos F. P., Parente M., Clark T., Morgan F., Barnouin O. S., McGovern A., Murchie S. L., and Taylor H. (2009) American Geophysical Union, Fall Meeting, P23A-1234.
- [2] F. P. Seelos, S. L. Murchie, D. C. Humm, O. S. Barnouin, F. Morgan, H. W. Taylor, and C. Hash (2011) 42nd Lunar and Planetary Science Conference, 1438.

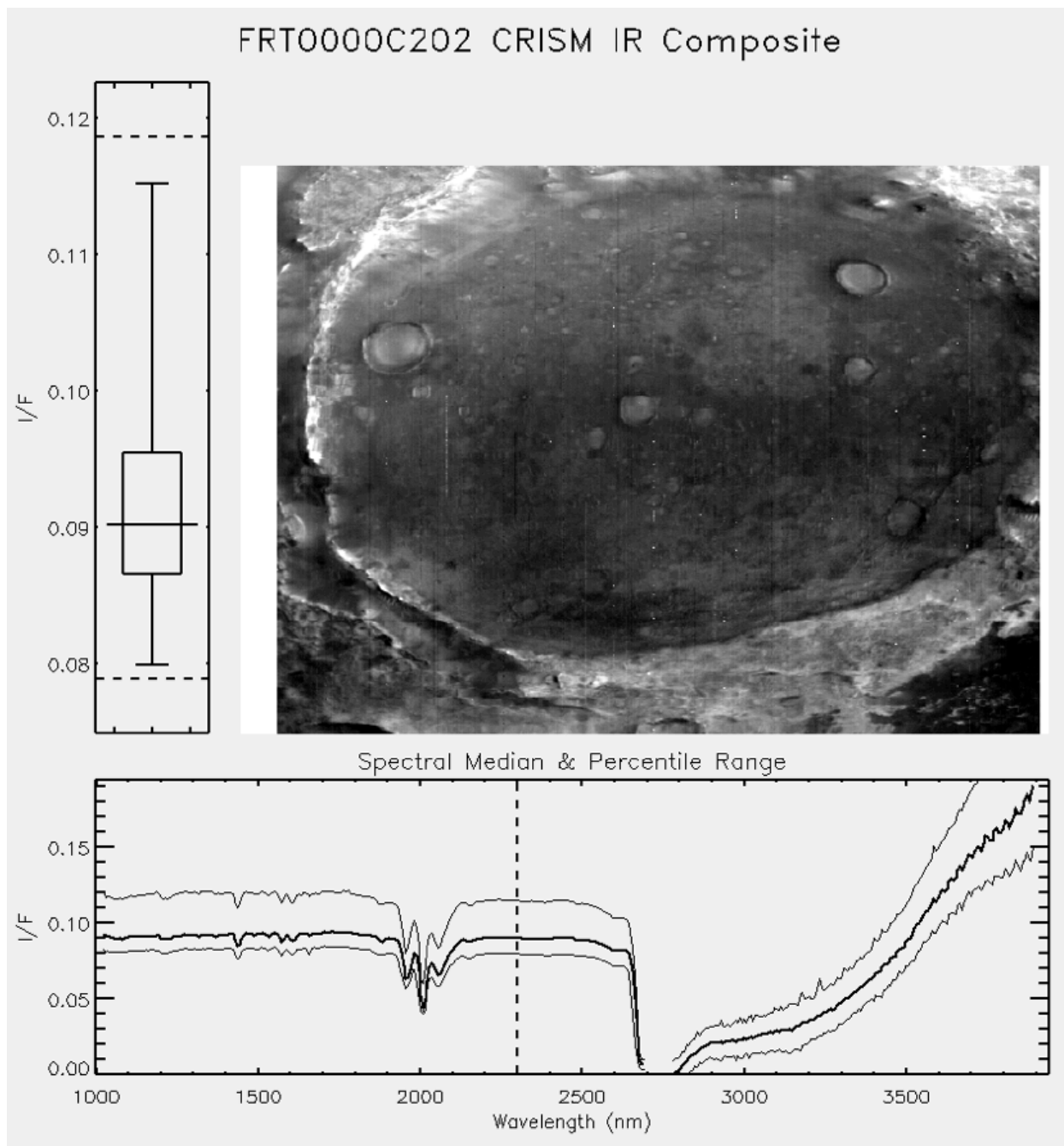


Figure N-2: Three panel composite view of FRT0000C202 segment 0x07 (central scan) input I/F IR image cube. Observation FRT0000C202 was acquired with an IR detector temperature of ~ 120.8 K. The systematic and stochastic noise components to be addressed by the filtering procedure are evident. The composite plot consists of: 1) Band 240 (~ 2300 nm) ground plane (x,t) image with a 1% linear stretch; 2) Boxplot showing the data distribution and stretch limits for the displayed band; 3) Median spectrum and [1,99]% envelope for the input image cube.

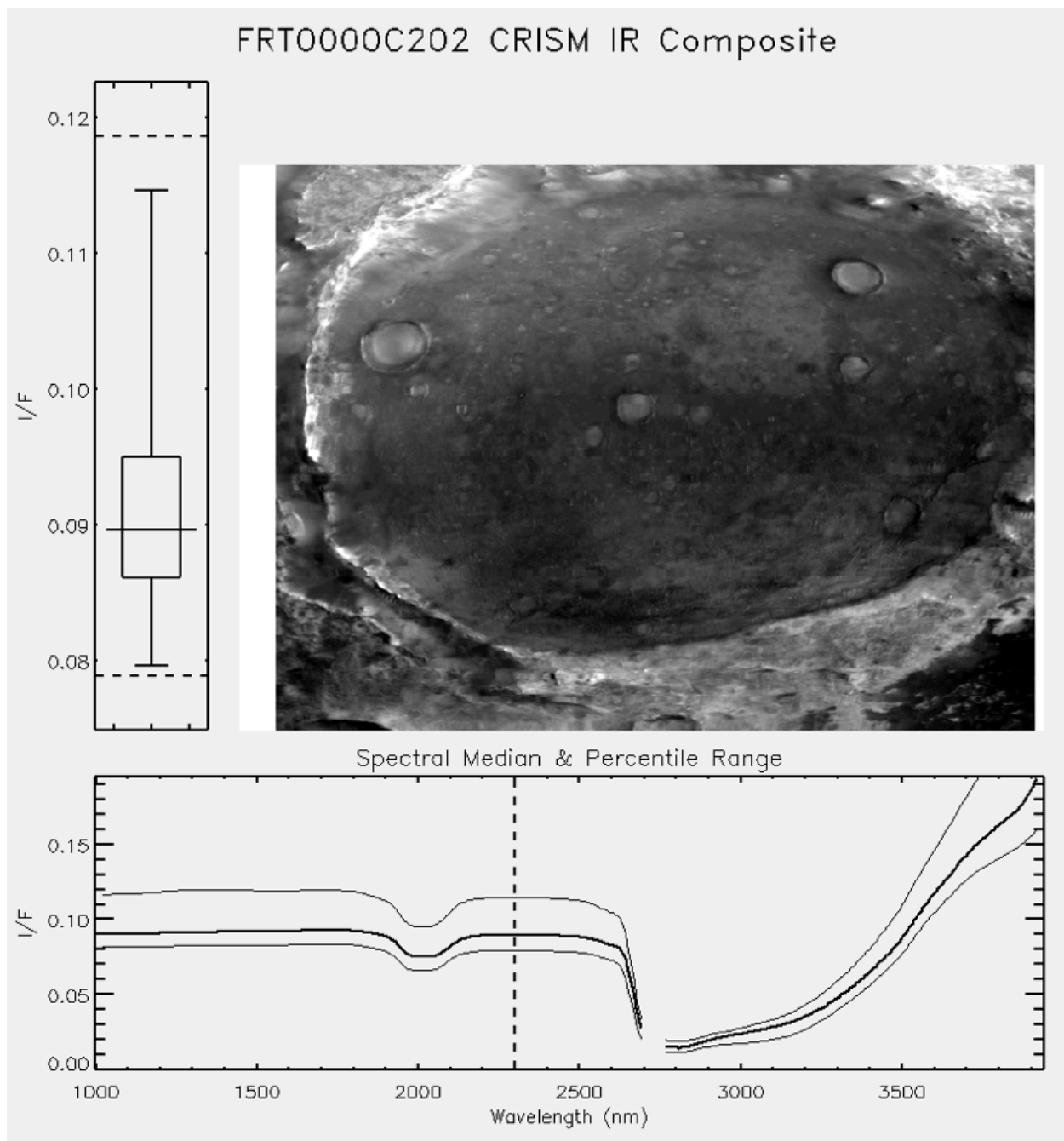


Figure N-3: FRT0000C202 reference cube. High frequency spatial information is retained while high frequency spectral information is discarded.

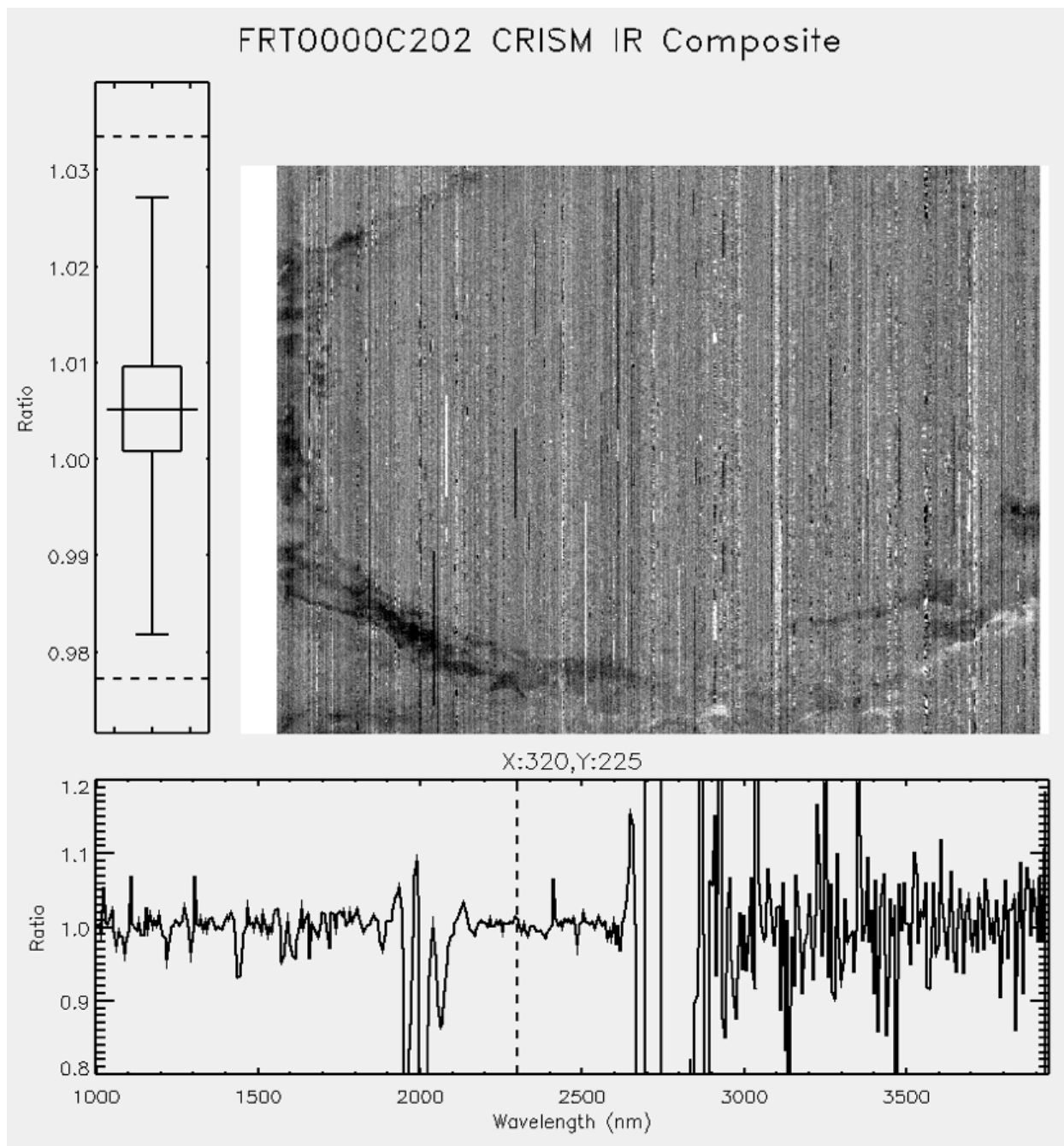


Figure N-4: FRT0000C202 ratio cube. Spatial pixel scale variability due to low-spectral frequency continuum variation is retained by the reference cube (Figure 3) but normalized out of the ratio cube. The ratio cube contains both high frequency noise and high frequency signal components. The spectral plot corresponds to the center pixel in the scene.

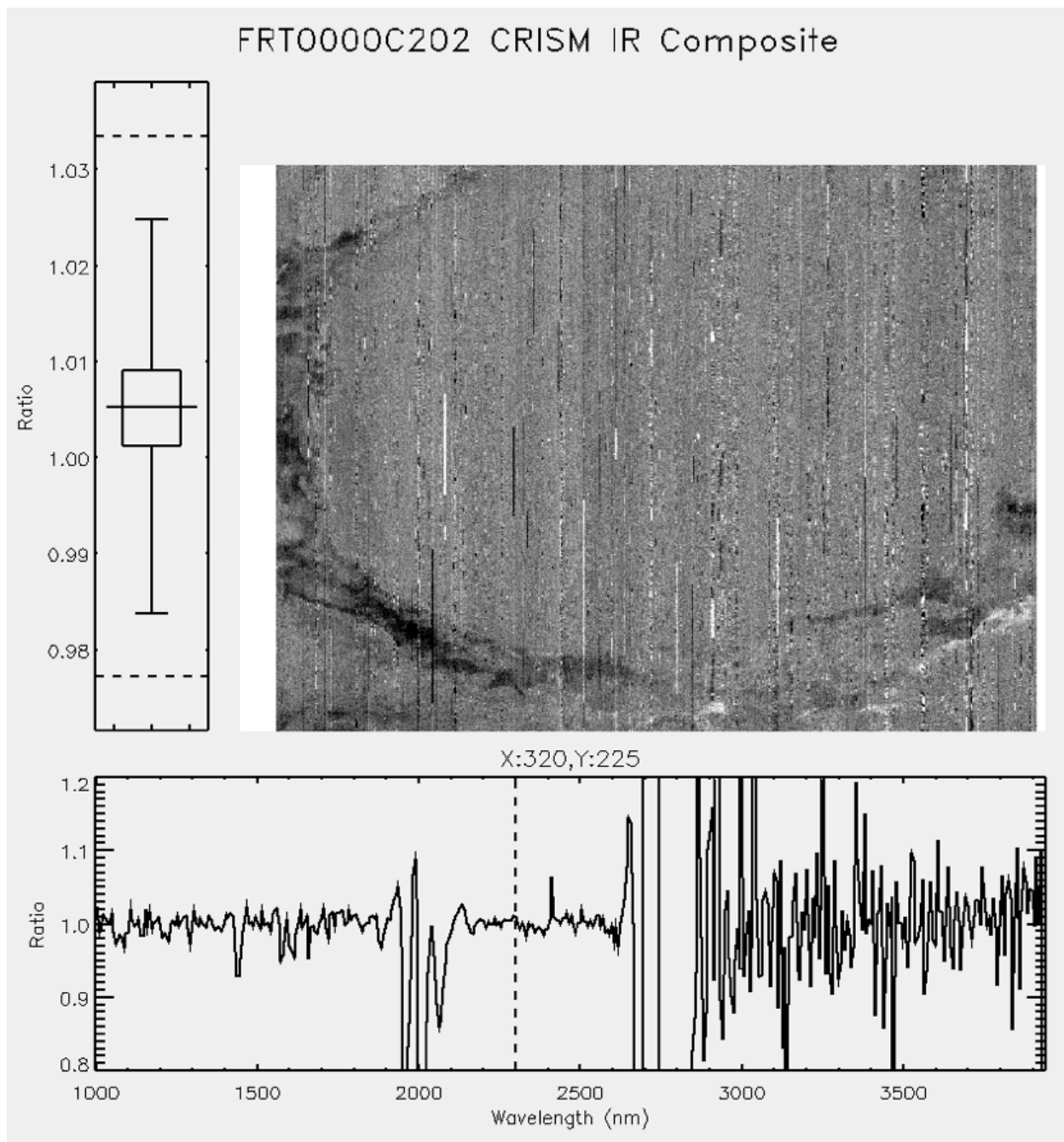


Figure N-5: FRT0000C202 ratio RSC cube. Systematic column-to-column (along track) bias has been mitigated.

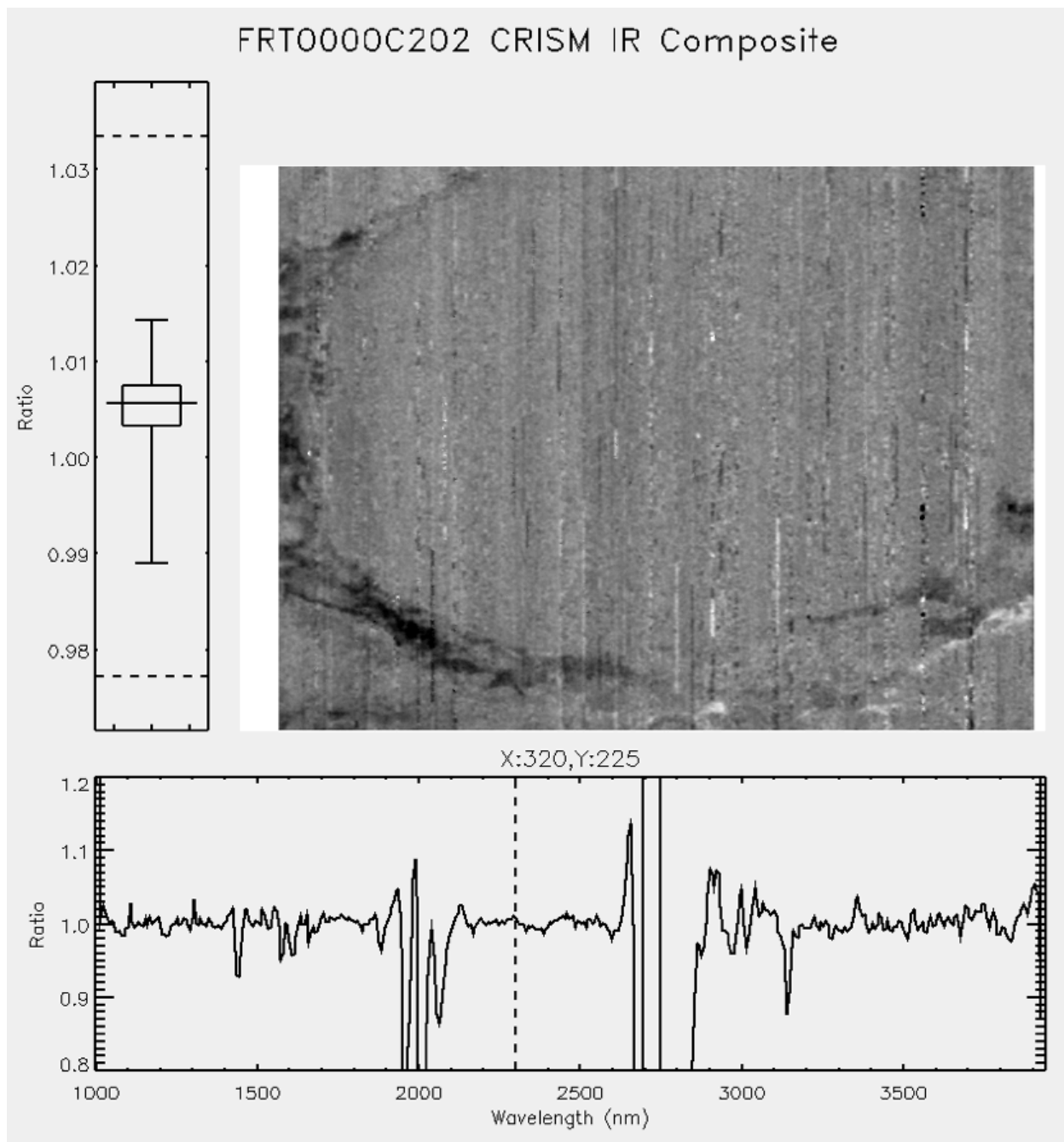


Figure N-6: FRT0000C202 resolve cube. Stochastic noise components have been removed while real high frequency spatial/spectral variability has been retained.

FRT0000C202 CRISM IR Composite

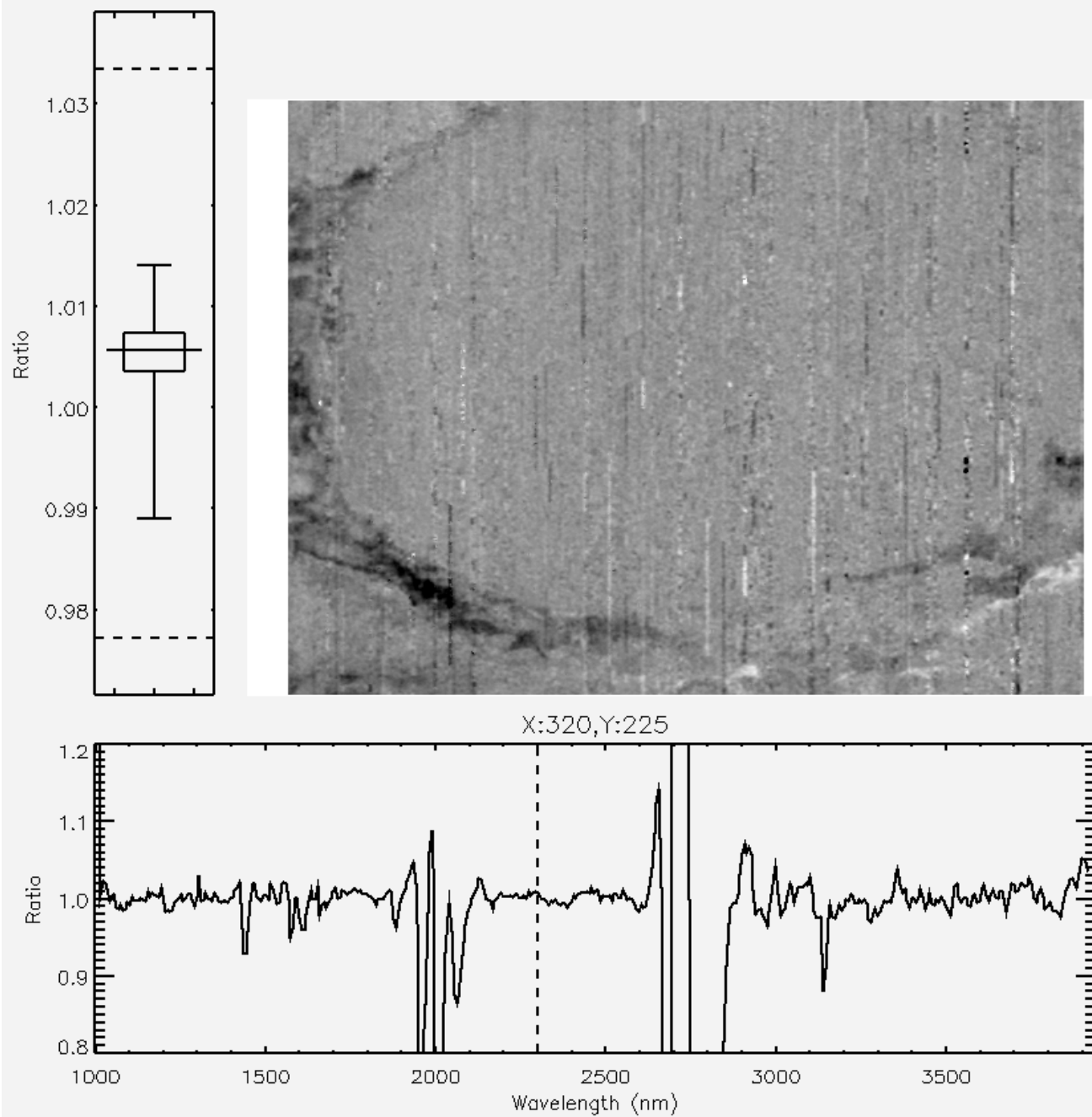


Figure N-7: RFRT0000C202 resolve RSC cube. Systematic along track banding has been mitigated.

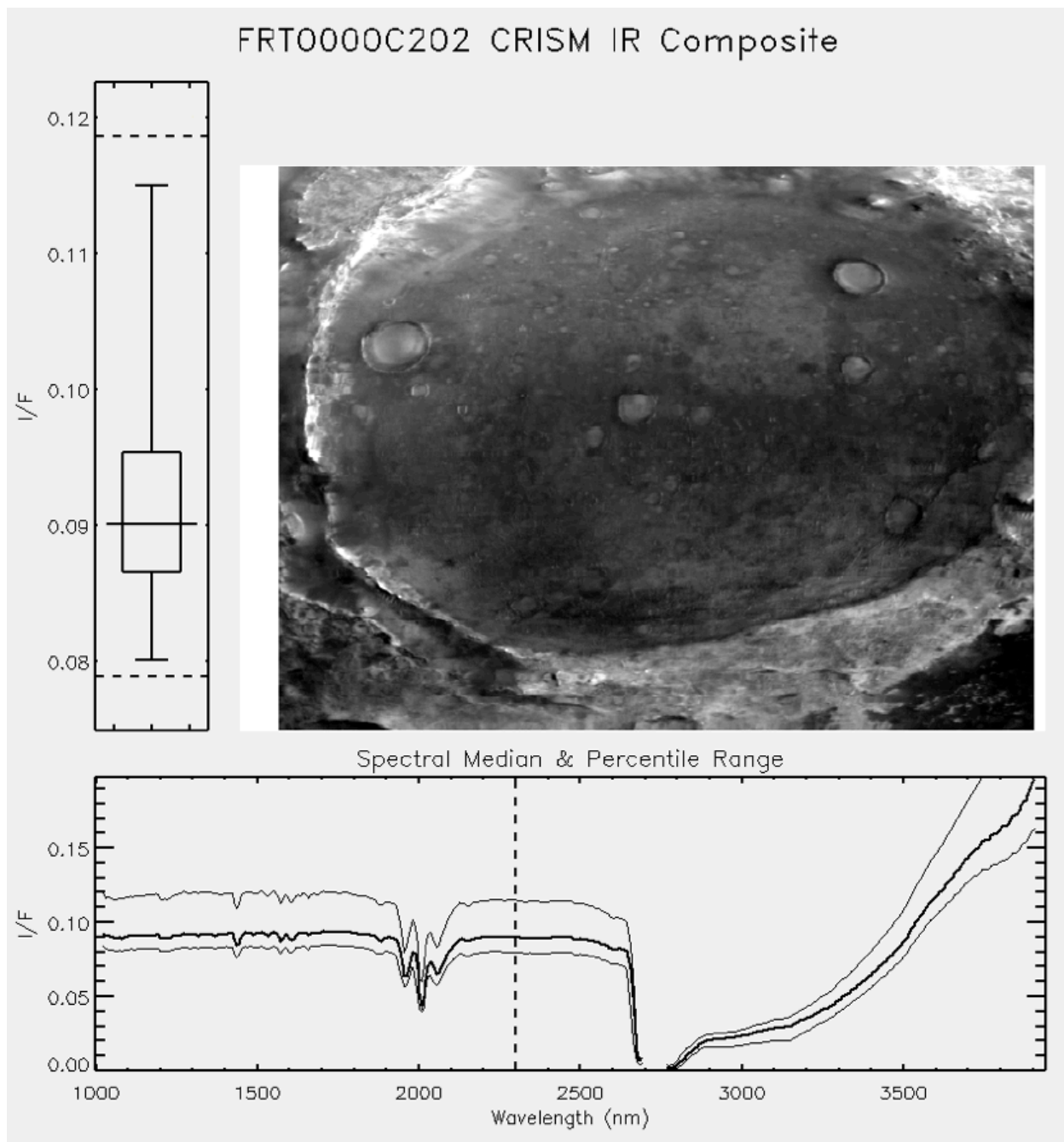


Figure N-8: FRT0000C202 restore cube – delivered to the PDS as FRT0000C202_07_IF165L_TRR3.IMG. Compare the ground plane image, median spectrum and spectral percentile envelope, and data distribution boxplot to Figure 2.

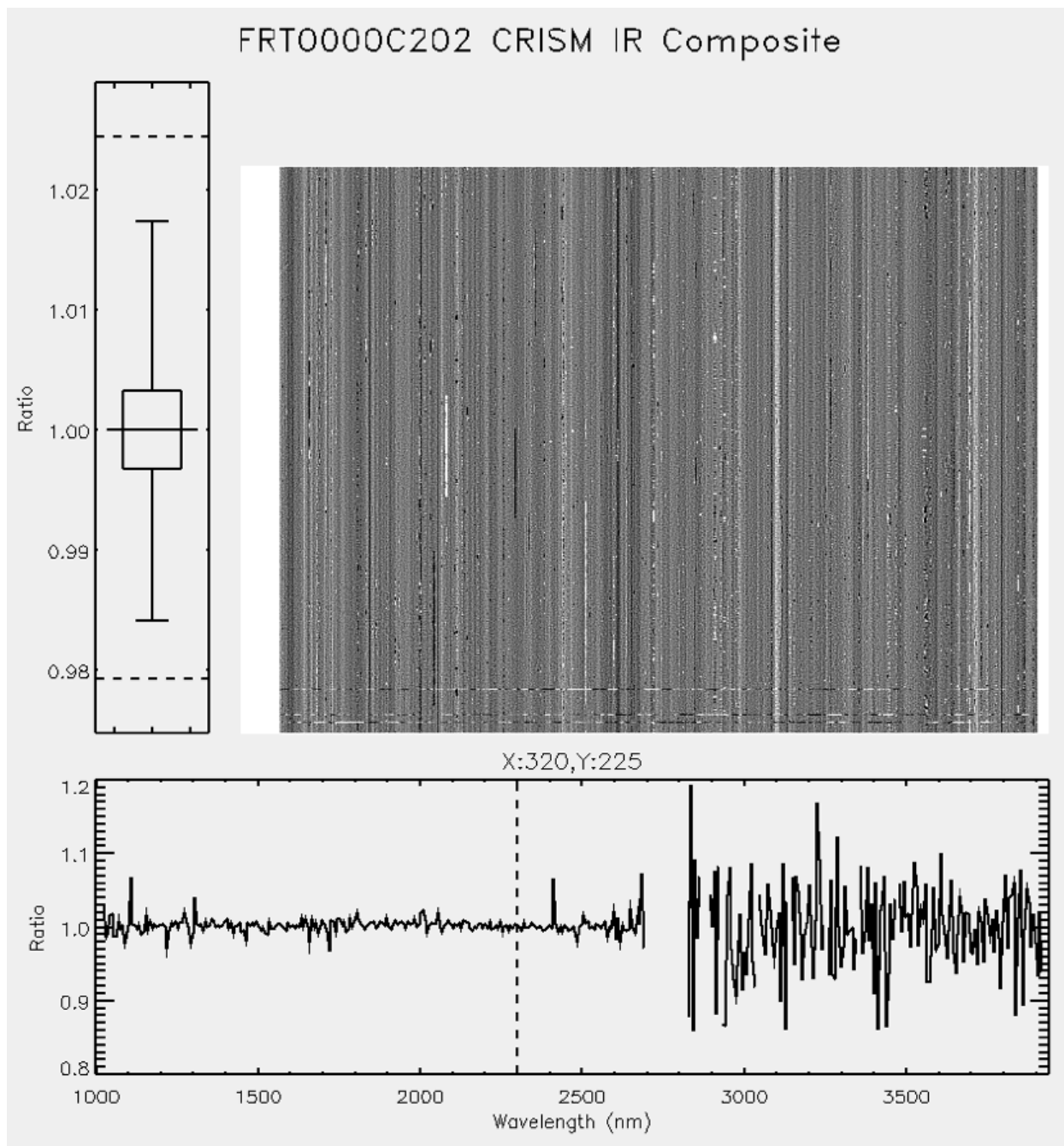


Figure N-9: FRT0000C202 input / output ratio cube showing the effect of the data filtering procedure. Note that the single pixel input/output ratio spectrum and band 240 ratio data are centered on unity.

APPENDIX O. DESCRIPTION AND USAGE OF ADRS